PRESTRESSED CONCRETE BEAMS WITH STIRRUPS SUBJECTED TO TORSION, BENDING AND SHEAR

by

Towfik Abdul Hussien Tahir

A thesis submitted for the degree of
Doctor of Philosophy

Department of Civil Engineering & Construction
The University of Aston in Birmingham.

July 1984

THE UNIVERSITY OF ASTON IN BIRMINGHAM

PRESTRESSED CONCRETE BEAMS WITH STIRRUPS SUBJECTED TO TORSION, BENDING & SHEAR

TOWFIK A.H. TAHIR Ph.D. 1984

SUMMARY

Reported in this thesis are test results of 37 eccentrically prestressed beams with stirrups. Single variable parameters were investigated including the prestressing force, the prestressing steel area, the concrete strength, the aspect ratio h/b and the stirrups size and spacing. Interaction of bending, torsion and shear was also investigated by testing a series of beams subjected to varying bending/torsional moment ratios. For the torsional strength an empirical expression of linear format is proposed and can be rearranged in a non-dimensional interaction form:

$$\frac{T}{T_o} + \frac{V}{V_o} + \frac{M}{M_o} + \frac{Ps}{P_o} + \frac{Fs}{F_o} = 1 + \frac{Pc_2}{Fsp}$$

This formula which is based on an average experimental steel stress lower than the yield point is compared with 243 prestressed beams containing stirrups, including the author's test beams, and good agreement is obtained.

For the theoretical analysis of the problem of torsion combined with bending and shear in concrete beams with stirrups, the method of torque-friction is proposed and developed using an average steel stress. A general linear interaction equation for combined torsion with bending and/or shear is proposed in the following format:

$$(fi)\ \frac{T}{T_u} = 1$$

where (fi) is a combined loading factor to modify the pure ultimate strength for differing cases of torsion with bending and/or shear. From the analysis of 282 reinforced and prestressed concrete beams containing stirrups, including the present investigation, good agreement is obtained between the method and the test results. It is concluded that the proposed method provides a rational and simple basis for predicting the ultimate torisional strength and may also be developed for design purposes.

Key words: prestressed concrete, beams, torsion, shear, ultimate strength .

ACKNOWLEDGMENTS

The author wishes to express his thanks to Dr. L.H.Martin, B.Sc., C.Eng., M.I.C.E., Head of the Department of Civil Engineering & Construction at the University of Aston in Birmingham, for his help, encouragement and supervision throughout this investigation.

Thanks are due to Mr. W.Parsons, Chief Technician in the Department of Civil Engineering at the University of Aston and for the staff of the Concrete Laboratories for their help during the experimental work.

Thanks are also due to Mr. I.A.Sparkes, Adviser to Overseas Students and Chairman of the Hardship Fund for providing financial support during different parts of this investigation. Also the support of the British Council for Aid to Refugees, the W.U.S. and the Father Domenique Foundation is sincerely acknowledged.

Special thanks are due to Mrs. L.Doogan for typing the thesis neatly and efficiently.

THE AUTHOR

The author graduated from the Department of Civil Engineering at Baghdad University in 1972. He spent the following three years as a site engineer. Since 1977, the author has been engaged as a research student in the Civil Engineering Department at the University of Aston in Birmingham.

No part of this work has been submitted in support of an application for another degree or qualification.

NOTATION

Subscripts 1,2,3 refer to modes of failure

i refers to level of investigating stresses on a section

j refers to level of steel

o refers to over reinforcement

A_ℓ	cross sectional area of longitudinal steel
Ap	cross sectional area of prestressing steel
As	cross sectional area of one leg of a stirrup
b	width of rectangular section
b'	shorter c/c leg of a stirrup
C	"cohesion" or min.confinement stress to develop concrete strength due to shear-friction
Cd	depth of compressed concrete due to twist-friction
d'	longer c/c leg of a stirrup
d_ℓ	effective depth of the section to the centroid
d_w	effective depth to the lower leg of a stirrup
d_n	depth of compression zone due to skew-bending
Ec,s	Young's modulus of Concrete and Steel repsectively
e	eccentricity of prestressing force
fc'	cylinder compression strength of concrete
fcm	maximum direct compressive stress in concrete due to bending moment
fct	shear stress due to torsion
fcu	cube compressive strength of concrete
M	applied bending moment
Mu	ultimate pure bending moment
pc1,2,3	direct stress in concrete due to prestressing at bottom, mid-depth and top respectively
P	prestressing force on the section
Ps	prestressing force on the steel

S	spacing of stirrups
T	applied torsional moment
Tu	ultimate pure torsional moment
υ	shear stress in concrete due to shear force
V	applied shear force
Vu	ultimate pure shear force
x	elastic depth of compression zone reduced by torsion
γ_c	shear strain in concrete
γ_s	shear strain in steel
$\theta_{1,2,3}$	angle of the skewed bending hinge at failure in modes 1,2 and 3 respectively
θ	angle of twist at ultimate
ρ_ℓ	ratio of longitudinal steel area to gross cross section of area = A_ℓ/bh (half-longitudinal steel)
ρ_ω	total volumetric stirrups steel ratio = $A_s(d' + b')/(bhS)$ (one leg)
ρ_{sv}	ditto for vertical leg of stirrup steel only = $A_s d'/(bhS)$
ρ_t	total steel content ratio = $(\rho_\ell + \rho_\omega) \cdot 2$
σ_n	normal stress on cross section
τ	tangential shear stress in cross section
τ_u	ultimate shear stress
	coefficient of friction

LIST OF CONTENTS

LIST OF TABLES

LIST OF FIGURES

LIST OF PLATES

CHAPTER ONE

REVIEW OF PREVIOUS WORK

1.1 INTRODUCTION

1.1.1 Analysis for Torsion

Torsion arises as a result of the eccentricity of the applied load acting normally to the longitudinal axis of the structural element. A prismatic element resists torque by building up shear stresses in the cross section.

From the point of view of structural analysis, the torsional moment can be considered as two components. The first is resisted by a circulating shear flow and covered by the theory developed by Saint-Venant. The second component, denoted as warping torsion, yields shear stresses resulting from the change in axial stresses. To satisfy the equilibrium condition, the sum of the Saint-Venant torsional moment and warping torsional moment must be equal to the total torsional moment of the applied load. However, it remains the task of structural analysis to deal with the structure as a whole and to determine the distribution of the torsional moment for a given load.

As far as the analysis of torsional shear stresses in a given cross section is concerned, taking into account only the conditions of the cross section under consideration, it is independent of whether the Saint-Venant torsional moment occurs separately or together along with a warping twist.(1).

In ... members with solid or hollow cross sections, Saint-Venant torsion usually predominates and warping torsion may be neglected.

Two types of torsion are possible in indeterminate structures. One results from equilibrium conditions and the other is required to satisfy compatibility. The first being a torque required to maintain equilibrium in the structure, the second is defined as the twist required to maintain compatibility in the structure (2). If on removal of the restraint redundant from such a structure, torsion is eliminated, then the torque is a compatibility one and when absent from the structure it remains a determinate one.

In general practice, for designers, lack of torsional resistance to the torsion arising from statical indeterminacy or continuity does not cause collapse (3). An instance of this type is the very often case in buildings; spandrel beams. Whereas equilibrium torsion set up due to statical determinacy or non-continuity needs to be resisted to avoid collapse. This occurs mainly in cases of curved or eccentrically loaded elements. Even in such simple structures, torsion for equilibrium may prove to be of minor importance, whereas compatibility torque in some indeterminate cases can turn to be of a major effect in concrete structures.

Torsion in concrete structures was generally considered as only a minor effect. Torque could also be a major effect as in curved girders or in girders with horizontal projections, and in spandrel beams at the corner without a column. More notable examples are the constructions of slender precast members, staircases without intermediate supports, spiral stairways and skewed archs. In each case, almost with no exception, torsion co-exists with bending and or shear. Thus the problem of combined torsion, bending and shear, while the most difficult to analyse, is, nevertheless, the most important to the designer.

1.1.2 Design for Torsion

Torsion being considered in the past as only a minor effect, has been ignored in the design of structural concrete members. It was assumed that it could generally be accommodated by the large factors of safety which were used in flexural design. As a new level of knowledge on material and loadings has been achieved, the load factors have been reduced and tended to be decided on a statistical basis rather than by the judgement of engineering experience. This, combined with the introduction of modern structures incorporating members subject to high torsional moments, dictated the need to take torsion into account explicitly in design.

For prestressed concrete in structural torsion, particularly, this demand is becoming more and more urgent with the growing use of prestressing in structures. One of the most practical cases in design for concrete torsion is that of large concrete members where the designer, from lack of better knowledge, tends to add stirrups to take the torsional moment. As there are definite limits for both the torsional and flexural shear strengths of reinforced concrete, irrespective of the amount of reinforcement, designers have to resort to prestressing giving much smaller members and simpler distribution of steel in the cross sections.

Design procedures for structural prestressed concrete subject to torsion are not yet fully developed and codified.

The Australian Code CA35-1963 (4), was the first to have a torsion clause for design of prestressed concrete structures in torsion. A complete design procedure is given by the CA35-1973 for prestressed concrete beams in combined torsion, bending and shear.

The provisions are based on the theoretical approach of Rangan and Hall (5) which assumes all steel at yield longitudinally and transversely. It is restricted to under-reinforced prestressed concrete beams with web steel, using an empirical formula to check that concrete does not fail prior to yielding of the steel.

The British Code CP110-1972 (7), deals with torsion for the first time in this country, but for prestressed concrete it suggests merely the general guidance given for design of reinforced concrete beams. The Code includes expressions for shear, torsion and bending that can be used independently of each other within certain limits. The expression for torsion, is based on a partial yield theory, though the presentation in the code may give the impression of an all yield theory (8).

1.1.3 Interaction of Torsion with Bending and Shear

The interaction of torsion, bending and shear is basically a three-dimensional problem. Consequently, for theoretical predictions of the behaviour and ultimate strength of a prestressed concrete beam subjected to combined loading, an interaction (and failure) surface must be developed. This can only be accomplished by representing the three variable parameters involved, in a three-dimensional space coordinate system (9).

No code of requirements for structural concrete has yet included such an interaction surface. However, a few theoretical approaches have been proposed for the analysis of the interaction between torsion, bending and shear (10, 11, 12, 13). None were intended as a complete solution, but only to cover the case where the steel yielded partially or completely. The complete solution is more difficult and further research is required to consider conditions where the steel does not yield and where the strength of the

concrete changes.

It can be concluded, therefore, that so long as the interaction problem of torsion is given basically different solutions, the provisions for the design of torsional shear reinforcement in prestressed concrete beams with stirrups cannot be identical for codes of practice from different countries.

1.2 REVIEW OF NON-STRESSED MEMBERS

Before reviewing the previous research in the prestressed concrete members, it is proposed to review the development of some aspects of work on torsion in non-stressed concrete sections.

1.2.1 Plain Concrete Members

The most important theoretical contribution to the further development of this field of knowledge is, undoubtedly, due to Saint-Venant (1797-1886). In 1853, he was the first to give an analytical solution for the problem of torsion in non-circular plain sections. Assuming an elastic, homogeneous and continuous member, he produced a solution in the form:

$$T = (\text{coefficient})\ b^2h\ (\text{maximum shear stress}) \qquad (1.2.1)$$

The coefficient involved in the torsional resistance of the section is a function of the ratio b/h, for which was proposed the approximate formula: $1/(3 + 1.8\ b/h)$. The influence of this work (14) was considerable and still provides a classical basis for the investigation into the torsional behaviour and capacity of most structural materials including concrete.

In the case of plain concrete members, St. Venant's equation was initially applied to determine the ultimate torque capacity. The concrete member subjected to torsion is, therefore, assumed to be elastic and homogeneous, until cracking occurs. The concrete

member resists the torque by shear stresses, distributed according to St. Venant's theory, which produce principal tensile stresses at an angle of 45^{o} to the rotational axis of the beam. Thus for stress equilibrium in the diagonal direction, the induced maximum shear stress is taken numerically equal to the maximum principal tensile stress. The latter being considered approximately equal to the uniaxial tensile strength of the concrete, the elastic torque capacity for a rectangular plain concrete beam, then becomes

$$T = (\text{coefficient})\ b^2 h\ f_t \qquad 1.2.1a$$

which corresponds to the ultimate torque of plain concrete beams failing at the apprearance of the first cracks. The plain concrete beam, therefore, is considered to fail, along a spiral twisting surface, when the tensile strength of concrete is exceeded. Moreover, no redistribution of stresses at failure is taken into account and only the stress equilibrium condition is considered.

St. Venant's basic assumption holds true until significant deformation takes place in the form of cracks, so the application of the theory to members whose failure torque corresponds to initial cracking, is perhaps justified. The equation 1.2.1a, however, was found to underestimate the torsional resistance of such members. The observed excessive strength was initially attributed to the non-elastic behaviour of concrete in tension, though the experimental results of tensile tests on concrete showed little or no plasticity ([15,16]). Furthermore, there have always been great difficulties in determining the tensile strength of concrete because it can be determined indirectly in various ways.

Despite failing to predict this excess of the strength shown by the experimental results, the general form of St. Venant's

elastic equation is considerably important. Similar comparable equations, for the case of pure torsion, are produced by the apparently different approach of the "skew bending theory" and assuming elastic behaviour of concrete in tension.

Bach (17) in 1911 extended St. Venant's theory to cover flanged plain concrete members. His method was based on dividing the sections into component rectangles and summing up their elastic torsional contributions to give the ultimate torsional strength:

$$T_u = (\frac{1}{3}) \quad [\frac{1}{b_w} \Sigma\ b^3h] \quad (ft)$$

where b_w is the width of the web and Σb^3h is the sum of the component rectangles which are assumed to be very narrow and hence the torsional coefficient is 1/3. The webs of concrete flanged members in general practice are usually far from narrow and therefore, according to St. Venant's original theory, correspond to values lower than 1/3. Thus the approximation would be expected to result in an unsafe estimate of the torque capacity.

Applying Bach's approximation to St. Venant's equation, however, gave very conservative results. That was thought to be due to ignoring the additional torsional resistance of the joints between the component rectangles. To visualize this effect of the joints and the elastic stress distribution throughout the cross section, Prandtl's membrane analogy method was employed (18). It was developed to obtain a more exact value of the elastic torsional strength, which is proportional to the volume under the deflected membrane, and the maximum shear stress, which is proportional to the greatest slope of the membrane. The method was not used widely and was generally confined to the laboratory.

The membrane elastic analogy developed later into the plastic sand heap analogy at the ultimate state, with a uniform shear stress distribution. In 1931, Nadai (19) gave the analytical solution for the torsional resistance of a fully plastic rectangular section in the form of:

$$T_u = (\frac{1}{2} - \frac{1}{6}\frac{b}{h})\ b^2h \text{ (the constnat shear stress)}$$

Assuming full plasticity, the ultimate shear stress for the concrete member subjected to torsion, is limited, therefore, to the maximum tensile stress of concrete. The full plastic assumption overestimated the torsional strength of concrete which is not an infinitely plastic material. The plastic theory, in its assumption of uniform shear stress redistribution at the ultimate load, was, however, more consistent with the experimental results than the elastic theory, particularly in the case of T-sections (20).

Turner and Davies (15), in 1934, reported tests on a few plain square, rectangular and T-concrete sections subjected to torsion. Considering various methods in analysing their test results, they assumed a limited stress redistribution based on the plastic behaviour of concrete in compression. The experimental results showed good agreement with their semi-plastic theory which was modified by an empirical factor.

In 1941, Marshall and Temb (16) tested plain concrete circular, rectangular and flanged sections. Their conclusion was that concrete, subjected to torsion, exhibits in its behaviour both elastic and plastic properties. For the purpose of assessing the ultimate torsional resistance of the non-circular sections, however, they suggested again a plastic redistribution of stresses at failure. They employed, like other previous researchers, the maximum principal

tensile criterion to predict the failure load and assumed therefore, that the failure mechanism is in the form of helical cracks. However, they observed that "with the exception of thin specimens, ... the fracture did not take spiral form ...".

In 1953, Cowan (21) concluded that since the problem of the partially plastic rectangular section has no simple analytical solution, the assumption of full plasticity may therefore be accepted as an approximation. He produced a general non-dimensional, theoretical solution on this basis.

In an attempt to clarify the failure mechanism of plain concrete subjected to torsion, Hsu (22) in 1966, tested ten rectangular beams, using high-speed photography. He came to the conclusion that failure took place about a skew axis of bending. Hsu also developed a theoretical approach for the ultimate load based on a failure plane at a variable angle to the longitudinal axis of the member. The solution based on the classical bending theory is essentially of the elastic torsional form:

$$T_u = (\text{coefficient}) \frac{b^2 h}{3} (f_r) \qquad (1.4)$$

The tensile strength of concrete is assumed to be related to the modulus of rupture, f_r, which is given by an empirical formula to vary with the size and the concrete strength. Hsu proposed an empirical factor of 0.85 to allow for the reduced tensile strength of concrete under torsion.. The ultimate torque as predicted by this equation, is about 65 per cent greater than that calculated by St. Venant's theory, for a ratio of h/b = 2 (45).

In 1971, Martin (23) constructed differently the basic equation for the skew bending solution of the interaction of torsion and

bending in plain concrete members. He achieved a general non-dimensional, theoretical solution of the form:

$$\left(\frac{T_1}{T_{ul}}\right)^2 + \frac{M_1}{M_{ul}} = 1 \qquad (1.5)$$

This form, for failure in mode 1, is of considerable importance since it is essentially the same solution introduced in 1953 by Cowan using a semi-plastic-elastic approach based on the maximum principal tensile stress failure criterion for concrete failing along a helix. When $M_1 = 0$ the interaction equation can be extrapolated to take the form

$$\frac{T_{1,2}}{T_{ul,2}} = 1 \qquad (1.6)$$

which is the special case of pure torsion, in mode 2 where T_{ul} is replaced by

$$T_{u2} = \frac{b^2 h}{3} f_{r2} = 2 \text{ (elastic sectional modulus) } f_{r2}$$

It is basically the same solution given by Hsu above involving an empirical constant. Analysing a distorted skew failure on a trapezoidal plane, clearly shown by Hsu's photographs, Martin gave also a theoretical basis for Hsu's constant in the form of a factor

$$\frac{1}{3 + \sqrt{\left(\frac{b}{h}\right)}} \quad \text{in mode 2}$$

Hsu (24) also extended the final solution of his skew failure theory to flanged sections by applying Bach's approximation method. As a result he had to impose empirical limits on the ratio of the effective flange width to the flange thickness.

By observing the failure mechanism of plain concrete Tee members under torsion and bending, Kirk and Lash in 1971 noticed that the failure, was completed by the rotation of the beam around a skewed bending axis. This confirmed the observations of Hsu about flanged beams tested under pure torsion.

Based on these experimental observations, Martin and Allos (25) extended theoretically the application of the skew bending analysis to cover the case of plain concrete Tee beams. They derived the relevant formula for the ultimate pure torsional capacity of the section from first principles using the distorted section at failure. Depending on the geometry of the section, the skew bending axis could be situated on either the top, the back or front face of the beam. The theoretical analysis gives good agreement with the available results, especially where the modulus of rupture is quoted.

In the same paper, the analysis (based on undistorted section) was further developed theoretically for plain concrete Tee beams subjected to combined loading. This produced the general non-dimensional theoretical solution of the form

$$\left(\frac{V_1}{V_{u1}}\right)^2 + \left(\frac{T_1}{T_{u1}}\right)^2 + \frac{M_1}{M_{u1}} = 1 \qquad (1.7)$$

$$\frac{V_2}{V_{u2}} + \frac{T_2}{T_{u2}} = 1 \qquad (1.8)$$

for modes 1 and 2 of failure respectively. These forms, equating the shear force to zero, are identical to the solution given by Martin in 1971 for rectangular plain concrete members under the action of torsion and bending.

These forms of the general non-dimensional interaction solution, are of particular importance for analysis and design purposes, because of their rational basis and versatility. The interaction curves can be extrapolated to the limiting condition of simple loading:

$$M_{u1,3} = (\text{factor})\ bd^2 f_{r1,3}$$

in pure bending, which is actually a standard modulus of rupture if a beam of a square section is used.

$$T_{u1,2,3} = 2\ M_{u1,2,3}$$

The expression for T_{u2} produces a line close to St. Venant elastic expression. The interaction between bending and torsion as given by Martin is similar to the one introduced by Cowan using a semi-plastic approach. The solution in mode 1 can, therefore, represent an Extended Cowan Simplified failure criterion, including the effect of flexural shear.

Since the interaction curves are based on the undistorted section, the equations 1.7 and 1.8 are applicable to all shapes of section. This makes the equations useful for the comparison of experimental results of differing section shapes, sizes and strength of concrete.

To achieve a reasonably accurate and rational method of assessing the ultimate strength of plain concrete under combined loading provides the theoretical basis for adding any reinforcing steel or prestressing force to the plain section.

1.2.2 Members Reinforced with Longitudinal Steel Only

PURE TORSION

In 1912 Bach and Graf were the first to investigate the behaviour and strength of plain and reinforced concrete members subjected to torsion. As a part of their experimental programme, they tested longitudinally reinforced beams. Their conclusion was that the longitudinal bars increased the torsional strength of plain concrete by only 9%. In continuing research, the test results of Andersen (26), Turner and Davis (15) and Marshall and Temb (16) showed also that the addition of longitudinal steel into a plain concrete beam has little effect on torsional behaviour. This was observed again in 1966 by Iyengar and Rangan. They confirmed experimentally that in pure torsion longitudinal steel, even if increased to 6%, increases the torsional strength of plain concrete by only 10%. The same conclusion was expressed by Hsu who wrote: "Therefore, a beam reinforced with longitudinal bars only can be taken conservatively as a plain concrete beam." (24). He suggested that his formula for pure torsion in plain concrete could also be used to predict the torsional strength of rectangular, T and L members containing longitudinal steel only. In this paper no comparison, however, was made with the available experimental data.

In a subsequent paper (27), Hsu showed that the test results indicate that pure torsional strength is accurately predicted by his equation. He also attempted to extend his theory to cover the case of combined loading.by suggesting a conservative interaction surface defined by an equation connecting torsion and shear. The shear strength was based on an empirical equation for diagonal

cracking in combined shear and bending. In this case, however, the shear strength greatly exceeded the values predicted by the interaction curve proposed by Hsu. He attributed this discrepancy to the fact that the shear strength was based on the development of the first diagonal cracking rather than on the final failure of the member. Hsu's conclusion was that: "To date no satisfactory interaction equation based on final failure, has been developed for beams without stirrups."

In 1971, Martin presented a theoretical procedure intended for ultimate strength analysis of longitudinally reinforced sections subjected to torsion and bending. He identified two modes of failure. In mode 2, singly reinforced beams are considered to behave as plain concrete beams. The interaction equation 1.6 gave very good agreement with the available test results reported by 11 investigators.

Allos and Martin (25) compared their theoretical analysis of plain concrete to Tee beams with small amounts of longitudinal steel. Using the cracking twisting moments of such beams, their analysis showed good agreement with the experimental results; $T_{test}/T_{theory} = 1.01$. The interaction equations, furthermore, showed good correlation with L-beams subjected to torsion and shear. These beams contained 0.6% steel of the web area.

TORSION WITH BENDING AND/OR SHEAR

Many investigators (6) concluded that longitudinal steel cannot be relied on to increase the pure torsional resistance of a rectangular concrete beam. Nevertheless, there was no serious analytical attempt by these early investigators to account satisfactorily for the effect of the including longitudinal steel in plain concrete members under torsion. Their analyses were based

on rather limited test results, from experiments mainly under pure torsion. Their solutions, mostly empirical, required equal volumes of longitudinal and transverse steels, and therefore could not be extrapolated to the more simple case of members containing longitudinal steel only.

Nylander in 1945 was the first to investigate the combined action of torsion with bending and/or shear in this type of member. He also gave the first theoretical solution for the case of torsion and bending in rectangular and T-sections. His theoretical approach was related to the theory for bending. Accordingly, if a beam is "underreinforced for bending", the combined action of bending and torsion should be taken into account. For this case the analysis was based on the superposition of the torsional effects of concrete and steel:

$$\text{Torque resistance} = T_c + T_s \qquad (2.2.1)$$

where T_c = torque resistance by the uncracked concrete zone of the section.

T_s = torque resistance by the shear forces in the longitudinal steel, acting approximately about the mid-point of the section.

The compatibility condition was not necessarily satisfied by Nylander's approach, since he had to assume a yield condition in the steel which was not related to the concrete strength. To achieve a solution he assumed, moreover, that the shear stresses and bending stresses in the steel were combined according to the criterion for yielding of Huber-Beltramis. This enabled him to derive a design expression for the longitudinal

steel area, as proportioned for the combined action of torsion and bending:

$$A_s = \frac{1}{f_s} \left[\left(\frac{M}{jd} \right)^2 + 3 \left(\frac{T - \alpha T_a}{d/2} \right)^2 \right]^{1/2}$$

M = bending moment

T = applied torque

T_a = allowable torque of the beam without bending

f_s = allowable steel stress

jd = internal moment arm

d = effective depth of the beam

α = a coefficient defines the portion of T carried by the uncracked portion of the beam

It is interesting to note that this expression can be rearranged to give a form of non-dimensional interaction between torsion and bending. On squaring both sides and rearranging

$$(A_s f_s)^2 = \left(\frac{M}{jd} \right)^2 + 3 \left(\frac{T - \alpha T_a}{d/2} \right)^2$$

$$1 = \left(\frac{M}{A_s f_s jd} \right)^2 + 3 \left(\frac{T - \alpha T_a}{A_s f_s d/2} \right)^2 \quad \ldots\ldots\ldots$$

This form is of considerable importance because it was obtained by later investigators.

Nylander gave no theoretical solution, however, for bending and torsion where the beam is "over-reinforced in bending", and steel does not yield. His justification was that if the beam is sufficiently over-reinforced for bending, such that the stress in the reinforcement is low, a moderate amount of bending does not decrease the torsional strength, but on the contrary increases it.

This effect was observed in ten experiments on over-reinforced rectangular sections containing 5.1% of longitudinal steel subjected to the more general case of combined torsion with bending and shear. Nylander also observed that flexural shear decreases the torsional strength and consequently proposed a linear interaction between shear and torsion of the form:

$$\frac{T}{T_o} + \frac{V}{V_o} = 1$$

T/T_o = ratio of ultimate torque for combined torsion and shear to ultimate pure torsion

V/V_o = ratio of ultimate shear for combined torsion and shear to ultimate shear for zero torsion.

Despite the controversial assumption of plasticity in concrete subjected to torsional shear stress the form is important because it was obtained later by the "skew bending" elastic approach. For the problem of torsion combined with bending, Martin, in 1971, produced an alternative form of the interaction solution, with different definitions of terms, related to the concrete strength:

$$\left(\frac{T_1}{T_{sul}}\right)^2 + \left(\frac{M_1}{M_{sul}}\right)^2 = 1 \qquad (2.2.2)$$

where $M_{sul} = A\ell f\ell y\ \ell a y$

$T_{sul} = M_{sul}\ \sqrt{\lambda_s}$

$\lambda_s = 3$ for Huber-Von Mise-Hencky criterion,

Martin considered this form as one of mode 1 failure based on yielding of the steel. Equation 2.2.2 involved the torsional lever arm. The theoretical solution on this case was also related to the case of failure in mode 1 controlled by failure of the

concrete. In the latter case, since the steel had been assumed not to reach yield, the value of the depth of compression zone was determined using an elastic analysis.

This elastic analysis was intended for ultimate strength and based on a "skew bending" failure mechanism. The depth of the compression zone was determined theoretically.

Cowan's simplified failure criterion was employed to combine the shear and bending stresses in concrete. The equilibrium of both moments and forces was satisfied about the skew axis. The theoretical procedure includes the compatibility of strains over the depth of the section and a linear stress-strain relationship of steel and concrete. To balance the shear stresses in the compression zone, Martin assumed a dowel force to act at right angles to the steel in tension.

The analysis produced the general interaction equation:

$$\left(\frac{T_1}{T_{cul}}\right)^2 + \left(\frac{2M_1}{M_{cul}}\right)^2 - \left(\frac{3M_1}{M_{cul}}\right) = 1 \qquad (2.2.3)$$

where $T_{cul} = \frac{1 - \sin \beta}{2} \; d \; d_n \; \ell a_1 \; f'_c$

$M_{cul} = km \; b \; d_n \; \ell a_1 \; f'_c$

The solution is for mode 1 based on failure of the concrete. It compared very well with the available test results, though very limited. Nonetheless, the theoretical solution for mode 1 is considered important because it is related to the general case of torsion and bending of rectangular cross section, as will be seen in reviewing prestressed members. In mode 2 of failure the torsional strength is governed by the tensile strength of concrete. Thus the theoretical solution is related to the case of plain concrete members where it has already been discussed.

Yielding Theories of Torsional Strength in Concrete Members Containing both Longitudinal and Transverse Steels

From Cowan's review of the literature (see ref.6), it can be concluded that in 1922 Graf and Morsch had tested reinforced sections. They observed that longitudinal bars alone and transverse steel alone are of little value, concluding that stirrups cannot take the horizontal shear (due to torsion). Consequently, a state of internal equilibrium must be considered in which the stirrups are stressed in tension. These test results were analysed by Rausch in 1929 , who gave the first theoretical solution for this type of member.

Rausch employed the space truss analogy, originally proposed by Morsch for shear strength analysis, to replace the concrete with compression struts and the steel reinforcement with tension bars. Rausch's analytical model was a space truss with constant inclinations of the diagonals. The angle of the diagonals with respect to the beam axis was taken to be 45^{o} for each face. This led directly to impose the requirement for a ratio of equal trnasverse to longitudinal steel in volume. By considering the equilibrium condition alone, the steel stresses were assumed at yielding and of equal values in both transverse and longitudinal directions. The solution was of the form:

$$T_s = \frac{2 A_s f_{sy}}{S} b'd' \qquad (3.1a)$$

This expression was supplemented by an equation that requires equal amount of longitudinal steel in the same volume:

$$T_s = \frac{A_l f_{ly} b'd'}{2(b' + d')} \qquad (3.1b)$$

$$\therefore \qquad \overline{A\ell} = \frac{b' + d'}{S} (2\ A_s) \qquad ; \qquad f\ell_y = f_{sy}$$

in which $A\ell$ is the total steel area in the longitudinal direction.

The form of equation 3.1a for torsional strength T_s, is analogous to the expression for V_s in the original truss analogy as developed by Morsch (6):

$$V_s = 2\ d' \frac{A_s\ f_{sy}}{S'} \tag{3.2}$$

In the classical shear analysis of Morsch, using the truss analogy, the compatibility conditions were not necessarily fulfilled and no stiffness ratio between the concrete struts and the steel bars was considered. While Morsch had assumed that the web of the beam will take all the shear force V_s, the equation 3.2 did not account for the influence of the web breadth, b, and was independent of b'. The method was intended to analyse cracked sections subject to shear force.

Rausch's solution, contrary to St. Venant's theory, was based on the circular section theory of torsion. Rausch obtained therefore for the rectangular section a maximum stress at the corners of the transverse steel where the elastic stress was, according to St. Venant, negligibly small. In 1934, Andersen (26) on the basis of his tests on square sections, produced a theoretical solution which was better related to the stress distribution of a rectangular section. Thus he assumed zero stress at the corners of a rectangle and a maximum stress at the middle of the sides of the transverse steel.

Andersen assumed, therefore, that only the bars at the centre of the wider face reached yield stress. Later in 1937, Andersen (26) showed also that the strength of the reinforced concrete

section, contrary to Rausch's theory, is approximately:

$$T = T_c + T_s$$

in which T_c is the strength of the plain concrete, and T_s is the additional strength of the reinforcement.

In contrast to the elastic theories, Marshall and Temb (16) in 1941 proposed the use of the plastic theory. They tested 24 rectangular and T-beams containing longitudinal steel and stirrups. The steel stress at failure of their test specimens was nowhere above the yield point. The solution was basically empirical and of the form:

$$T_u = T_{cu} + T_{su}$$

in which T_u = ultimate torque of a reinforced concrete section.

T_{cu} = strength of corresponding plain concrete section.

T_{su} = strength contribution of reinforcement.

This solution also required equal longitudinal steel and ties, within rather limited percentages of steel, established empirically.

In 1950, Cowan (41) attempted a precise elastic solution by equating the strain energy stored in the beam to the external work done by the applied twisting moment. It was considered that the strength is that for plain concrete plus the strength for the stirrups.

$$T = T_c + T_s$$

in which, T_c = St. Venant's elastic strength for plain concrete.

To evaluate T_s, Cowan, adopting St. Venant's distribution of stress, assumed (like Andersen) a parabolic variation of strain in the web steel with a zero strain at the corners and maximum strain at the centre. Then,

$$T_s = 1.6 \frac{A_s f_{sy} b'd'}{S} \qquad (3.3)$$

This proved to be 20% different from Rausch's equation 3.1a and closer to Andersen's. However, in summing up the total strain energy, Cowan assumed the torsional resistance to be equally divided between the tensile strain energy in the steel plus the compressive strain energy in the concrete. Implying that concrete has no tensile strength.

Later, in 1953, Cowan ([21]), pointed out that "the inelastic deformation in the concrete does not immediately produce plastic strains in the steel, since the yield strain of the steel is at least twice as much as the ultimate tensile strain of concrete. The steel, therefore, remains elastic almost up to the point of failure; the beam may sometimes fail before the steel yields". Thus, Cowan suggested his solution to be on the safe side at ultimate strength in the following form:

$$T_u = T_{cu} + T_s$$

in which T_s being equation 3.3 and

T_{cu} = Nadai's plastic strength for plain concrete, equation 1.3.

This form is considered important, since it has been developed later by an approach based on the skew bending theory.

All these theories assumed helical twisting of beams up to failure and the torque is carried partly by the concrete and partly by the steel. This expressed the equilibrium conditions but did not necessarily ensure the compatibility conditions, while Rausch assumed that the transverse steel takes the full amount of the principal tension, implying that $T_c = 0$, Andersen and Cowan assumed that the torque is shared equally by the concrete and steel.

1.3 PRESTRESSED CONCRETE MEMBERS WITH NO TRANSVERSE STEEL

In the search for methods of strengthening concrete subjected to torsion, many investigators have studied the effect of adding transverse and/or longitudinal steel to plain concrete. It can be concluded from the previous part of this review, that the investigators agreed that using longitudinal steel alone had little effect. The combination of longitudinal and transverse steel, however, considerably improved the effectiveness of including steel. Among the early investigators, Nylander, in 1945 was the first to suggest the possibility of using the prestressing force as a method to increase the torsional strength of concrete.

In 1952, Cowan and Armstrong ([28]) set out to investigate the effect of prestressing on the torque capacity. They tested nine rectangular beams without web steel, post-tensioned by four unbonded bars. Prestressing increased the torsional strength of concrete, and this was confirmed by the observations of Nylander. It is interesting to note that Cowan and Armstrong and Nylander studied the problem as a part of an investigation into torsion combined with bending, where the concrete was subjected to a state of biaxial stress. Their conclusion from the tests was that for prestressed members under relatively high torsion, the cracking moment coincided with the ultimate torsional strength. With higher moment/torque ratios, the ultimate strength was greater than that corresponding to the formation of the first crack.

For predicting the cracking torsional and bending moments, Cowan in 1953 produced a general non-dimensional theoretical solution for members with no stirrups. He used the maximum principal stress theory, and assuming a uniform prestressing. The general

form of the interaction equation was identical to that for plain concrete:

$$(\frac{T_1}{T_o})^2 + (\frac{M}{M_o}) = 1$$

The values of T_o and M_o were calculated in the same manner as for plain concrete but with the effect of prestressing being incorporated, so that both terms at the first crack were increased. Although this theory was also applicable for the ultimate strength for mode 2, it was not intended for beams which show extensive cracking before failure in mode 1.

In 1957 Humphreys (29), carried out an extensive investigation under pure torsion, and tested 94 post-tensioned rectangular members of varying width to depth ratio. 90 beams were uniformly prestressed by an unbonded central bar, and the others were eccentrically pre-tensioned. The prestressing force varied between 0 to $0.75f'_c$. His conclusion was that the torsional strength might be increased by prestressing well beyond the strength of plain concrete, and reported an increase of 250 per cent. He used the classical criterion of the principal tensile stress modified by the prestress to predict the cracking moments. This was achieved by increasing the principal tensile strength of concrete as a function of $\sqrt{1 + \frac{Pc_2}{ft}}$; where ft is the tensile strength of concrete. This was similar in form to the factor derived by Cowan in mode 2.

Humphrey's test results seemed to agree reasonably with those predicted by this method but modified by empirical constants derived from the same test results.

In 1960, Gardner (30) reported the first investigation on non-rectangular prestressed beams . It included tests on 16

eccentrically prestressed concrete I-beams, subjected to combined bending and torsion. The beams were tested in a range varying from pure torsion to a moment/torque ratio = 1.

To predict the cracking moments, Gardner used St. Venant's elastic theory, taking ft = 0.707 f_r. For assessing the ultimate strength, however, he assumed full plasticity. This assumption of a uniform distribution of shear stress compared better with the experimental torque than the elastic theory.

In 1960 also, Zia[40] reported tests on rectangular, T and I-beams. He modified the Cowan simplified criterion by considering a closer approximation of Mohr's generalised internal friction theory. The modified criterion like the original one clearly indicated that up to a certain limit, prestressing may result in a substantial increase of the apparent strength of concrete.

Zia also observed for the flanged sections, a behaviour different from the rectangular ones. After diagonal cracking in the webs, the flanges tended to arrest the development of the crack, resulting in a significant increase in the ultimate strength. In all the rectangular beams where no stirrups were provided, failure was sudden and took place at the cracking load.

Zia was also the first to examine the effect of transverse steel on the prestressed concrete beams subjected to pure torsion, and will be reviewed in the next section.

In 1962, Swamy (31) undertook an investigation into combined bending and torsion using prestressed hollow box beams. He tested 20 beams post-tensioned with uniform distribution of prestress. Four of the beams included stirrups. He found that a large increase in the torsional strength of the beams occurred due to prestressing. Swamy attributed this to the effect of pre-compression which reduced

the principal tensile stress due to torsional shear and producing a sudden failure. He also reported an increased torsional strength when a small amount of stirrups was provided.

Swamy, however, did not differentiate between the increases due to stirrups and those due to prestressing, but was certain that adding stirrups would lessen the violence of failure. He showed that his experimental results were not satisfactorily predicted by the classic failure theories. No explanation was offered to explain the distinct differences shown by the tests between the bending failure and the primary torsion failure, and the transition from crushing to cleavage. His conclusion was that "the mechanism of failure of concrete was complex and not well defined for many stress combinations". Despite these difficulties, Swamy showed that if plastic behaviour is assumed in concrete, then the interaction curve between bending and torsion can be approximated by

$$(\frac{T}{T_o})^2 + (\frac{M}{M_o})^2 = 1$$

Although this circular curve agreed with the lower bound of his test results, the upper bound was greater by about 14%. It shows a reduction of torsional strength due to bending.

Reeves (32) from tests on 42 T-beams with no stirrups subjected to torsion and bending, showed a substantial increase in torque due to bending. His tests were carried out with an eccentric prestressing force and the prestress varied from zero at the top to 13.79 N/mm^2 at the bottom fibre. He compared the elastic and plastic theories in an attempt to derive an expression for the pure torque capacity. From a statistical comparison he favoured using the St. Venant's theory with the torsional shear stress taken equal to the concrete modulus of rupture.

To represent the behaviour of his test beams, he proposed an empirical interaction curve in form of a polynomial. This was based on a regression analysis to fit the test results. The parabolic shape is considered to be important and shows the same trend observed by Nylander and Cowan for concrete members with longitudinal steel only, and reinforced concrete members respectively.

In 1967 Hsu (33) analysed the test results of Humphreys, Nylander, Cowan and Zia. His conclusion, like Reeves', was that neither the plastic nor the elastic stress criterion agreed with the experimental results. Hsu had already attempted to clarify the torsional failure mechanism of plain concrete members. He found that torsional failure for uniformly prestressed rectangular members with no stirrups was also due to bending around a skew axis, identifying mode 2 and 3 of failure. He proposed, therefore, a failure criterion originally developed for plain concrete with the effect of prestressing bending incorporated. This approach resulted in an expression of the form:

$$T_u = (T_{up})\sqrt{1 + 10\,\frac{P_{c2}}{f'_c}}$$

The factor accounting for the effect of prestress as given by Hsu is a function of $\frac{P_{c2}}{f'_c}$ and involves empirical constants. It compared favourably with the experimental results from tests under pure torsion.

Cowan in 1953 derived a similar formula from the principal tensile stress failure criterion, assuming an elastic-plastic stress distribution. Hsu's expression which is basically elastic shows that prestressing can substantially increase the pure torsional capacity of a member (in mode 2 of failure).

Employing Cowan's simplified criterion, Evans and Khalil (34) presented in 1970 a theoretical approach for the mode 1 of failure in concrete members subjected to bending and torsion. The approach was intended for cracking and ultimate strength analysis. The ultimate torsion theory was based on the assumption that after cracking, torque is only resisted by the compression zone, and implying that the steel does not take any torsion.

However, they computed the depth of the compression zone as if it were due to pure bending, and implied that torsion had no significant effect on the depth of compression zone. This is in contradiction with the theoretical notion introduced years earlier by Lessig that the depth of the compressive zone in concrete members reduces as the M/T ratios reduces changing the mode of failure from mode 1 to mode 2.

To substantiate their theory, Evans and Khalil (34) tested 12 beams with eccentric prestress whilst seven of their beams had uniform prestress. The ratios of M/T varied between 0.8 and 12.7. Their observation confirmed again that beams failed abruptly at the formation of the first crack (mode 2) under high torsion effect, whilst other beams sustained additional torque after the first cracking (mode 1). Their conclusion was that "it is difficult to derive one experssion to predict the ultimate moments of all beams under any combination of bending moment and twisting moment.' This conclusion is the same as Swamy's who also attempted to make use of Cowan's criterion in mode 1.

The approach of Evans et al is considered important because it is based on the strength of compressive zone and attempted to define the depth from equilibrium of moments and forces. In the "crushing mode", the plastic distribution was also related to the depth of the compressive zone.

In 1972 Wainwright (35) tested 17 beams post-tensioned with one unbonded prestressing tendon, giving an eccentric distribution of prestress. The range of M/T ratios varied between 0.3 and 17.8. He identified mode 1 and 2 of failure. He also detected a mode 3 of failure under a low M/T ratios and when the prestress at the top of the section was low or even tensile (35). Martin and Wainwright (36) in 1973 analysed the results and developed a rational approach for beams with no transverse steel subjected to bending and torsion. The theory covered the three observed modes of failure and compared favourably with 125 test results. By setting the prestressing force to zero in mode 1, the basic expression retains the form of equation (2.2.3) developed by Martin for members containing longitudinal steel only. Mode 2 is a rationally achieved solution with the effect of prestress incorporated. The latter being zero the equation takes the form of equation 1.6 for plain concrete members.

In 1974, Woodhead and McMullen (37) published a report and theory for 26 test beams with and without stirrups, subjected to combined torsion, bending and shear. They also proposed interactive curves and presented theoretical analyses. Their work will be reviewed in the next section.

In 1976 Cooper (38) tested 32 beams under bending, torsion and shear. The ratio of M/T varied from 0.1 to 18.9. He observed modes 1 and 2 of failure but none of his beams failed in mode 3. In 1977, Cooper and Martin (39) analysed the results in an attempt to improve on Woodhead et al approach. They tried to extend a theoretical precedure.to include the effect of shear force on the interaction of bending and torsion. However, in mode 1, the shear stresses are assumed to be additive and equal to the maximum shear

stress in concrete. The theory compared with 184 test results, showed a good agreement. The theory is shown to apply to both conditions where the prestressing steel is free to move in the duct, and where the steel is bonded.

For interaction surface, Martin and Cooper preferred to use a series of cross sections parallel to the M/T plane for different values of shear, and proposed a theoretical moment/torque/shear interaction surface. In the paper the theory was substantiated only by Cooper's test results in regions of low shear force.

1.4 PRESTRESSED CONCRETE MEMBERS WITH STIRRUPS

In 1960 Zia (40) was the first to investigate experimentally and theoretically the effect of including transverse steel in prestressed concrete members. Commencing with the case of pure torsion, he tested 68 specimens of plain, reinforced, and prestressed concrete. The prestressed tests on beams with no stirrups have been reviewed in the previous section. Zia incorporated stirrups in six rectangular beams of cross section 101.6 mm × 304.8 mm with 50.8 mm × 254 mm stirrups of 32.26 mm^2 cross-sectional area. Some beams were uniformly pretensioned while others were eccentrically prestressed. His conclusion was that transverse steel increased the torsional strength and provided a considerable ductility by delaying failure.

Zia followed the traditional approach of superposition in analysing the concrete members with transverse steel:

$$T_u = T_c + T_s$$

where T_c is the cracking moment of the member computed by using St. Venant's elastic torsion theory with the shear torsional stress being based on Zia's Modified Criterion.

T_s = the the moment resisted by the transverse steel

$$T_s = 1.6 \times \frac{A_s f_{sy} b'd'}{S}$$

Zia determined T_s by using Cowan's equation (21) assuming the steel to reach yielding value. This tends to conflict with the analysis of a rectangular section on the basis of St. Venant's elastic, homogeneous and continuous section. Zia noticed that from the torque/angle of twist experimental curves of his test beams

with stirrups, which indicated that the stirrups yielded prior to failure of the test beams. (Zia did not use any steel strain gauges to substantiate this). Consequently, he computed the resisting moment of the web reinforcement based on yielding and as a constant quantity added simply to that part of moment resisted by concrete. The latter was in some cases, three times greater than T_s. This is obviously consistent with the basic assumption of Cowan that torque is shared equally by the concrete and steel. Zia's approach is furthermore contradicted by his own observation of "under-reinforcement" in transverse steel, where the torsional resistance would be expected to be entirely dependent on the transverse steel and the strength a function of the reinforcement factor, $(A_s f_{sy} b'd'/S)$. Zia's equation failed to predict satisfactorily the strength of ordinary reinforced members, and this was particularly evident in the case of his I-beams.

Zia's empirical equation is however important in its form which implies that a theoretical expression must also follow the same line. The complete theoretical solution has proved to be more difficult and needed more tests to consider conditions where transverse steel does not yield or its yield is governed by the concrete. This required a better understanding of the torsional shear distribution in concrete and establishing the relevant failure criterion for concrete under combined stresses. Zia contributed to this and his modification of Cowan's Simplified Criterion has been reviewed.

Zia considered the cleavage type of failure which is characteristic of failure under low M/T ratios (mode 2) and observation of his own tests on prestressed beams subjected to pure torsion. Cowan presented his criterion of failure in crushing as a sequel of

investigating members loaded in higher M/T ratios (mode 1). No theoretical explaination was given for the transition from one mode of failure to the other. This required not only modifying the criteria of failure of concrete but also understanding specifically the mechanism of failure of concrete members subjected to combined loading. From her experimental work on reinforced concrete under combined torsion and bending, Lessig (42) changed radically the concept of the failure on a helical surface. She identified modes 1 and 2 based on the mechanism of failure around a skew bending axis. Lessig did not however conduct any tests on prestressed concrete beams.

In 1965 Murashkin investigated the influence of prestress on the torsional capacity. From his work on a few unstressed and prestressed beams, he came to the conclusion that if the tensile steel approached yielding then the prestressing force would have no influence on the ultimate capacity of the beams failing in mode 1. The prestressing force however, has a pronounced effect in increasing the cracking resistance. Thus if the failure occurs due to cracking (mode 2), the ultimate strength of the beam will be higher. One interesting feature of this work is that it was carried out under approximately constant M/T ratio of 2.5. The number of the test beams was limited to five beams of 170 × 210 mm cross section, and prestressed by four tendons giving concentric or eccentric prestress.

In 1966 Okada et al (44) published more test results. They tested six post-tensioned eccentric beams of 100 × 200 mm cross section containing both 54 × 154 stirrups of 6 mm diameter and four bars of 13 mm diameter as longitudinal reinforcement. The M/T ratios varied between 0.4 and 2.4. They followed Cowan's approach

and used a theory based on the superposition hypothesis in the form of;

$$T = T_c + T_s$$

where T_c = the visco-elastic limit for prestressed beams

$$T_s = 1.6 \frac{A_s f_{sy} b'd'}{S}$$

Since the concept of superposition was the fundamental assumption of almost all the researchers in their analyses of sections with transverse steel, it needed further examination. Hsu (45) carried out a series of tests in pure torsion using solid and hollow rectangular sections. The beams were not prestressed. The overall dimensions and reinforcement being the same, the test results indicated that the ultimate torque of the hollow sections was comparable to that of the solid sections though the latter had higher cracking strength, as was expected. His conclusion was that the core action is not an acceptable explanation of the torque resistance attributed to concrete, T_c. The same conclusion was reached independently by Lampert and Thurlimann in 1968 (46) but both investigations used non-prestressed members.

Hsu and Lampert et al gave two apparently different theoretical explainations to the same experimental observation. For Lampert it seemed that the ultimate strength corresponds to the yield moment of a space truss. This is a restoration of the basic premises of Rausch (6) who assumed forty years earlier that the transverse steel would take the full amount of the principal tensile stress, implying that $T_c = 0$. Lampert argued therefore, later in 1971 (11) that the prestressed member can be treated as a non-stressed member by using the truss analogy for predicting the

ultimate torque. This was based on the assumption of yielding and the necessary equation for the truss was derived, subject to torsion and bending.

On the other hand, Hsu drew the conclusion that T_c is the shear resistance of the compressive zone of concrete when skewed bending takes place. Hsu, however, did not attempt to define this compression zone theoretically. Instead, he followed the apparently easier path of extending empirically his existing reinforced concrete theory by incorporating the effect of prestressing.

Hsu and Kemp in 1969 (47) showed that the effect of prestressing is to increase the contribution of the concrete to the ultimate torsional strength, while the contribution of the transverse steel remains unchanged. Thus, they proposed again a formula of the form:

$$T = T_c + T_s$$

where $$T_c = \frac{x^2 y}{3}\ 2.4\ \sqrt{f'_c}\ \left(2.5\sqrt{1 + 10\ \frac{\sigma}{f'_c}} - 1.5\right)$$

$$T_s = \left(0.66 + 0.33\ \frac{y_1}{x_1}\right)\ \frac{x_1 y_1 A_s f_{sy}}{S}$$

From the form of the equation it is clear that the addition of transverse steel above a certain minimum value causes a linear increase in the torsional resistance in a manner similar to reinforced concrete beams. The expression has in fact the same form as the one originally observed by Hsu for concrete beams.

To ensure yielding, Hsu and Kemp imposed an upper limit empirically on transverse steel to avoid a compression failure. They also limited the prestress independently according to the empirical provision of $0.45\ f'_c$. No comparison was made with available test

results, though the formulation of the original expression and its successive extensions (for reinforced concrete and uniformly prestressed members with no stirrups), was largely dependent on experimental data of plain, reinforced and plain web prestressed members.

In 1969 Bishara (10) also reported more tests and proposed a corresponding theoretical expression. He tested 24 pre-tensioned beams, eight of which were of 101.6 mm × 304.8 mm cross section containing 44.45 mm × 247.65 mm stirrups of 6.35 mm in diameter. The beams had longitudinal shear reinforcement consisting of four bars of the same diameter. Both eccentric and uniform prestress distributions were used. M/T varied between (2.7) and (0.7). M/Vh ratio was (2.75). At the failure of the test beams, ultimate load was on average 15% higher than the cracking loading. To account for the excessive strength, Bishara assumed plasticity in concrete under torsion. Otherwise, he followed the line of Zia's approach to account for the web steel. For pure torsional capacity,

$$T = T_c + T_s$$

where $$T_c = 10\, k_p\, V_p \sqrt{f'_c} + 12\, f_{av}$$

in which f_{av} = average effective prestress

V_p = volume of plasticity membrane on section having unit slope

$T_s = 1.6\, x_1 y_1\, A_s f_{sy}/S$

Plastic distribution was assumed for computing T_c, which was considered by Zia to be the cracking moment of plain concrete, and it included an empirical factor of plasticity $k_p = 0.85$ depending on the concrete strength f'_c. The approach was essentially empirical and produced polynomial interaction equations of the form:

$$\frac{T_u}{T_{uo}} = 1.0 + 2.3 \left(\frac{M_u}{M_{uo}}\right) - 3.3 \left(\frac{M_u}{M_{uo}}\right)^2$$

$$\frac{T_u}{T_{uo}} = 1.0 + 2.3 \left(\frac{V_u}{V_{uo}}\right) - 3.3 \left(\frac{V_u}{V_{uo}}\right)^2$$

for rectangular beams subject to a constant M/V ratio.

The equations were compared with Bishara's own test results. This is a similar method to the one produced by Reeves (32) earlier. Both tried to find the best polynomial fit with their own test results and are therefore not necessarily applicable to other tests and conditions of loading from other investigators. Bishara's prediction was that: "using classic equilibrium equations with well defined rupture criterion may lead in the future to more reliable expression for predicting the ultimate strength."

For his PhD thesis in 1970, Gangarao (49) conducted tests of combined torsion and bending on 40 beams, the cross sections were 152.4 mm x 304.8 mm containing stirrups of 6.35 mm in diameter with and without longitudinal mild steel. M/T varied between 0.55 and 8.35.

In an attempt to overcome some of the theoretical difficulties faced by previous researchers, Gangarao and Zia (50) analysed the results of the former's tests. They developed a skewed bending theory to predict the failure in torsional mode and in bending mode. In mode 1 the analysis was based on yielding of either stirrups or the longitudinal prestressing steel. The analysis was claimed to be applicable also to reinforced concrete members when these are treated as a special case by setting the prestressing force to zero. They, however, proposed a square and tri-linear empirical interaction curve for prestressed rectangular beams with and without mild reinforcement..

Evans and Khalil in 1970 reported more tests under torsion and bending. Their tests were on 12 beams eccentrically prestressed by post-tensioning with four 7 mm unbonded wires. Cross sections were 127 mm × 203 mm containing stirrups of 6.35 mm in diameter and 63.5 mm or 101 mm in spacing. The M/T varied between 0.8 and 12.7. From comparing these tests with others on beams with no stirrups, they concluded that the use of web reinforcement made failure more progressive. They noticed that stirrups increased the torsional capacity of a member but there was a limiting percentage of web reinforcement beyond which the increase in torque was small. Under high M/T ratios the increase in percentage of stirrups had no apparent effect on the torsional strength. Their conclusion was that the increase in torsional strength due to prestressing is much greater than that due to web reinforcement.

Further tests on members containing stirrups and subjected to torsion, bending and shear were reported by Mukherjee and Warwaruk in 1971 (9). The M:T ratios varied between 0.23 and 13.6, whilst the M:Vh variation was between 1.7 and 6.3. The cross sections were 152 mm x 305mm prestressed by pre-tensioning of 4 - No. 5/16 seven wire strands with either zero or 50.8 eccentricities. The tests of combined loading included 22 beams containing both stirrups and longitudinal non-stressed reinforcement. The effects of torsion combined with bending only were investigated also by testing 20 beams. A further 4 beams were tested subject to pure torsion.

Mukherjee and Warwaruk noted that a pure torsional strength formula was not established. As for the interaction problem, their conclusion was that neither the elastic nor the plastic theory accounted for the beneficial effect of bending moment on the torsional resistance of prestressed beams. From a comparison of their test results with the polynomial espressions as proposed by Reeves and Bishara, Mukherjee et al favoured a second degree polynomial to express the interaction in their test results. The variation of prestress and eccentricity was incorporated in the form of a non-dimensional coefficient $= (2\frac{pc2}{fc1} + \frac{e}{d})$. The solution for torsional and bending was, therefore, in the following form:

$$\frac{Tu}{Tuo} - (\text{Coefficient})\frac{Mu}{Muo} + \left(\frac{Mu}{Muo}\right)^2 = 1.$$

When: $Tu/Tuo > (2\frac{pc2}{fc} + \frac{e}{d})$

Alternatively, for the interaction of torsion with bending and shear, the following form was presented:-

$$\frac{Tu}{Tuo} - (\text{Coefficient})\frac{Mu}{Muo} + \left(\frac{Mu}{Muo}\right)^2 + \left[1 - \left(\frac{Mu}{Muo}\right)^2\right]\frac{Vu}{Vuo} =$$

From empirical considerations a limit was set on this equation in the form of:-

$$(Tu/Tuo)/(Mu/Muo) \quad \left(2\frac{Pc2}{fc} + \frac{e}{d}\right).$$

The pure shear strength of a beam, Vuo, was also estimated on an empirical basis.

These forms of the interaction solution were based on a statistical regression analysis of the test results and were not suitable for a graphical comparison. Mukherjee and Warwaruk concluded that the variation of web reinforcement did not affect the non-dimensional interaction forms if a "minimum" amount of stirrups was provided and "over-reinforcement" was avoided. These boundary conditions, however, were not clearly defined.

In 1973, McMullen and Woodhead (37) published the results of their experimental study of 18 beams of 152mm x 305mm cross-sections, eccentrically prestressed by pre-tensioning of 6-12.7mm dia. 7 wire strands. 15 beams contained stirrups. The M/T and M/Vh ratios varied between 1.8 and 25.8, and 5.3 and 6.4 respectively. They found that the initial torsional stiffness was independent of the prestressing force but increased after cracking as the prestressing force increased, and decreased as the T/Vb ratios decreased. This latter effect was also observed in other investigations (9,13).

One interesting feature of McMullen and Woodhead's experimental programme was to examine the effect of varying the prestressing force on the interaction of torsion, bending and shear. For beams with no stirrups and of lower average level of prestress (:pc2=0,1fc), the torsional strength did not reduce below the value for pure

torsion until the values of M/Mu and V/Vu ratios exceeded 25 per cent in combined loading. For the beams of higher prestressing (:pc2 = 0.2 f$\acute{c}$) and containing stirrups, the torsional capacity increased above pure torsion with a small amount of flexural moment and shear. The combined bending strength could be as high as Muo in pure bending,even when a torque equal to 30 per cent of Tuo was simultaneously applied.

McMullen and Woodhead analysed these test results, and for beams with no stirrups they proposed interaction curves of the form:

$$\frac{Mu}{Muo} + \frac{Tu}{Tuo} = 1$$

$$\frac{Vu}{Vuo} + \left[\frac{Tu}{Tuo}\right]^2 = 1$$

Alternatively, for beams with stirrups the proposed curves were of the form:

$$\left[\frac{Mu}{Muo}\right]^2 + \left[\frac{Tu}{Tuo}\right]^2 = 1$$

$$\left[\frac{Vu}{Vuo}\right]^2 + \left[\frac{Tu}{Tuo}\right]^2 = 1$$

McMullen and Woodhead, like Mukherjee etal. (9), found that "pure" shear strength, Vuo, could not be determined experimentally in absence of bending. Consequently, they defined Vuo, in their curves as the shear force acting at failure , of a beam subjected to bending and shear alone. It is noted that although they preferred to use two-dimensional interaction curves for torsion-

bending and torsion-shear, their torsion-shear equations cannot be compared to equations proposed by other investigators because different definitions for the pure shear strength, Vuo, are adopted.

In a subsequent paper (51), Woodhead etal. elaborated on a theoretical procedure for analysing prestressed and unstressed concrete members of differing sections. This analysis for the ultimate strength was based on the skew bending theory and was shown to give good agreement with a large number of available test results. It was claimed to cover over-reinforced and partially under-reinforced sections. Their theory is given a special place in a next chapter.

Henry and Zia (13) published in 1974 the results of extensive tests on 32 beams, all of which contained trasverse steel. The cross-sections were 152mm x 305mm prestressed by pre-tensioning 5 or 4 strands of 9.5mm diameter giving eccentric or concentric distribution of prestress. The M/T and M/Vh ratios varied respectively from (0.41) to (13.4) and from (0.98) to (5.11). The stirrups were 6.3mm in diameter and spaced at 7.6cm, giving a web volume percentage of about 0.573. In addition the cross-sections were longitudinally reinforced by 4-12.6mm bars located at the corners. Their study showed that the initial torsional stiffness, before cracking occurred, was nearly independent of the prestressing force (including eccentricity). They reported that the cracking torque increased slightly, with a small increase of eccentricity and with a small increase in the prestressing force, but was significantly affected by the M/T ratio. Henry et al. also found that the torsional stiffness increased after cracking with increasing prestress and

decreased as the T/Vb ratio decreased. This was confirmed by the previous observations of McMullen and Woodhead and Warwaruk.

From a comparison with other test results of previous investigators (49, 9, 10), Henry and Zia attempted to express the interaction between torque and bending in a nondimensional interaction diagram of the form:

$$\left[\frac{Tu}{Tuo}\right]^2 + \left[\frac{Mu}{Muo}\right]^2 = 1$$

This equation is similar to those produced earlier by Nylander(20) and Mukherjee and Warwaruk(9). On the other hand it is apparently different from the circular interaction curve as proposed by McMullen and Woodhead (37) who also adopted a different definition for Vuo. Henry and Zia, however, interpreted Vuo as the theoretical ultimate shear in absence of torsion. Their conclusion was that in the presence of a shear force combined with torsion and bending, the behaviour and the ultimate strength of the test beams were in agreement with the skewed bending theory. Consequently two modes of failure were recognised for analysis. The transition point from the bending mode to the torsion mode of failure was not well-defined, but the ratio of M/T= 4.5 was, however suggested as critical.

In 1976, McGee and Zia (52) reported tests on a total of 45 beams subjected to torsion, shear and bending. Sixteen of these beams had web reinforcement of a low percentage and made of black annealed wire of 4mm diameter. Their test beams were designed to assess the minimum amount of reinforcement required under combined

loading. The cross-sections were 152mm x 305mm, pretensioned with six or five 7-wire strands, giving uniform or eccentric prestress. All the beams containing stirrups were, however, eccentrically prestressed by two strands of 9.5mm diameter and three strands of 12.7mm diameter. The (M/T) ratios varied between 0.64 and 9.o9 and (2T/Vb) ratios between 1.45 and 8.94.

Using the maximum principal stress theory of failure, McGee and Zia - developed theoretical interaction curves to predict the cracking loads. The elastic theory was applied assuming a limiting tensile strength for concrete taken equal to $7.5\sqrt{f'c}$ psi They reached the conclusion that the web reinforcement provided in their investigation was not adequate to develop the required postcracking ductility and strength.

It can be seen from this survey that an increase in the prestressing force increases the torsional cracking resistance and the ultimate strength in combined loading. This is particularly evident when the T/Vb ratio is high. The magnitude of the prestressing force significantly affects the shape of the interaction diagrams for combined loading, particularly in the region of low M/T ratios. The many investigators who worked on the problem appreciated this effect, but their main concern was to account for the effect of the stirrups separately. This necessitates additional experimental work to investigate single variables such as the effect of varying the prestressing force, longitudinal steel area, the transverse steel size and the spacing of stirrups. One important parameter, beside the member size effect, is to

study the effect of varying the concrete strength.

Table 1.1 shows a general outline of previous experimental investigations into torsion of rectangular prestressed beams with stirrups. It is clear from this synopsis that until 1969 no test was reported on such members subjected to torsion combined with bending moment and shear force. In 1969, Bishara (10) reported tests on eight pretensioned rectangular beams in combined loading. The seventies, however, witnessed growing prestressed concrete research in the fields of torsion involving pure torsion and torsion combined with bending and shear. With the exception of the works of Okada(44) and Evans et al.(34) on post-tensioned beams, pretensioning type of prestress was generally used. Although post-tensioned beams are encountered in general practice and have also the advantage of enabling the research worker to measure the prestress, directly; there are no published experimental data on such members containing stirrups and tested in combined torsion, bending and shear.

Torsional theories are still too empirical, and more rational approaches are needed. It is, therefore, important in addition to accumulate more test results, to develop basic research in the fields of torsional, flexural and shear strengths.

To resist torsion, the design engineer usually added closed stirrups to tie up the corners of the concrete member. Prestressing could provide an attractive alternative but little is known about when a prestressed beam is under-reinforced for torsion and no definite limits are theoretically established for over-reinforcement either. The minimum requirements of stirrups

TABLE 1.1 PREVIOUS TESTS ON RECTANGULAR PRESTRESSED CONCRETE BEAMS WITH STIRRUPS IN TORSION, BENDING AND SHEAR

INVESTIGATOR	b x h (mm x mm)	S (mm)	PRESTRESS		TORSION ONLY	TORSION & BENDING ONLY	TORSION BENDING & SHEAR	TOTAL
			Type	Distribution				
ZIA (40) (1961)	101.6 x 304.8	101.6	PRE.	U. & E.	6	-	-	6
MURASHKIN (43) (1965)	170 x 250	100	?	U. & E.	-	5	-	5
OKADA (44) (1966)	100 x 200	100	POST.	U.	2	6	-	8
BISHARA (10) (1969)	101.6 x 304.8	101.6	PRE.	U. & E.	-	-	8	8
GANGARAO (50) (1970)	152.4 x 304.8	50.8,76.2 & 101.6	PRE.	U. & E.	7	33	-	40
KHALIL (34) (1970)	127 x 203	63.5 & 101.6	POST.	E.	2	12	-	14
MUKHERJEE (9) (1971)	152.4 x 304.8	50.8 & 76.2	PRE.	U. & E.	4	20	22	46
McMULLEN (37) (1973)	152 x 305	51, 101 & 254	PRE.	E.	2	-	15	17
HENRY (13) (1974)	152 x 305	76	PRE.	U. & E.	-	-	32	32
McGEE (52) (1976)	152 x 305	114	PRE.	E.	1	-	11	12
		GRAND TOTAL			24	76	88	188
		Subtotal for POST-TENSIONED			04	18	NONE	022

PRE: Pretensioned
POST: Post-tensioned
U. : Uniform
E. : Eccentric

are also not clearly defined in codes of practice from different countries.

1.5 CONCLUSIONS

As a result of this review it became clear that reasonable progress has been achieved in the fields of the experimental and theoretical study of plain and reinforced concrete members. In the case of prestressed concrete beams with no stirrups, some rational methods of analysis have been achieved through extensive research. From the review of the previous research on pre-stressed concrete beams with stirrups, in particular, the following conclusions are drawn:

1. Insufficient experimental results are available particularly in the case of post-tensioned concrete beams.
2. Previous investigations were generally aimed at solving the general interaction problem of combined loading and little or no systematic investigation was carried out into the influence of single variable parameters.
3. The theoretical analyses were not entirely rational and the too empirical approaches need further verification.
4. Theoretical work is required to solve the problems of when a prestressed beam is under-reinforced or over-reinforced, and to resolve the question of the minimum requirement of stirrups to resist torsion.

5. Theoretical work is also required to relate the torsional and the flexural-shear strength (and deformation) of the member, to provide the design engineer with more realistic values when proportioning concrete members in the structure subject to combined torsion, bending and/or shear.

CHAPTER TWO

EXPERIMENTAL INVESTIGATION

2.1.1 INTRODUCTION

The experimental work programme consisted of preparing and testing thirty seven post-tensioned eccentrically prestressed rectangular beams, all with web reinforcement. The beams were designed and tested so that the effect of the following parameters upon the torque capacity and the interaction of torsion with bending and shear could be investigated:

I The prestressing force.

II The area of the prestressing steel.

III The concrete strength.

IV The depth-to-width ratio.

V The applied bending-to-torsion ratio.

VI The size of stirrups.

VII The spacing of the stirrups.

2.1.2 Numbering System

The test series were numbered in Roman numerals from I to VII in the order of the parameters as listed above. The beams were numbered for preparation purposes in groups from A to G. There was a subgroup called AA. Within the group, the beams were identified by Arabic numerals.

2.1.3 Test Series

The test programme contained seven series and one sub-series.

Series I consisted of eleven beams (No.A1-11) tested to observe the effect of varying the prestressing force. All other parameters

were kept constant as far as possible throughout the series. The prestressing force ranged from zero to 150 kN.

Series II contained six beams (B1-6). The only variable was the area of the tensile steel and the influence of this parameter was observed. The tensile area varied from 115.5 mm^2 to 346.5 mm^2.

Series III contained five beams (Beam G1-4 and B 2) tested to examine the effect of changing the concrete strength. The range of f'_c was between 25 N/mm^2 and 50 N/mm^2.

Series IV consisted of five beams (D1-3, B2 and C2) with different depth-to-width ratios, to study the influence of the aspect ratio upon the torque strength. The overall depth of the cross section, which was the same throughout all the series, was kept constant and only the width varied. Range of h/b ratios varied from 1.25 to 2.18. $\{\frac{d'}{b'} = 1.31 \text{ to } 2.84\}$

Series V contained five beams (Beams E1-5) similar to those of Series I and III except that the prestress force and the concrete strength was kept constant. The tests were carried out under different bending to torsion ratios so that the interaction of torsion, bending and shear could be observed. The range of M/T ratios varied from 0.1 to ∞. {0.1 to 17.2}

Series VI consisted of four beams (Beams F1,2 and E2,3). The only difference of Beams F1, 2 with respect to Beams E2,3 of series V was that the size of stirrups was changed to observe the effect on the strength in combined loading. This was demonstrated by using two sizes uzt. 4 mm and 6 mm stirrups.

Series VII consisted of five beams (F1,2 and G1-3). The beams G1-3 were identical to those of group F except that the spacing of the stirrups changed. The change was from 70 mm to 140 mm.

TABLE 2.1.

SERIES		I	II	III	IV	V	VI	VII	SUB-I	TOTAL
Parameter varied in the investigation		Prestressing Force kN	Prestressing Steel Area mm^2	Concrete Strength N/mm^2	h/b ratios mm/mm	M/T ratios kNmm/kNmm	Stirrups' size mm	Stirrups' Spacing mm	Prestressing Steel Depth mm	
Range of Variation	from	0.0	115.5	25*	1.25 1.75	0.1	4 6	70 70	103** 120	
	to	150	346.5	51.5	2.18	∞	6	140	135	
Beams used in the investigation	Designation of beams	A1-11	B1-6	C1-4, B-2	D1-3, B-2, C-2	E1-5	E2,3, F1,2	F1,2 G1-3	AA1, A-11, AA2	
	Number of beams	11	6	5	5	5	4	5	3	44

* Values of f'_c

** implying a variation of eccentricity from 13 mm to 49 mm correspondingly

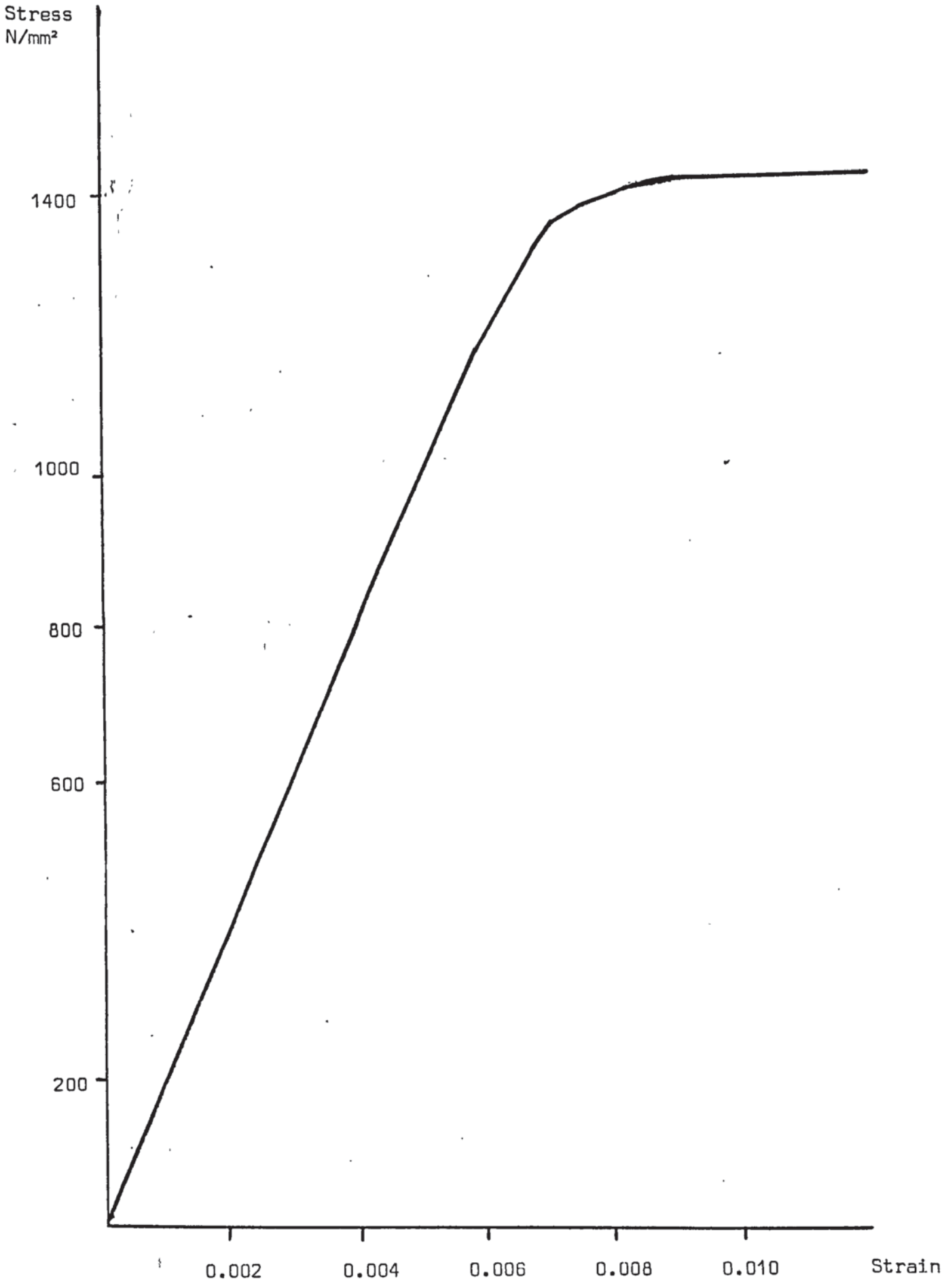

Fig.(2.1) Stress-Strain Curve for Prestressing Steel

Sub-series I consisted of three beams (AA1,2 and A-11) with identical average level of prestress, strength of concrete and web reinforcement. The total prestressing force was kept constant but the eccentricity was varied by changing the depth of the upper tensile steel from 87 mm to 55 mm and 119 mm for AA1 andAA2respectively.

A complete listing of the test series and the parameters considered in this investigation is presented in Table (2.1). Details of the beam groups and their characteristics are discussed under 2.5 (Details of Test Beams).

2.2 MATERIALS

2.2.1 Steel

High tensile prestressing wires of 7 mm diameter, were used throughout the experimental work. The properties of the steel were determined from the tensile test performed on a 300 mm long wire..

The stress-strain curve for the prestressing steel is shown in Figure (2.1). A mild steel of 6 mm diameter bar was used in reinforcing the test beams longitudinally throughout the work. It was used as well as web reinforcement in the six beams of Groups G and F.

4 mm diameter annealed wire was used to make stirrups for all the test beams except beams of Groups G and F.

Table (2.2) shows the properties of the prestressing wire and the web reinforcement.

2.2.2 Concrete

Ordinary Portland cement was used to prepare the mix which was nominally 1:1:5:3.0 by dry weight with a water to cement ratio of 0.5.

Table 2.2 PROPERTIES OF THE PRESTRESSING WIRE AND THE REINFORCEMENT STEEL

Diameter mm	Cross-Sectional Area mm²	Yield Stress N/mm²	Ultimate Tensile Strength KN	Young Modulus KN/mm²
4	12.56	342.0	4.54	180.37
6	28.27	382.0	15.72	218.27
7	38.50	1426.0 *	63.64	208.20

* Based on 0.2% strain

Table 2.3 SERIES III CONCRETE MIX AND STRENGTH

BEAM	Mix proportions by weight				ACTUAL AT 28 DAYS	
	WATER	CEMENT	SAND	GRAVEL	fcu	f'_c
C1	0.65	1	2.3	3.5	29.37	25.0
C2*	0.50	1	1.5	3.0	49.65	35.0
C3	0.45	1	1.8	2.8	47.0	39.0
C4	0.33	1	1	1.5	68.63	51.52

* Typical mix used throughout the other series

Coarse aggregate of 10mm maximum size obtained from Perry Barr pit and Packington sand were used. The sieve analysis of the aggregates has shown Zone B. When it was necessary, with aggregates being delivered in several batches, the mix design was slightly modified to make up for the target strength of the mix. The target cylinder compressive strength of the mix of 35 N/mm^2 at 28 days was normally achieved. See Table (3.2.2), Control Test Results. This mix was used to make the concrete for 34 beams.

In the case of the beams of Group C (Series III), which were devoted to investigate the effect of changing the concrete strength, three more mixes were designed to give the nominal cylinder compression strengths of (25), (40) and (50) N/mm^2 at 28 days. For the other beams of this group the usual common mix referred to above was used again. These nominal mix designs and the actual concrete strengths achieved at testing of Series III, are shown in Table (2.3).

2.3 CONCRETE CONTROL SPECIMENS

Alongside each of the main test specimens, the following specimens were cast :

(a) Three 100 mm cubes for compression cube strength test.

(b) Two 150 x 300 mm cylinders for compression cylinder strength test.

(c) Two 150 x 300 mm cylinders for the indirect tensile split cylinder strength test.

(d) Two 150 x 300 mm cylinders to determine Young's Modulus.

(d) Two 100 x 100 x 600 mm beams for the standard modulus of rupture test.

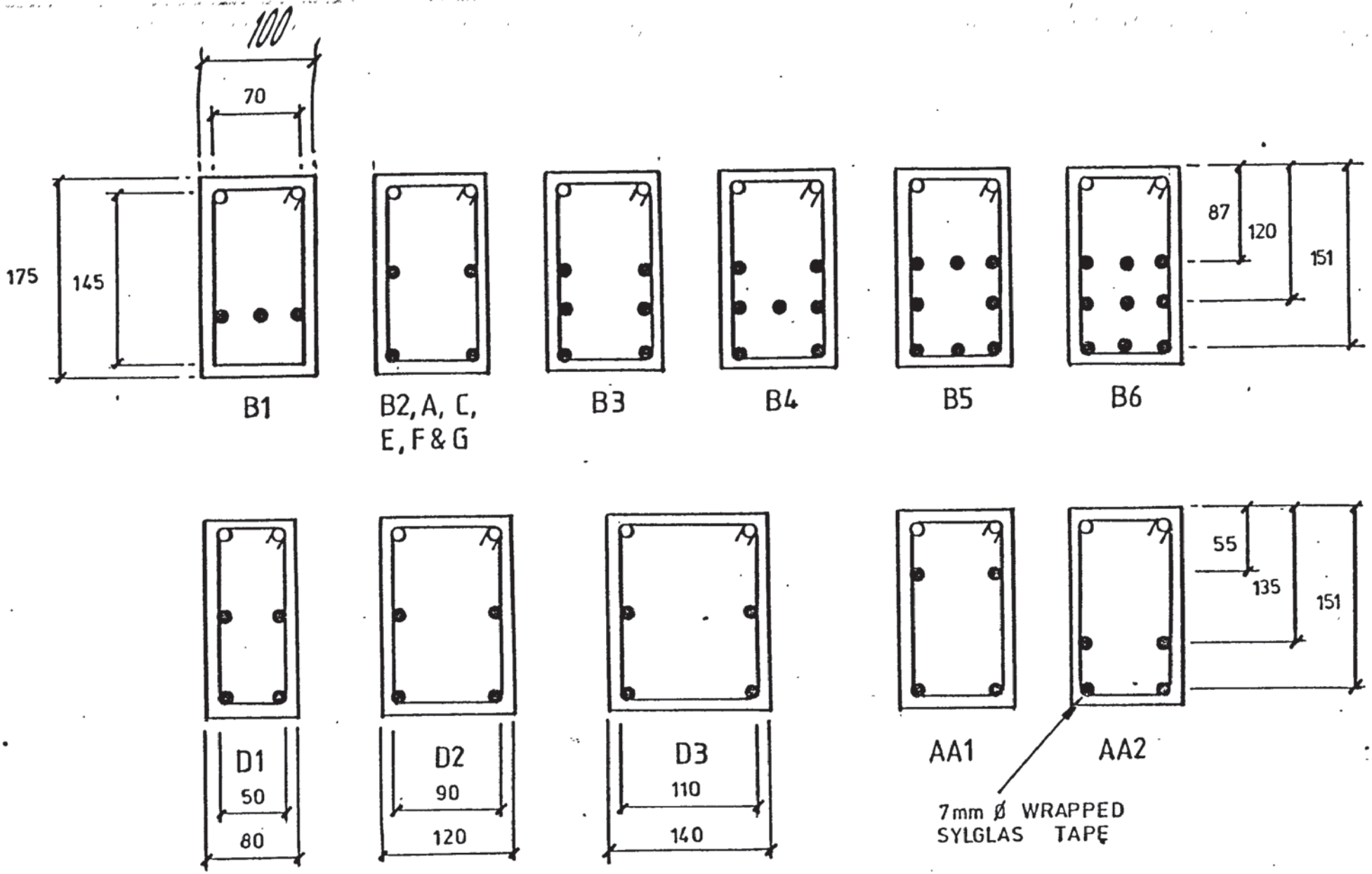
100
70
175
145
B1
B2, A, C,
E, F & G
B3
B4
B5
B6
87
120
151
D1
50
80
D2
90
120
D3
110
140
AA1
AA2
55
135
151
7mm ø WRAPPED
SYLGLAS TAPE

These control specimens were cured for 27 days in the same tank containing the main test beam. Details of curing are described under 2.4. They were tested in accordance with the British Standard 28 days after casting.

The test results are presented in Tables (3.2.1) and (3.2.2) discussed in the next chapter.

2.4 MIXING, PLACING AND CURING OF CONCRETE

The required mix proportions were weighed and carefully handled to avoid any unnecessary losses before reaching the mixer's loading-hopper. A linear "Cumflow" No 1A mixer was utilized to make the concrete.

Before casting took place, the mould for the test beam (see 2.5) and the moulds for the control specimens (see 2.3) were cleaned, oiled and checked to detect any damage caused by previous use.

The electric wires, extended from the steel strain gauges (see 2.6.1), and the prestressing wires and other metalwork were finally inspected in place before the concrete was placed.

The concrete was compacted during placing by means of a poker vibrator. In the case of the beams of Series II, which were manufactured to investigate the effect of increasing the tensile steel, it was impractical to use the poker vibrator because of the close spacing of the longitudinal steel wires. Thus the concrete of the main specimens of Group B, together with the associated control specimens, was placed with the help of a vibrating table. Both methods of concrete consolidation were found satisfactory.

The main and control specimens were cured in a special curing tank and automatically sprayed with water once a day for 27 days. They were then removed out of the tank and left under the normal

conditions of the laboratory in order that the surface be dry enough for the attachment of the concrete strain gauges (2.6.2).

2.5 TEST BEAMS

2.5.1 Groups of Test Beams

For preparation purposes the thirty seven beams were classified according to their general arrangements and design characteristics, into seven groups (Group A-G) and one subgroup (Sub-group AA). The groups A, C and E contained twenty beams, with the same cross sectional dimensions, arrangements of prestressing steel and details of reinforcement. Only the concrete mix used might differ in strength and in the average level of prestress to which it was to be post-tensioned at testing.

Groups F and G each contained three beams similar to those of Group A, except that the stirrups used were 6 mm diameter mild steel and the spacing varied.

In sub-group AA which contained two beams identical to Beam A-11, the depth of the upper layer of the prestressing steel varied.

Groups B and D contained six and three beams respectively. In B types of beams the configuration of the prestressing steel varied. One, two and three layers of steel were used with two or three tendons in each layer. The beams of Group D were of different cross-sectional dimensions and areas. Although the overall depth of the cross section was kept constant, together with the average prestress across the depth, the width was successively varied.

A listing of the beam groups and their characteristics is presented in Table (2.1). A detailed account of the general arrangements and the particular features of each group and its beams is given in the following section.

2.5.2 Details of Test Beams

Typical cross sections of the test beams are shown in Figure (2.2). A general description of a typical beam is presented first. The particular features of each group are discussed with reference to the typical test beam of Group A.

The test beam had a nominal cross section of 100 x 175 mm and was 3000 mm in length. It was post-tensioned eccentrically by four 7 mm diameter high tensile steel wires. These wires were arranged in upper and lower layers. Further longitudinal reinforcement was provided by two 6 mm diameter mild steel bars located to the corners in the 'compression zone'. While these bars were bonded to the concrete, the prestressing wires were allowed to move, so that the beam could be post-tensioned. To achieve this end, the wires were wrapped in Sylglass water-proofing tape.

The prestressing force was applied so as to produce zero stress at the top fibre and a predetermined compressive stress required at the bottom fibre of the cross section. Thus the prestressing stress distribution was a triangular with 28 mm eccentricity as measured from the centroid of the section. It was possible to determine prestressing strains in each wire using the strain gauges attached to the wires monitoring the steel strain. Gauges were also fastened to the longitudinal bars.

The beam contained closed stirrups made of black annealed wire of 4 mm diameter at spacings of 70 mm. One stirrup at least was gauged with four strain gauges, one on each leg. The stirrup was gauged assuming that the failure, and/or cracking section, would be intercepted by such gauged stirrups. In many cases this did not occur.

The annealed wires and the tendons were straightened to facilitate the manufacturing of the stirrups and to help in achieving more accuracy of assessing the prestressing force.

The steel was cut to the required lengths of the tendons, bars and stirrups and the bar's ends were shaped into standard hooks. Considerable care was taken in manufacturing the stirrups so as to be as exact and consistent as possible. A replacement was always substituted for a stirrup which did not fit. The spacings of the stirrups were marked on both the longitudinal reinforcing bars, and the stirrups were then fastened to the bars by means of ties.

The strain gauges were attached to at least one of the stirrups and also the longitudinal bars and the tendons. This procedure will be discussed in section (2.6) Instrumentation.

The attached strain gauges were water-proofed and their leads were soldered to the electric wires and plastic tubes of 12 mm diameter and 140 mm length were inserted to protect the gauges glued to the tendons. The tendons were covered with Sylglass tape. The reinforcement cage and the tendons were then assembled and carefully placed in the mould.

The casting mould was made of plywood and lined with formica. It was cleaned, oiled and put together before the steel-work was secured in place. A metal plate was placed at each end of the mould to serve as a support for the tendons anchorage using friction wedges. Wood wedges were inserted between the end of the mould and another metal plate used as a temporary reaction support. Before casting started, a small prestressing force was applied to the tendons which were anchored using the friction wedges bearing on the reaction plate. This method was necessary to hold the prestressing wires securely in place during the placing and compacting of concrete.

2.5.3. Particular Features of Test Beams

Group A: consisted of eleven beams. The cross sectional dimensions, arrangement of prestressing steel and details of reinforcement have already been discussed above. The parameter considered in investigation was the varying of the prestressing force. The beams were post-tensioned to different levels of prestress. The prestressing force varied from 0.0% (in Beam A-1) to 60% (in Beam A-11) of the ultimate tensile stress of the tendon; the percentages being based on four wire tensile strength. See Table (2.2).

Table (2.4) gives the actual prestressing effects on the tendon, in each layer of steel, and upon the concrete section and also shows the relevant characteristics of this group of beams.

This group provided the main specimens of Series I, and were tested under approximately "constant" bending to torque ratios. The test procedure will be described later.

Group B: consisted of six beams. The main variable involved was the amount of the prestressing steel. In the remainder of the beams, it was necessary to vary the position of the prestressing steel, but the prestressing steel's centroid, however, was kept constant and was 32 mm below the centroidal axis of the section.

In the beam B-1, only three tendons were used, arranged in one layer, and located at 32 mm below the centroidal axis of the concrete section. The steel was increased by increasing the number of tendons and one more tendon was added to each succeeding beam. Beam B-6 contained nine tendons distributed in three layers.

In addition to the depth of the tensile steel, the eccentricity of the prestressing force also was kept constant. The prestressing tendon force was varied in the different layers so as to give a constant average level of prestress at the

Beam	Prestressing Force on the Steel			Eccentricity mm	P_{tot} %*
	Lower Layer N	Upper Layer N	P_{tot} kN		
A1	Nil	Nil	Nil	Nil	0.0
A2	5691.147	5619.006	11.31	32.2	4.55
A3	9981.00	10838.00	20.819	30.68	8.38
A4	19317.832	20359.88	39.677	31.159	15.97
A5	26688.00	26688.00	53.376	32.0	21.49
A6	33936.98	33366.41	67.303	32.3	27.10
A7	45256.00	46010.00	91.266	31.74	36.7
A8	49450	53270	101.718	30.81	41.35
A9	62740.76	74718.11	137.459	28.9	55.34
A10	54506.76	75299.486	132.288	26.87	57.2
A11	65648.583	83162.888	148.811	28.23	59.9

* percentage based on ultimate tensile strength of four wires

TABLE 2.4 SERIES I STRESSES ON THE STEEL DUE TO PRESTRESSING

centre of the section, with almost the same effects of prestress at the top and bottom fibres of the various beams.

One particular problem in the process of post-tensioning these beams, was to make up for the losses in the prestressing force, which were aggravated by the use of multi-layers of steel.

Every effort was made to assess accurately the prestress loss in each tendon and several attempts were required to readjust the prestressing force. The final prestress effects when testing of the beams commenced are presented in Table (2.5). The table gives also all the relevant data concerning this group of beams.

The concrete for this group of beams was compacted during casting with the help of a vibrator table.

The tests on these beams, which were used in Series II, were carried out under approximately the same 'constant' bending to torque ratio as Series I.

Group C: contained four beams with a variable concrete strength. The beams were, otherwise, identical to the typical beam of Group A. The concrete for the beam C-2, however, was of the same common mix used throughout the other groups, and produced the expected cylinder compression strength of 35 N/mm^2.

Table (2.3) gives the relevant data and the concrete strengths of the beams of this group. The concrete mixes have already been discussed in section 2.2.2.

The beams of Series III were tested under bending to torque ratios identical to chose of Series I and II.

Group D: contained three beams with the main variable of the h/b ratio. The height of the cross section of the beams was kept constant and only the width varied. The typical width of 100 mm was reduced to 80 mm in the case of beam D-1 and increased to be 120

Table 2.5 SERIES II

i - VARIATION OF PRESTRESSING STEEL AREA

Beam	Area of Steel in layers:			Area Total mm²	Strains Total due to Pre-stress	PC2 N/mm²	Total P KN
	lower	middle	upper				
B1	-	115.5	-	115.5	17150	≅7.80	130.200
B2	77	-	77	154.0	17150	"	137.469
B3	77	77	77	231.0	16505	"	132.299
B4	77	115.5	77	269.5	16740	"	134.183
B5	115.5	77	115.5	308.0	17180	"	137.710
B6	115.5	115.5	115.5	346.5	[17360]	"	139.153

ii - VARIATION OF TOTAL STEEL CONTENT

Beam	$\frac{A\ell}{bd\ell}$ %	$\frac{As\ .2\ (b'+ d')}{bd\ell\ S}$ %	Total Steel %
B1	0.9705	0.653	1.624
B2	1.294	"	1.947
B3	1.941	"	2.594
B4	2.265	"	2.918
B5	2.588	"	3.241
B6	2.912	"	3.565

and 140 mm for the beams D-2 and D-3 respectively. Accordingly, the stirrup's centre to centre dimensions were 51, 91 and 111 mm by 145 mm. The depths to the upper and lower layers of the prestressing steel were kept consistent with those of the typical beam. The mould was readjusted so as to accommodate the desired cross sectional dimensions of the beams.

Throughout the group, the average level of prestress across the depth of the concrete section was constant and the eccentricity the same as that of a typical beam. To accomplish this with a variable cross sectional area the total prestressing force applied to the tendons was varied accordingly.

Table (2.6) gives full details of the characteristics and the particular features of this group of beams, together with those of Beams B-2 and C-2, in total were the test specimens for Series IV. The tests on this series were carried out under the same combined loading ratios of the series previously discussed.

Group E: contained five beams identical with the typical beam described above. The variable was the applied bending to torque ratios. Table (2.1) gives the relevant data of those beams which constituted Series V.

The beam E-5 was tested under no torsion. The bending to torque ratio was reduced in the following beams in the series until the point load was zero in case of the beam E-1 which was tested under its own weight and pure torsion. The sequence of loading was changed in this series and will be discussed further in section (3.3).

Group F: contained three beams identical to those of Group A, except that the stirrups used were of 6 mm diameter mild steel. The beam F-O was post-tensioned to less than the predetermined prestress applied to the other two beams of the group.

Table 2.6 SERIES IV - BEAM CHARACTERISTICS

Beam	h	b	h/b	d'/b'	Gross Area mm^2	pc2 N/mm^2	P total KN
D1	175	80	2.18	2.84	14000	6.99	97.857
{C2} {B2}	175	100	1.75	2.04	17500	7.83	137.0
D2	175	120	1.458	1.59	21000	7.82	164.22
D3	175	140	1.25	1.31	24500	7.82	191.59

Beam	b mm	$\frac{As2\ (b'+d')}{bd\ S}$ % (1)	$\frac{A}{bd}$ % (2)	(1 + 2) %
D1	80	0.741	1.618	2.359
C2, B2*	100	0.653	1.294	1.947
D2	120	0.595	1.078	1.673
D3	140	0.553	0.924	1.477
Group F**	100	1.467	1.294	2.761
Group G***	100	0.734	"	2.028

* common characteristics of all the test beams except Group B (excluding Beam B2), and the groups of beams listed herein.

** As=28.3mm²

*** S = 140mm, (As=28.3)

Group G: concerned three more identical beams, the only difference being the spacing of the stirrups which was doubled to become 140 mm.

The relevant data of these two groups of beams constituting Series VI and VII that dealt with the effects of web reinforcement variation, are shown in Table (2.1).

The loading ratios of testing of the two series were such as to cover a specific range of M/T ratios.

2.6 INSTRUMENTATION

The prestressing force was assessed directly from the strains in steel and the loading effects on the concrete were assesed by measuring the concrete strains. The members were therefore instrumented with steel and concrete strain gauges. Additional mechanical gauges were used to measure the twist angles and the deflections.

2.6.1 Steel Strain Gauges

Tokyo Sakki Kenkyujo PL-5-11 type of electric resistance strain gauges were used to monitor directly the strains on the steel. For each beam, four strain gauges were glued to at least one stirrup, one at each leg. Two gauges were glued to each prestressing wire. Moreover, the longitudinal bonded bars were also gauged.

The positions of the strain gauges were sanded and degreased with a trichloroethane solution, and an ammonia solution was used to neutralise the surfaces.

The strain gauges were then glued to the steel with the adhesive provided by the manufacturer. When the strain gauges had adhered to the steel, electric wires were soldered to the gauge leads. Water proofing was achieved by applying an M-Coat G paste. The further steps in protecting the gauges were described in section 2.5.2.

2.6.2 Concrete Strain Gauges

PL-60-11 electric resistance strain gauges (120 ohms) were used to monitor the longitudinal concrete strains.

After marking the positions on the surface of the beam (section 2.5.2), the surfaces were sanded with an emery paper and cleaned. A thin film of F88 dental cement of Tridox products was applied to the position. The strain gauges were then gently pressed to the surface and left to adhere. When the adhesive cement had dried, the gauge leads were soldered to electric wires connected to the Peekel.

An initial reading of all the strain gauges was recorded.

2.7 TESTING OF BEAMS

After 27 days of casting, the beams were moved out of the curing tank. For handling purposes, the upper layer of the prestressing steelwas post-tensioned by an initial small amount of prestressing force. The tendons were safely anchored by using the friction wedges, and the prestress effects on the steel were recorded. The beam remained in the laboratory until dry so that the concrete strain gauges could be attached to the surface.

The steel strain gauges were connected to the extension box of the Peekel, and after a set of initial readings were taken, the strain gauges were disconnected and the beam was ready then for setting up in the test rig.

A prestressing jack was used to post-tension the beams. The required elongation of each wire was carefully measured and the amount of prestress was further checked by the pressure on the hydraulic jack. This was to check the strain gauge readings on the wires.

TABLE (2.7) PRESTRESSING FORCE AND EFFECT

BEAM	Prestressing Force on the Steel kN		Prestress N/mm^2	
	Upper LAYER	Lower LAYER	Bottom of beam (- compression)	Top of beam (+ tension)
A1	0.00	0.00	0.0	0.0
A2	5.69	5.69	-1.37	+0.072
A3	10.90	10.03	-2.46	+0.070
A4	20.58	19.32	-4.73	+0.170
A5	26.85	26.84	-6.45	+0.317
A6	33.85	33.84	-8.18	+0.440
A7	45.90	45.89	-10.98	+0.489
A8	53.27	50.03	-12.17	+0.367
A9	74.47	54.33	-14.18	-0.540
A10	75.33	62.40	-15.77	-0.027
A11	84.19	65.47	-16.87	-0.236
C1	77.80	64.44	-16.21	-0.046
C2	85.46	70.79	-17.81	-0.051
C3	74.85	62.00	-15.60	-0.045
C4	72.20	59.81	-15.04	-0.043
E1	84.73	70.18	-17.65	-0.051
E2	82.87	68.65	-17.27	-0.049
E3	81.10	67.18	-16.90	-0.048
E4	78.39	64.94	-16.33	-0.047
F0	62.75	58.93	-14.34	+0.437
F1	74.83	54.60	-14.45	-0.347
F2	80.83	66.96	-16.84	-0.048
G1	67.96	67.94	-16.29	+0.754
G2	75.12	62.22	-15.65	-0.045
G3	85.59	70.90	-17.83	-0.051
AA1	79.72	72.43		

The measurements were recorded using a Peekel indicator type B105. This was adjusted to the appropriate gauge factors and connected to a dummy to compensate for the change in temperature.

The final prestressing force and effect for each beam is shown in Table (2.7), which gives the effective prestressing values at the commencement of loading.

The loading was initiated by flexural bending to stabilise the strain gauges, and then a predetermined bending load was applied followed by the corresponding increment of torque. The strain and mechanical gauge readings were recorded. The second increments of bending and torsion were applied in the same sequence. The combined loading thus built up until cracking occurred. Every effort was made to detect the initial crack and the subsequent growth by checking the concrete surface and watching the Peekel.

After cracking, the predetermined increments were reduced proportionately as failure was approached. The failure was usually indicated by the sudden drop of the torsion hydraulic jack. The maximum readings of the torsional jack before reduction and the final bending load were taken as the ultimate torque and bending load respectively. The steel and concrete strain gauges, the twist and deflection gauges were taken as far as possible at the ultimate load.

The primary test results are presented in Table (3.3). The table gives also the initial cracking and failure positions, which were measured from the left hand support.

2.8 TEST RIG

All beams were tested using a portal testing rig in the Structural Concrete Laboratory. The rig was suitable to apply a point load in the centre of the test span. The beam was simply supported and subjected to torsion by means of lever arms fixed at the ends. Whilst the left hand lever arm was fixed to the rig frame, the right hand side one was connected via a universal joint to a hydraulic jack. The latter was provided by a proofing ring which was calibrated up to an accuracy of 14 Nmm per division. The effective span was 2900mm from centres of supports.

The test rig has been used and described previously by Cooper (38), Allos (57) and Jolla (58) where full details are reported.

Mechanical dial gauges of Batty type were fixed at the centre and the two ends to measure the vertical deflection at the centreline of the beam and the twisting rotation of the torsional lever arms. Whereas the flexural deflection was measured by reading the dial gauge directly, the rotations were calculated from the vertical movement of the end dial gauges.

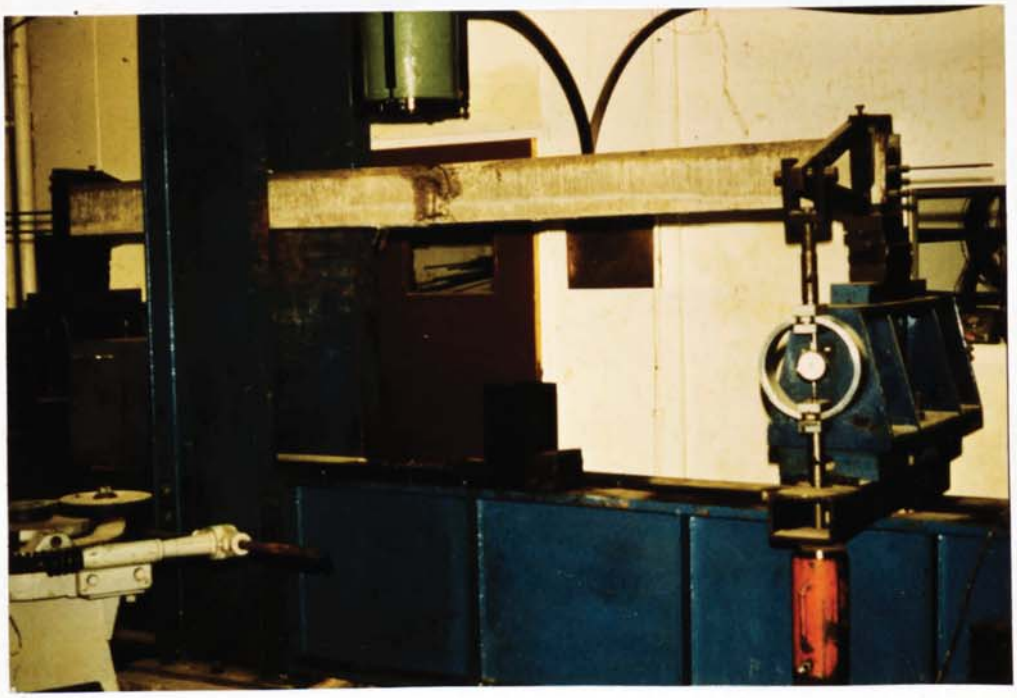

PLATE (2.0) GENERAL VIEW OF TEST RIG

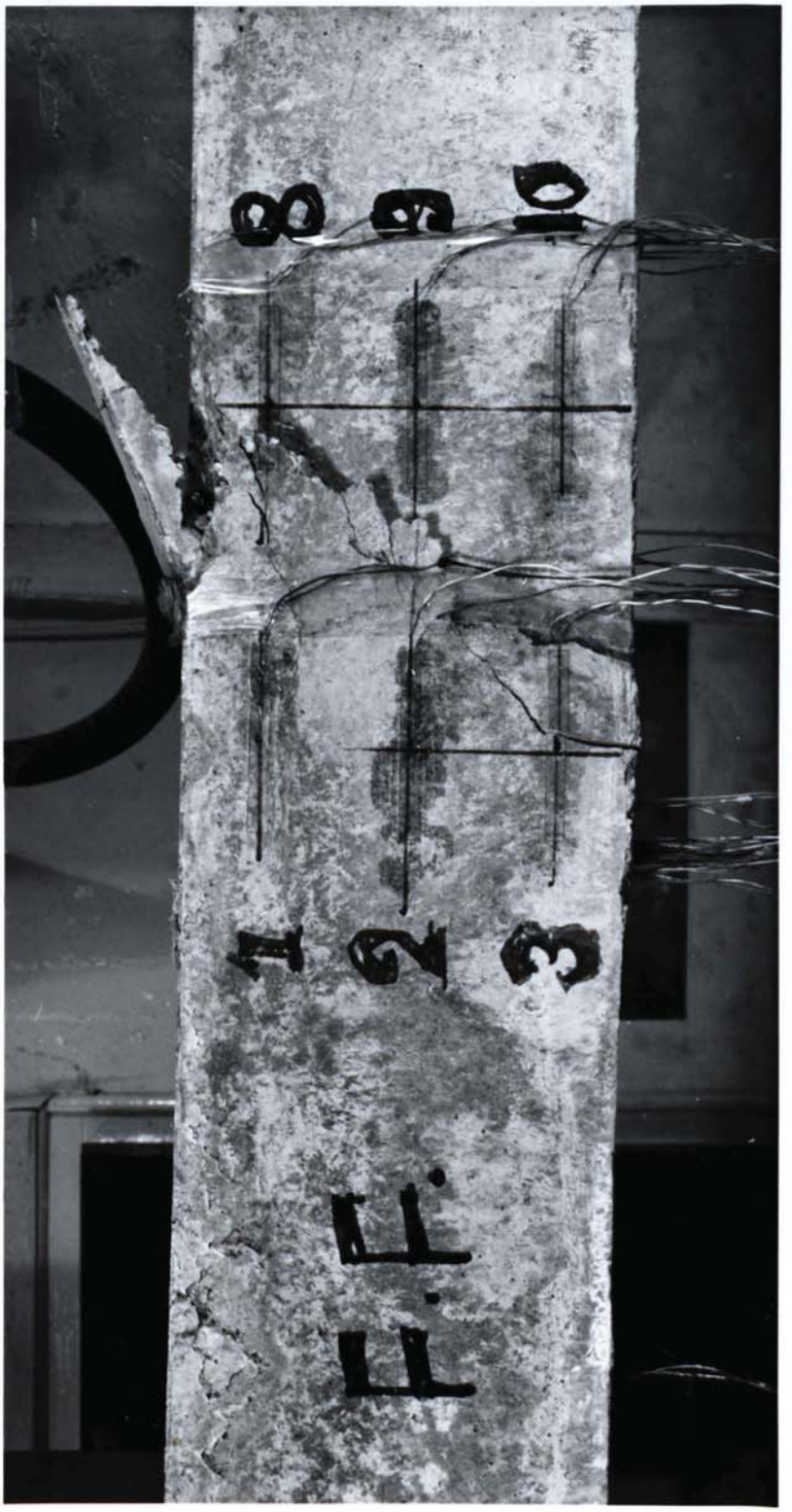

PLATE (2.1) FAILURE CRACKING PATTERN OF BEAM B-6. A FRONT FACE VIEW.

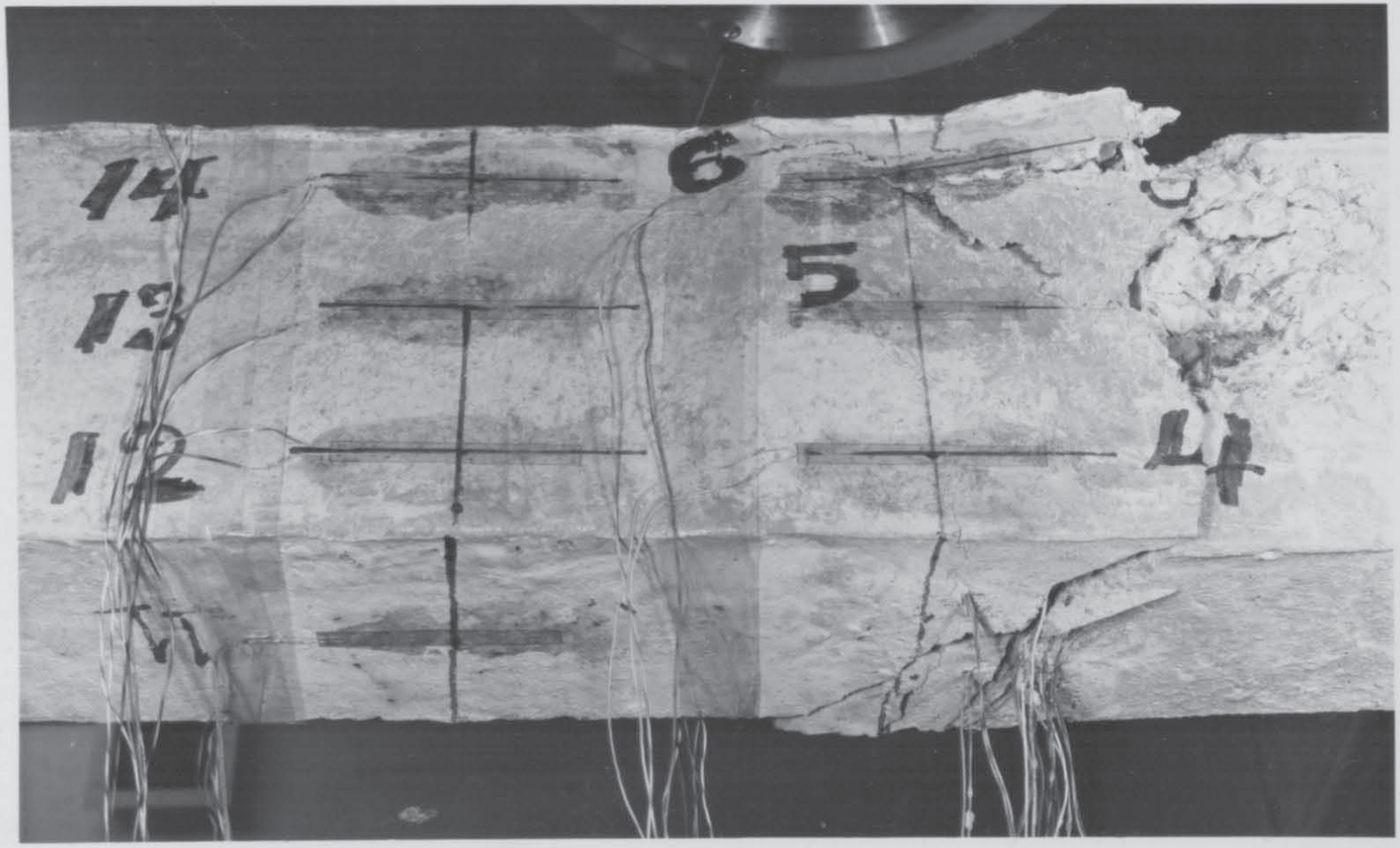

PALTE (2.2) FAILURE CRACKING PATTERN OF BEAM B-6 A BACK FACE-BOTTOM VIEW

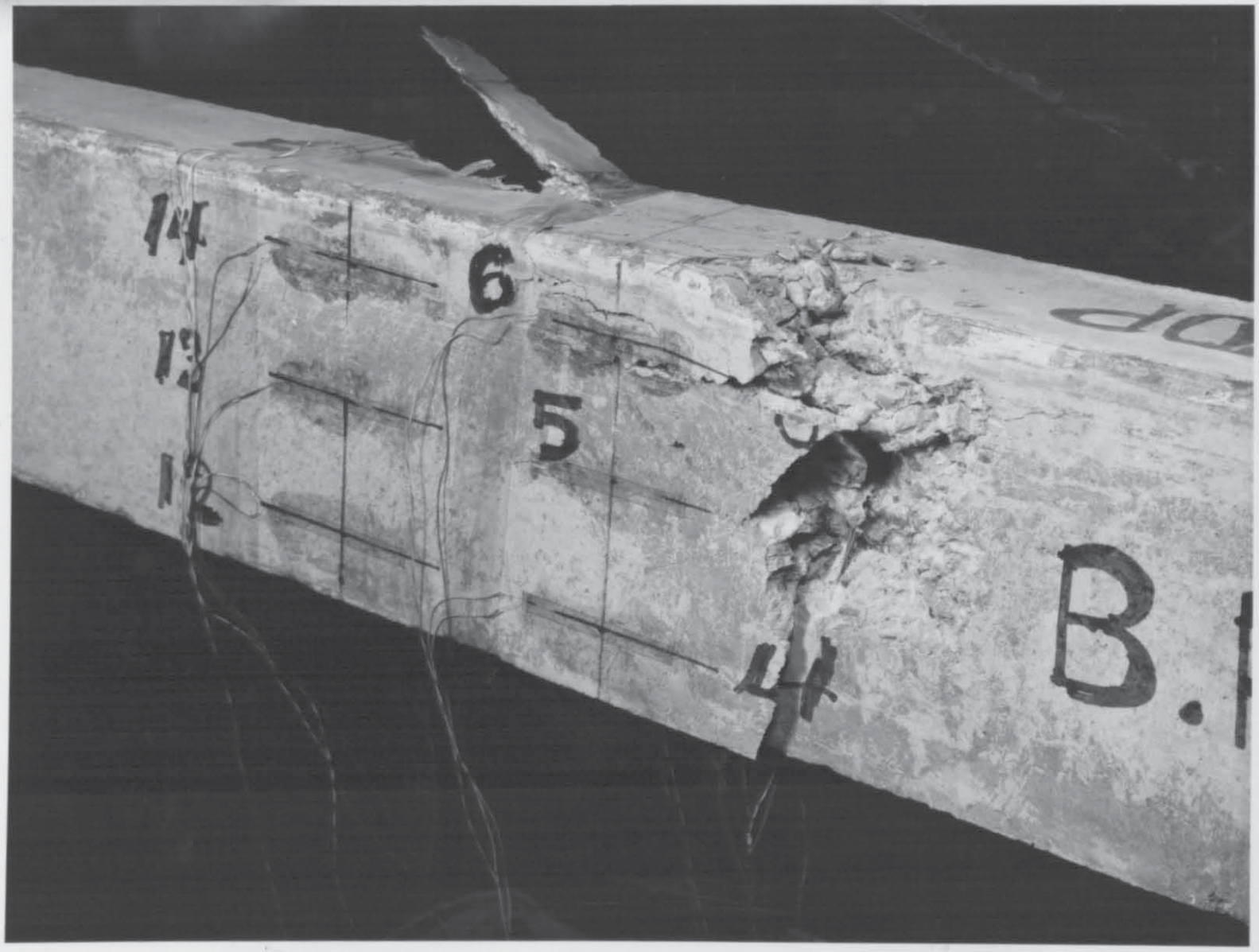

PLATE (2.3) FAILURE CRACKING PATTERN OF BEAM B-6 A BACK FACE-TOP VIEW

CHAPTER 3:

TEST RESULTS & FAILURE OF BEAMS

3.1. INTRODUCTION

In this Chapter the ultimate strength and other limit states of the thirty-seven test beams are presented, e.g. cracking capacity and cracking patterns at failure. Conclusions are drawn from the experimental observations and discussion of the differing single variable parameters as investigated in the main series. The first section, however, examines the test results of the concrete control specimens which accompanied the testing of the main beams.

3.2 Test Results of Concrete Control Specimens

These test results may be divided into two groups. The first group includes the test results of the control specimens from the beams C1, C2,3 and 4, which were tested to investigate the effect of the concrete strength as the major variable. The control specimens in this group therefore served to monitor the varying concrete strength over the required range. The second group includes the control specimens from the other 33 beams, in which the concrete strength was the constant parameter and the control results therefore monitored the target strength.

3.2.1.

The control specimens results for the four beams included in this subsection are shown in the following table.

The results include the value of Young's modulus of the concrete and the Poisson's ratio. In the case of the test beam C2, the latter two values are missing because of the malfunction of the strain gauges. Also the result of the indirect tensile cylinder split test, fsp, for beam C3 was omitted due to experimental error.

Table (3.2.1) Test Results of Control Specimens.

Test Beam	f_{cu} N/mm^2	f'_c N/mm^2	f_{sp} N/mm^2	f_r N/mm^2	E_c kN/mm^2	ν
C1	29.37	25.00	2.242	2.480	26.858	0.1338
C2	49.65	35.00	3.300	3.590	-	-
C3	47.00	39.00	-	3.700	32.373	0.1495
C4	68.63	51.52	4.449	4.828	39.200	0.1816

Table 3.2.1. summarises the results of testing twenty-six cylinders and eight prism beams, from which it is concluded:

a. The cylinder compressive strength, f_c', varied between 85% and 75% of the cube compressive strength, f_{cu}. With increasing the strength the ratio of f_c': f_{cu} tended to decrease.

However, if the strength ratio, f_c': f_{cu}, is regarded as independent of the variation in strength, the main strength ratio is equal to 0.78 with a standard deviation of 0.06 and a coefficient of variation of 7.7% The limit of the variation of the cylinder compressive strength considered in this part of work was between 25 and 50 N/mm^2.

b. The split cylinder tensile indirect strength, f_{sp}, varied between 90% and 92% of the mean value of the standard rupture modulus of tensile strength, f_r. The ratio f_{sp}: f_r was approximately constant and less sensitive to the variation in strength than the ratio f_c': f_{cu} was as discussed in (a).

c. Young's modulus of concrete increased directly proportional to the compressive cylinder strength, 'f_c'. The variation suggested a parabolic relationship and the simple formula $E_c = 5000\sqrt{f_c'}$ was sufficiently accurate for the analysis of the test results. A mean of 1.068 was obtained for the ratios of E_c test/ E_c formula. With increasing compressive cylinder strength, this empirical formula, was conservative.

d. An increase in the Poissons's ratio was evident with increasing the cylinder' compressive strength. As the latter increased from 25 N/mm^2 to 51.52 N/mm^2, the Poisson's ratio increased by 35.7% indicating higher "elasticity" produced by higher strength concrete mixes. It is noted that the maximum aggregate size was constant and the strength increased was achieved by reducing the mixing water weight and adjusting the sand and gravels weight in the mix.

The relation between the two tensile strength indexes vtz. the cylinder split and the standard rupture, and the water/cement ratio is linear for both tensile strengths.

3.2.2

The test results of the control specimens for the remaining thirty-three beams are presented in Table (3.2.2.) For each series of beams the mean, standard deviation and coefficient of variation were computed and are listed in the table. From these test values of 84 cubes, 130 cylinders and 88 prisms for the grand total of thirty-three beams concrete, the following conclusions are made:

a. The mean cylinder compressive strength was 76% of the cube compressive strength.

The mean value of the cube compressive test was 49.04 N/mm^2. The cube strengths varied between 53.63 N/mm^2 and 44.45 N/mm^2 with a coefficient of variation of 9.36%. The cylinder compressive tests were more consistent, with a mean of 37.08 N/mm^2, a standard deviation of $\pm$ 2.73 N/mm^2 and a coefficient of variation of 7.37%.

b. The split cylinder tensile strength was 87% of the standard modulus of rupture for tensile strength.

The mean value of the splitting cylinder tensile tests was 3.18N/mm^2 with a coefficient of variation of 9.53%. The coefficient of variation was 10.20% in the case of the standard modulus of rupture tests that resulted in a mean of 3.67 N/mm^2 and a standard deviation of $\pm$ 0.37 N/mm^2

Table 3.2.2.4. TEST RESULTS OF CONTROL SPECIMENS

Beam	f_{cu} N/mm^2	f_c N/mm^2	f_{sp} N/mm^2	f_r N/mm^2
A1	50.50	38.20	3.73	3.34
A2	43.99	34.78	3.332	3.223
A3	32.53	25.86	2.200	2.285
A4	45.70	35.54	3.473	3.610
A5	43.13	34.50	2.710	3.112
A6	44.90	34.89	2.640	3.470
A7	48.02	35.95	3.600	3.820
A8	40.70	32.56	3.013	3.222
A9	45.63	35.46	2.910	3.510
A10	44.67	34.18	3.183	3.650
A11	42.00	37.235	3.218	3.520
B1	48.50	36.00	-	3.960
B2	50.70	35.735	3.381	4.310
B3	49.68	41.60	3.324	4.712
B4	51.10	36.60	3.204	4.052
B5	45.73	36.60	2.986	3.252
B6	50.13	37.10	3.388	3.640
D1	49.50	37.20	3.220	3.880
D2	50.20	36.70	3.280	3.950
D3	51.70	38.20	3.310	3.980
E1	59.83	41.82	3.650	3.980
E2	50.00	43.52	3.180	3.740
E3	53.10	38.23	3.706	3.830
E4	56.30	39.72	3.020	3.460
E5	49.43	37.07	3.540	3.940
F0	46.47	32.59	2.723	3.720
F1	48.73	38.25	2.740	3.820
F2	57.80	42.84	3.056	3.840

continued

TABLE 3.2.2. Test Results of Control Specimens

Beam	f_{cu} N/mm^2	f_c N/mm^2	f_{sp} N/mm^2	f_r N/mm^2
G1	50.53	40.06	2.800	3.800
G2	45.20	33.95	3.056	3.240
G3	55.87	38.25	3.056	3.840
AA1	54.66	36.61	3.060	3.280
AA2	44.80	34.63	2.820	2.880
Mean	49.04	37.08	3.180	3.670
S.D N/mm^2	4.59	2.73	0.300	0.370
Coefft of Var.n%	9.36	7.37	9.53	10.19
A Beams				
Mean	44.92	35.33	3.181	3.448
Coeff.t of varn%	5.99	4.24	10.90	6.09
B Beams				
Mean	49.31	37.27	3.257	3.988
Coeff.t of Varn%	3.65	5.33	4.62	11.65
E Beams				
Mean	53.73	40.07	3.419	3.79
Coe ft. of varn%	7.29	5.85	7.92	4.89
E,F & G Beams				
Mean	52.11	38.75	3.155	3.736
Coefft of varn%	8.77	3.38	10.58	5.44

Table (3.3-1) FAILURE LOADS OF BEAMS

Beam	Y_1 mm	Bending Load kN	Ultimate Torque kNm	Ultimate Bending moment	Ultimate Shear Force kN	Bending to Torsional moments ratios	$\frac{2T}{Vb}$ Ratios
A1	1450.0	9.00	1120.0	6570.0	4.56	5.90	4.90
A2	1400.0	6.00	1274.0	4740.0	3.03	3.70	8.40
A3	1450.0	7.00	1400.0	6710.0	4.99	4.80	5.60
A4	-	7.50	1036.0	7070.0	5.25	6.80	3.95
A5	1510.0	6.00	1260.0	5750.0	4.53	4.60	5.56
A6	1650.0	11.00	2100.0	8350.0	7.10	4.00	5.90
A7	1480.0	11.00	2282.0	9420.0	7.01	4.10	6.50
A8	1365.0	10.00	2366.0	7370.0	5.04	3.10	9.40
A9	1620.0	16.00	2538.0	11740.0	9.59	4.60	5.30
A10	1475.0	16.00	3402.0	13010.0	9.51	3.80	7.20
A11	1360.0	17.00	3542.0	14790.0	9.95	4.20	7.10
B1	1385.0	7.00	1428.0	5390.0	3.53	3.77	8.09
B2	1425.0	13.00	2604.0	9280.0	6.51	3.56	8.00
B3	1413.0	11.30	2310.0	8010.0	5.67	3.47	8.15
B4	1525.0	10.00	1890.0	6930.0	5.04	3.67	7.50
B5	1450.0	14.00	28880.0	10150.0	6.99	3.63	8.01
B6	1466.0	13.00	2240.0	9330.0	6.51	4.17	6.88
C1	1437.0	9.00	1918.0	6730.0	4.54	3.50	8.45
C2	1380.0	11.00	2324.0	8132.0	5.54	3.50	8.40
C3	1315.0	13.00	2730.0	9086.0	6.57	3.33	8.31
C4	-	12.00	2520.0	8690.0	5.99	3.45	8.41
D1	1500.0	6.00	1288.0	4634.0	3.02	3.60	10.66
D2	-	13.00	2758.0	9653.0	6.54	3.50	7.03
D3	1400.0	16.00	3388.0	11960.0	8.04	3.53	6.02
E1	-	-	3500.0	360.0	0.43	0.103	162.80
E2	-	10.00	3178.0	7440.0	5.04	2.34	12.61
E3	1485.0	19.50	2730.0	14400.0	9.78	5.27	5.58
E4	1450.0	24.00	1160.0	19030.0	13.50	17.20	1.63
E5	-	-	000.0	21930.0	15.50	0.0	0.00
F0			2128.0	9860.0	6.51	4.60	6.50
F1	-	-	3570.0	7660.0	5.01	2.20	14.25
F2	1479.0	19.50	2450.0	14400.0	9.78	5.88	5.01
G1	1421.0	10.00	3528.0	7650.0	5.02	2.20	14.10
G2	-	15.00	3150.0	12150.0	9.02	3.90	6.98
G3	-	19.50	2128.0	13810.0	9.52	6.49	4.47
AA1	-	16.00	3080.0	13230.0	9.50	4.50	6.20
AA2	-	-	3780.0	2610.0	11.12	0.70	6.80

3.3. FAILURE & CRACKING LOADS OF BEAMS

The ultimate strengths of torsional, flexural bending and shearing loads for each of the thirty seven beams are presented in Table 3.3-1. The table includes the values of ratios of bending to torsion and the parameter 2T/Vb for each beam at failure. The position of the failure section as measured from the left hand support (y_L) together with the bending single point load are also listed.

Table 3.3-2 contains the corresponding cracking loads and

TABLE (3.3-2) CRACKING LOADS OF BEAMS

Beam	YL mm	First Crack	Cr. Load KN	Cr.Torque KNmm	Cr./Uit. B.L.ratio	Tcr/Tu ratios	Location of failure
A1	1450.00	SOFFIT					TOP
A2			2.00		0.33		
A3			1.00		0.14		
A4			5.00		0.53		
A5			4.00		0.67		
A6			3.00		0.27		
A7			10.00	2282.0	0.91	1.00	
A8			9.00	2156.0	0.90	0.91	
A9			14.00		0.88		
A10			14.00		0.88		
A11							
B1	1345.0	FRONT	6.00	1288.0	0.86	0.90	TOP
B2	1388.0	SOFFIT	12.00	2534.0	0.92	0.97	
B3	1450.0		8.00	1680.0	0.71	0.73	
B4	1537.0		9.00	1890.0	0.90	1.00	
B5	1451.0		7.00	1470.0	0.50	0.51	
B6	1440.0		10.00	2100.0	0.77	0.94	
C1	1525.0	FRONT	9.00	1918.0	1.00	1.00	TOP
C2	1380.0		11.00	2324.0	1.00	1.00	
C3	1315.0	SOFFIT	13.00	2730.0	1.00	1.00	
C4	1462.0		11.00	2310.0	0.92	0.92	
D1	1475.0	BACK	4.00	868.0	0.67	0.67	FRONT
D2	1515.0	SOFFIT	13.00	2758.0	1.00	1.00	
D3	1385.0	SOFFIT & FRONT	15.00	3178.0	0.94	0.94	
E1							
E2			10.00	3178.0	1.00	1.00	
E3	1540.0		19.50	924.0	1.00	0.34	
E4	1450.0		24.00	644.0	1.00	0.58	
E5							
F0							
F1							
F2	1418.0		19.50	1470.0	1.00	0.60	
G1	1275.0		10.00	1918.0	1.00	0.54	
G2			15.00	3150.0	1.00	1.00	
G3	1420.0		17.00	2100.0	0.87	0.99	
AA1			15.00	2940.0	0.94	0.95	

positions of the beams with the cracking ratios of the torque and bending force.

3.4. General Behaviour and Failure Patterns of Beams:

Beam Group B

Beam B1

The bending load and the torque were increased by increments of 1000 N and 210 Nm. At the sixth increment a crack developed almost simultaneously at the front and bottom faces. The torque cracking capacity was 1288 KNmm combined with a flexure load of 6KN. On increasing both loads by 120 kNmm and 1 kN respectively another crack developed at the front face and the torque gauge dropped slowly to 728 kNmm.

The maximum torque before reduction was 1498 kNmm combined with a 7 kN point load. These values are, therefore, taken to represent the ultimate strength of this beam. It was noticed that the cracked beam when approaching failure did not utilize the existing initial crack. Instead, the main failure crack developed at the front and soffit faces of the beam at a distance of nearly 175mm from the initial crack and parallell to the latter.

From the shape of the failure crack pattern of beam B1, it can be concluded that the failure was a mode 1. The compressive concrete zone, which is clearly observed at the top face, is 455mm long and has an average depth of 75mm, as determined with the aid of the concrete strain gauges at the front and back faces. The maximum tensile concrete strain, 1335 microstrain was recorded by the gauge at the lower strain gauge level close to the soffit of the beam.

Beam B2

The flexural load and the torsional moment were increased by increments of 1kN and 210 kNmm respectively. When the point load was 12kN, the first crack appeared at the soffit face, of the beam at a distance of nearly 60mm from the centreline towards the left hand support. This first crack propagated almost instantly to the front face (see figure B2). The corresponding torque was then 2534 kNmm.

The beam had been subjected to a further bending load whereas the applied torque had had an increase of 70 kNmm before failure was achieved. Thus the failure bending load was 13kN combined with an ultimate torque of 2604 kNmm.

Figure B2 shows the failure crack pattern which is not typical for a mode 1. The initial tensile crack at the bottom face progressed along an inclination of approximately 42^{o} to penetrate the front and back faces. The plastic compressive

zone established itself at the top face with a sudden explosion and crushing of concrete at the back face. This compression zone which included also cleavage lines at the front face had an estimated average depth and length of 95mm and 470mm, respectively. The maximum longitudinal concrete strain was 998 microstrain in compression at the top face of the beam. The maximum stirrups stress was however 270 N/mm^2 in the front face leg, which is lower than the yeilding stress of 342 N/mm^2.

Beam B3

The loading sequence was determined by increments of bending 1 kN load followed by 210kNmm torque until cracking occurred. The first crack took place at the intersection of the front and bottom faces on the centre line. The cracking load was 8kN combined with a 1680 kNmm of twisting moment. With the subsequent load increments, the crack developed into the bottom face and towards the mid-height of the front and back faces. The tensile crack at the bottom face was inclined at 60^o to the front and back faces the failure "cracking" angles were 40^o and 73^o respectively. These tensile cracking lines were discontinued by the compressive zone which formed at the top face of the beam. The estimated depth of this compression zone was about 58mm with an approximate length of 385mm.

As it can be seen from Figure B3, the mode of failure is type 1. This corresponded to an ultimate bending load and torque of 11.3 kN and 2310 kNmm, respectively.

Beam 4

The loading started by sequential increments of 1kN and 210 kNmm, flexure and torque respectively.

The first crack took place at mid-depth of the back face and almost simultaneously another cracking line developed at the lower end of the front face. The latter crack started at a point 40mm to the right hand of the centre line (see Figure B4).

The cracking flexural and torsional loads were 9kN and 1890 kNmm, respectively. The beam whilst sustaining an increment of the bending load of 10kN, failed before the torque increment could have been applied. The cracking torque capacity therefore represents actually the ultimate torsional strength in the case of this beam.

The failure crack surface as shown in Figure B4 is a complicated surface and of a dual nature. On the one hand it can be regarded as a mode 2 form of failure but restricted from full development by the crushing of concrete at the top face of the beam. Alternatively, a possible mode 1 could explain the tensile cracks at the bottom and back faces. This reasoning finds support in the severe vertical deflection following the first cracks. It was noticed however, that the concrete at the back face exhibited crushing. From this discription it may be concluded that the failure of beam B4 represented a form which was fully compatible with any of the three classical modes of failure. Nonetheless using conventional terms the B4 failure can be considered

as a mode 1/2.

Beam B5

The loading in the case of this beam was built up by the same sequential increment discussed before. The first crack was noticed at the front face in the form of a very small tensile crack at a distance of 35mm from the centreline towards the left hand support. The cracking flexural load was 7kN and the torque cracking capacity was recorded as 1470 kNmm. On the continuing the loading a further crack developed at the soffit face of the beam.

The ultimate strength was achieved at a flexural laod of 14kN and a relatively high torsional moment of 2800 kNmm. The mode of failure can be considered like the beam B4 as mode 2/1. This failure, at the intersection of modes 2 and 1 is shown by the small increase of the vertical deflection with no sudden rise as would have been expected for a primary flexural type of failure (i.e. a mode 1) The failure ended into a moderate explosion of the concrete which was apparently in compression at the top face of the beam. The maximum longitudinal concrete strain at this face was 935 microstrain. Whereas the maximum tensile concrete strain was 1920 microstrain and occurred at the front face.

As far as the stirrups stresses are concerned the maximum stress occurred at the leg close to the soffit face of the beam and

was 86 N/mm^2, much too lower than the yielding point, whereas in the front and back legs the stresses were as low as 37 and 6 N/mm^2, respectively,

Beam B6

The first crack appeared at the bottom face of the beam and developed into the back face more slowly than in the front face. The cracking load was 10 kN and the torque cracking capacity was 2100 kNmm. Severe vertical deflection followed the first crack which occurred at a distance of 1440mm from the left hand support.

From Figure B6 it is seen that the crack failure pattern resembles basically the feature of a typical mode 1 failure. The compressive zone at the tope face of the beam is 75mm deep and 325mm long. It is noticed that this zone is inclined with an angle of 70^o to the transverse axis of the beam. The final cracking line at the bottom face, however, did not pass through the initial cracking line which was nearly parallel to the transverse axis. Instead, the failure crack developed along a line inclined at an angle of 37^o with the longitudinal axis of the beam.

The maximum longitudinal compressive strain of the concrete was 1280 microstrain and occurred at the top face. The maximum tensile strain was recorded by the lower strain gauges at the back face, close to the soffit face of the beam, and was 1255 mircostrain.

The steel in both the longitudinal and the transverse directions did not reach yeilding. The maximum stress indicated at the back face leg of the stirrups was 78 N/mm^2. The same leg was at a stress of $40N/mm^2$ at cracking. The cracking and failure stresses in the front face leg were comparatively lower at 30 and 36 N/mm^2 respectively.

Beam Groups C and D

Beam C1

The first crack developed at the mid-depth of the front face. The crack travelled downward along a line making an angle of 53^o with the centre line, at the soffit face of the beam. The other end of the crack at the front face was intersected by the compressive zone which formed at the top face.

The initial cracking corresponded to the ultimate torque capacity of 1918 kNmm and the ultimate flexure load of 9kN. The maximum compressive strain in the concrete of 785 micro strain was recorded at the top face of the beam.

The failure, coinciding with the first crack, was sudden and extremely explosive. This might give the impression of a mode 2 type of failure. On the other hand the severe vertical deflection and the crushing of concrete at the top of the beam, all suggest a mode 1 form of failure. The failure of beam C1 is considered as a restricted mode 2 which did not fully develop because of the crushing of the concrete at the top of the beam at a comparatively low stress.

This can be attributed to the low strength concrete used in casting this beam, fc' = 25 N/mm^2. The failure in terms of the classic modes, is a mode 1/2. The compressive zone at the top had an average depth of 38mm and a length of 410mm.

Beam C4

The first crack developed under a flexure load of 11 kN and a torque of 2310 kNmm. This crack appeared at the soffit of the beam and travelled to the front and back faces.

The maximum torque was 2520 kNmm combined with 12kN, bending load, after which the torque reduced. These values are, therefore, the ultimate torque and the ultimate bending load respectively. The failure was gradual although the "plastic" concrete zone did not fully develop at the upper face of the beam. The failure took basically the form of a mode 1 with particular features of concrete cleavage. (Figure C4). This was evidently due to the high concrete strength in this case which was more than 50 N/mm^2 (fc')

The steel did not reach yielding and the bottom leg of the gauged stirrup showed a compressive stress of 28N/mm^2.

Beam D1

The incremental increases of 1kN and 210 kNmm were also applied for this beam. The first crack appeared at the intersection

of the front face and the soffit and developed into the latter reaching the back face with an angle of approximately 15^{o}. The point load was 4 kN and the torque cracking moment 868 kNmm. In the back face the crack reached about one third the beam depth. After that the strain gauges and mechanical dial gauges had stablized, a further 1000 N was applied to the beam combined with 210 kN mm torque. This extended the cracks at the front and back faces. In the latter the crack had reached nearly three quarters the depth, with associated crushing of the concrete. The crack at the soffit deepened but remained sharp without crushing.

When the flexure load was 6kN and the combined torque was 1288 kNmm, the crack advanced and more debris was observed at the back face near the top where a clear line of cleavage parallel to the top face of the beam, became evident. In the front face the crack line changed its direction and travelled towards the top along a line at an inclination of approximately 60^{o}. A the top face of the beam, concrete failed in form of crushing combined with cleavage. It was interesting to note that the concrete strain gauge at the soffit was indicating a small compression. The vertical deflection, however, was relatively large.

It is difficult, therefore to assign the beam failure mechanism to a specific classic mode of failure, but from the overall behaviour and pattern of cracking it is perhaps justified to consider it as a mode 1/2. If a mode 1 were adopted to describe the failure of the beam D1, then the cleavage compressive concrete zone had a depth of 50mm and an inclined length of 325mm with an angle of about 74^{o} with

the transverse axis of the beam.

In the case of this beam also the steel stresses did not reach the yield point. At cracking the tensile stress in the back face leg of the gauged stirrup was 28 N/mm^2 and increased to 68 N/mm^2 immediately before failure. In the top and front faces legs the very low compressive stresses of 10 and 3 N/mm^2 at cracking, increased to 7.4 and 15 N/mm^2 in tension. At failure, these low values jumped to 205 and 123 N/mm^2 at the top and front faces legs respectively The steel yield stress being 342 N/mm^2, the maximum stirrup's stress was 60 percent of the yield stress.

Beam Group E

Beam E1

This beam was tested under self-weight and pure torsion. The cracking torque coincided with the failure load of 3500 kNmm. The failure was sudden and was noticed to start as a crack on the front face near the mid-depth. This crack, which occurred at a distance of 600mm from the right hand support, propagated towards the soffit face of the beam more slowly than it approached the top.

Failure occurred with an explosion at the back face where the concrete crushed, while the bottom face spalled. The back face showed consequently extensive debris due to the crushing of the concrete. In contrast, the top face showed clear tensile

cracks without any debris.

The crack pattern at failure (cf. Figure E1) resembles the features of a mode 3 of failure combined with a mode 2. Thus the failure can be labelled as mode 3/2 or simply mode 3 if only the final ensued failure surface is considered.

The top and back face legs of stirrups were stressed in compression at failure producing 140 and 80 microstrains respectively. In contrast the tensile stresses in the front and bottom legs of the stirrup were as low as 20 and 68 N/mm^2 respectively.

Beam E2:

The bending load was increased in average increments of 1kN accompanied by torque increments of 210 kNmm. When the point load reached10 kN it was held constant, and the corresponding torque was 2128 kNmm. This was then increased by subsequent increments. During this stage, the vertical deflection was constant indicating no change in the applied bending load.

Cracking initiated at the front face when the torque was 3178 kNmm and this value represented the maximum reading on the tensile proofing ring attached to the torque jack. An explosion was followed instantly by a sudden drop in the torque. Consequently, the 15th increment marked the failure of beam E2.

From examining the crack pattern at failure (cf. Figure E2), it is clear that the failure was complex. At the top face little or no debris was present. One of the two observed cracking lines was tensile while the other was a line of cleavage which continued across the front face with the same slope to the soffit of the beam. The bottom face showed crushed concrete debris which was linked up with the compressive area of concrete that occupied the lower half of the back face of the beam where the shear stresses were subtractive. From these observations and analysing the steel and concrete strains, it can be deduced that the failure had a dual character and it is labelled, therefore, mode 2/3.

Beam E3

The sequence of loading was such as to apply a predetermined bending load of 19.5 kN in increments, while holding the beam free of torque rotation. The single point load had already been fully applied when the first torsional increment was applied. As the torque resisted by the member was 910 kNmm a very slight crack became visible at the front face and back face corners just above the soffit level. No vertical deflection change was indicated by the mechanical dial gauges before the torque had actually reached 2520 kNmm. Now that the cracking had developed, it propagated toward the mid-depth at both back and front faces.

Finally the beam failed with a maximum torque load of 2730 kNmm.

The failure was explosive and excessively severe vertical deflection was recorded. Although it is proposed to consider the failure as mode 1, the real failure surface was more complicated (cf. Figure E3) and spalling of concrete took place at the soffit of the beam.

Beam E4

This beam was loaded in bending by a predetermined vertical load which was increased until it was 24 kN, during which the beam was kept free from any torque rotation. This was ensured by monitoring the torque hydraulic jack's tensile proofing ring, the dial gauges and the movement of the torque lever arms. When the torsional moment was 644 kNmm, the first crack developed immediately beneath the single point load which was kept constant although it tended to reduce during the testing time.

The beam resisted four more increments of torque which brought the torque resistance to a maximum of 1106 kNmm. Then the torque dropped off very quickly towards zero and it was not possible to maintain the twisting moment by using the hand pump. Consequently it was concluded that E4 had failed subjected to 1106 kNmm torque combined with 24 kN bending load. The beam failed in mode 1.

Beam E5

This beam was tested under bending and shear only with no torsion.

The bending load was applied in increments of 2kN until the vertical force was 10 kN. Henceforth the load was increased by increments of 1kN. The first crack occurred at a load of 22kN at the soffit of the beam in tension. The vertical deflection was relatively low even after the first crack which took place directly beneath the vertical load.

The failure load was 28 kN. Severe deflection was noticed and a compressive hinge was apparently formed at the top of the beam.

Beam Groups F and G

Beam Fo

Increments of 1kN bending load and 210 kNmm torsion moment were used in the case of this beam also. The first crack appeared at the soffit face of the beam, 80mm from the centreline towards the left hand support (Cf. Figure 10). The cracking flexural and torsional capacity were 10kN and 2128 kNmm, respectively. These values corresponded to the ultimate strength of the beam which was badly damaged but nonetheless failed with no sudden explosion. The failure was rather gradual and the mechanism was such as to establish a compressive zone on the top face where the concrete consequently crushed while the torque gauge reduced to zero.

The failure was therefore a typical model 1. It was noticed that because of the lower prestressing force applied to the beam no spalling concrete took place.

Beam F1

The first cracking line was noticed at the front face of the beam where the shear stresses were additive. This corresponded to a flexure load of 10 kN and 3570 kNmm torque. Eventually the beam failed with no further load applied, and the failure which was explosive, coincided with the cracking capacity.

It was noted that the failure cracking line did not follow the existing first crack line. Concrete crushing debris was evident at the back, soffit and top faces of the beam. From examining the failure surface in Figure F1, it can be deduced that the failure mechanism was in reality a complex one. Features of a classic mode 2 were evidenced by the first cracking appearing at the front face and concrete crushing taking place at the back face at failure. But contradictary signs of tensile cracks, split due to cleavage and concrete crushing did in fact co-exist at the front and top faces and the soffit of the beam. In view of the complexity of the beam failure it is proposed, here, to regard it as a mode 2/3 failure. Nevertheless severe vertical deflection was recorded on failure. No strain gauges indicated yielding in the gauged stirrup or in the longitudinal steel. The concrete strains were relatively low. The maximum reading of the four concrete strain

gauges intercepting the failure section was 260 microstrain in compression at the top of the beam while the maximum tensile strain of 294 microstrain was recorded at the soffit.

Beam F2

At the sixth flexure load increment when the point load was 19.5kN the first torsion increment was applied.

The first crack appeared when the torque was 1470 kNmm, which was the total of three successive increments. The crack started at the soffit and propagated very slowly to the back and front faces. The torsional moment was increased then to 1680 kNmm, and as a result the crack proceeded towards the mid-depth at the front face though it ceased to make any progress at the back face of the beam. This situation persisted under a further increase in the torque to become 1890 kNmm. At the following increment of torque, which was 210 kNmm, the crack grew at the back face approaching the mid-height. In the front face the crack had reached beyond the mid-depth of the section. When the torque was 2310 kNmm the crack line extended beyond the mid-depth at the back face too. The maximum recorded torque load was 2450 kNmm when the failure was established with a relatively low-noise explosion accompanied by a rapid increase in the vertical deflection.

The failure as indicated in Figure F2 is complex and not a typical mode 2 or 1 and is therefore labelled as mode 2/1

Beam G1

The sequence of loading was such as to apply increments of vertical bending force while holding the beam free from any torsional moment. It was, therefore, necessary to keep the beam in a horizontal position by adjusting the torque lever arms. This was achieved by the combined action of the bearing pads at the supports and at the application point of the vertical load, which were arranged to counter-act and adjust the restraining effect of the torsionsal arms.

The predetermined vertical load was first applied in ten increments and when this load had reached 10kN it was kept constant throughout the test. The torsion moment was then applied in 210 kNmm increments. When the torque was 1918 Nm, at the 9th increment, the first visible crack appeared approximately on the intersection of the soffit and the front faces at a distance of 340 mm fromthe centreline towards the left hand support. After this initial cracking torque the beam resisted a further 5 increments to reach failure.

The failure was explosive and the concrete crushed at the top and back faces. The concrete at the front face showed less distress while at the soffit well established tensile cracks were present and no debris was noticed. The mode of failure can be discribed as a mode 2/1 (cf. Figure G1).

Beam G2

The ultimate load coincided with the first crack of 15kN and 3150 kNmm, flexural load and torque moment respectively. The failure was violent with an explosion of crushed concrete at the top and front faces.

More debris appeared at the back face which was characterised by the presence of well defined splitting lines. The mode of failure was identified as mode 2/1.

The steel strain gauges indicated no steel yielding. The maximum stress in a stirrup leg occurred at the front face leg and was equal to 41 N/mm^2, much less than the yielding stress. However, the maximum longitudinal compressive strain occurred at the mid-depth of the front face where it was equal to 945 microstrain. In contrast the maximum tensile concrete strain, 465 microstrain was recorded at the soffit of the beam.

Beam G3

This beam was subjected to 2128 kNmm torque combined with a 10kN point load. The applied torque was maintained while the bending load was increased by increments of 1kN.

When the flexure load was 17kN, the first crack developed at the soffit face and extended slowly towards the front and back faces. With a further increase of 1kN, the crack propaged towards the mid-depth at the front

and back faces (Cf.. Figure G3).

The beam reached failure when the bending load was 19.5kN. The failure was explosive and it utilized the main tensile crack at the soffit of the beam where some concrete crushing was noticed. The top face also showed a crushing concrete area, with debris.

While the front face, at the extremities of the failure line connecting the top and bottom faces of the beam, showed the existence of some debris ~~[illegible]~~ a main tensile line of cracking characterized the failure surface. This surface of the cracked concrete in the front face was further complicated by the presence of a line of cleavage which did not fully develop. On the other side, the back face showed a full crushing of concrete. If only the front and back faces of the beam at failure are considered, a classic mode 2 form of failure is described and is supported by the examination of the twisting deformation. It is noticed, however, that the mode 1 could have developed along the tensile crack at the soffit and by crushing of the concrete at the top face. However from analysing the readings of the deflection dial gauge, it is apparent that no large vertical deflections occurred.

Because of the complexity of the failure surface of beam G3 which contained features of a mode 2 combined with a less developed mode 1, the failure mode is identified as mode 2/1.

The front face stirrup's leg was stressed in compression at failure to 82 N/mm^2. The maximum tensile stress, however, was recorded in the top leg at 68 N/mm^2.

3.5 VERTICAL DEFLECTION

The bending force - central deflection curves for all the beams are presented in the figure (3.5.1) through (3.5.7). The increment by increment deflections as measured by the mechanical dial gauges at the centreline of each beam can also be obtained from Fig.(3.5.1) to (3.5.7).

The influence of M/T ratio variation:

For the beam E1 tested subject to self-weight and torsion only, a maximum upward deflection of 0.33mm was recorded. With increasing the M/T ratio to 2.3 in the case of beam E2, the maximum deflection also increased to 3.71mm, downward. As the bending moment was increased further, increasing deflections were recorded.

In the case of beam E3, with a ratio of M/T = 5.3, the vertical deflection at cracking (at front and back faces of the beam) was 7.90mm. After cracking the bending deflection curve, which was basically linear from the origin uptil observing the first crack, showed a great reduction in the slope and flattened into a plateau with the beam undergoing an extensive increase in deflection. The latter occurred subject to approximately a constant applied bending force. (: only the torque was increased to reach failure). Nonetheless the maximum value of deflection was 47.24mm at failure. (On releasing the external loading after failure, however the beam 'recovered' from some of this deflection which reduced

to a value of 30.30mm).

Further increase of the M/T ratio had the effect of creating a zone of non-linearity introduced between the basically linear parts of the bending - deflection curve joining respectively the point of self-weight on the bending axis intercept to the cracking deflection and the latter to the failure deflection. Reference is made to beam E4 (Figure 3.5.5) tested subject to a M/T = 17.2 ratio. The beam showed a cracking and maximum deflection of 19.76mm and 22.71mm respectively.

Further reduction of torsion smoothened evermore the non-linear zone. The bending-deflection curve of the beam E5, which was tested subject to pure bending and a shear force, for instance, shows clearly such pattern. The maximum deflection was 30.10 mm as compared to a cracking delfection of 9.96mm.

In the three beams, discussed above, it is noted from their bending-deflection curves that the 'cracking point' is located rather higher than the 'end' point of the first linear zone of the curve. As this could be due experimentally to the difficulty and consequently, the delay in marking the first visible cracks instanteously on their occurrence; it can also be attributed to the development of 'micro-cracking' that might have existed under much lower loads.

The effect of increasing the Prestressing Force (and its eccentricity)

This effect can be examined by studying the bending-deflection curves

of beams A1, to A11, AA1 an AA2. No detailed study is attempted here, but an outline of the deflectional behaviour and the limit state is presented.

The beam A1, tested with zero prestressing force, deflected considerably at failure. The maximum deflection recorded was 56.80mm, one increment before ultimate load, which was the last deflection reading. As this beam was cracked subject to self-weight when placed on the test rig and before applying any live torque or bending load, the first deflection reading was therefore, regarded as the "cracking" displacement which was 7.21 mm. Reference is made to the curve shown in Figure (3.5.1).

Applying an effective amount of a prestressing force equal to 11.373 kN to the beam A2 did not affect the basic features of the beinging deflection curve as described above for beam A1.

The advantageous effect of the presence of a prestressing force upon the behaviour of the deflecting beams was pronounced increasingly as the applied prestressing force increased to 20.95 kN, 39.90 kN and 53.69 kN in beams A3, A4 and A5 respectively. In all these beams the initial semi-linear line segment was generally extended by shifting the visible cracking level. A non-linear segment followed which was linked up with the final line-segment of the curve. For the latter, the reduction in the slope was evident but not severe. The effect of increasing prestressing on the bending - deflection curve was clearly pronounced by the failure deflections of the beams:

A3, A4 and A5 which were 39.22mm, 21.26mm and 18.92mm respectively.

Beam A6 which was post-tensioned by an effective force of 67.69 kN, marked a transition stage between the lower and higher prestressed beams. The cracking deflection was 12.50mm downward but preceeded by an upward deflection of 1.68mm. By contract, the maximum deflection was 61.1mm which as high. One specific feature after cracking was the development of a very noticeable non-linear segment accounting for a 25mm, or 40%, of the maximum deflection. At the end of this segment, the curve changed slope and consequently followed the trend of a straight line increase. The latter represented roughly anouther 40% of the total deflection recorded at failure.

For beams A7, 8 and 9, prestressed by forces ranging from 41.8 to 63.4% of the tendons yielding force of the tendons, the resistance to vertical deflection improved considerably and exhibited a longer and steeper initial semi-linear segment. The latter was observed to run smoothly into a much clearer non-linear intermediate part prior to end up by the final part of the curve, which was nearly flat. Cracking and maximum deflection were in the order of 6.71mm, 29.24mm, 5.89mm, 29.24mm and 8.36mm, 21.46mm respectively. It is noted from the Figure (3.5.1) of the bending deflection curves of these beams that the visible "first crack" points are located well away from the initial semi-linear segments and are at the end of the non-linear segment. It was difficult experimentally to detect first visible cracking with any reasonable

degree of precision. In addition internal cracks may be present.

Increasing the prestressing force further extended the linear portion of the curve. The transition from the initially near straight-line part into the final load segment took instead the form of a sharp reduction in slope. The failures of both beams A10 and 11 with prestressed froces as high as 128kN and 150 kN respectively, were brittle and no clear visiable warning of failure was given by the increasing deflections. The deflections were for beams A10 and A11 respectively: 4.52mm and 26.65mm, and 6.27mm and 22.25mm at cracking and ultimate stages respectively. The prestressing force therefore cannot be increased indefinitely because excessive prestressing can lead to explosive brittle failures. Similarly, the advantage of reducing vertical deflection cannot be utilised without limits, because a beam with a very limited vertical deflection may fail in mode : 2(or 3), as was the case in beams A10 and A11 and (AA1).

At a relatively high level of prestress similar to that applied to beam A11 (:150kN), the increasing (or decreasing) of eccentricity achieved by lowering (or raising) the upper layer of the prestressing steel, did not have any significant effect. Fig. (3.5.1C) shows the curves of AA1, A11, A9 and AA2 beams. The latter which has an eccentricity of 49mm. resisted the live bending load of 18kN and deflected downward at the centreline by 7.01mm at failure, which was in mode 3. In contrast beam AA1, where the eccentricity was 13mm, the failure occurred at 16.o kN as the cracking load (crack being at front

face) and a vertical deflection of 5.92mm. The failure was in mode 2. Apart from the absence of the ascending end-part from the both curves, a direct comparison with bean AA1 was therefore, not possible because the numerical values of cracking and limit state deflection referred to were from differing modes of failure.

Figure (3.5.2) shows the bending force - deflection curves for the six beams of Group B, in which the prestressing steel area was increased. The maximum deflections were 8.69mm, 8.51mm, 13.69mm, 9.07mm 8.89mm and 21.16mm for beams B1,B2,B3, B4 B5 and B6 respectively. The variation of deflection was fairly minor, if beam B6 was excluded. The latter, however, deflected in fact 11.68mm, one increment before failure. In general, the shape of the curves was similar, with a smooth change of slope until failure took place.

The effect of increasing the concrete strength on the bending force-deflection curve is shown in the Figure (3.5.3). As the concrete strength increased from beam C1 to beam C4, the slope of the initial near straight line segment of the curve, also increased. This was followed by a region of non-linearily leading smoothly to a much shorter and steeper end-segment. Close to failure beam C1, in particular, exhibited a drastic increase of deflection, from 4.93mm up to a maximum of 26.77mm. The rate of this increase, however, was low. Maximum deflections were 8.10mm, 6.96mm and 8.92 for beams C2, C3 and C4 respectively.

The effect of varying the b/h ratio, by increasing the breadth only, was demonstrated by testing beams D1,2 and 3. The results are shown

in Figure (3.5.4). As expected, the torsional and bending cracking capacity increased substantially. In contrast, the cracking displacement, for the three beams, was constant and equal to 4.83

The locations of the cracks for beams D1,2 and 3 were at the back face, bottom face and at the bottom and front faces respectively. In beam D2 no ascending segement line was observed and non-linear segment did not develop either, hence the cracking displacement coincided with failute deflection. For beam D3, the cracking dispacement deviated from the initial slope-line and was followed by a much reduced slop-line to produce a maximum value of 9.02mm deflection. Beam D1 also exhibited some postcracking deflection which was recorded up to 10.52mm as a maximum. The transition from the precracking stage was not, however, gradual but abrupt and discontinuous. The first slope-line, in particular, was non-linear and the "first visible crack" was considerably delayed and occurred well beyond this first segment of the curve.

It is recalled that in the beginning of this subsection the deflectional behaviour of the E beam group was discussed. The effect of increasing the size and spacing of the stirrups for these beams is as follows: The beam F1, for instance, represented a counterpart of beam E2 in design and loading ratio which was fixed at 2.2 as a value for M/T ratio. It is shown in the Figure (3.5.6) that up to cracking the effect was not a large increase in the slope of the first near straight line of the curve. The latter for beam E2 however, was marked by non-linear fluctuation and was curtailed shortly

after cracking. With heavier stirrups in beam F1, much longer end-part of the curve extended the deflection to a maximum of 20.32mm. Subjected to a higher M/T ratio of 5.88, the beam F2 showed signs of cracking (at the soffit) accompanied by a deflection of 7.57mm whilst its maximu deflection was 11.94mm. The last two numerical vlues should be compared with those obtained from beam E3 7.90,, and 9.57mm (penultimate) or 47.24mm at failure. Finally, doubling the stirrups spacing of beam F2 in beam G3 resulted in cracking and maximum deflections for the latter equal to 9.58mm and 11.58mm respectively.

The general trend of the curves of the paired beam groups E, F and G are presented in the Figures (3.5.5.6 and 7). The cracking and maximum deflections for these beams are presented in the following table:

Table DEFLECTIONS OF GROUPS E, F and G

Beams	M/T ratio		Cracking	Maximum
E2	2.34		3.71mm	3.71mm
F1	2.20	Av 2.25	2.74mm	20.32mm
G1	2.20		3.58mm	6.60mm
E3	5.27		7.90mm	(9.37mm)
F2	5.88		7.60mm	11.94mm
G3	6.49		9.58mm	11.58mm

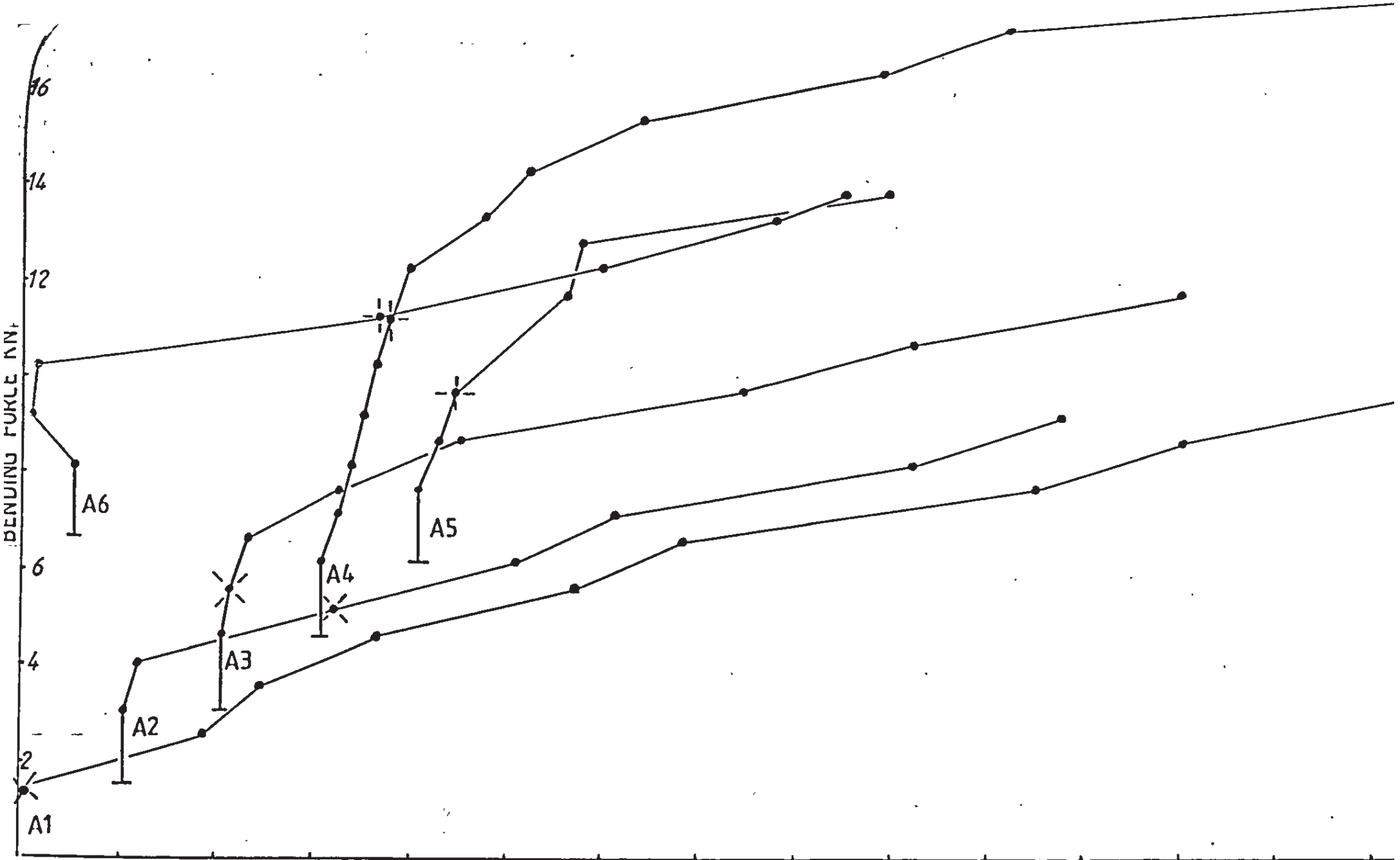

FIGURE 3.5.1a RELATIONSHIP BETWEEN BENDING LOAD & CENTRAL DEFLECTION - SERIES

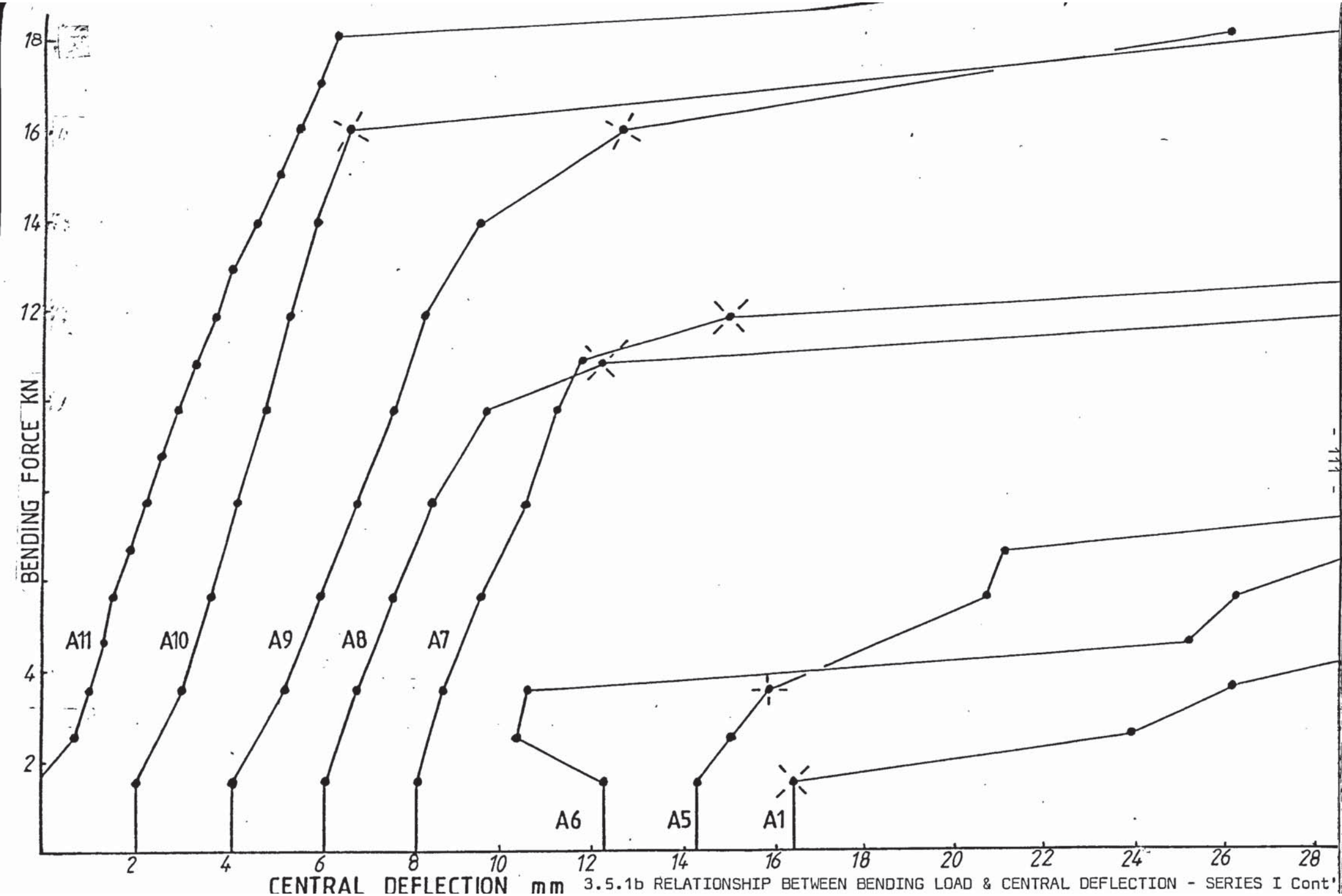

3.5.1b RELATIONSHIP BETWEEN BENDING LOAD & CENTRAL DEFLECTION - SERIES I Cont'

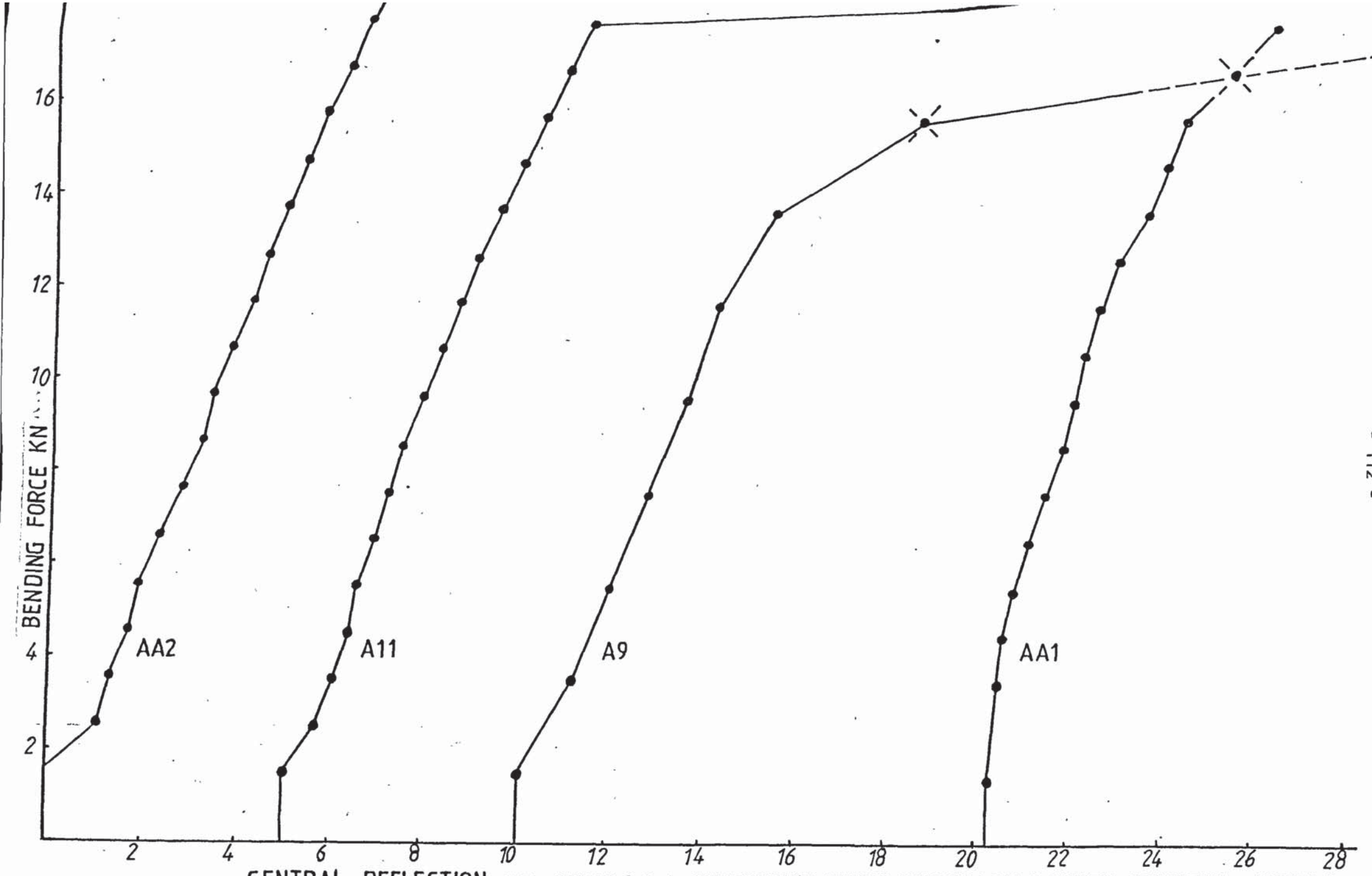

FIGURE 3.5.1c RELATIONSHIP BETWEEN BENDING LOAD & CENTRAL DEFLECTION - SERIES I Cont'd.

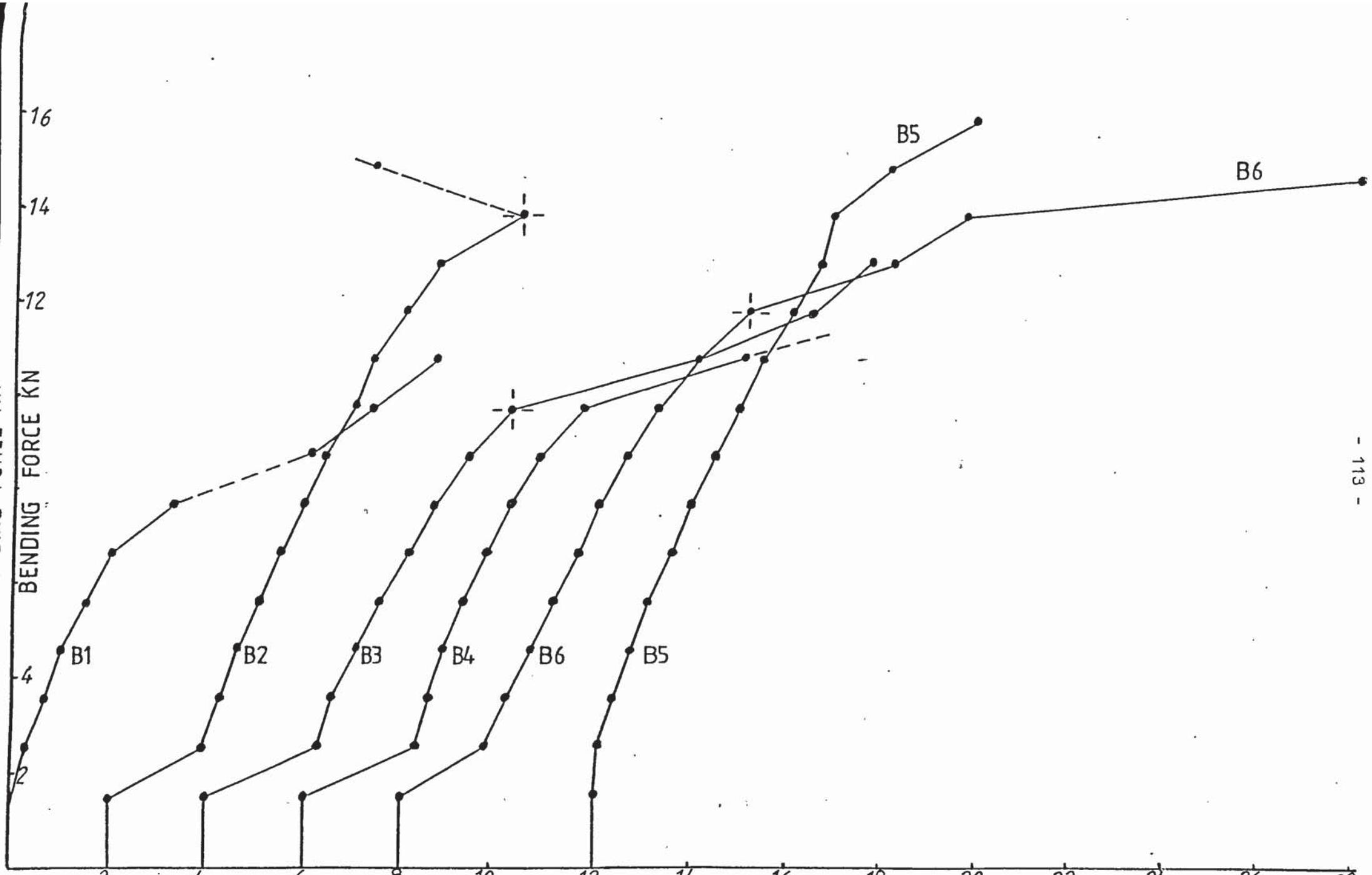

FIGURE 3.5.2 RELATIONSHIP BETWEEN BENDING FORCE & CENTRAL DEFLECTION SERIES II

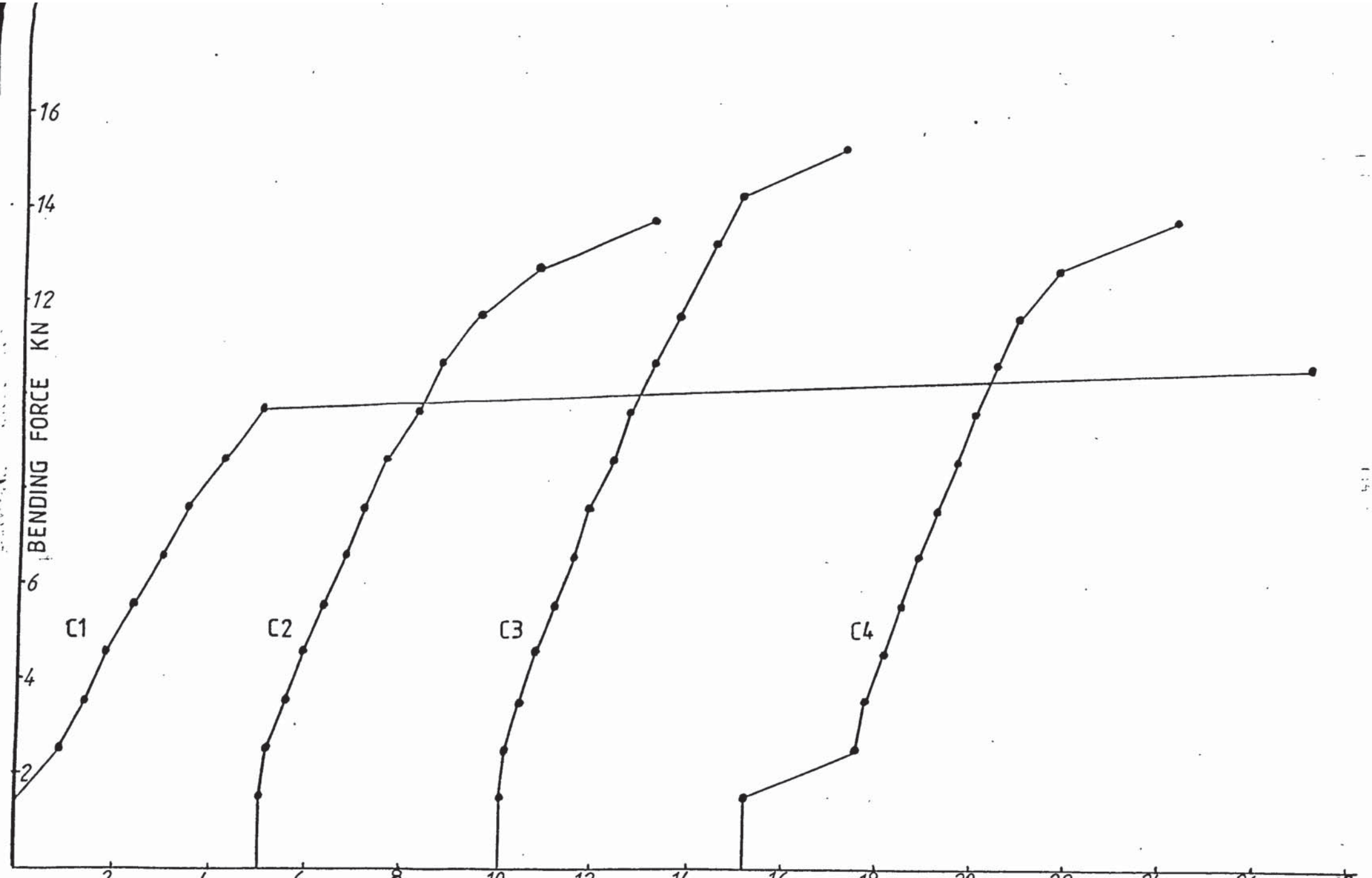

FIGURE 3.5.3.RELATIONSHIP BETWEEN BENDING FORCE & CENTRAL DEFLECTION - SERIES II.

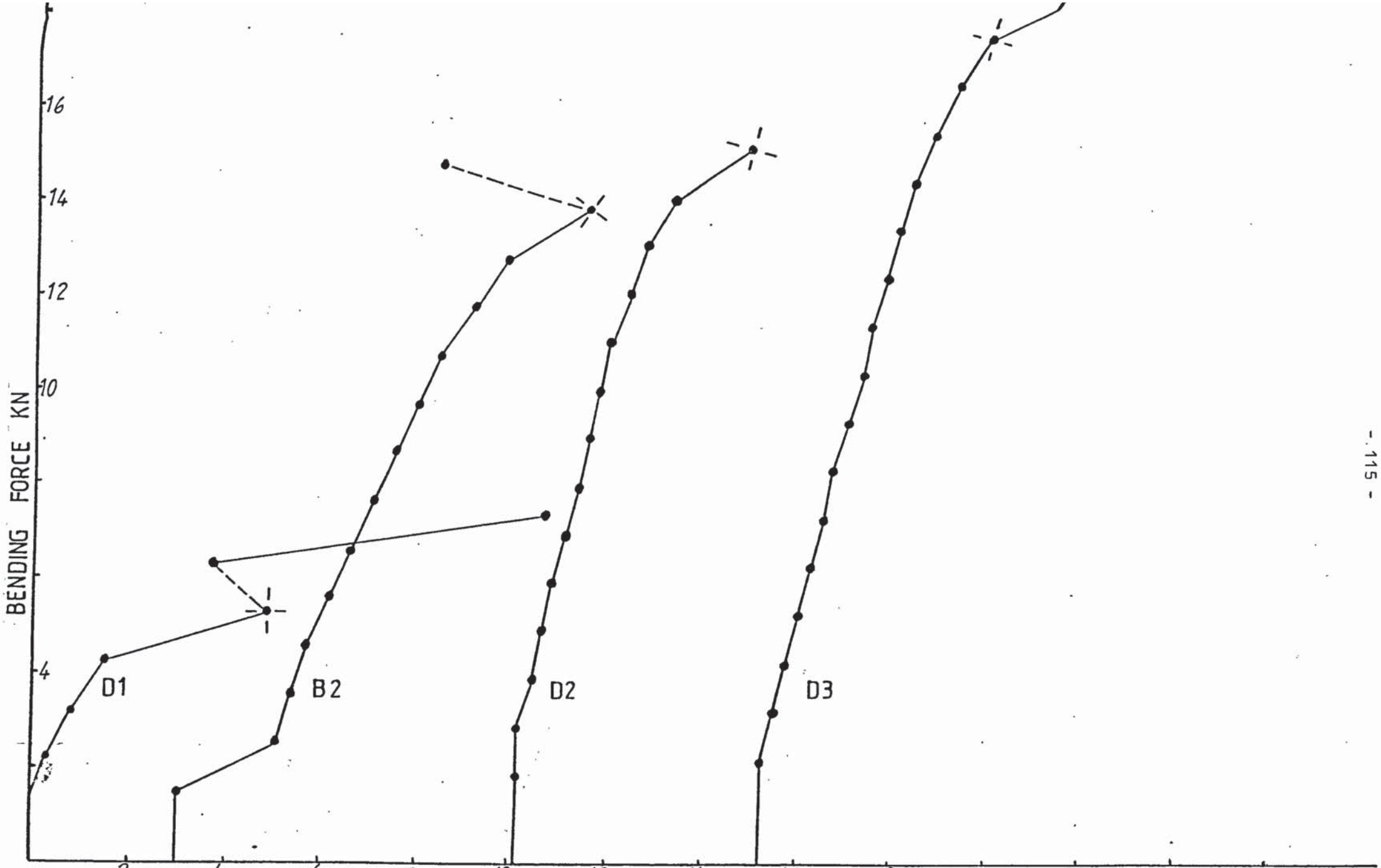

FIGURE 3.5.4. RELATIONSHIP BETWEEN BENDING FORCE & CENTRAL DEFLECTION - SERIES IV

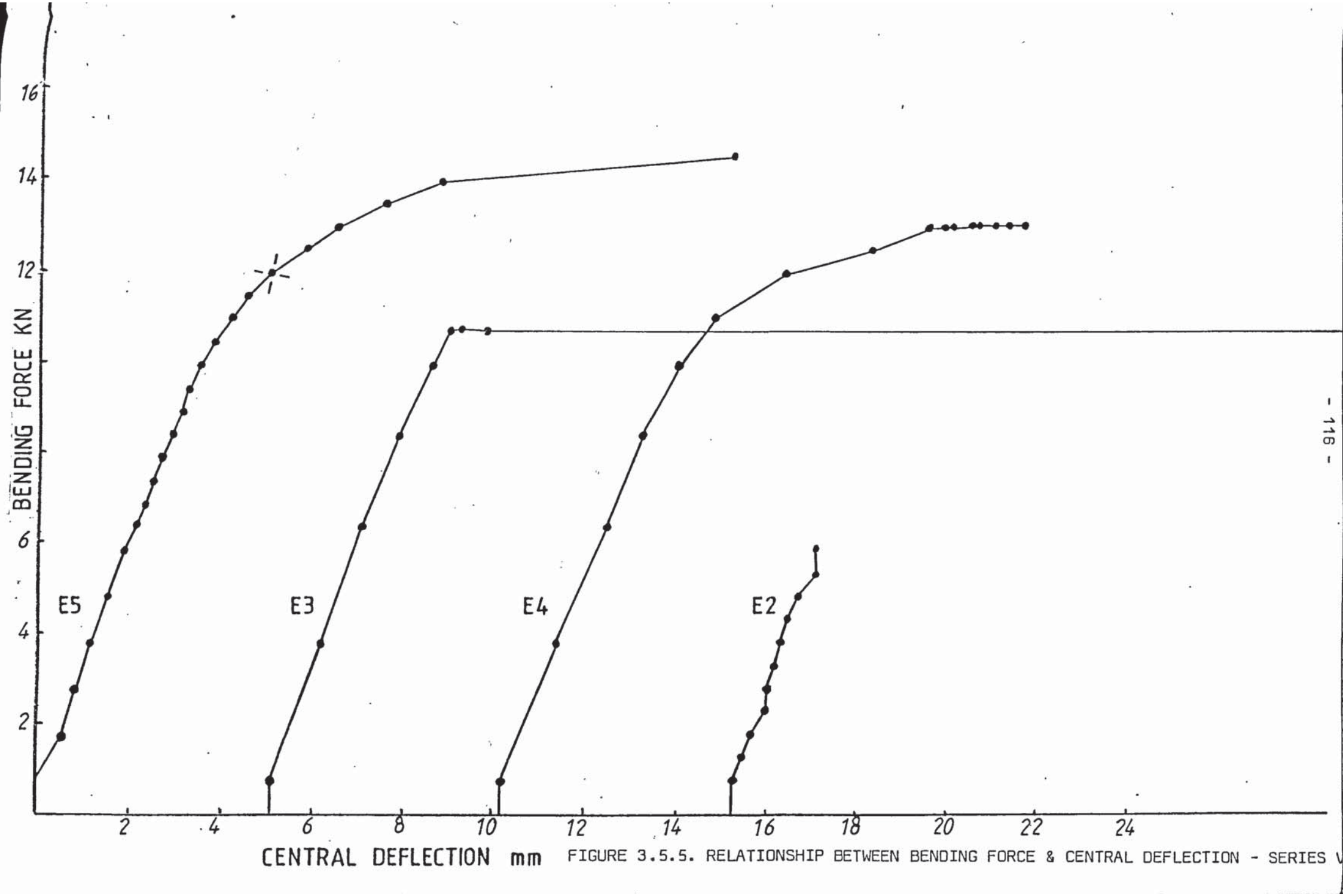

FIGURE 3.5.5. RELATIONSHIP BETWEEN BENDING FORCE & CENTRAL DEFLECTION - SERIES V

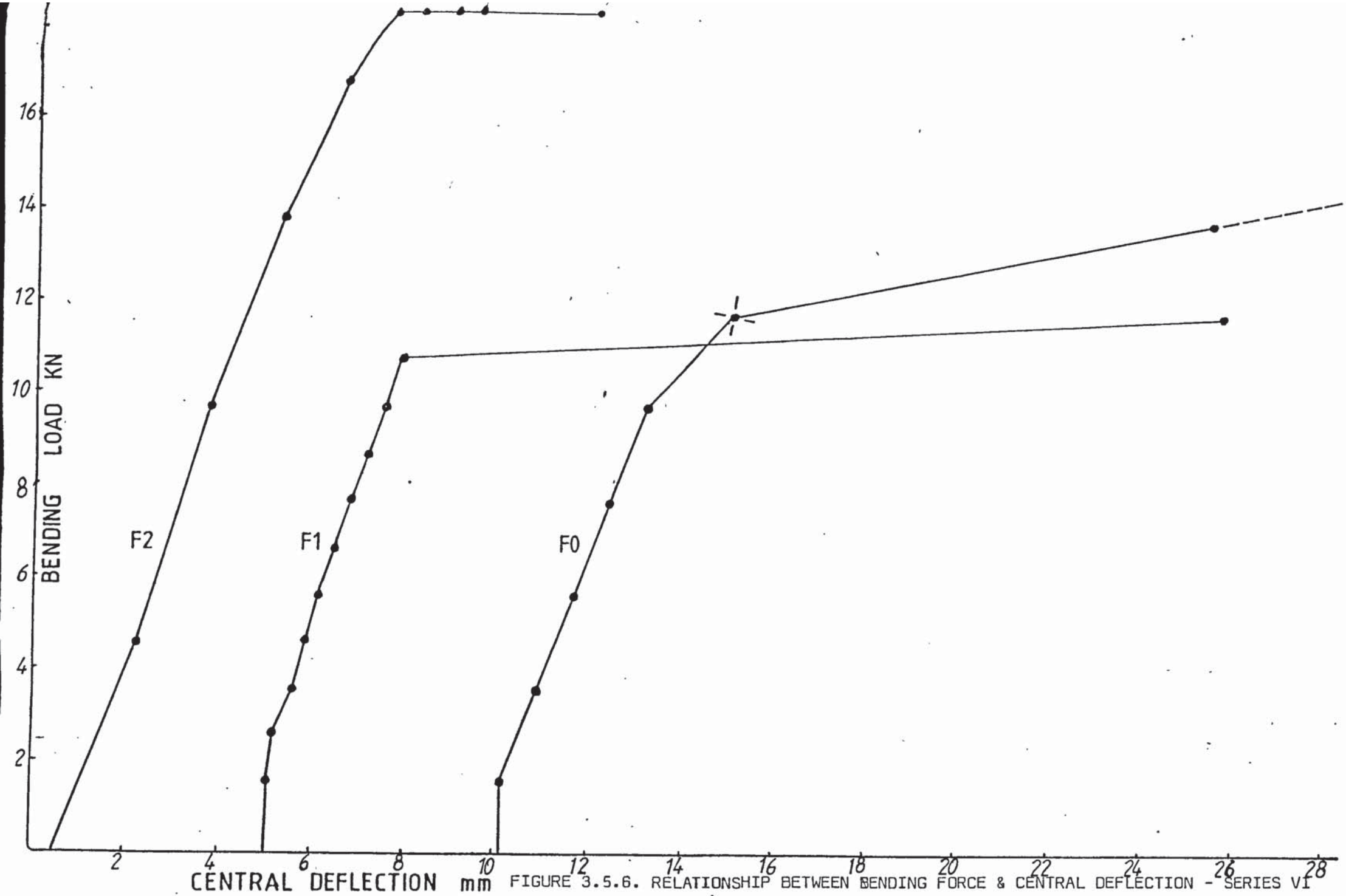

FIGURE 3.5.6. RELATIONSHIP BETWEEN BENDING FORCE & CENTRAL DEFLECTION - SERIES VI

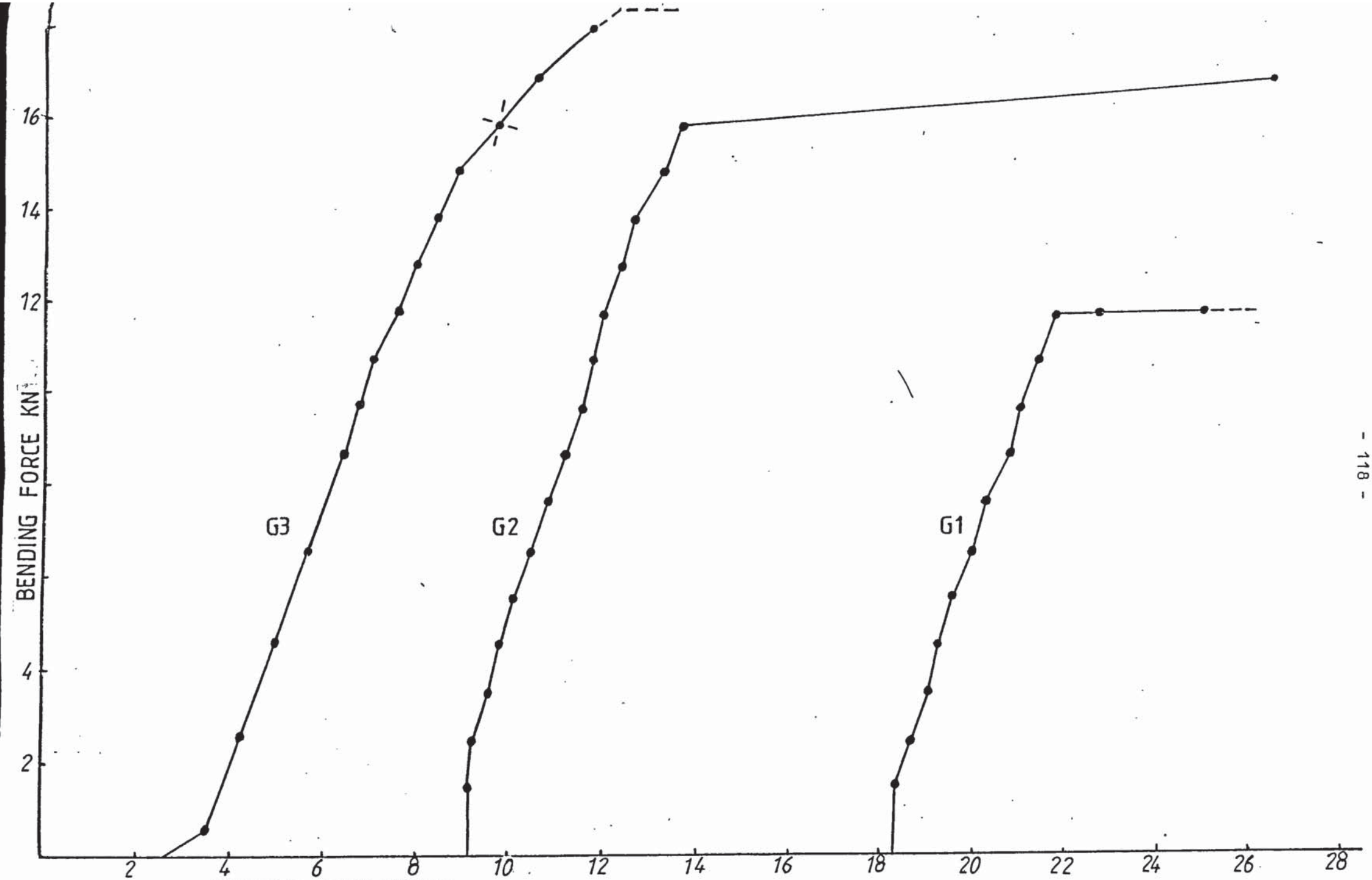

FIGURE 3.5.7. RELATIONSHIP BETWEEN BENDING FORCE & CENTRAL DEFLECTION - SERIES VII

3.6 TORSIONAL ROTATIONS

The torsional moment rotation curves for the thirty-six beams tested subject to torsion and combined loading are presented in graphical form in the Figure (3.6.1) through (3.6.6). The numerical vlues for the incremental increased of rotation as measured by the mechancial dial gauges at the end of each beam, can be obtained from Fig.(3.6.1) to (3.6.6).

A most general shape of the curve would be described as rising through the origin with a certain slope, known in the literature as the Initial Torsional Stiffness (I.T.S). Increasingly reducing in slope over a range of semi-linearity, the curve runs into a semi-non-linear bend leading generally, through a substantial drop in slope to near-plateau limit line. The plateau was generally the ultimate torsional strength of the tested beam, but in some beams a descending (or ascending) branch of the curve was observed. In addition to the varying stiffness properties along the curve, the maximum and cracking rotations are of main concern in this discussion. Furthermore, in the analysis of torsional deformations, a number of parameters is involved including prestress, concrete strength, geometrical shape, torsion span etc, on which variation the rotation and strength may depend.. In this subsection, it is proposed to examine the rotational curves of the tested beams and assess the effect of the variation of such parameters upon the behaviour and deformations.

Increasing the prestressing force as can be seen from Figure (3.6.1a), did not substantially affect the initial slope of the torsion

in rotation curve, provided that the beam was not pre-cracked. The average value for the I.T.S. was 328 kNm^2 with a standard deviation of 42.64 kNm^2 and a 13% as the coefficient of variation of the total of seven beams from A4 to A11 within a range of variation of the prestressing force from 15 to 64% of the tendon "yeild" force. This average value is 67.5% of the elastic:

St. Venant stiffness as calculated from : $K = \frac{0.213\ E_c\ hb^3}{2(1+\nu)}$

and substituting 30 kN mm^2 and 0.15 as nominal values for E_c and ν respectively. Such elastic formulae assume that the section is uncracked. Therefore it is expected for the partially uncracked and the precracked section to deviate considerably from the elastic stiffness as calculated above. Actually beam A1, which was cracked before applying the live loading, showed in an initial stiffness of 58.80 kNm^2, which is only 12% of the elastic value. In contrast to beam A1, with no prestress, the beam A2 which was prestressed to 5% showed a very high initial stiffness which on cracking in the next increment, however, dropped to 51.46 $KN \cdot mm^2$

The beam A3, prestressed by 8% rotated by only 0.056 and 0.112 rad ($mm \times 10^{-6}$) respectively before and immediately after cracking. Cracking occurred at 15% of the ultimate torque resistance of this beam. From the curve of this beam, in figure (3.1.1a) it is seen that during the interval in which the applied torsion was increased to 30% of the ultimate strength, the rotation remained constant. On continuing the loading further, a sudden drop in the slope occurred which became approximately 43.96 kNm^2 when the applied torque was

44% of the ultimate. It was, also, observed that a third reduction in the slope had occurred reducing the stiffness to 23.53 kNm^2. The maximum rotation in beam A3 was 50.52 rad/mm x 10^{-6} which was high compared to the two beams A1,A2 and the two beams A4,A5 prestressed by 0, 5% and 15,22% respectively. As the average maximum rotation for these four beams was 25.00 $\pm$ 4.04 (16.2%) rad/ (mm x 10^{-6}), the exceptionally higher value for beam A3 is thought to be due mainly to the lower concrete strength ($fc' = 25.86\ n/mm^2$) used unintentionally in casting this beam.

It was observed that with increasing prestress, the first slope reduction took place under higher torque for the same rotation and consequently the torsional stiffness increased as the prestressing force increased.

The cracking and maximum rotations for Series A beams are shown on the Fig.(3.6.1a,b). It is obvious, from these values, that increasing the prestressing force had a dual effect. Increasing the rotational angle at which cracking became visible was accompanied by a decrease in the maximum rotation at failure. An extreme case is beam A11 (cf. Figure 3.6.1b) prestressed by 64% where a rotation of 19.16 rad/(mm x 10^{-6}) represented the roations at both the cracking and maximum load. This sudden brittle failure is to be avoided in design on the grounds of the requirements for ductility and post-cracking strength.

Figure (3.6.1a,b) might be divided into three regions:

I - beams prestressed from 0 to 25% of the tendon "yield" force

II beams prestressed from 25 to 55% of the tendon "yeild" force
III beams prestressed as high as 65% of the tendon "yield" force.

Region I included five beams, discussed above, all of which (except some particulars concerning beam A4) showed an early cracking but good postcracking rotational performance which improved as the prestressing force increased. It was also found that increasing prestress affected the final pre-failure segment of the curves e.g. curve A6.

Region II: Increasing the prestressing force resulted in a flat peak. In the case of beam A6 (prestressed by 27%) ample warning of the impending failure was given because the failure followed a period of increasing rotation under unrising torsion. This type of behaviour has been observed by previous reseachers. Zia (1961)(40) used similar observations to argue that the stirrups yielded in his prestressed beams. In 1968 Hsu (45), however, regarded the flatness of the curve as a sign of a state of equilibrium according to his model of skew-bending for reinforced concrete beams. The readings from the stirrups strain gauges of beam A6 in the present investigation invalidated Zia's argument in this case because yielding was not present in all of the four legs. A "critical equilibrium state" is considered to be a satisfactory explanation. This agrees with Hsu's interpretation and does not assume yielding of the stirrups.

On further increase of the prestressing force, the first approximate straight line segment of the curves developed with diminished non-linearity. The slope at the end parts decreased with sudden drop

in the load resistance but generally not very large ultimate rotations.

Region III included beams prestressed to nearly 60% prestressing the curves of beams A10, A11 showed longer and more developed initial line-segments. These were followed by a less clear non-linearity segment with a slightly upward inclined end- part as can be seen from Figure 3.6.1b

It is noted, here, that eccentricity (or depth of upper steel layer) was found to be of no major consequence for the torsional rotation, compared to beams of similar properties. Reference is made to Figure (3.6.1b) in which the rotations of beams AA1 (:e=10mm) and AA2 (:e = 49mm) are plotted.

It is deduced from Figure (3.6.2) that increasing the tensile (prestressing) longitudinal steel, in five intervales, from 0.66 to 1.98% did not affect the origin slope of the torque - rotations curves. The initial torsional stiffness was consequently, considered to be independent of the quantity of the prestressing steel. In Table (3.6.2-1), the Initial Torsional Stiffness values of the series II beams are presented. These values varied between 278 kNm^2 and 355 kNm^2 with a mean of 316 kNm^2 and a coefficient of variation of 12.03%.

TABLE 3.6.2-1

Beam	$m\%$	$\int l\%$	$\int t\%$	I.T.S
B1	1.497	0.660	1.101	300.0 kNm^2
B2	1.99		1.321	333.3
B3	2.994		1.761	242.4
B4	3.493		1.981	363/6
B5	3.992		2.200	336.0
B6	4.491	1.980	2.421	323.10

$\sum_{1}^{6}$ 316.4 ± 38.05 kNm^2

c.v. = 12.03%

$\int_s = 0.441\%$

TABLE 3.6 -2-2

Beam	Cracking T.S.	Ulimate State Tors. S.
B1	188.235 kNm^2	148.750 kNm^2
B2	250.890	127.450
B3	227.030	161.540
B4	198.950	198.950
B5	207.040	174.550
B6	218.750	152.38

Cracking T.S.:

$\sum_{1}^{6}$ 215.15 $\pm$ 20.35 kNm^2

c.v. = 9.5%

U.T.S:-

$\sum_{1}^{6}$ 160.60 $\pm$ 22.26 kNm^2

c.v. = 13.86%

The behaviour after visible cracking was not simple and non-linear variation was also observed in some of the ending parts of the curves of the B group beams whilst some others were

approximatley straight lines. The examination of the behaviour of the test beams was complicated by two laboratorial difficulties. Firstly, there was in many cases the delay betweem the occurrence of the 'first' crack and its observation. Secondly, as the obversation was limited to "surface" cracks only, it was noticed in addition that in some cases a certain crack was identified assuming it was the first, but in subsequent increments, of load, however, such a crack closed and/or a different crack was found which might have occurred earlier. Consequently, it was not easy to mark on the curve where cracking initiated so as to divide the curve into segments for examination. In addition to these difficulties, it was not possible to control the exact mode of failure for the tested beam.

Nevertheless if straight lines are drawn between the visible cracking and ultimate rotation points and the origin - two indexes can be calculated. The slope of the line drawn from the origin to the point of cracking rotation is called the Cracking Torsional stiffness (C.T.S). Similarly, the Limit Torsional Stiffness (L.T.S) is defined by the slope of the line joining the maximum torque rotation and the origin. Their use in this subsection is to provide a convenient means for the assessment of the torsional stiffness. In Table (3.6.2-2) the values of C.T.S and L.T.S are presented for Group B beams. The cracking torsional stiffness varied between 195kNm^2 and 236 kNm^2 with a mean of 215 kNm^2 and coefficient of

variation of 9.5%. The mean value of 68% of the I.T.S.

In the table are given also the values of the limit torsional stiffness. These values fluctuated between 183 kNm^2 and 138 kNm^2 with a mean of 161 kNm^2 and 13.86% as a coefficient of variation. The mean value is only 50.9% of the initial torsional stiffness. (One special case was the post cracking behaviour of beam B3 - cf. Figure (3.6.2) which changed not only slope after cracking but followed a hyper-bolic path to failure). The higher coefficient of variation in comparison with 9.46% for the Cracking Torsional Stiffness suggests that the rotation near failure may not be totally independent of the longitudinal prestressing steel ratio, even if unbonded.

The minimum and maximum rotations at failure were 8.687 and 20.387 rad/(mm x 10^{-6}) which occurred in beams B1 and B2 respectively. This increase appeared to be independent of the steel percentage, but the rotations at cracking and ultimate stages are listed in the following table:

Beam	Cracking	Ultimate	(ult. - Cracking)/Cracking
B1	6.40	8.69	0.358
B2	10.12	20.39	1.015
B3	7.42	14.31	0.929
B4	9.52	9.52	-
B5	7.10	16.53	1.328
B6	9.58	14.14	0.476

TABLE (3.6.2 -2) Series II Torsional Rotations (inrad3mm x 10^{-6}

The effect of increasing the total steel volume percentage ($\int t$), by increasing the web steel content ($\int s$) only, was observed by testing Groups F & G beams, the torsional rotation curves of which are presented in Figure (3.6.6). From the latter the values of I.T.S. were computed and are presented in the following table:

Beam	I.T.S.	Average $\frac{M}{T}$	cr.	ult.
G3	303		5.63	6.82
G2	400	4.20	-	20.18
G1	327		4.96	16.68
F1	286		5.87	25.4
F2	385	4.23	1.66	9.21
F0	267		6.11	17.11
E1	328		-	-
E2	375		-	12.32
E3	345	3.81	2.91	10.995
E4	132	17.20		
(B2)	333	3.56	10.12	20.39

I.T.S. Mean = 335.7 kNm^2

S.D. = 42.87 kNm^2 For total : 9 beams

C.V = 12.77%

Table (3.6.2 -4) Beam Groups E,F and G INITIAL TORSIONAL STIFFNESS (in rad3mm x 10^{-6})

The initial stiffness varied from an average of 335.7 kNm^2 between 378.5 kNm^2 and 292.8 kNm^2 with a coefficient of variation of 12.77%. This low value suggested that the initial stiffness was independent of the web steel percentage and spacing of stirrups as provided in this investigation. The ultimate rotations were affected by size and spacing of stirrups. Interchanging the 4 mm - size stirrups (in E beams) by 6mm - size in F beams resulted into an increase of 18.3% over the average ultimate rotations of E beams. Conversely, the cracking rotation decreased and hence the average cracking rotation of F beams was only 53.8% of that for the corresponding E beams.

With increasing the spacing only in G beams, their average cracking rotation decreased below 10.26 rad/mm x 10^{-6} as compared to 4.55 rad/mm x 10^{-6} in F beams. In contrast, the average ultimate rotation increased as the spacing decreased, from 14.56 rad/mm x 10^{-6} to 17.24 rad/mm x 10^{-6} in G and F beams, respectively. Reference is made to the following table:

Group Beams	Size: Spacing	Ave. cr	Ave. u
F	6mm : 70mm	4.55 rad/mmx10^{-6}	17.24 rad/mmx10^{-6}
G	6mm : 140mm	10.26	14.56
E	4mm : 70mm	8.45	14.57

TABLE (3.6.2 -5)

Table (3.6.2-5) Beam Groups F,G and E The effect of stirrup size and spacing on the average cracking and ultimate torsional rotation.

Finally, increasing both the stirrups size and spacing produced an increase in the cracking average rotation from 8.45 rad/mm x 10^{-6} to 10.26 rad/mm x 10^{-6} in E and G beams respectively. However, the average ultimate rotation remained constant at an average value of 14.56 rad/mm x 10^{-6} for the total of six beams in both the groups E and G.

In the Figure (3.6.5) increasing the M/T ratio is seen to have a considerable affect on the initial torsional stiffness. The variation was inversely proportional and with an increase in M/T ratio from 2.34 (beam E2) to 17.20 (beam E4), the I.T.S. decreased from 375 kNm^2 to 132 kNm^2, respectively. The initial torsional stiffness, instead was found to vary directly proportional to the loading ratio 2T/Vb. Hence, for the beams E2, E3 and E4, the initial stiffness of 375 kNm^2, 345 kNm^2 and 132 kNm^2 corresponded to the 2T/Vb ratios of 12.60, 5.60 and 1.60 respectively. For the same beams, the maximum rotations recorded were: 12.32, 10.995 and 8.31 rad/(mm x 10^{-6}) respectively. This suggests a directly proportional variation of the maximum rotation with the 2T/Vb ratio. It is, therefore, concluded that the initial torsional stiffness and the maximum rotations at ultimate load varied directly proportional to the loading ratio 2T/Vb.

In Figure (3.6.3) the torsion-rotation curves for Series III beams are presented. It is noted that with increasing the concrete strength the cracking load increased and the general form of the curve became more linear and the slope increased. The initial torsional stiffness, in particular, increased with increased concrete strength from 133 kNm^2 for C1 to 286 kNm^2 and 533 kNm^2 for beams C2 and C3 respectively. Despite the considerable increase in the concrete strength of beam C4 over that of C3, the former exhibited an initial stiffness of 286 kNm^2. However, the maximum recorded rotation of 13.64 rad/mm x 10^{-6} occurred in beam C2. By contrast, the beam C4 exhibited the minimum rotation at cracking which was 8.29 rad/(mm x 10^{-6}) two increments before failure. At failure, the maximum rotation 12.36 rad/mm x 10^{-6} was recorded. This value was very close to the maximum value occurring in C2 and within 2.1% of it.

In Figure (3.6.4), the torsional-rotation curves of the beams D1, D2, and D3 are presented. It was noted that with increasing the width of the beam, the torsional resistance and the rotational performance improved progressively. In particular, the initial torsional stiffness increased from 308 kNm^2 to 500 kNm^2 and 677 kNm^2 for the three beams respectively.

The cracking and ultimate rotations for the beams D1, D2 and D3 were 5.39, 14.11 rad/mm x 10^{-6}, 10.42, 10.42 rad / mm x 10^{-6} and 6.78, 9.45 rad mm x 10^{-6} respectively. Therefore as the width increased the final torsional rotation produced at the limit state

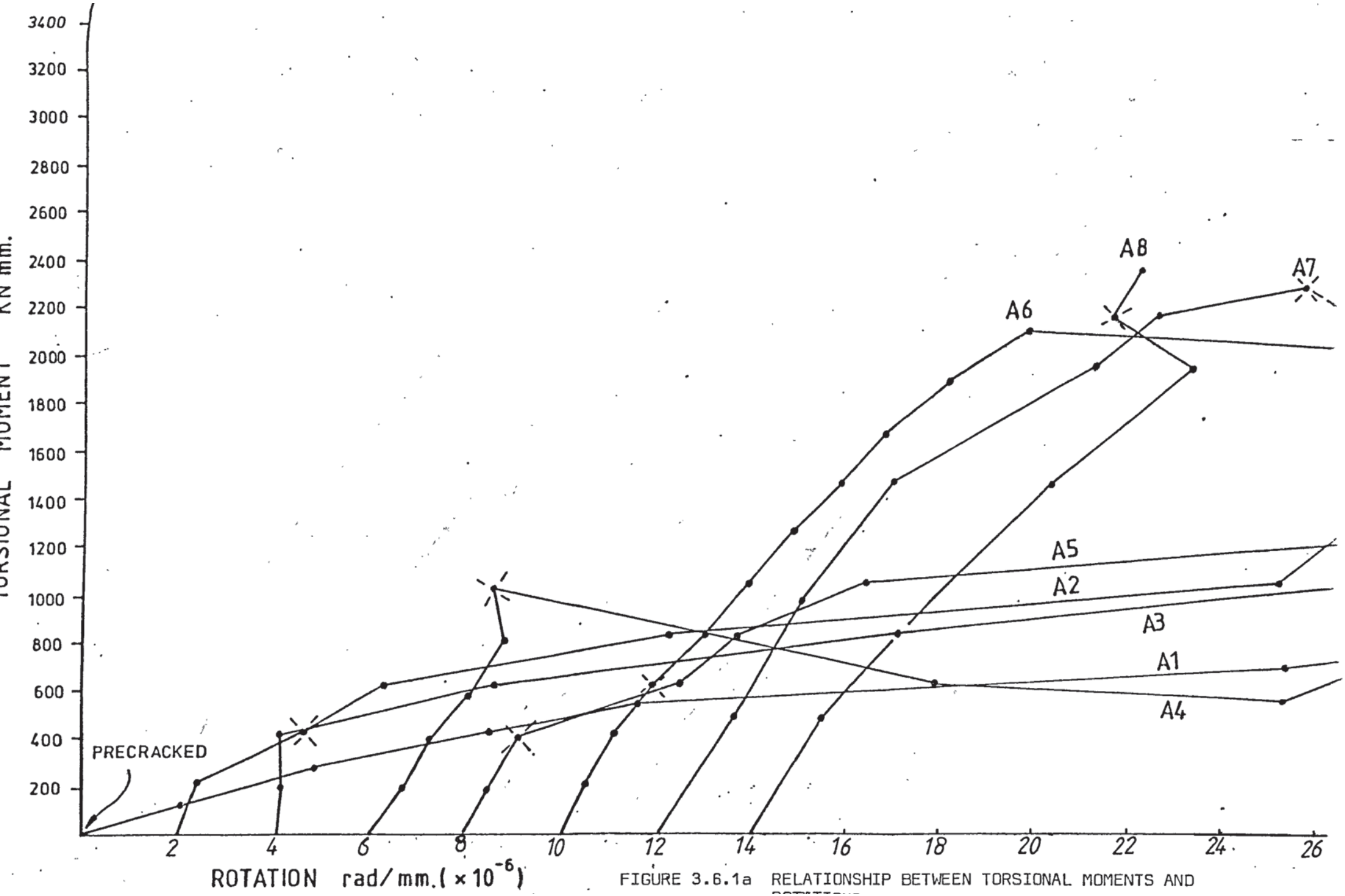

FIGURE 3.6.1a RELATIONSHIP BETWEEN TORSIONAL MOMENTS AND

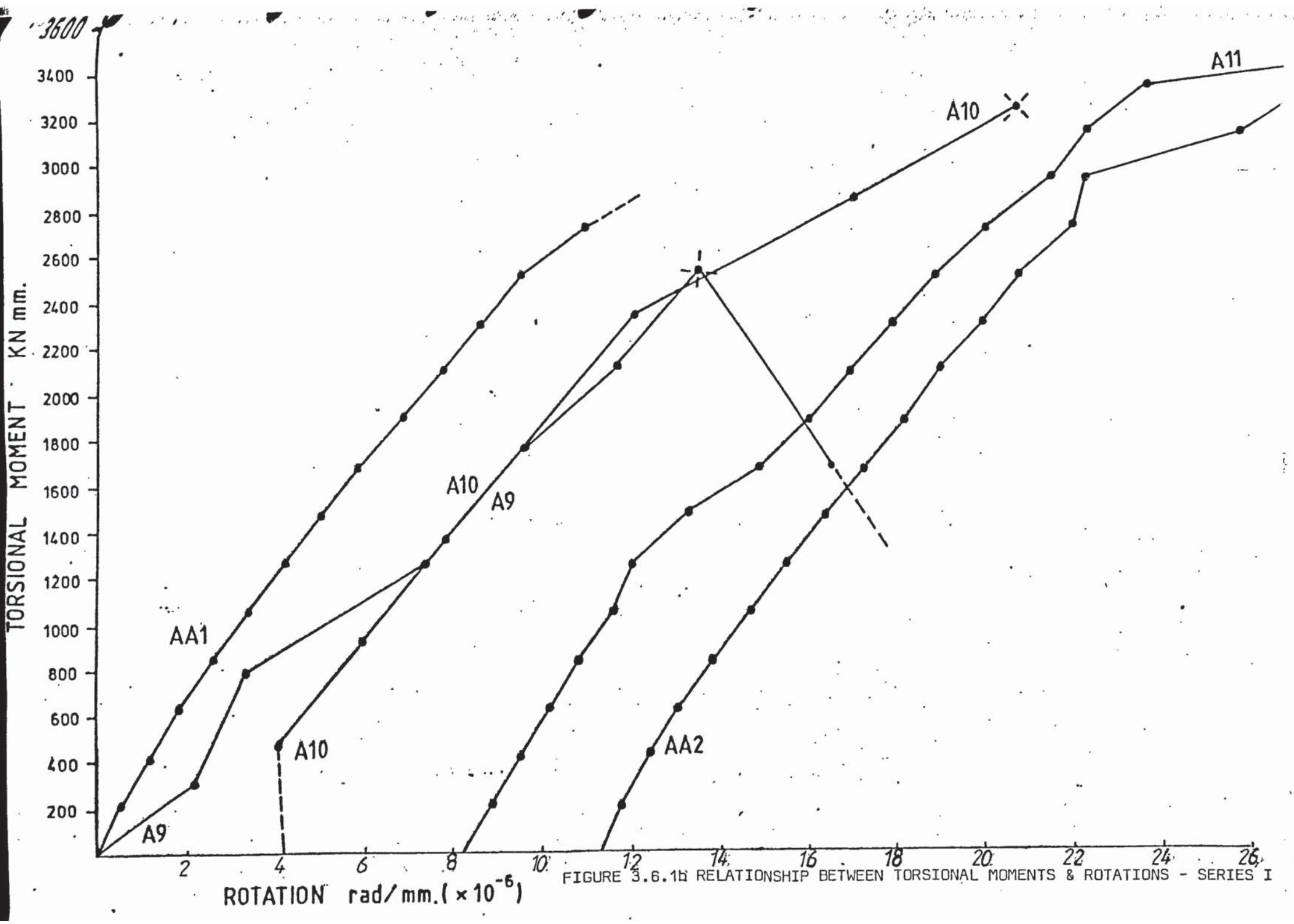

FIGURE 3.6.1b RELATIONSHIP BETWEEN TORSIONAL MOMENTS & ROTATIONS - SERIES I

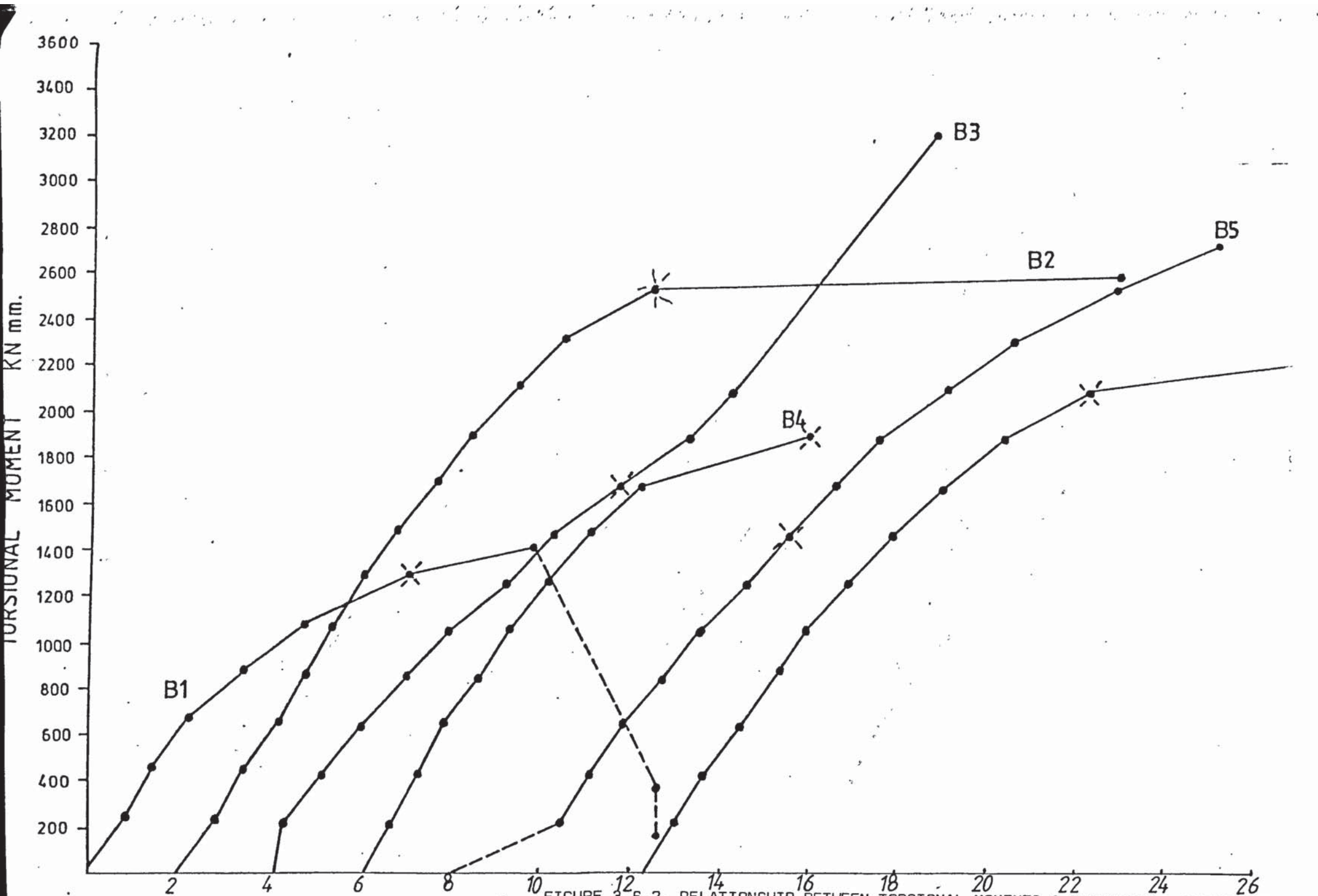

FIGURE 3.6.2. RELATIONSHIP BETWEEN TORSIONAL MOMENTS & ROTATIONS - SERIES II

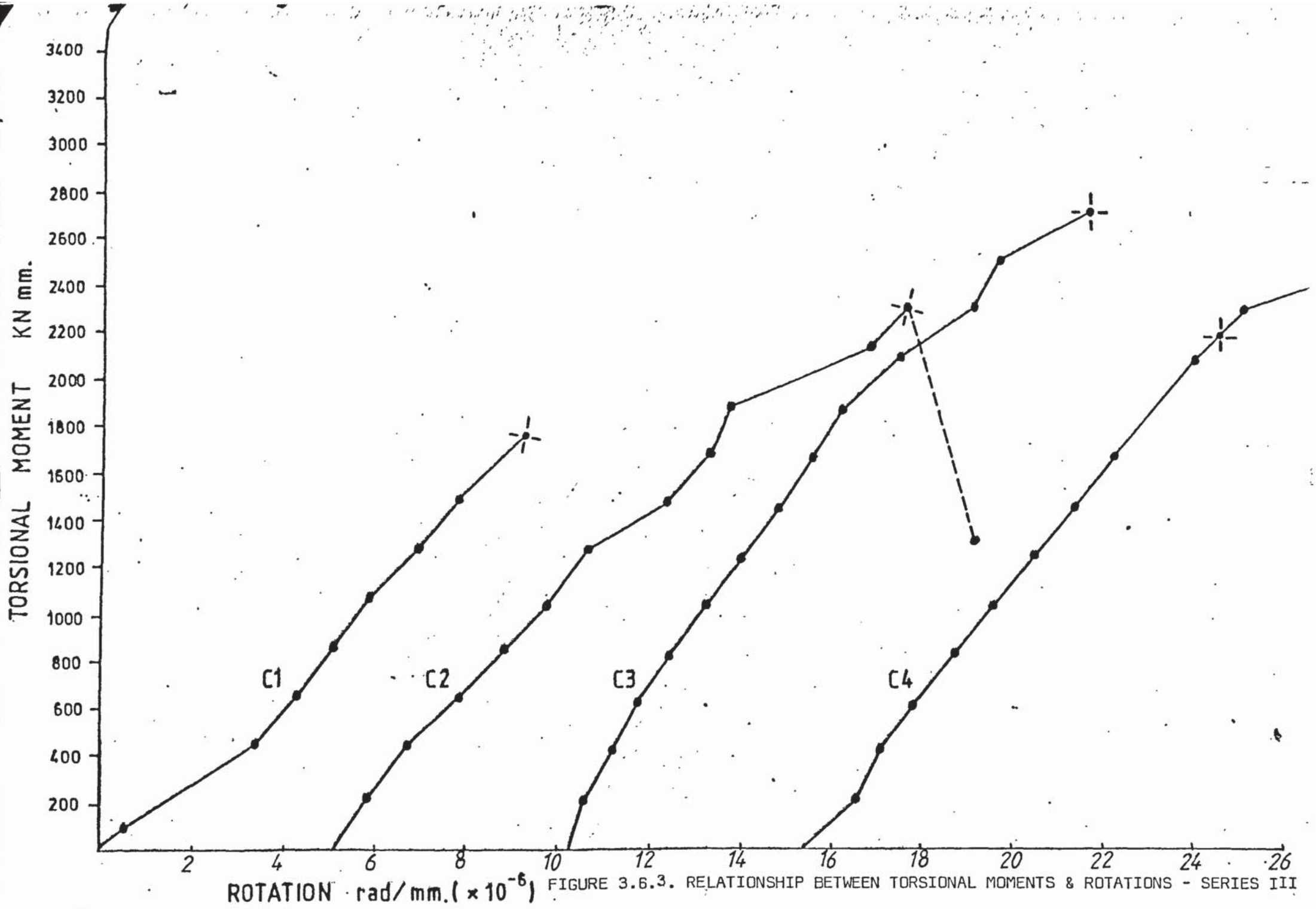

FIGURE 3.6.3. RELATIONSHIP BETWEEN TORSIONAL MOMENTS & ROTATIONS - SERIES III

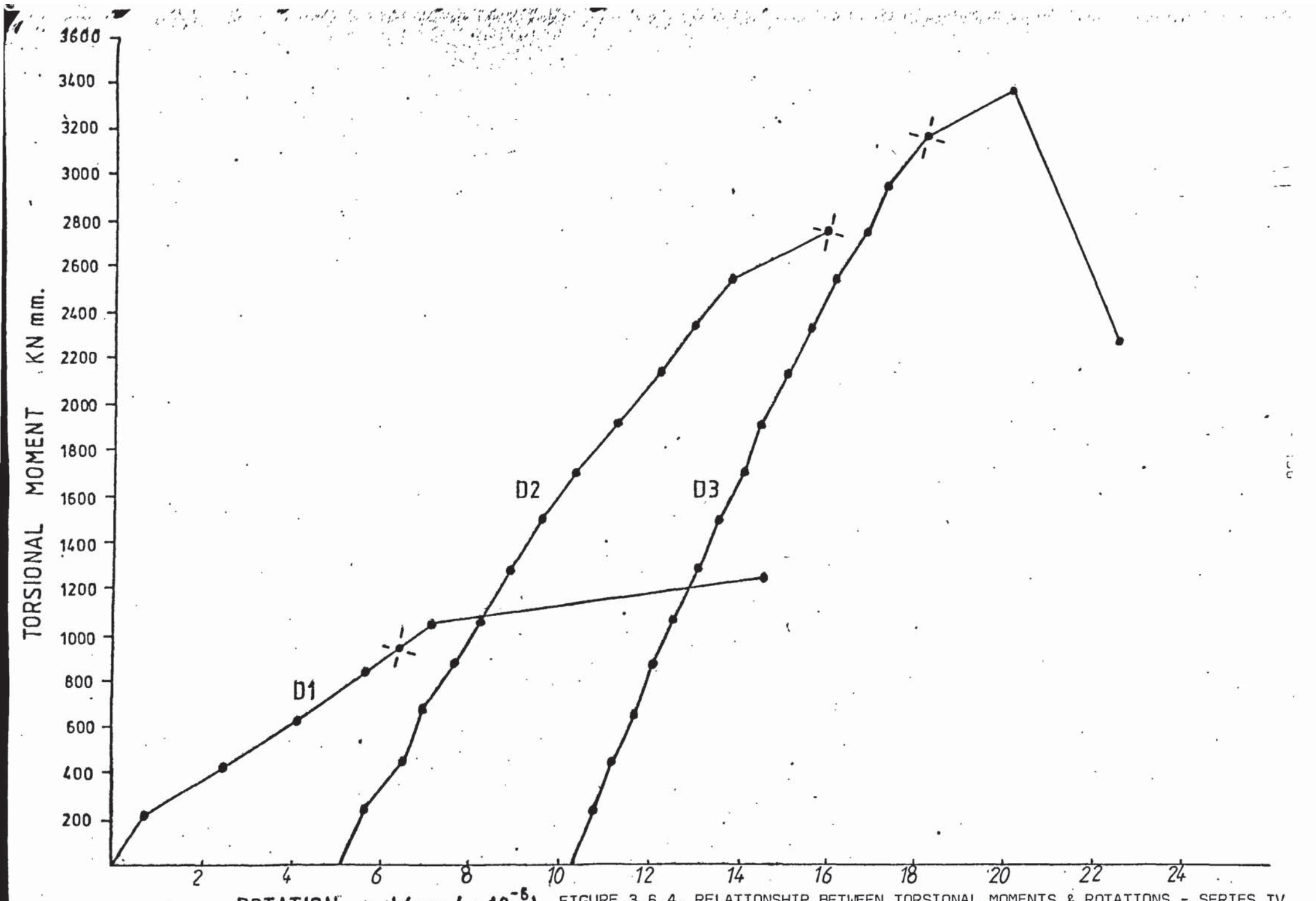

FIGURE 3.6.4. RELATIONSHIP BETWEEN TORSIONAL MOMENTS & ROTATIONS - SERIES IV

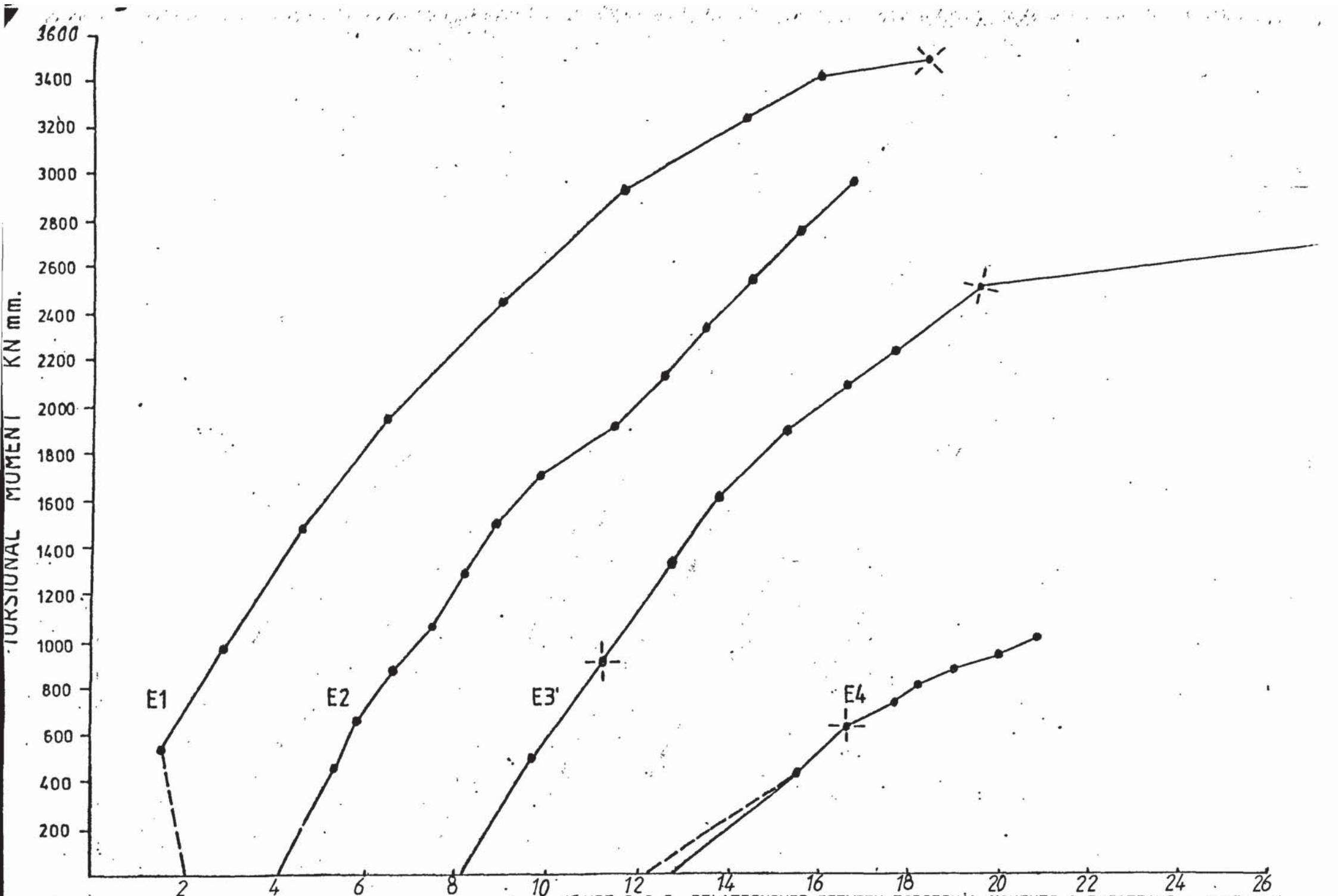

FIGURE 3.6.5. RELATIONSHIP BETWEEN TORSIONAL MOMENTS & ROTATIONS - SERIES V

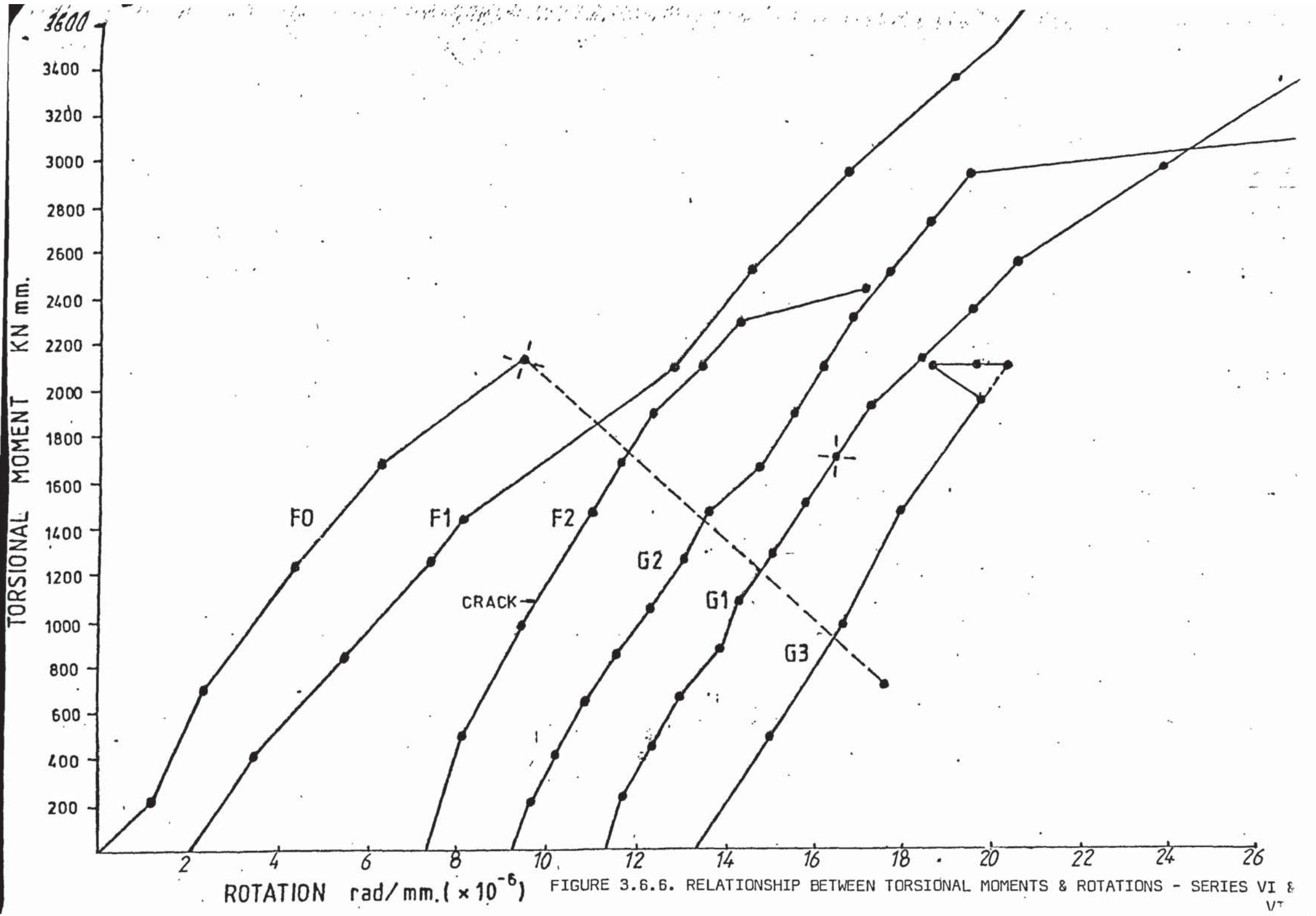

FIGURE 3.6.6. RELATIONSHIP BETWEEN TORSIONAL MOMENTS & ROTATIONS - SERIES VI & VI

decreased. Conversely, the ratios of $(\theta_u - \theta_{cr}) / \theta_{cr}$ were respectively 1.62 and 0.39 in D1 and D3 showing, on the other hand, the loss in ductility with increasing the width.

3.7. STEEL STRAINS

These were measured by means of electrical resistance strain gauges. Unfortunately, some of the strains readings were lost on the Data Logger which was used during the testing of beams A11, AA1, AA2, and E5. The strains from thirty-three beams were prepared in graphical form and are discussed in this section. The graphs included the variation of the strains in the four legs of the stirrups, in the two bonded longitudinal mild steel bars and in the prestressing wires - versus the torsional moment and/or the bending force.

In Table (3.7.1) of this section, the stress change due to loading at the final state of strain in each leg and the prestressing wires are presented. For all the beams included in this table, it is concluded from checking the strain states that none reached yielding. Furthermore, in no beam in this investigation did rupture of any prestressing wire occur.

In the beams prestressed by lower forces, as the figures for series 1 show the increase in the tendons forces was more significant.

TABLE (3.7.1.)SUMMARY OF MAXIMUM RECORDED STEEL STRESSES & CONCRETE STRAINS FROM TEST BEAM

BEAM	STIRRUPS LEGS N/mm²				LONGITUDINAL STEEL N/mm²		CONCRETE STRAIN
	TOP	F.F.	BTM.	B.F.	MILD	PRESTRESS	
A1	Yield	23.0	-2.0	-7.0	130.0	431.0	-
A2	-138.0	22.0	-	21.0	219.0	788.0	-
A3	29.0	-63.0	-4.0	22.0	--	416.0	-
A4	251.0	Yield	32.0	Yield	-Yield	342.0	-
A5	Yield	Yield	-	76.0	Yield	56.0	-
A6	-	-	-	-	-	-	-
A7	70.0	-	168.0	26.0	272.0	-	850
A8	12.0	Yield	158.0	34.0	-110.0	84.0	465
A10	-Yield	29.0	-Yield	48.0	-100.0	-9.8	711
B1	-	-	-	-	-	54.0	1240
B2	-	Yield	-	19.0	-	-	1135
B3	-	Yield	10.0	-	-	134.0	1035
B4	184.0	28.0	-	-	-	105.0	-
B5	-	52.0	93.0	-6.0	-	62.0	935
B6	38.0	39.0	-	Yield	-	90.0	1280
C1	26.0	21.0	15.0	7.0	-	62.0	900
C2	57.0	-42.0	30.0	50.0	-	66.0	475
C3	-	-	-	-	-	-	1000
C4	-	-	-31.0	-	-	77.0	-
D1	222.0	133.0	-	74.0	-	43.0	445
D2	-84.0	-Yield	34.0	24.0	-	76.6	-
D3	-	-	-	-	-	58.0	1250
E1	-57.0	23.0	Yield	Yield	Yield	04.0	285
E2	-	-	-	-	-	32.0	1060
E3	-	-	-	-	-	72.0	980
E4	118.0	Yield	114.0	-	-Yield	183.0	-
F0	123.0	-32.0	Yield	-63.0	-Yield	-	1090
F1	246.0	-Yield	143.0	40.0	-	27.0	260
F2	-	-50.0	68.0	99.0	-106.0	80.0	1075
G1	-	-	-	105.0	-	109.0	2315
G2	-	33.0	32.0	-	-63.0	44.0	490
G3	73.0	-89.0	34.0	-	-151.0	58.0	800

The maximum strain increase of 1460$\mu\varepsilon$ in a single wire was recorded in the beam A2 which was prestressed to nearly 5% of the yielding force as based on a proof stress of 1426 N/mm^2. The strain was 452.7% of the prestress plus self-weight strain, effective at the commencement of the test.

In many beams, the failure cracking surface did not, however, intercept the gauged stirrups. From an examination of the stirrups strains no yielding due to loading was recorded in all of the four legs of a gauged stirrup.

3.8. CONCRETE STRAINS

These were mainly the longitudinal concrete strains induced by the loading and monitored across the depth of the beam. The strain profiles produced from the readings following each loading increment were prepared.

The main use of the concrete strain gauges, which were arranged on the beam surface parallel to the bending moment plane, was to trace the development of the neutral axis. The depth of the compressive, zone was computed for the beams failing in 'mode 1' or "mode 2" and values are presented in Table (3.8.1.). In the tensile zone

TABLE (3.8.1) DEPTHS OF COMPRESSION ZONE

BEAM	(1) from strain gauges (mm)	(2)from surface cracking (mm)	AVERAGE OF : Col.1 + Col.2(mm)	Max.Longitudinal concrete strain με
A1	35.00			920
A2	42.50			-
A3	45.00			725
A5	54.00			670
A6	65.00	65.00	65.00	660
A7	65.00			505
A8	61.00			465
A10	73.50			835
B1	90.00	89.00	90.00	810
B2	94.00	76.00	85.00	1140
B3	93.00	78.80	86.00	770
B5	62.50	59.00	61.00	940
B6	64.00	63.00	64.00	1270
C1	82.80	-	83.00	900
C2	66.50	-	67.00	(600)
C3	77.00	-	77.00	1000
C4	77.00	73.50	75.00	890
D1	42.50	50.00	46.00	-
D3	97.50	-	98.00	770
E1	135.00	-	135.00	180
E2	-	-	-	1060
E3	51.00	58.40	55.00	430
F0	131.00	-	131.00	1090
F1	134.00	142.50	138.00	260
F2	71.00	67.50	69.00	950
G1				
G2	108.00	115.00	112.00	950
G3	86.00	102.50	94.00	800

Table (3.8.2.) VALUES OF BOND/SLIP FACTOR

	Average change in steel strain με		Average change in concrete strain με				
	up.layer	1.layer	upper	lower	B1 upper	B1 lower	B1 average
A1	0620	1345					0.4400
A2	0557	1460					0.5807
A3	0638	2240					0.7650
A4	0458	1078					0.7466
A5	-	0310					0.2815
A6							0.1914
A7	0030	0320	-	0355	0.086	0.320	0.2029
A8	0020	0200	0598	1107	0.033	0.1807	0.1068
A9							
A10	0036	0044	1099	0809	0.0328	0.0518	0.0423
A11							
B1		0090					0.1670
B2		0131	0179	1774	0.0432	0.0740	0.0586
B3	0005	0433	0599	2359	0.0083	0.1835	0.0959
B4							0.1710
B5	0010	0298	1205	1895	0.0083	0.1573	0.0828
B6	0030	0340	0883	2354	0.0340	0.1444	0.0892
C1	0020	0290	0725	1701	0.0276	0.1705	0.0990
C2	0035	0293	0750	1739	0.0467	0.1685	0.1076
C3	-0085	0220	-0606	1403	0.1402	0.1568	0.1485
C4	0052	0364	0678	2584	0.0767	0.1409	0.1088
D1	0143		0861		0.1660		
D2	0210	0133	1265		0.1661		
D3	0051	0174	1668	1671	0.0306	0.1041	0.0674
E1	0015						
E2	-0030	0118		1277	0.0482	0.0924	0.0703
E3	0020	0348	0683	2317	0.0293	0.1502	0.0898
E4	0195	0873					
F0							
F1	0011	0121	0606	0984	0.0181	0.1229	0.0705
F2	0078	0383	0828	4708	0.0942	0.1759	0.1350
G1	0545	0098	0548	1185	-	0.0827	0.0827
G2	0033	0198	0553	1214	0.0596	0.1631	0.1114
G3	0020	0290	0616	1471	0.0325	0.1972	0.1148

the concrete strain gauges were generally fixed to the surface of the beam at levels equal to the prestressing wires depths from the top face of the beam. The concrete and steel strain readings (at the same level) were, thus, used to compute the Bond-Slip factors of the tendons relative to the adjacent concrete. These values are presented in Table (3.8.2.)

It was noticed, in many cases, that the strain gauges did not always intercept the visible cracking and/or failure sections. When the gauge lines were close to the failure crack excellent agreement was found between the visual measurements and the values estimated from the concrete strain in measurements for the compressive depth. As mentioned before the depths of the compressive zone for beams where the "mode 1" was eminent are presented in Table (3.8.1) of this section in which for each beam two values of the compression depth are sited.

The maximum compressive longitudinal concrete strain, in group B beams, was recorded in beam B6 and measured 1270 $\mu\varepsilon$. In C and D beams the maximum were 1000 $\mu\varepsilon$ and 770 $\mu\varepsilon$ and occurred in the beams C3 and D3 respectively. Wherever possible, the max. compressive strains were recorded and their values are presented in the same Table (3.8.1). The tensile longitudinal strains, however, were less reliable but were useful to estimate the values of the bond-slip factor.

3.9 INTERACTION OF TORSION, BENDING AND SHEAR

The failure loads of the beams have been presented in section 3.3

Table 3.3.-1 andin thissection are presented graphically.

Interaction of Torsion and Bending Moment:-

In Figure (3.9-1) the interaction curve of torsion with bending moment is presented. The ultimate torsional and bending loads of series V beams which were tested subject to varying M/T ratios, are connected by straight lines extending from pure torsion (beam E1) to bending and shear only (beam E5). The interaction line represents the range of loading from a mode 3 form of failure of beam E1 to a mode 1 failure of beam E4. The latter was tested subject to a M/T ratio of 17.2. Conversely, on reducing sufficiently the bending load on such a beam a mode 2 of failure would become imminent around M/T ratios less than the wide range of 5.0 - 3.0. It is evident that the use of such limits of M/T ratios to identify specific modes of failure cannot be consistent throughout the full range of test beams. The figure confirms experimentally that the problem of M-T interaction in prestressed beams was further complicated by the variation along the radial paths away from the origin towards the interaction curve.

For series V beams the overall trend could be approximated to a semi-circular curve as the one shown on the figure. Upon this E1-E5 curve, the influence of the following parameters are now considered:

Influence of increasing the stirrups size could be noticed

from the position of the line connecting the ulitimate strength of beams F1 and F2 in which 6mm size ties were used. At nearly 7500 kNmm bending moment, beam F1 was capable of resisting 25.6% more torque than a beam such as E2. The line F1 - F2, however, shows a reduction effect when extended towards higher bending moments. At about 14500 kNmm bending moment, the beam F2 had a reduced capacity of nearly 90% of the torque resisted by beam E3.

Hence the trend indicated by these limited tests, though not conclusive, suggests that the increase of the web percentage of stirrups as provided has a significant effect on the interaction curve in high torsional regions only, whereas there is little influence at higher bending moments.

Influence of doubling both the size and the spacing of the stirrups is indicated by the interaction line G1,G2,G3. At high torsional loads beam G1 was 11% stronger than a counterpart beam E2. In contrast the beam E3 at a lower torsional level resisted 28.3% more torque than did beam G3. Therefore the G beams tended to interact in a manner similar to F beams, along an interaction line running between the two line of F and G beams.

To assess the effect of inclusion of stirrups in the beams of the present investigation as compared to beams without web steel, results are compared with the extensive test results from Cooper (38) who had tested identical beams in his Series II, but with no stirrups and a shorter shear span.

In Figure 3.9.-1 Cooper's beams are plotted and connected by straight lines. As the number of the points is far too larger, the emerging shape of the interaction curve is more refined than the curve of E beams of this investigation. Generally the trend is similar with a beneficial margin of higher strength produced by providing the author's beams with stirrups. It is also noted that this gain in torsional strength was on the whole smaller than the gain obtained in the bending moment by the beams with stirrups at lower levels of torsion. Reference is made to Figure 3.9.-1.. The shorter shear spans (600mm and 800mm) over which Cooper's beams were tested should affect the ultimate load, but this should not greatly affect the general shape of the interaction curve.

To examine further the effect of the presence of a shear force in the author's beams as compared to similar beams in which such a shear force was absent, use is made of some test results produced by Evans and Khalil (34). Their beams were very similar to the author's beams, with identical prestressing wires and unbonded, but tested in absence of any shear force in the test span. The beams had a cross-sectional ares, area of one leg of stirrups and a spacing each larger than that of the author's beams by the ratios of 1.47, 2.20 and 1.46 respectively. Four beams of Evans et al., scaled down by a factor of 1.47 are shown on Figure 3.9.-1 Despite the approximate scaling method, the test results are in the range of the E series, interaction curve.

All of the author's beams and the compared beams referred to above

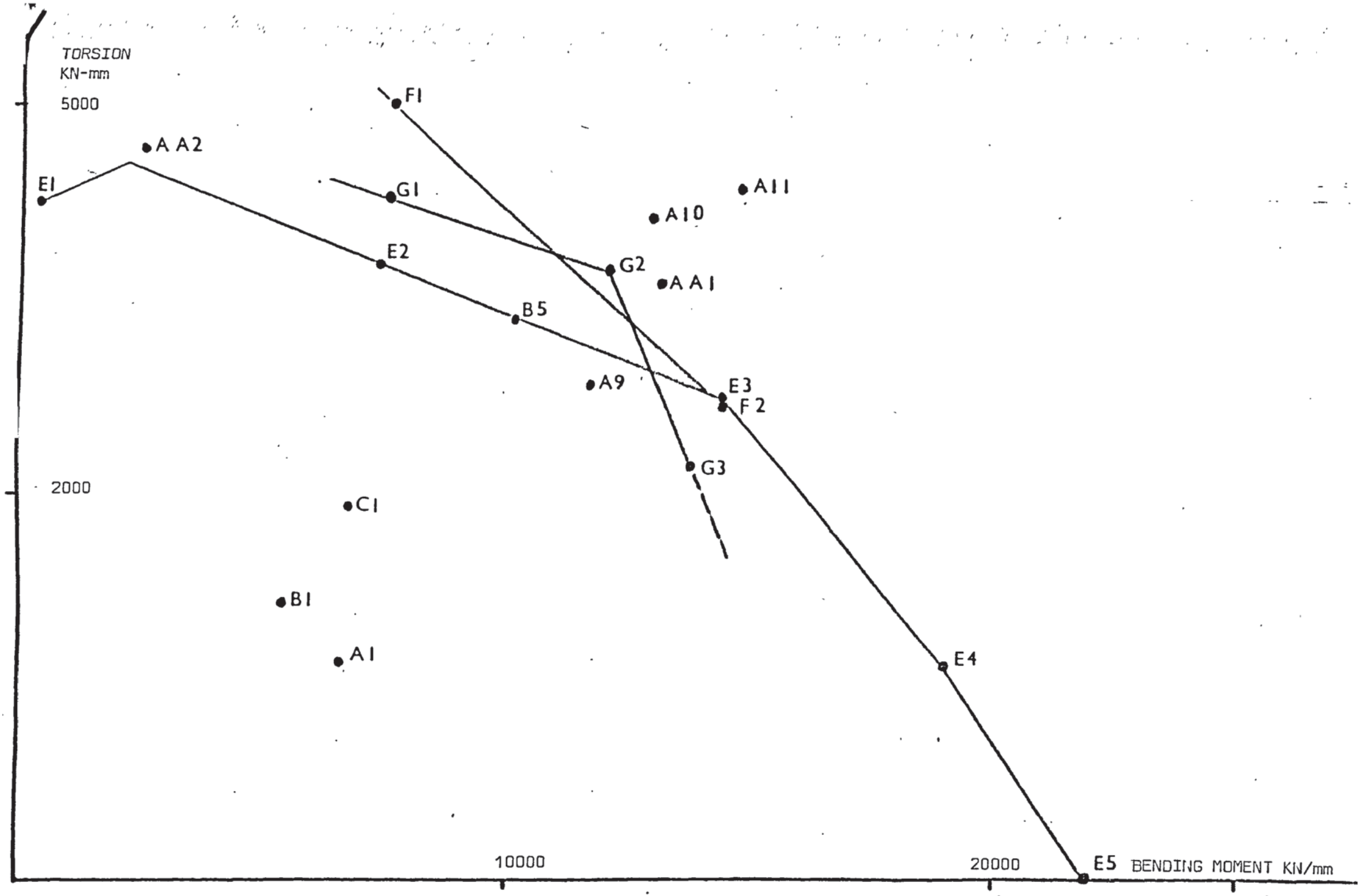

FIGURE 3.9.1. INTERACTION OF TORSION AND BENDING MOMENT.

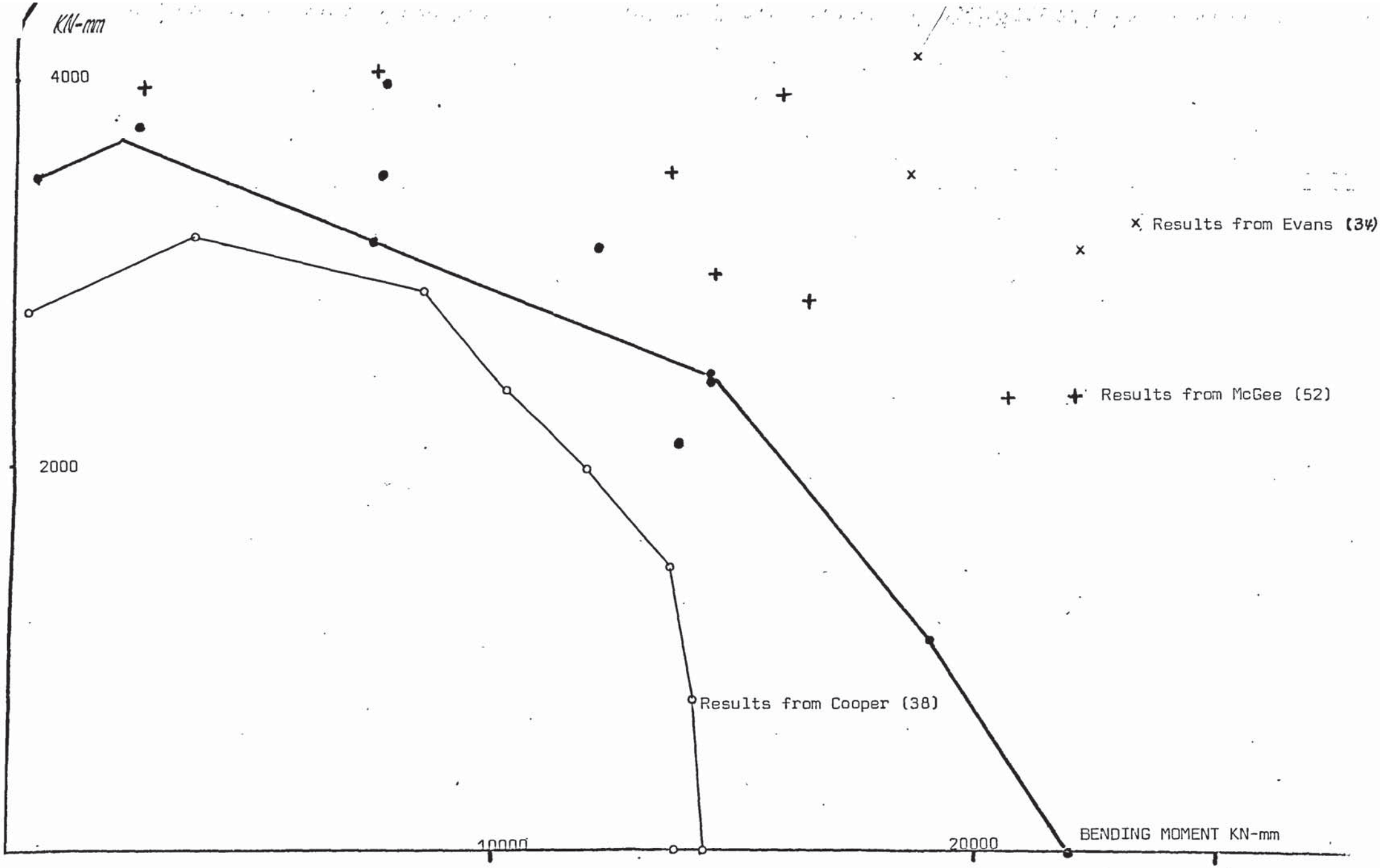

FIGURE 3.9.1a. INTERACTION OF TORSION AND BENDING MOMENT FOR THE PRESENT & PREVIOUS INVESTIGATIONS

wer unbonded and post-tensioned. It was thought relevant to include a few pretensioned bonded beams in this discussion. The interaction points of egiht beams tested by McGee and Zia (52), containing stirrups - 4mm and hence comparable to the web steel used in this investigation, were therefore plotted in Figure 3.9-1. Their cross section was 2.65 times larger than the author's E-beams, so they were accordingly scaled down by a factor of (1/2.65). It is seen that these beams too followed the general trend outlined by the E - interaction curve. It seems that bonding has an insignificant effect whenever M/T ratio is less than 2.0 and shearing force is very small, whereas the strnegth margin over unbonded beams increases by nearly 20% with M/T ratios around 8.0 in the presence of a moderate shear force. Reference is to Figure 3.9-1.

INTERACTION OF TORSION AND SHEAR;-

The torsional and shearing loads are plotted versus each-other in Figure 3.9-2. The loading points of group E beams are connected by straingt lines. The emerging interaction curve thus produced is discussed herein.

The E beamsinteraction curve of torsion with shear is clearly more linear than the curve of torsional interaction with bending moment. It mainly, consists of two semi-linear branches meeting at the loads points of beam E3 which at failure, has had a ratio of 5.58 for the (2T/vb) parameter (and a M/T ratio of 5.27). Reference is made to Table 3.3-1.

It is noted, with particular reference to beam E3, that it is laying in the same vertical shear plane, of a 10.0kN force, with beams F2 and G3. It can be deduced, from Figure 3.9.-2 containing these beams, that doubling the size of the stirrups did not have a beneficial effect on the torsional strength because beam F2 actually failed with a 10% strength margin below beam E3. The non-beneficial effect of increasing the spacing was observed in beam G3 which contained the same size of stirrups as F2 but with twice as much spacing and therefore, an equal web steel percentage as beam E3 was present. Beam G3, nonetheless, failed at a torsional capacity level of 22% below the torsional strength of beam E3.

Subject to a higher (2T/Vb) ratio of 12.6 (and a lower M/T ratio of 2.34) that situation was reversed in the case of beam E2. The latter, being on the interaction curve, and laying in the same vertical shear plane of 5.0 kN force as beams F1 and G1, was on the average 10% weaker than either of these two beams i.e. increasing the size resulted in an increase of over 10 per cent in the strength.

It can be deduced, therefore, that in presence of moderate shear forces e.g. 5.0 kN, decreasing the web steel percentage by about 50%, through doubled spacing, resulted in the drop of strength by 13%. Also when fixing the web steel percentage by reducing the size to 50% and at the same time cutting the spacing by half, a torque reduction amounting to 11% could be observed. Whereas subject to higher shear forces (e.g. 10.0 kN) increasing the web steel size by two times could lead to a counter effect of reducing the strength by 10%,

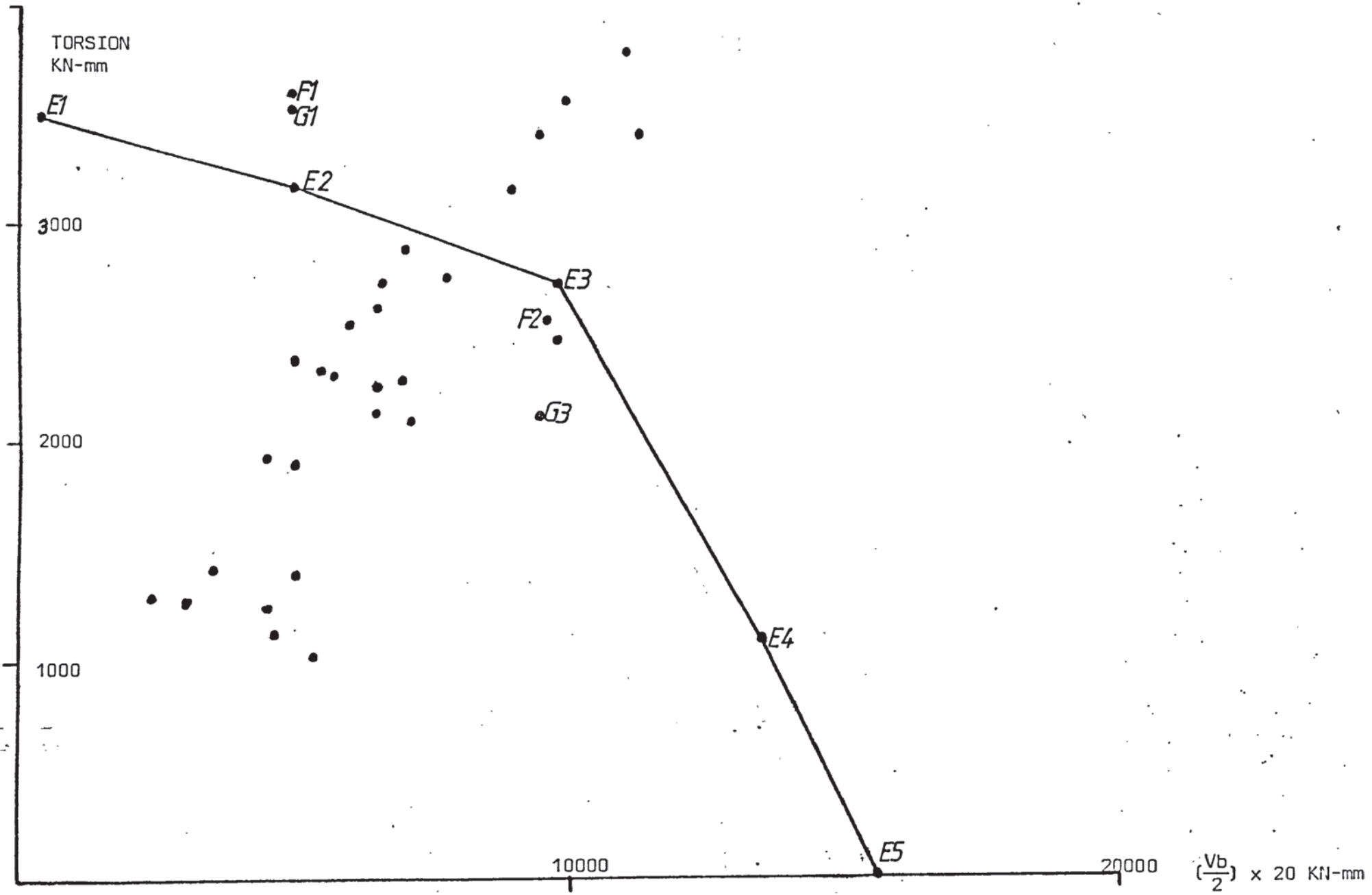

FIGURE 3.9.2. INTERACTION OF TORSION AND SHEARING LOAD

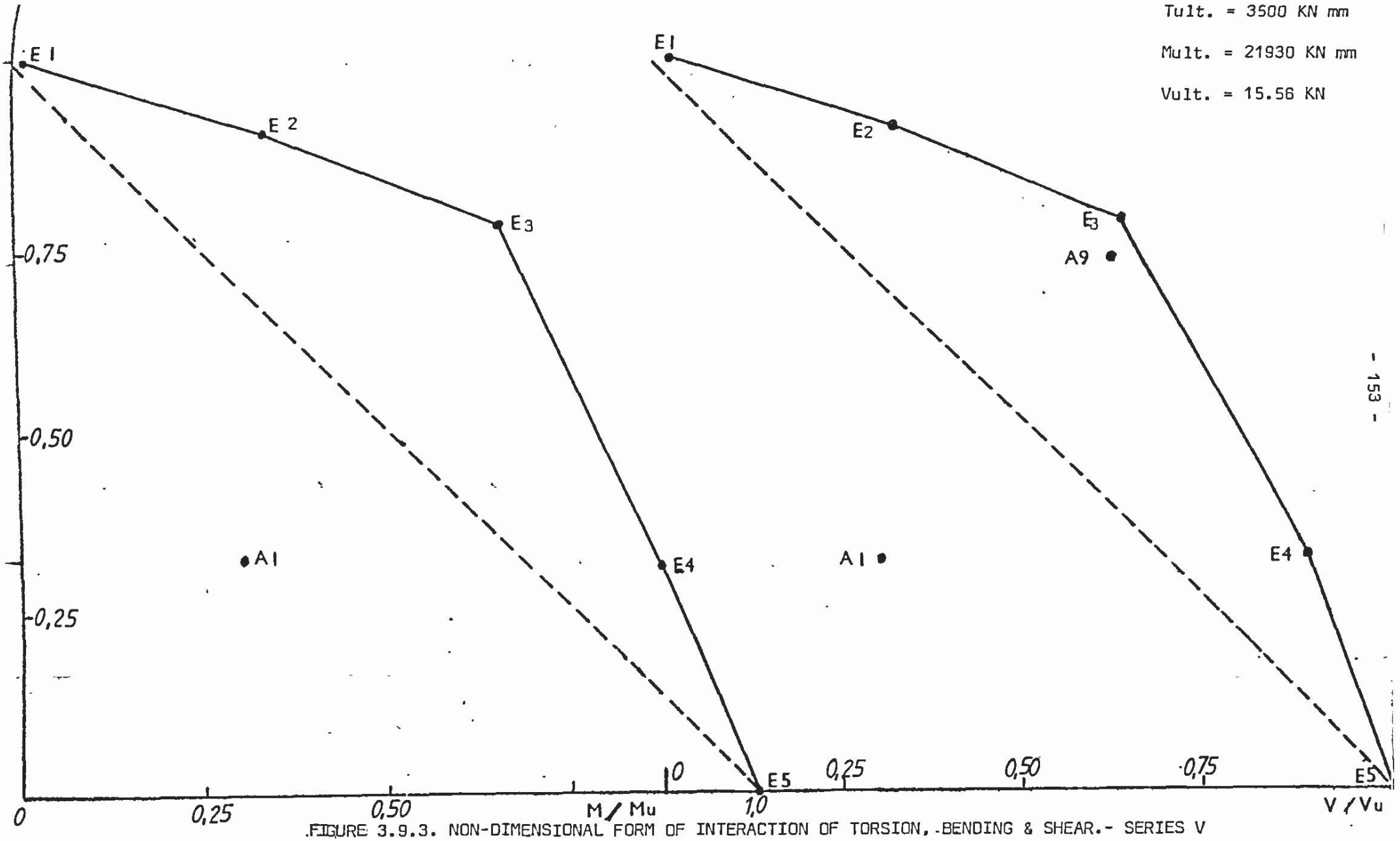

FIGURE 3.9.3. NON-DIMENSIONAL FORM OF INTERACTION OF TORSION, BENDING & SHEAR.- SERIES V

resuming the initial web percentage by doubling the spacing as well, has led to a further loss of strength of 13%.

Generally, beyond some increasing of the web steel percentage stirrups effect on the ultimate strength of the test beams was not significant and even unbeneficial. This effect depended heavily on the amount of shear force present in the test span.

3.10 A simplified Graphical Representation of the Combined Loading Test Results of Beams

The concrete cross section is subjected to direct stress due to the prestress and the bending moment. It is also subjected to shear stresses due to the shear force and the torsional moment,

By simple addition the average tangential stress =

$$\frac{K_t}{b^2 h} T + \frac{V}{bh} \qquad (3.10.1)$$

Adding up the axial stresses normal to the cross section, the resultant stress =

$$\frac{M}{0.85\ bh^2} + \frac{Ps}{bh} + \sum \rho_j \bar{f}_j \qquad (3.10.2)$$

where $la_1 = 0.85h$

Ignoring vector addition the summation of the total stresses applied at the section:

$$\frac{kt}{b^2h}T + \frac{V}{bh} + C_1\left[\frac{M}{0.85\,bh^2} + \frac{Ps}{bh} + \sum \rho_j \bar{f}_j\right] \qquad (3.10.3)$$

This is equated to a maximum shear crushing stress $= 2f_{sp}\ (1 + pc2/f_{sp})$

and with $f_{sp} = 3.12\ N/mm^2$ which is the average for series I beams:

$$\sqrt{fc'}\ (1 + 0.32\ pc2)$$

if $ft' \cong f_{sp} \cong 0.5\sqrt{fc'}$ (3.10.4)

The basic equation is therefore:

$$\frac{kt}{b^2h}T + \frac{V}{hb} + C_1\left[\frac{M}{0.85\,bh^2} + \frac{Ps}{bh} + \sum \rho_j \bar{f}_j\right]$$

$$= 2\,f_{sp}\ (1 + pc2\,/\,f_{sp}) \qquad (3.10.5)$$

The method is visualized by plotting the total numerical value of the applied stresses against the "theory" stress in a diagram form.

Diagram 3.10.1 represents the interaction of the loading stresses and the shear resistance of the beams. A line of 45^{o} is drawn from the origin. It is noted that this line is in good agreement with the experimental results. In Table 3.10.1 the Test/Theory ratio relation is presented and the mean value, standard deviation and coefficient of variation are found for the total of thirty-six beams to be 1.02, 0.13 and 12% respectively. The experimental constant C_1 involved in these calculations was 1.20. The term $\sum \rho_j f_j$ is the sum of the longitudinal and transverse stell ratios ρ_l and ρ_s respectively multiplied by the corresponding experimental average stress increase in the tendon, longitudinal mild steel and the induced stress in the stirrups.

It is also noted that the Test/Theory line divides the test results into two main groups. The group of beams below it includes ten beams all of which were uncracked by flexure at the soffit.

The rest of the test beams with a ratio of Test/Theory $\geqslant 1$ were cracked by flexure at the bottom. These beams can, however, be divided into two groups with the horizontal line through an intercept of Test/$\sqrt{fc'}$ $=$ $(0.67\ fc' / \sqrt{fc'})$ N/mm^2 being the dividing boundary. Beams located higher than this line were observed to have crushed with compression shear characteristics and although the bending moments applied were sufficient to crack them at the bottom fibre (and hence they are above the 45^{o} line in the diagram) these beams failed in "mode" 2. It is reasonable, from the diagram and distribution of the test points, to regard a value of

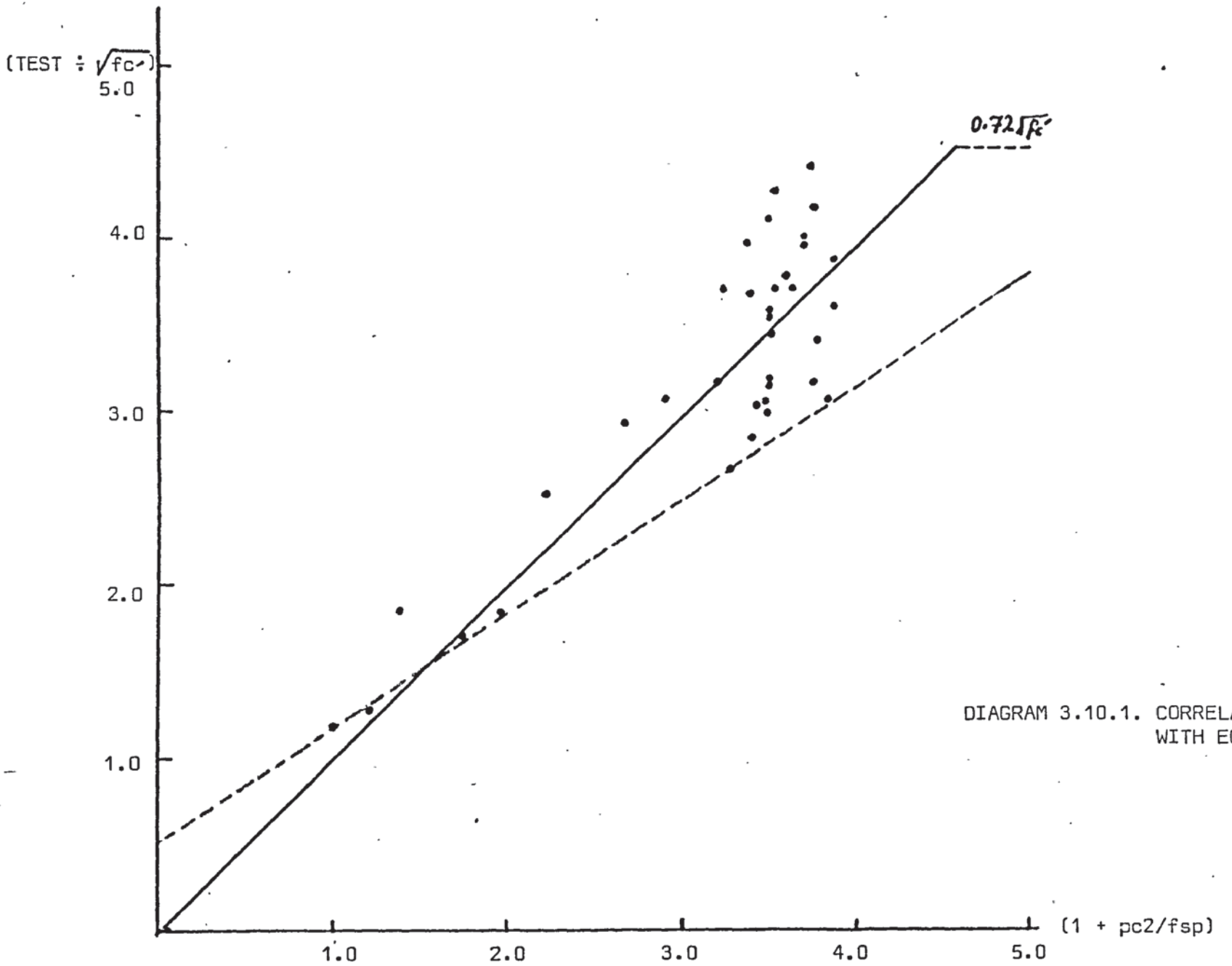

DIAGRAM 3.10.1. CORRELATION OF TEST BEAMS WITH EQUATION (3.10.5.)

$(\text{Test}/\sqrt{fc'}) = 4.5$ as an upper limit which corresponds to a maximum stress of 0.72 fc'.

In conclusion the constructed stress interaction diagram enables to distinguish three main regions of the interaction surface covering beams: cracked in flexure shear, cracked in web-shear and crushed in shear compression. The test beams compared favourably with the distribution over these regions. Although more work is needed to improve on the diagram, the assumption of a simple shear criterion to govern the total interaction is reasonably justified by the obtained accuracy. For the web cracked beams, which gave ratios < 1.0 it was indicated that their failure was not governed exactly by the 45^{o} line. A better critical line is shown on the same diagram by skewing the 45^{o} line so it makes a slope of 0.65 with the x axis. The Test axis is intercepted at a ratio of $(\text{Test}/\sqrt{fc'}) = 0.5$. Hence an equation of this form is apparently the governing "criterion":

$$\frac{\text{Test}}{\sqrt{fc'}} - 0.5 = 0.65 \ (1 + 0.32 \ pc2) \quad (3.10.6)$$

Should be noted that the both sides of the equation are dimensionless. The experimental strength according to this equation can be interpreted as consisting of an apparent shear constant and a variable component which depends on the direct stress multiplied by a coefficient = 1.2.

A general non-dimensional strength equation can be written to express the interaction of loadings and may be presented in the following form:

$$\frac{\sum \text{Test Stresses}}{\sqrt{fc'}\,(1 + 0.32pc2)} = 1 \qquad (3.10.7)$$

or more explicity in terms of ultimate strength loads:

$$\frac{T}{T_o} + \frac{V}{V_o} + \frac{M}{M_o} + \frac{Ps}{P_o} + \frac{Fs}{F_o} = 1 + \frac{P.c2}{fsp} \qquad (3.10.8)$$

in which:

$$T_o = \frac{1}{Kt}\, b^2 h \sqrt{fc'} \quad ; \quad k_t = 3 + \sqrt{\frac{b}{h}}$$

$$V_o = bh\sqrt{fc'}$$

$$M_o = \frac{1}{C_1}\, 0.85\, b\, h^2 \sqrt{fc'} \quad ; \quad C_1 = 1.20$$

$$P_o = \frac{1}{C_1}\, bh\sqrt{fc'}$$

$$F_o = \frac{1}{C_1}\, bh\sqrt{fc'}$$

$$\text{and } F_s = \sum \left[A_l\, \bar{f}_l + \frac{2\, A_s\, (b' + d')\, \bar{f}_{sv}}{S} \right]$$

Note: an empirical formula for $\bar{f}_l$ is derived later and given in Eqn.(6.1.2).

Table (3.10.1) CORRELATION OF TEST AND FORMULA FOR DIAGRAM (3.10)

Beam	τ N/mm^2	f_{cm} N/mm^2	TEST	THEORY	Test/Theo.
	1	2	3	4	
A1	2.67	4.62	1.18	1.00	1.18
A2	2.91	4.56	1.27	1.21	1.05
A3	3.29	6.12	1.85	1.38	1.34
A4	2.52	7.59	1.70	1.73	0.98
A5	2.96	7.92	1.83	1.98	0.92
A6	4.91	10.08	2.54	2.24	1.14
A7	5.30	12.23	2.92	2.68	1.09
A8	5.37	12.07	3.06	2.89	1.06
A9	5.995	15.83	3.67	3.36	1.09
A10	7.85	17.13	4.27	3.54	1.21
A11	8.17	18.67	4.40	3.74	1.18
B1	3.27	12.64	2.65	3.28	0.81
B2	5.96	15.29	3.56	3.51	1.01
B3	5.28	14.36	3.05	3.42	0.89
B4	4.34	13.99	3.03	3.45	0.88
B5	6.58	15.71	3.72	3.52	1.06
B6	5.18	14.08	3.16	3.18	0.99
C1	4.38	14.45	3.76	3.60	1.05
C2	5.31	16.06	3.61	3.86	0.94
C3	6.23	15.16	3.43	3.50	0.98
C4	5.75	14.65	2.84	3.41	0.83
D1	4.70	13.57	2.995	3.50	0.86
D2	4.50	14.74	3.18	3.50	0.91
D3	3.68	15.72	3.14	3.50	0.90
E1	7.54	12.38	3.08	3.83	0.80
E2	7.11	15.41	3.41	3.77	0.91
E3	6.42	18.40	4.01	3.71	1.08
E4	3.15	20.19	3.70	3.62	1.02
F0	4.94	16.21	3.71	3.23	1.15
F1	8.85	15.73	3.97	3.37	1.18
F2	5.82	20.09	3.96	3.70	1.07
G1	7.86	14.51	3.53	3.49	1.01
G2	7.28	16.68	4.11	3.51	1.17
G3	5.11	18.76	3.86	3.86	0.999
AA1	6.85	19.13	3.16	3.78	0.84
AA2	8.75	15.81	4.17	3.76	1.11

Series	No. of Beams	MEAN	S.D.	C.V.
I	11	1.11	0.11	9.8%
All	36	1.02	0.13	12%

1. $\tau = \dfrac{3 + \sqrt{b/h}}{b^2 h} T + \dfrac{V}{bh}$

2. $f_{cm} = \left[\dfrac{M}{0.85\ bh^2} + P_s/bh + \sum f_j F_j \right] \times 1.20$

3. Test $= \left[(1) + (2) \right] \div \sqrt{f_c'}$

As can be seen from Table (3.10.1) the correlation with the test results is good. The formula is particularly in good agreement with the beams of series I producing a mean of 1.11 with a S.D. of 0.11 and a coefficient of variation of 9.8% whilst for the total of thirty-six beams the method produces a mean of 1.02 with a S.D. of o.13 and coefficient of variation of 12%. This indicates that the format of equation (3.10.8) is correct and may be developed further following the same form.

3.11. Conclusions From Experimental Investigation:

As a result of examining the general behaviour of the tested beams and from the variation of their failure loads in relation to the single variable parameters as were investigated and described in this chapter, the following conclusions are achieved at this stage:-

1. Full yielding did not occur in either the prestressing tendons or the stirrups legs were generally less than yield. When yielding did occur it was never present in all the four legs of a gauged stirrup.

2. The modes of failure as detected in this experimental investigation included the three classic modes. Transitional modes were also noticed.

3. It was impossible to measure the cracking angles with any

degree of accuracy. Nevertheless from these tests failure always followed the appearance of cracks or coincided with the first cracking. This depended on the following factors:

a) the prestressing force (and its eccentricity)

b) the prestressing steel area

c) the aspect ratio h/b

d) the concrete strength

e) the stirrups' size and spacing

f) the M/T ratio.

The shear span, however, was kept constant in these tests.

4. The torsional resistance is directly proportional to the increase in the prestressing force (and its eccentricity, in combined loading).

Series I indicates that the relationship can be approximated to a straight line. See Fig.(3.11.1)

5. The torsional resistance is directly proportional to the increase in the prestressed steel area. Series II indicates that a parabolic relationship fits the test results. See Fig. (3.11.2)

6. The torsional resistance is inversely proportional to the increase in the h/b ratio and the relationship can be expressed as a straight line. See Fig.(3.11.4)

7. The effect of increasing the concrete strength is to increase the torsional strength as a parabolic function. See Fig.(3.11.3)

8. Increasing the stirrups size and spacing did not have a pronounced effect on the ultimate strength especially under higher M/T ratios. The effect of including the stirrups in these tests can be described as a binder confining the intially cracked section, providing that a minimum area of stirrups is present and a maximum spacing is not exceeded.

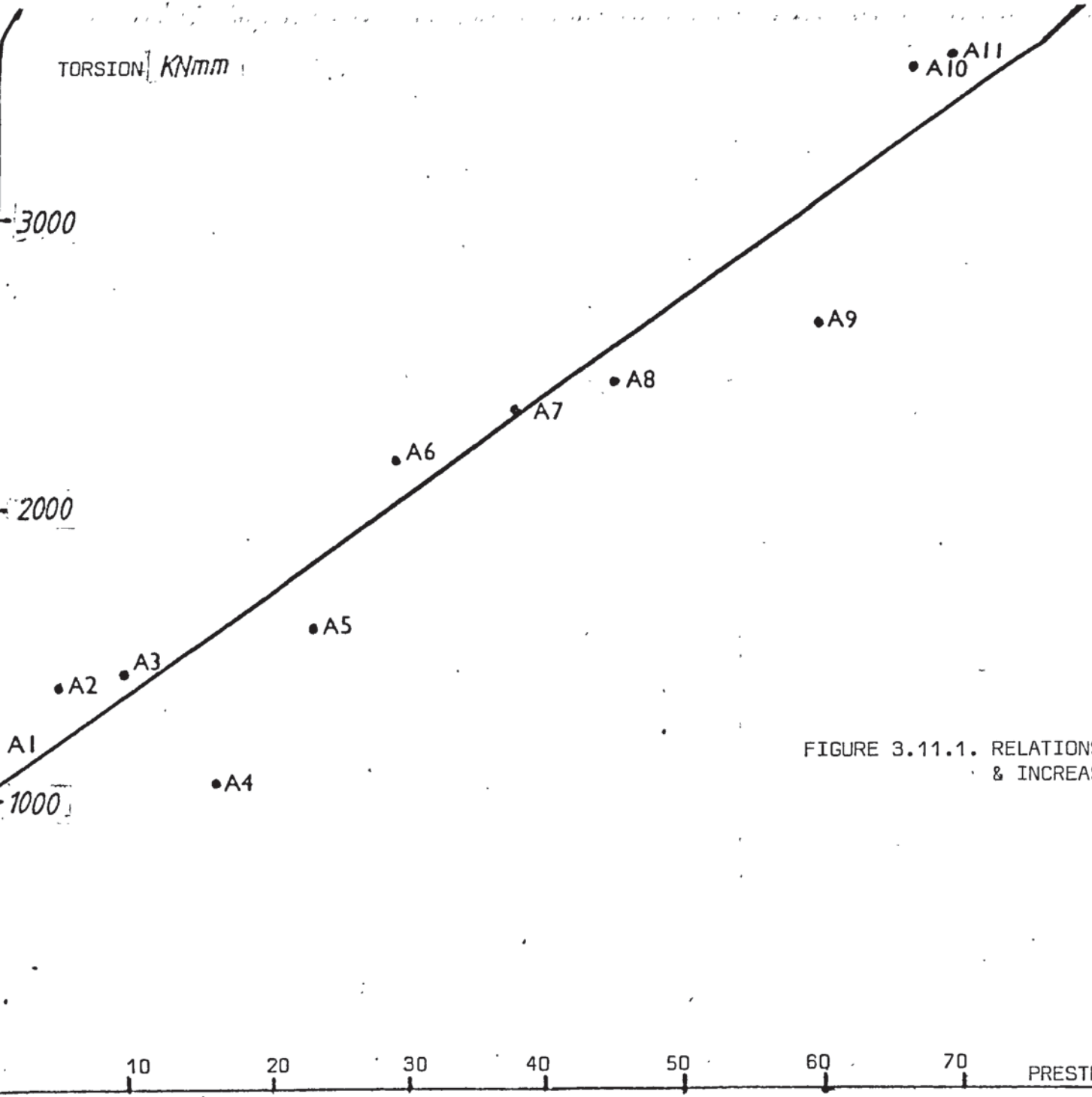

FIGURE 3.11.1. RELATIONSHIP BETWEEN TORSIONAL STRENGTH & INCREASING PRESTRESSING FORCE. SERIES I

FIGURE 3.11.2 RELATIONSHIP BETWEEN TORSIONAL STRENGTH & INCREASING PRESTRESSING STEEL. SERIES II

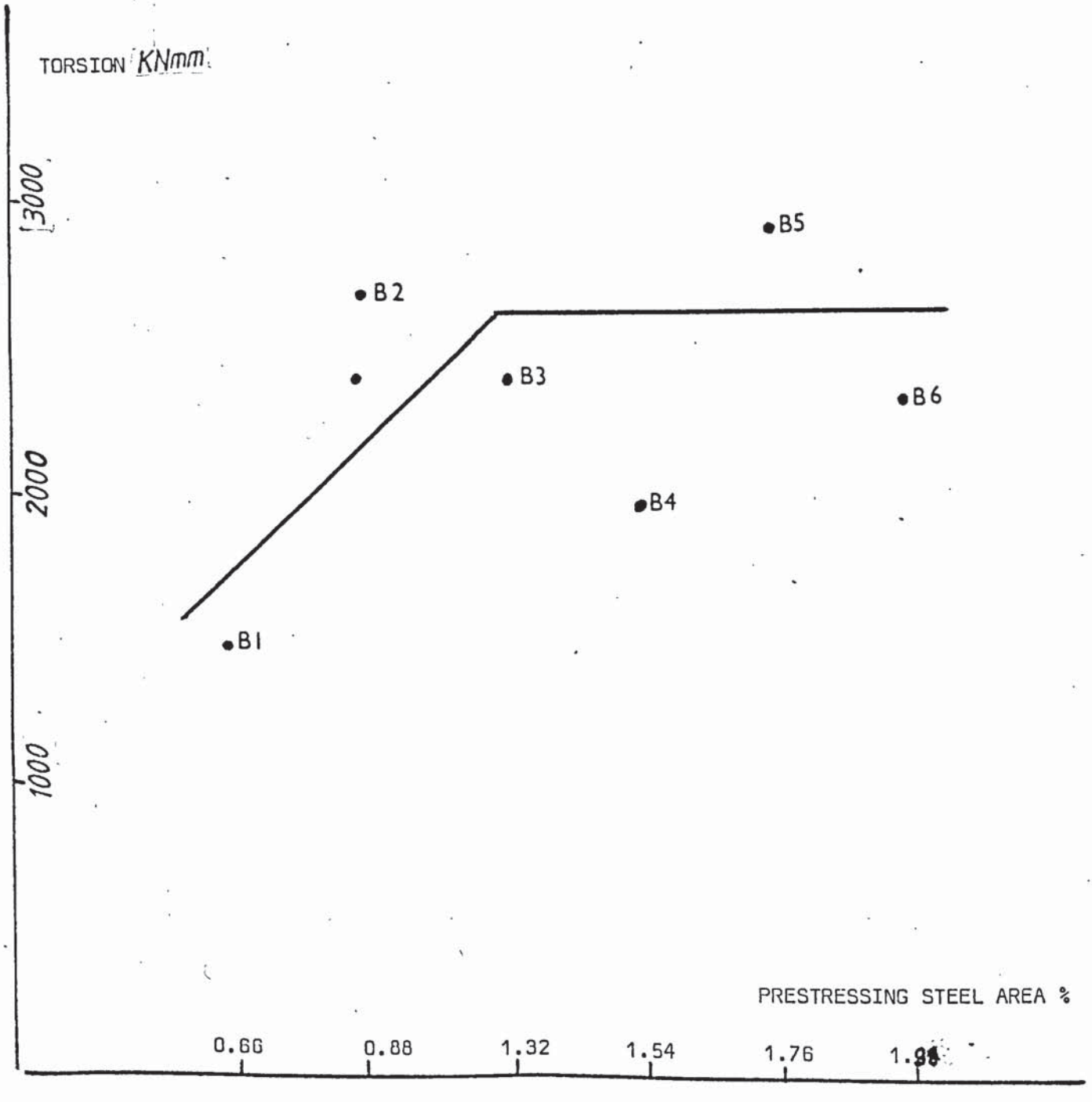

FIGURE 3.11.3. RELATIONSHIP BETWEEN TORSIONAL STRENGTH & INCREASING CONCRETE STRENGTH. SERIES III

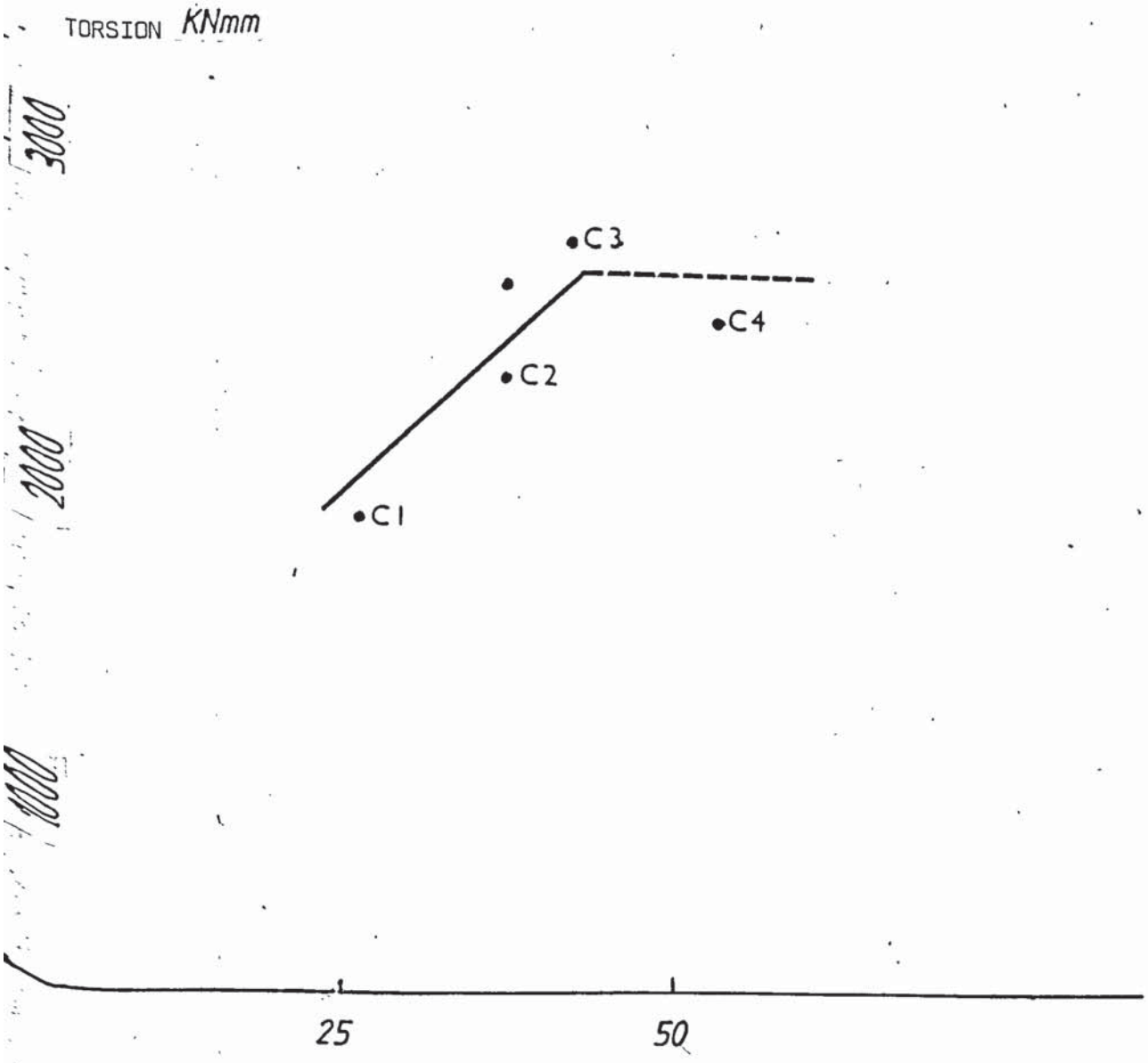

FIGURE 3.11.4. RELATIONSHIP BETWEEN TORSIONAL STRENGTH & INCREASING h/b RATIO SERIES IV

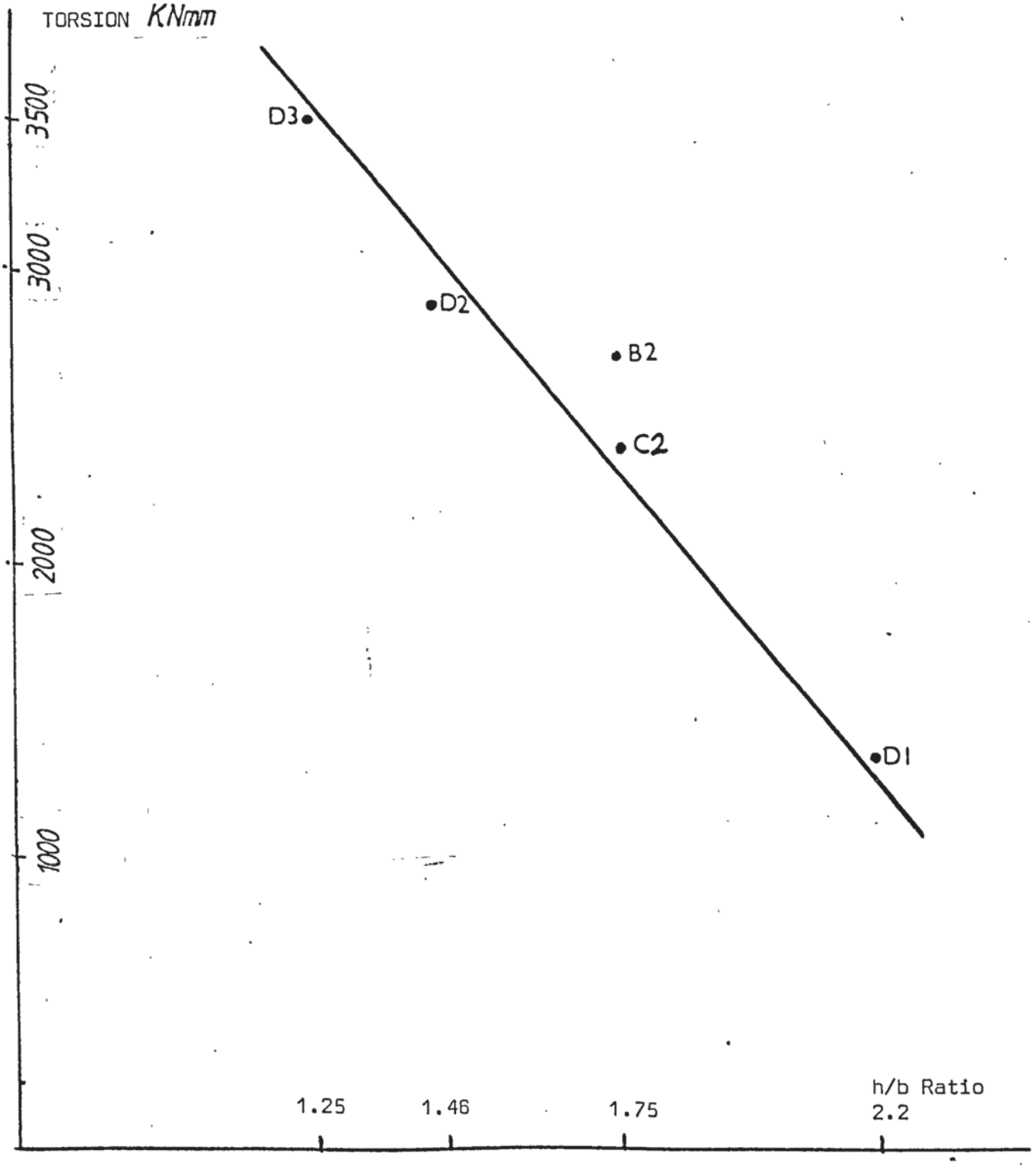

CHAPTER 4

ANALYSIS OF TEST BEAMS APPLYING STEEL - YIELDING METHODS

4.1. INTRODUCTION

In this chapter an attempt is made to assess the experimental ultimate strength of the author's beams by means of existing methods of analysis. The assumptions necessary to apply these theories are out-lined in each case, and the outcome of the comparison with the given theory is presented in the form of a TEST/THEORY diagram. As the measure of the accuracy of the applied method, the mean, standard diviation and coefficient of variation of the test results with respect to the given theory is calculated. The critical value and mode of failure, wherever predicted, are compared to the observed values and characteristics and examined with particular reference to the masurements obtained by the strain and mechanical dial gauges and the corresponding visual evidence from the failure cracking patterns - already presented in Chapter 3.

Prior to the detailed analysis, however, section 4.2 presents comments on the relevance and development of the main methods available to analyse the combined torsion problem. Subsequently the necessary conclusions are drawn from the analytical work and the advantages and disadvantages of the existing methods are emphasised.

4.2 Analysis for Torsion Bending and Shear

For the theoretical prediction of the behaviour and ultimate strength of concrete members subjected to combined torsion, bending and shear, an interaction surface must be developed. This will

meet the need for a usable tool for design and research purposes and the analysis of test results. To develop a complete interaction surface a sound analytical method is needed to cover the whole range of combined loading and to take into account the variation of materials strength and geometrical characteristics of the tested beams. A large number of test results are, therefore, required to establish the validity of such a method. In addition to the experimental results available in the literature, this investigation adds a further thirty-six beams.

Unfortunately, the available analytical methods are not suitable to be presented in an interaction form. As an alternative previous investigations (9,10, 37) produced experimental curves of the interaction surface. These empirical curves were applicable only to the test results of that investigation and are not suitable for a graphical comparison with test results from other investigators.

Two analytical methods viz Space-Truss theory and Skew Bending theory, have been applied to the analysis of the interaction between torsion, bending and shear. Neither was intended as a complete solution, but only to cover the case when the steel yeilded. The complete solution is more diffcult and further research is required to consider conditions where the steel does not yield and where the strength of the concrete varies.

4.3 Analysis of Test Beams using Lessig - Marashkins Theory (1965)

Backing her theory with the observed skew bending failure surface, Lessig (⋅ 42) studied force, moments - equilibrium conditions and derived the necessary formula for the ultimate torque. The latter was evaluated by differentiation with respect to the inclination of the compression zone. To achieve a solution for the depth of the compression zone an empirical method. was later established

4.3.1 Theory - Mode One

The basic expressions were formulated originally for reinforced concrete sections. Murashkin (43) from testing an exploratory set of prestressed and non-stressed beams containing stirrups and with out stirrups showed, however, that the theory could be applied also to prestressed beams. For further particulars of Murashkin's beams and test procedure reference is made to Chapter 1 and the appendix.

After making the assumption of a completely yielded steel, the basic theoretical expression for the torsional strength is:

$$T\left[\frac{C_1}{b} + \frac{M}{T}\right] = \left[f_{ly}\ A_l + f_{sy}\ \frac{A_s\ C_1^2}{S(2h+b)}\right]\left[d_1 - \frac{dn_1}{2}\right]$$

To achieve a solution for this equation the two unknowns dn_1, the

depth of the neutral axis , and C_1, the projected length of the inclined skewed bending axis, need be evaluated. To determine these, the following two equations were presented by Lessig:

$$dn_1 = \left[f_{ly} A_l + f_{sy} \frac{A_s C_1^2}{S(2h+b)} \right] b / \left[C_1^2 + b^2 \right] R_b \qquad \ldots\ldots 4.3.2$$

in which

$$C_1 = -b \frac{M}{T} + \left[\left(\frac{bM}{T} \right)^2 + \frac{f_{ly} A_l S}{f_{sy} A_s} (2h + b) \right]^{\frac{1}{2}}$$

and

$$C_1/b = -M/T + \sqrt{(M/T)^2 + \frac{f_{ly} A_l S}{f_{sy} A_s b} (2h/b + 1)} \qquad \ldots\ldots 4.3.3$$

4.3.2. Application to Test Beams

In applying the theory to the author's test beams, it was assumed that the total of the longitudinal steel, A_l , was concentrated at an effective depth, d_l . For steel yielding stresses, the two values of 342 N/mm^2 and 1426 N/mm^2 were used for f_{sy} and f_{ly}, respectively. It was not clear, however, what concrete control specimens test result should be used for R_b defined as the compressive strength of concrete.

Consequently, it was assumed to be 0.85 fc', but a reduced value of (2/3) fc' was used to cater for the stress interactionin the presence of torsion and shear.

The theoretical predictions of ultimate strength of the test beams are presented in Table 4.1. and compared to the experimental results in the following subsection.

4.3.3. Test/Theory

In Fig. (4.1.) the theoretical predictions are plotted versus the experimental strengths for the test beams. Moreover the ratios of the test result to the theoretical strength were computed and are given in Table 4.1

For a total of thirty-six beams, the mean ratio is 0.65 with a standard deviation of 0.21 and coefficient of variation of 32%. For a twenty-one beams cracked in flexure, however, those values were respectively 0.67 $\pm$ 0.24 and 36%. The method is, therefore, unconservative and generally not consistent with the variation of the experimental strength in relation to the basic parameters varied in this investigation.

4.3.4. Discussions

In the discussion of these ratio results for the author's beams, it is noted that for Murashkin's six beams in Series A a mean ratio of 1.103 $\pm$ 0.102 could be calculated with a coefficient of variation of 9.3%.

This large difference between Murashkin's test results and the author's in accuracy and consistency must be attributed mainly to

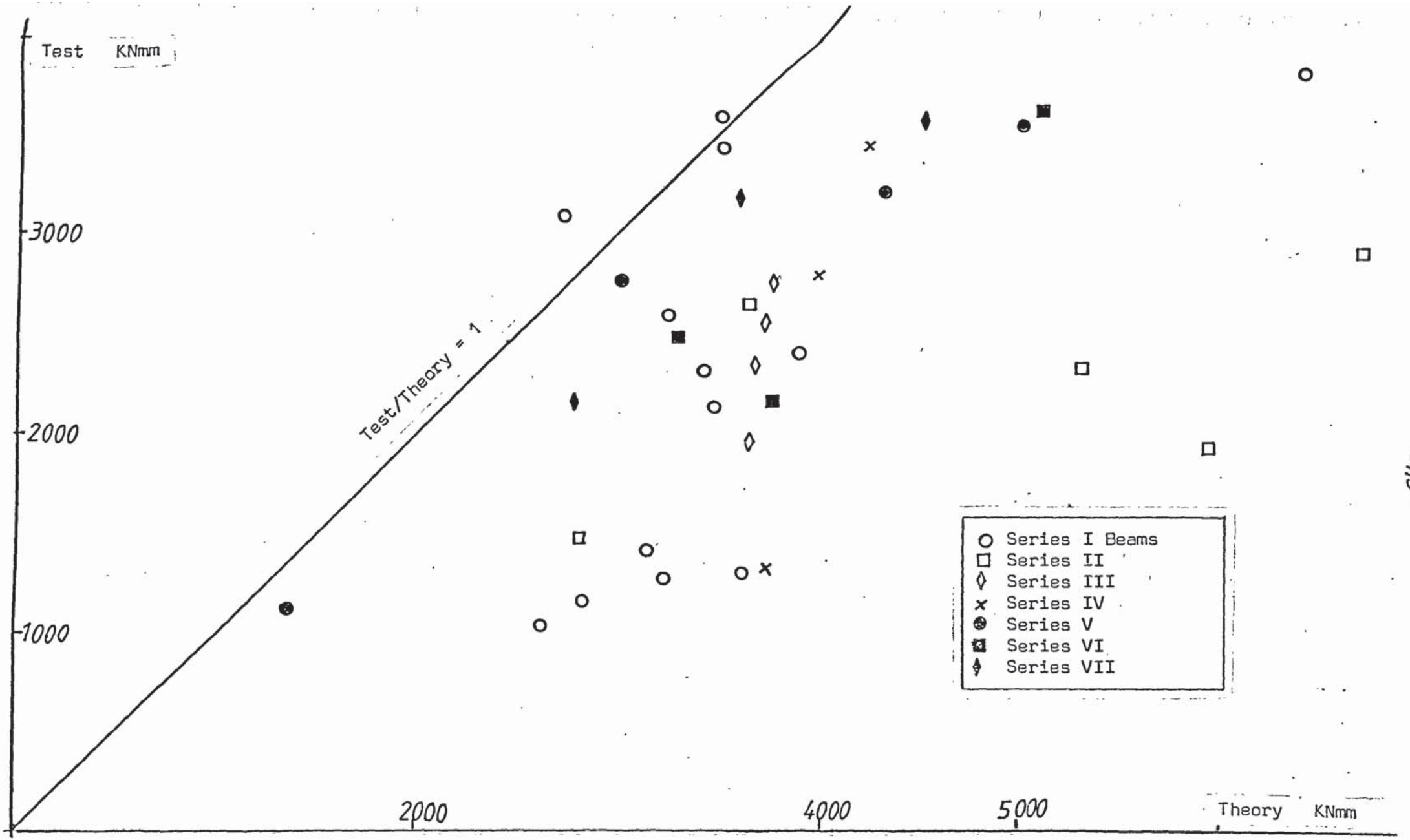

FIG.(4.1): LESSIG-MURASHKIN'S THEORY COMPARED TO TEST BEAMS

Table 4.1. Analysis of Test Results by Murashkin's Theory

Beam	Test Torsion kNmm	Theory Mode 1 kNmm	Ratio of Test/ Theory 1	Theory Mode 2 kNmm	Ratio of Test/ Theory 2	Ratio of Test/The Critical
A1	1120.0	2799.5	0.40	4136.3	0.27	0.40
A2	1274.0	3543.8	0.36	4440.0	0.29	0.36
A3	1400.0	3101.7	0.45	4177.2	0.34	0.45
A4	1036.0	2572.8	0.40	3967.1	0.26	0.40
A5	1260.0	3192.3	0.40	4210.3	0.30	0.40
A6	2100.0	3419.0	0.61	4248.9	0.49	0.61
A7	2287.0	3381.0	0.68	4309.9	0.53	0.68
A8	2366.0	3818.0	0.62	4482.8	0.53	0.62
A9	2538.0	3194.6	0.79	4182.1	0.61	0.79
A10	3402.0	3499.8	0.97	4360.7	0.78	0.97
A11	3542.0	3344.8	1.06	4362.9	0.81	1.06
B1	1428.0	2748.2	0.52	3530.3	0.40	0.52
B2	2604.0	3607.4	0.72	4419.7	0.59	0.72
B3	2310.0	5241.7	0.44	6223.9	0.37	0.44
B4	1890.0	5880.9	0.32	6999.3	0.27	0.32
B5	2880.0	6630.1	0.43	7909.4	0.36	0.43
B6	2240.0	6925.0	0.32	8606.5	0.26	0.32
C1	1918.0	360212	0153	4396.7	0.44	0.53
C2	2324.0	3632.9	0.64	4440.5	0.52	0.64
C3	2730.0	3719.8	0.73	4447.7	0.61	0.73
C4	2520.0	3680.5	0.69	4479.2	0.56	0.69
D1	1288.0	3673.5	0.35	4206.2	0.31	0.35
D2	2758.0	3934.9	0.70	5009.1	0.55	0.70
D3	3388.0	4170.0	0.81	5485.4	0.62	0.81
E1	3500.0	6345.3	0.55	4960.4	0.71	0.71
E2	3178.0	4266.6	0.75	4628.2	0.69	0.75
E3	2730.0	2980.0	0.92	4223.6	0.65	0.92
E4	1106.0	1338.3	0.83	3089.6	0.36	0.83
F0	2128.0	3707.9	0.57	5373.4	0.40	0.57
F1	3570.0	5055.9	0.71	5824.4	0.61	0.71
F2	2450.0	3253.8	0.75	5213.0	0.47	0.75
G1	3528.0	4467.2	0.79	4850.4	0.73	0.79
G2	3150.0	3551.0	0.89	4523.9	0.70	0.89
G3	2128.0	2720.0	0.78	4240.0	0.50	0.78
AA1	3080.0	2682.7	1.15	-	-	1.15
AA2	3780.0	6347.4	0.60	-	-	0.60

Series A: Mean = 0.61, Standard Deviation = 0123

Coefficient of variation = 37.9%

Total 36 beams: Mean = 0.65, Standard Deviation = 0.21

Coefficient of variation = 32.2%

two reasons: experimental and theoretical. The former is related to the lowered strength values of the author's test beams due to the use of unbounded tendons and the presence of a transverse shear force in the test span. This force also caused a variable bending moment throughout the test span which affected the consistency of the results when compared to Murashkin's results obtained under a constant M/T ratio. In the experimentation method as followed in the present investigation the tested beams included a wide range of variables. By contrast, Murashkin's beams were limited in number and basically constant parameters were involved. His prestressing steel had a strength much lower than was used in this work.

Theoretically; for the author's beams the predictions made by Murashkin's method are almost independent of the prestressing force. Thus in the Diagram 4.3.4, the series A points are generally along a line running parallel to the Test axis. From Table 4.1 also it is obvious that the predictions of the analysis is in poor agreement with the test values. Hence the too high coefficient of variation of 38% resulting from applying the method to series I group A beams. Nonetheless it is noted that the numerical accuracy improved as the prestressing force increased to nearly 60% P_s^y in the case of beams A10 and A11. (Murashkin's beams were generally highly prestressed, in some beams as high as ninety percent P_s^y) (43)

With increasing the prestressing steel, the accuracy of the method was adversely affected. This was apparently because the steel-yielding assumption increased the strength estimate regardless of the strain compatibility, concrete strength and prestress level.

This same trend was noticeable when the h/b ratios were reduced. An increase of 263% in the test strength was under-estimated by the theory to be 113%. The relatively broad beam D3 is seen to be the closest to the 45^{o} line. This is reasonable because beam D1 was the smaller in cross-section, thus to obtain the same prestress level as in beam D3 the tendons were tensioned by a prestressing force lower than was required to post-tension D3 beam. It is reasonable to expect the latter beam to reach yielding in the tendons before D1 beam. Experimentally, beam D3 did not yield, however, and the increases in the tendon forces were much lower than those occurred in case D1.

Finally, it may be deduced from Diagram 4.1 that for the E beams tested subjected to variable M/T ratios, the theory was reasonably accurate. The accuracy, however, varied depending on M/T ratios from 0.83 in case of E4 beam to 0.75 for beam E2. The method does not extrapolate satisfactorily to the simple loading case of pure torsion thus the test/theory ratio produced for E1 beam was 0.55.

4.3.5 Further considerations:

Although based on a reasonably realistic machanism of failure clearly indentifiable from experiments, Lessig's solution was not simple or easy to handle in an interaction form for mode 1. The theory ignores the shear force because the moments are conveniently taken at the centre of the compressive zone. The steel forces in the tensile zone are known by the assumption of yielding and the tensile strength of concrete is taken as zero.

Apart from the lack of attention to compatibility conditions, a serious criticism that can be levelled at this theory is that equlibrium is not satisfied for the moment and force equations. In this respect Yudin (1962) (42) also noted that Lessig's original expressions were incomplete and further equations were needed. In an attempt to justify the theory Lyalin (42) pointed out that this is not required because rotation takes place about the skewed plastic hinge. Lyalin also presented a simpler derivation of the Lessig's ultimate equilibrium equations which required the solution of only two equilibrium equations.

In mode 2, however, the method which predicts a linear interaction between flexural shear and twisting moment does not extrapolate to the simple case of pure shear. Calculations of the test beams strength according to mode 2 predictions were also made and are also tabulated in Table 4.1 With the exception of beam E1 in pure torsion, the theory is not critical for mode 2 but in many cases this is contradicted by the experimental observation as presented in Chapter 3.

The objective of this section was to examine the author's test results by an all-yield theory. From the comparison with Lessig-Murashkin's method, it is deduced that the beams tested were generally far below the "yielding" strength.

4.4 Analysis of Test Beams using Rangan and Hall's Simplified Theory (1973)

Collins et al, (1968) (56) and Rangan and Hall (1973) (5), modified Lessig's method to apply to reinforced and prestressed concrete beams subjected to combined loading. Rangan and Hall 's simplified method for prestressed concrete beams is similar in the analytical approach, i.e. optimization of the torque, but is further simplified by assuming the neutral axis coincides with the horizontal leg of the stirrups.

4.4.1 Theory - 3 modes

Following Walsh et al. and Collins et al, who first analysed a third mode of failure for reinforced sections, the theory also considered solutions for three modes of failure for prestressed members. In addition a semi-empirical equation was derived by Rangan et al. and will be discussed in sections 4.7 of this Chapter.

In mode 1 the solution was presented in the form of:

$$T_1 = M_o \frac{2r}{1 + 2\,h/b} \tan\theta_1$$

where

$$\tan\theta_1 = \sqrt{(M/T)^2 + \frac{1 + 2\,h/b}{r}} - M/T$$

in which M_o = 26350 kNmm for the Series A, C, E etc of the beams tested by the author, and defined as the product of the prestressing steel yielding force times its effective depth. Therefore, the assumption of yielding for the (longitudinal) prestressing steel is apparently made.

For mode 2, Rangan et al, realised the difficulties associated with assuming that all of the steel yield. ·d when applied to situations where high torsion and shear force were involved. The flexural capacity in Mode 1, M_o, was re-determined using a reduced area of prestressing steel and hence used in the torsional strength equation for mode 2 expressed as:

$$T_2 = \frac{M_o}{1 + \frac{b'V}{2T}} \sqrt{\frac{4r}{1 + 2\,b/h}\, R_2}$$

in which

$$R_2 = \frac{\frac{1}{2}(A_l' + A_l) + (f_{py}/f_{ly})\,\beta_2\,A_{ps}\,\frac{b'}{d'}}{A_l + \frac{f_{py}}{f_y} \times 1 \times A_{ps}}$$

4.4.2 Application

For the test beams series A,C, E, etc. M_o is calculated to be 26350 kNmm, in mode 1. In mode 2, $R_2 = 0.196$ and

$\beta_2 = 0.5 \times \frac{b}{2} \times \frac{l}{b'} = 0.375$ where the factor 0.5 is assumed as the yielding portion of the steel since the theory text does not contain more detailed guidance.

For mode 3, $R_3 = M_o(3) / M_o(1) = 0.481$

4.4.3 Ratio of Test/Theory

The results for each mode are listed in Table 4.2. The highest mode value is taken as the critical. For twenty-five beams the theory predicts a failure in mode 2. Only two beams fail in mode 1 and one more in mode 3. The remaining eight beams fail, according to the theory, in shear- compression. This mode of failure is considered in section 4.7.

For the total of thirty-six beams, however; the numerical correlation is apparently good if expressed as a mean of 1.044 with a standard deviation of 0.30 and a coefficient of variation of 29%.

4.4.4 Discussion

Although the mean value is very good, as it can be seen from

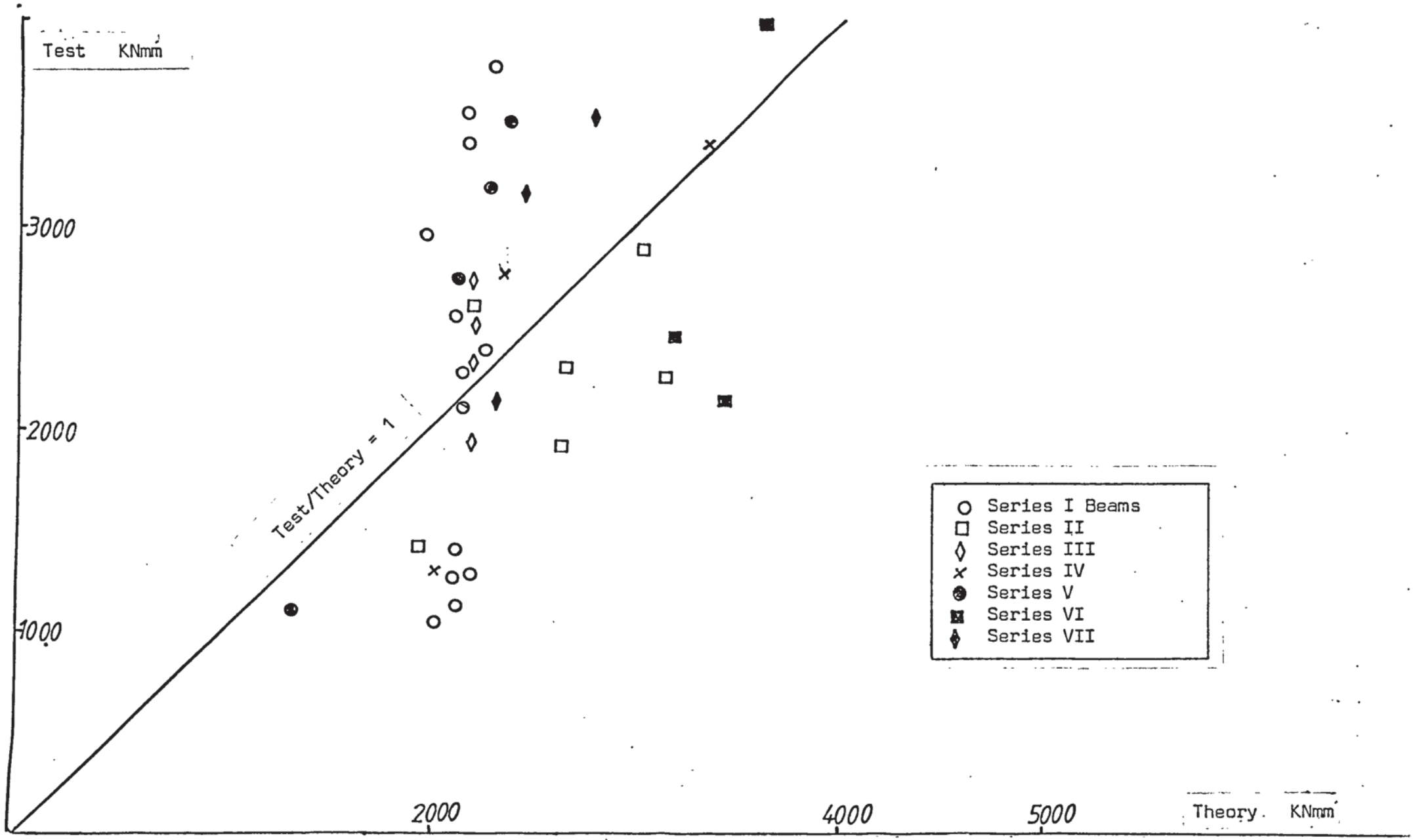

Fig.(4.2): RANGAN AND HALL'S THEORY COMPARED TO TEST BEAMS

Table 4.2 Analysis of Test Results by Rangan - Hall's Theory

Beam	Test Torsion kNmm	Theory Mode 1 kNmm	Ratio Test Theory (1)	Theory Mode 2 kNmm	Ratio Test Theory (2)	Theory Mode 3 kNmm	Ratio Test Theory (3)	Ratio Test Theory Critical	
A1	1120.0	2489.5	0.45	2094.0	0.53	4561.3	0.25	0.53	*
A2	1274.0	2874.1	0.44	2208.3	0.58	3747.6	0.34	0.58	*
A3	1400.0	2672.7	0.52	2126.8	0.66	4143.0	0.34	0.66	*
A4	1036.0	2340.2	0.44	2031.8	0.51	4951.4	0.21	0.51	*
A5	1260.0	2714.2	0.46	2124.7	0.59	4056.5	0.31	0.59	*
A6	2100.0	2824.4	0.74	2140.0	0.98	3839.7	0.55	0.98	
A7	2282.0	2795.4	0.82	2159.9	1.06	3895.0	0.55	1.06	
A8	2366.0	2996.3	0.79	2226.1	1.06	3535.2	0.67	1.06	
A9	2538.0	2702.9	0.94	2112.7	1.20	4079.8	0.62	1.20	
A10	3402.0	2853.8	1.19	2178.9	1.56	3784.8	0.9	1.56	
A11	3543.0	2786.3	1.27	2178.0	1.63	3912.5	0.91	1.63	
B1	1428.0	2383.6	0.60	1945.6	0.73	2489.4	0.57	0.73	
B2	2604.0	2905.1	0.90	2198.3	1.18	-	-	1.18	
B3	2310.0	4192.8	0.60	2644.1	0.87	-	-	0.87	
B4	1890.0	4394.1	0.43	2610.4	0.72	-	-	0.72	
B5	2880.0	4425.0	0.65	3023.6	0.95	-	-	0.95	
B6	2240.0	4601.4	0.49	3146.9	0.71	-	-	0.71	*
C1	1918.0	2916.1	0.66	2209.2	0.87	3672.4	0.52	0.87	
C2	2323.0	2918.0	0.80	2208.0	1.05	3668.9	0.63	1.05	
C3	2730.0	2952.5	0.92	2206.4	1.24	3609.1	0.76	1.24	
C4	2520.0	2928.2	0.86	2208.5	1.14	3651.1	0.69	1.14	
D1	1288.0	2371.3	0.54	2003.7	0.64	-	-	0.64	*
D2	2758.0	3368,8	0.82	2349.3	1.17	-	-	1.17	*
D3	3388.0	3913.1	0.87	3356.1	1.01	-	-	1.01	
E1	3500.0	3701.5	0.95	2381.9	1.47	2613.3	1.34	1.47	
E2	3178.0	3161.8	1.01	2266.4	1.40	3276,4	0.97	1.40	
E3	2730.0	2588.3	1.05	2125.7	1.28	4328.2	0.63	1.28	
E4	1106.0	1335.1	0.83	1676.2	0.66	-	0.11	0.83	
F0	2128.0	3586.9	0.59	3420.8	0.62	-	0.26	0.62	
F1	3990.0	47.68.4	0.84	3627.6	1.10	-	0.26	1.10	
F2	2450.0	3181.1	0.77	3322.8	0.74	-	0.26	0.77	
G1	3528.0	3518.2	1.00	2550.8	1.38	3713.7	0.95	1.38	
G2	3150.0	3089.2	1.02	2433.9	1.29	4436.6	0.71	1.29	
G3	2128.0	2547.6	0.84	2315.3	0.92	5751.4	0.37	0.92	
AA1	2940.0	2465.8	1.19	1991.1	1.48	3880.3	0.76	1.48	
AA2	3780.0	3486.6	1.08	2300.5	1.64	2301.5	1.64	1.64	

Mean + Standard Deviation (%)

Series A
Mode One: 0.73 ± 0.29 (39.5%)
Mode two: 0.94 ± 0.39 (41.0%)

All Modes ** 0.99 ± 0.34 (34.7%)

All series

All modes ** 1.04 ± 0.30 (28.9%)

* Shear - compression formula governs Cf. Table 4.7.2.1.
** Including shear - compression failure.

Figure 4.2 that the scatter is high and the high coefficient of variation indicates that some of the theoretical assumptions may not be correct.

1. The theory is independent of the prestressing force. This is evident from the format of the theory and clearly shown when compared to the test results I A - beams. For these eleven beams, in particular, the ratio of test/theory = 0.94 $\pm$ 0.39 with a coefficient of variation of 41% all failures being confined to mode 2. In the laboratory only two beams definately failed in this mode, whereas the rest failed in mode one or by web crushing. This if only the mode 1 analysis is applied a mean and a standard deviation of 0.73 $\pm$ 0.29 results with a 39.5% as a coefficient of variation. A little more accuracy can be achieved by considering the results from the shear-compression formula and this will be discussed later.

2. The theory is unconservative for test beams prestressed by less than 35% P_s^y as well as beams with increased quantities of prestressing steel. e.g B_3 and B_6 beams.

3, The theory in mode 2 is conservative producing, for high torsion a Test/Theory ratio of 1.47 for beam E1 (pure torsion) but less accurate with higher bending moment e.g. for beam E4 the test ratio = 0.83.. Similarly the theory is conversative for a high prestress force e.g. A10 and A11 beams. In both case of prestress force and M/T variations, the ratio of Test/Theory varied favourably when the test torque generally exceeded the theoretical value.

It is concluded that this method is not fully suitable for the analysis of the interaction between the combined loadings and adopts an empirical approach to the problem of shear strength. For this case Rangan et al produced an independent expression on the basis of partial yield of stirrups. No clear restraints were imposed in mode 2, however, to ensure that only a "reduced portion" of the longitudinal steel would yield with the yield of the stirrups.

When applied to the author's beams, the method in mode 2 was closer to a partial yield theory. Hence a relatively better accuracy was obtained compared to the other yield theories when applied in analysing the test strengths of the present investigation.

4.5 Analysis of Test Beam using Woodhead- McMullen's Theory (1974)

In an attempt to modify Lessig 's method to account for the presence of flexural shear, McMullen and Woodhead (51) presented an alternative method for prestressed members.

4.5.1. Theory - Torsion Mode, Analysis A

This phase of the analysis, according to McMullen et al, represented an all steel yield theory which conformed to a mechanism of mode 2 failure in the terminology of Lessig's theory for reinforced sections. In extending that theory to apply to prestressed beams, the inclination of the skewed axis was

determined from an elastic cracking analysis. The latter considers the cracking initiated at one wider side and spreading with the same angle to the top and soffit faces. The failure cracking surface at failure being enclosed by the crushing compression hinge on the opposite wide side. In this procedure the depth of compressive zone (or the neutral axis) is therefore ignored initially.

As opposed to Rangan and Hall's theory (1973), however, the theory includes a value for the depth of the neutral axis x', from equilibrium of forces normal to the skew axis plane. Nonetheless it is recommended that x' should be confined within the concrete cover so that any steel be excluded from the compression zone.

4.5.2. Application

The theory in its torsion mode - Analysis A requires that the quantities of (b v/T), P_s^y , $P_{s\ eff}$ and f_c' be known. To calculate the x' value an equivalent rectangular stress block is assumed related to x' by a factor k_1. Series C beams excepted, K_1 is calculated for the author's beams as based on an average value = 0.85 - 0.05 (5377 p_{si} - 4000 p_{si})/1000 = 0.78, in which 5377 p_{si} (37.08 N/mm^2) is the mean test value of f_c' for thirty - three beams Cf control specimens results - Chapter 3. Whereas this value is substituted in the equation of x', for 0.85 k_1, the actual test values of f_c' are otherwise used. Following the notations of the paper the following values are found for the author's beams :- a = a_1 = 20.5mm and a_2 = 15mm.

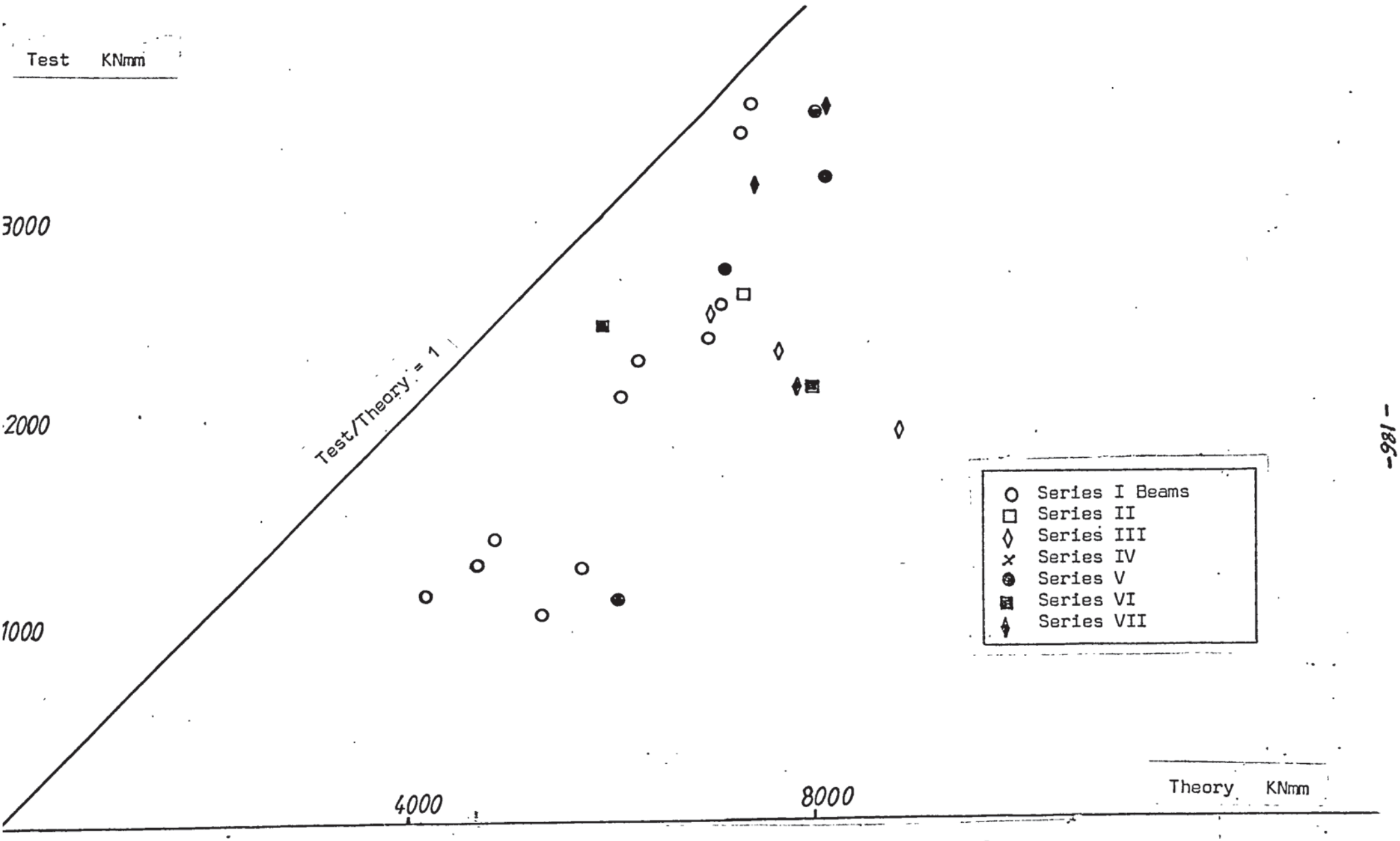

Fig.(4.3): WOODHEAD-MCMULLEN'S THEORY COMPARED TO TEST BEAMS

4.5.3. Ratios of Test/Theory

The correlation between Theory and the test results is presented in Fig. 4.3. but the ratios of Test/Theory are not tabulated in this section. The Theory includes also the theoretical values of the depth of compression zone and its inclination with the long axis of the beam.

4.5.4. Discussion

It is clear from Fig. 4.3. that the predictions are generally twice the experimental values. Foe Series I - A beams. the ratio is on the average 0.32 of the test value and 0.09 standard deviation with a coefficient of variation of 26.5%. This may be also assessed from the variation of the predictions for these eleven beams with respect to the Test-Theory line as shown in Fig. 4.3 This theory is considered as an improvement on Murashkin and Rangan and Hall's analyses; both of which were independent of the prestress force. The theory is related to the prestressing by depending initially on an elastic cracking angle for the inclination of the skewed axis and then forces equilibrium is satisfied normal to the axis. As a result the theory is also sensitive to the variation of concrete strength. See the points representing beams C1, 2 and 4 in Diagram 4.3. The stronger the concrete the more accurate the theory became.

The higher the torsional moment the closer the predictions made by the theory came to the test values of beams involving variable ratios of M/T, web steel percentage and stirrups spacing. Reference

is respectively made to beams E1,2 and 3 F1, 2 and G 1 and 2 in the diagram When lower values of torsion mement occurred, however, the analysis is not as accurate, but nevertheless, for the latter mentioned thirteen beams the mean was 0.37 $\pm$ 0.08 with C.V. = 22%.

In conclusion, although the method is extended to include the variation of the bending moment due to the shear force, the latter does not appear in 'mode 1" and in the 'torsion mode' the accuracy of the analysis is unfavourably affected in presence of high shear forces. The method is iterative and can not be presented in the interaction form. The analysis A for the all yield situation indicated that no test beam reached yield in mode 2 in this investigation and this agrees with the experimental observations presviously presented.

4.6 Analysis of Test Beams using Elfgren et al's Interaction Theory (1974)

The skew bending theory formed the basis for all the previous methods whereas , the Truss Analogy orginally suggested by Rausch in 1929 formed the basis for alternative theories. The original model was a 45^{o} inclined diagonal truss applied to the simple loading case of pure torsion. The method was refined in 1969, by Lampert (11) to cover a more general case of torsion with bending, introducing a "space truss model with variable inclinations of the diagonals". The same approach was also extended to include torsion, bending and shear by Elfgren (**59**). The latter model differed from that of Lambert by considering the centrelines of the stirrups to govern the

cross-sectional dimensions (b' x h') of the failure plane. By contrast, Lampert made the observation that the diagonal forces in the "shear wall" were deflected into the adjacent wall by means of the longitudinal corner bars whose location would determine the cross-sectional dimensions ($b_o \times h_o$). Lampert regarded this difference as important for the small cross section usually involved in testing. This is of considerable significance for prestressed concrete beams because it implies that the prestressing steel which is not located at the corners can be also relied on as torsional steel.

In Elfgren's method it is assumed that the yielding of "all" the steel occurs in three sides, whereas the unyielded stirrups in the fourth side define the hing (along the compression zone) around which the beam rotates at failure. In Lampert's failure mechanism two unyielded longitudinal corner bars define the hinge at failure. All the stirrups and the rest of the longitudinal steel yield on all four sides of the cross sections. Lampert, however, did not consider the possibility of one unyielded longitudinal bar defining the hinge at failure. Such a possibility will not violate his "possible hinge" rule because the hinge in this case also does not pass through the enclosed failure area.

Lampert (11) also extended the space truss theory for reinforced beams to prestressed beams. He showed that with respect to ultimate strength, prestressed members could be treated as non-prestressed members with an equivalent amount of reinforcement.

He argued that if the additional strain up to yield in tendons and bars were approximately the same, then only the yield force of the steel is significant.

4.6.1. Theory - 3 Modes

In 1974, Elfgren et al (59) presented a simplified method for the analysis of the reinforced concrete beams. Three modes were analysed and appropriate solutions derived. As was proposed by Lampert no basic differences existed between reinforced and prestressed beams, as far as ultimate strength was concerned.

4.6.2. Application

To examine the accuracy of the theory when applied to prestressed concrete beams the interaction equation of Elfgrn et al. have been applied to predict the ulitmate strength of the authors test beams.

Based on 382 N/mm^2 (of the mild steel) unified strength: the equivalent areas at top and bottom corners were respectively $97.0mm^2$ and $477.8\ mm^2$. at each top corner, an area of $28.27\ mm^2$ was added to represent the existing mild bar.

4.6.3 Test/Theory

For the eleven beams of Series I, the analysis in mode 1 produced a mean of 0.59 ± 0.31 with a coefficient of variation of 53%.

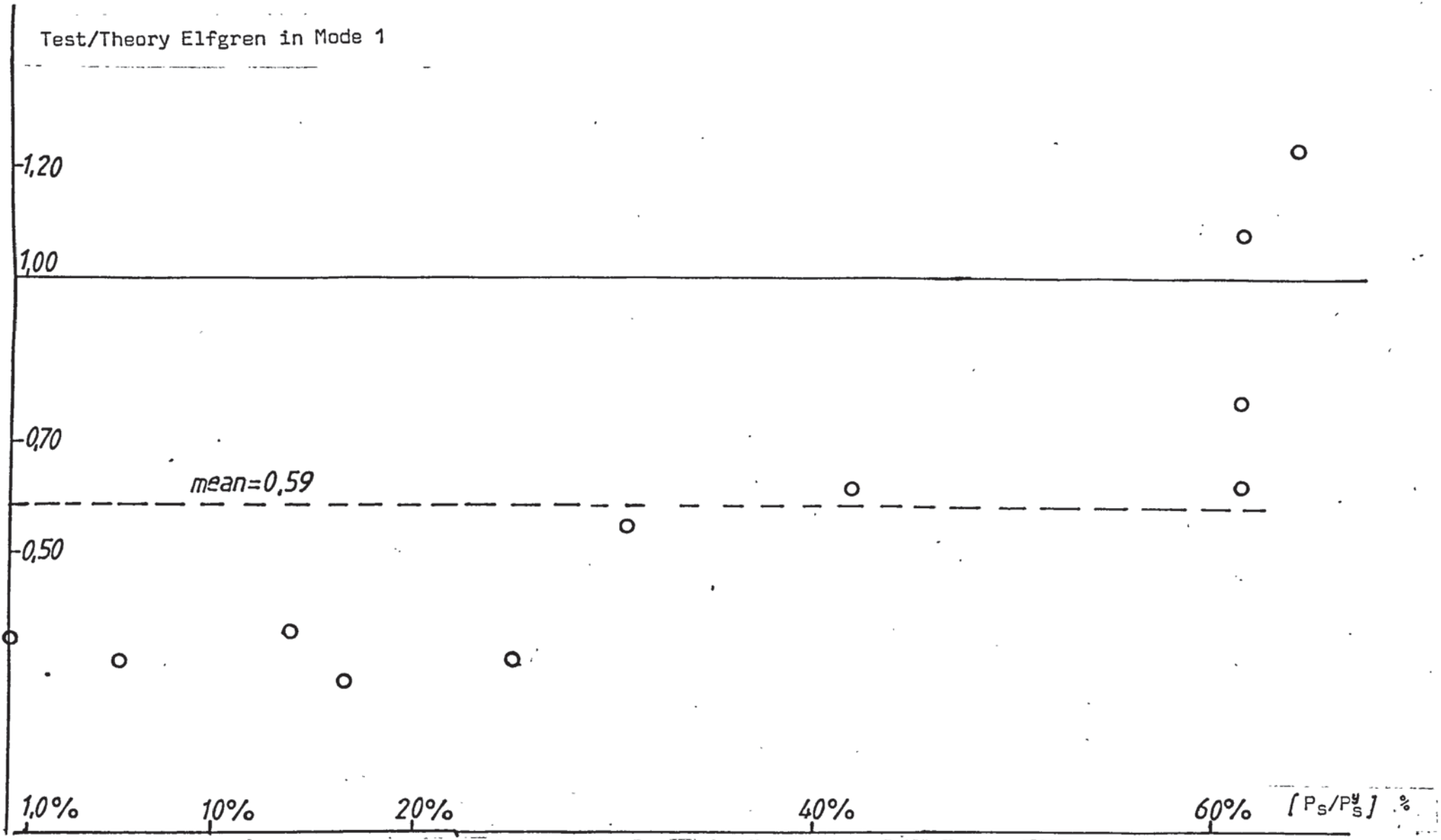

Fig.(4.6.3): ELFGREN et al THEORY FOR MODE 1
COMPARED TO THE TEST RESULTS OF SERIES I

Plotting the ratio of test/theory against prestressing percentage which is the main parameter of variation in series I a definite pattern can be observed. Referring to Figure 4.6.3. the accuracy is improved as the Prestressing Force % or pc^2/f_c' increases. Thus for eleven beams, prestressed to more than 30% P_s^y, a mean of 0.80 ± 0.19 is obtained with a variation of 23.7%. For seventeen beams, in mode 1 a mean of 0.64 ± 0.27 with a C. V. = 41.6% is obtained. The correlation is much improved if the beams of series I are excluded: for six beams with nearly equal prestressing, a mean = 0.75 ± 0.09 (12,6%) can be ontained.

4.6.4. Discussions

Elfgren's theory was based on yileidng of the steel and was intended to ensure within certain limits of reinforcement that both categories of steel longitudinal and stirrups, would yield simultaneously. A value of $\tan\alpha = 1$ was given to be ideal for this case. It was, however, suggested that if $\cot\alpha_t$ had a value within the range $0.5 < \cot\alpha_t < 2$, yielding usually is obtained in both categories of reinforcement. Reference is made to Elfgren et al. (**59**).

Therefore, the ratio of test "yield" theory = 0.64 indicates that the beams strength was lower than the yielding strength. The high scatter, however, reveals that some of the theoretical assumptions are not correct. Elfgren's interaction surface is based on an "all yield"

assumption of the steel but this does not ensure that the concrete does not fail prior to the yield of reinforcement. For such cases it is necessary either to estimate the concrete failure load by some other means e.g. Cowan's dual criterion, or to limit the range of applicability of the yielding theory to exclude these cases. The approach, seen as a Space Truss analogous theory, implies that the concrete contribution to the torque resistance is nil.

4.7. Analysis of Test Beams using Partially Steel-Yielding Methods of the General Form: $T = T_c + T_{sy}$:-

To improve the correlation between his test results and the current theory, Andersen (26) was the first to produce the above form for torsion in reinforced concrete. This form consists apparently of a concrete term T_c and a steel term T_s. The introduction of prestressing to the section introduces a direct compressive stress in the concrete which interacts with the shear stress resulting from torsion. Zia (40) was the first a analyse prestressed sections applying Cowan's simplified concrete failure criterion for the purpose of determining T_c, which Zia took as the cracking moment. In contrast T_s was an invariable quantity similar to the one accounted for by Rausch or Cowan. As the controversy continued about the qualtitive nature of the T_c term, the T_s term remained as the stirrup yield moment. Thus the longitudinal steel was not required to yield and the prestressing effect was absorbed

in T_c.

4.8.1 The Shear - Compression Equation By Rangan & Hall

Rangan and Hall (5) distinguished between two types of failure: a flexure type failure on a skew plane and a flexure shear type of failure. The theory for the three modes for the former type have already been covered in section 4.4. It was not possible for them to extend the theoretical analysis of these modes to consider the situation where, in presence of torsion and shear, the strength is reduced below that predicted in pure flexure. Describing this failure as a shear compression type, and as a sequel to the skew bending analysis, a semi-empirical formula was produced for the strength in such a mode of failure.

The stirrups were assumed to yield but not the longitudinal steel (prestressing and non-stressed). The torsional strength was the sum of a concrete resistance and the stirrups resistance: $T = T_c + T_s$. In evaluating these two components, Rangan and Hall opportioned the concrete strength and the stirrups area between the torsion and the shear force. A linear interaction: $\frac{Tc}{T_{co}} + \frac{Vc}{V_{co}} = 1$ was assumed to evaluate the term Tc.

The McGee and Zia's Formula (1974)

With fewer assumptions but with heavier reliance on empirical

consideration of a large number of test results, McGee and Zia (52) produced a similar formula of the general form:-

$$Tu = \alpha_1 b^2 h \quad 6 \sqrt{f_c'} \left[\sqrt{1 + 10\, pc_2/f_c'} - K_{web} \right] + T_s$$

in which $k_{web} = \frac{1 - 0.133}{\alpha_1}$ and from a computer analysis the factor α_1 was determined as equal to $\frac{0.35}{0.75 + b/h}$. The interaction of shear - torsional stresses was also included, on the basis of the American Code requirements, combined with the prestress effect.

Although no claim was made by McGee and Zia about the theoretical basis of their equation it was at the time an attempt to unify the treatment of reinforced and prestressed members in the ACI Code, in which (318-71) the first torsion phrase was derived on the basis of a skew - bending theory.

4.8.2 Application to the Test Beams

Both formulae were applied to analyse the test results of the beams in this investigation.

In Tables 4.5 and 4.6 the computed elements of Rangan-Hall's and McGee-Zia's theories respectively are presented and the experimental strengths are divided by the theoretical predictions to calculate the ratios of Test/Theory. These results are also presented in a

graphic form in Figures 4.7.2.1. and 2.

4.8.3 Correlation of Tests and Predictions

As a measure of correlation the test/theory ratios were calculated. The formula by Rangan et al. when applied to the total of thirty-six beams resulted in a mean of 0.84, and standard deviation of 0.20 and a coefficient of variation of 23.4%. For the same beams, McGee-Zia's formula produced a mean of 0.88, a standard deviation of 0.23 and 26% as a coefficient of variation.

4.8.4. Discussion

The agreement between the outcome of the two analyses is better than previous theories. The reasonably low coefficient of variation of both methods, differing by 10%, indicates a better correlation with the tests than any of the "all yield" methods applied in the fofegoing sections. The average ratio of test/theory = 0.86 is interpreted as that none of the longitudinal steel had yielded in the tests. Futhermore, by McGee-Zia's formula as a criterion, only 11 beams can be regarded as failing at "only the stirrups yielding" strength The implication being that for beams at the same strength level and below the theory line the stirrups stresses should be below the yield also. Reference is made to Figure 4.7.4.2. Figure 4.7.4.1 shows the same trend if Rangan-Hall 's method is adopted.

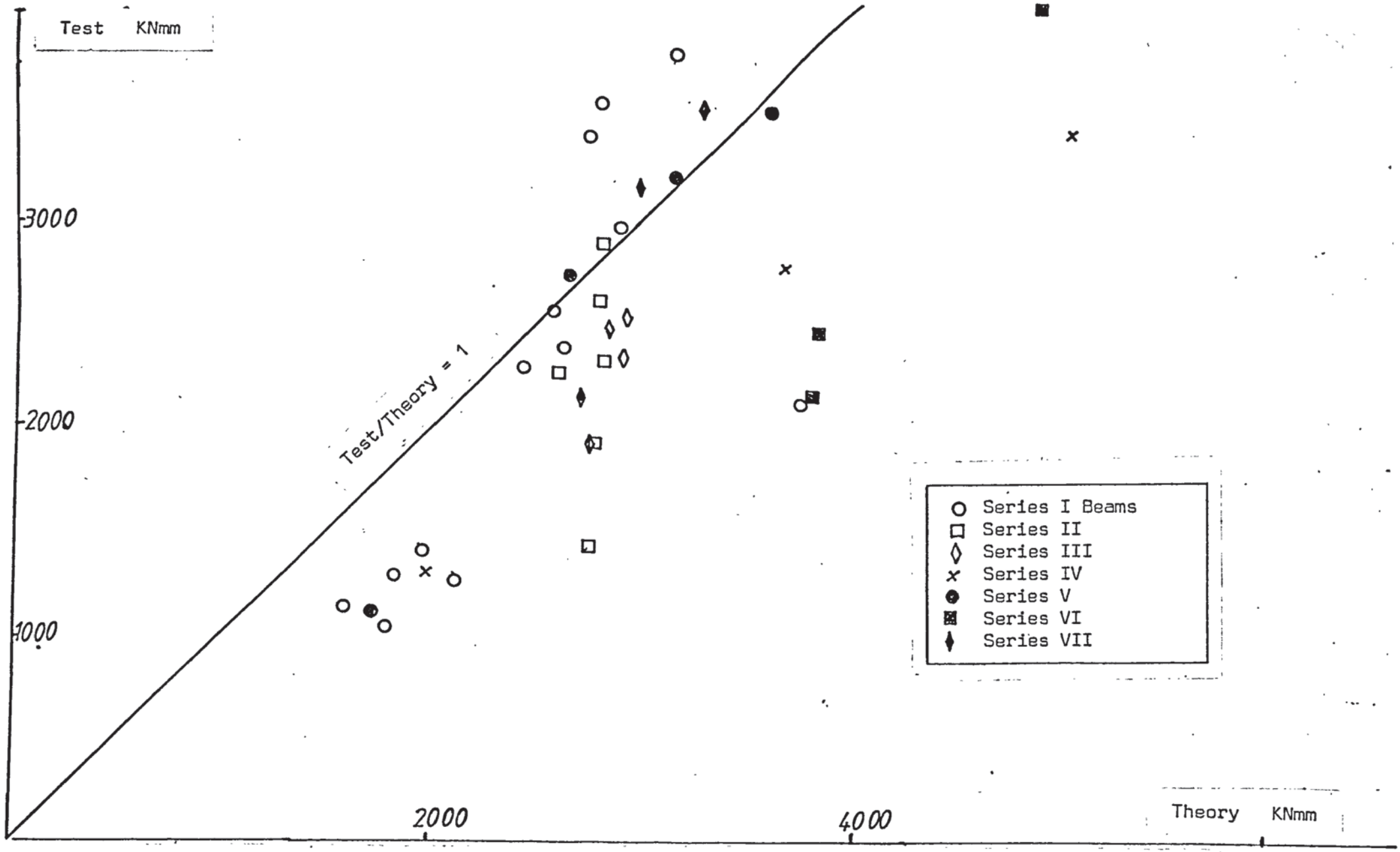

Fig.4.7-2.1): RANGAN & HALL'S THEORY : SHEAR-COMPRESSION COMPARED TO THE TEST BEAMS

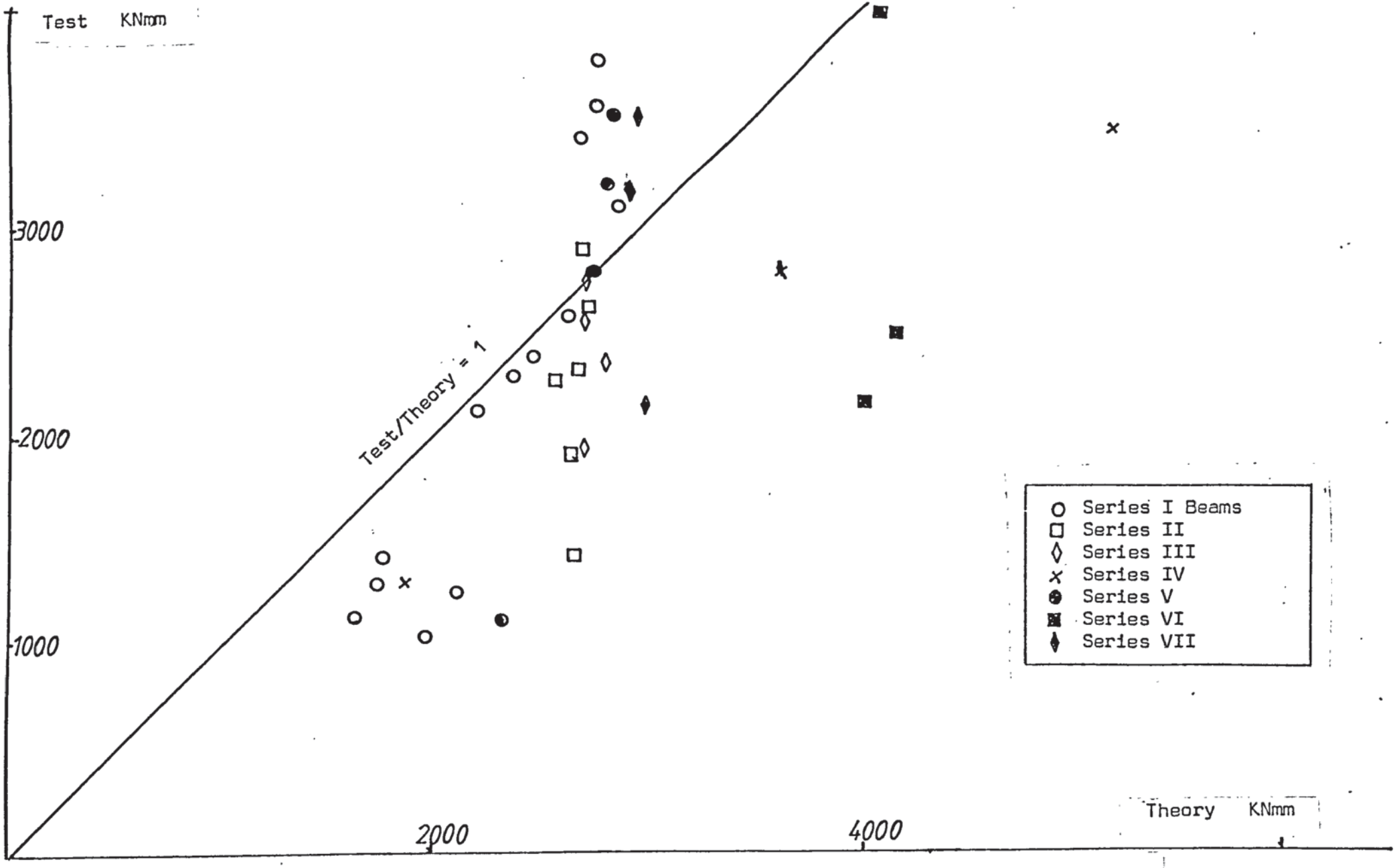

Fig.(4.7-2.2): MCGEE & ZIA'S THEORY (WITH SHEAR INTERACTION) COMPARED TO THE TEST BEAMS

In comparison to the test results of series I - A beams, (McGee - Zia) produces a mean and standard deviation of 0.88 ± 0.23 with a C.V. = 26%. For the same eleven beams (Rangan - Hall) results in a mean and standard deviation = 0.85 ± 0.24 with a C.V. = 28%. The relatively higher coefficinet of variation, for both methods is an indication that some of the assumption e.g. stirrups legs yield are not realistic and the presstressing force, in particular, is not accounted for correctly.

Table 4.5 Analysis of Test Results by Rangan - Hall's Forumla

Beam	Test Shear Force kN	Test Torsion kNmm	Theory kNmm	Test / Theory	
A1	4.56	1120.0	1575.2	0.71	*
A2	3.03	1274.0	1814.8	0.70	*
A3	4.99	1400.00	1707.3	0.82	*
A4	5.25	1036.0	1786.2	0.58	*
A5	4.53	1260.0	2100.0	0.60	*
A6	7.10	2100.0	3720.0	0.56	
A7	7.01	2282.0	2427.7	0.94	
A8	5.04	2366.0	2628.9	0.90	
A9	9.59	2538.0	2563.6	0.99	
A10	9.51	2402.0	2743.5	1.24	
A11	9.95	3542.0	2811.1	1.26	
B1	3.53	1428.0	2746.2	0.52	
B2	6.51	2604.0	2800.0	0.93	
B3	5.67	2310.0	2817.1	0.82	
B4	5.04	1890.0	2779.4	0.68	
B5	6.99	2880.0	2823.5	1.02	*
B6	6.51	2240.0	2604.7	0.86	*
C1	4.54	1918.0	2740.0	0.70	
C2	5.54	2324.0	2905.0	0.80	
C3	6.57	2730.0	2843.8	0.96	
C4	5.99	2520.0	29.30.2	0.86	
D1	3.02	1288.0	1981.5	0.65	*
D2	6.54	2758.0	3677.3	0.75	
D3	8.04	3388.0	5056.7	0.67	
E1	0.43	3500.0	3608.2	0.97	
E2	5.04	3178.0	3146.5	1.01	
E3	9.78	2730.0	2650.5	1.03	
E4	13.50	1106.0	1710.5	0.65	

continued

FO	6.51	2128.0	3800.0	0.56
F1	5.01	3990.0	4865.9	0.82
F2	9.78	2450.0	3828.1	0.64
G1	9.02	3150.0	2971.7	1.07
G3	9.52	2128.0	2693.7	0.79
AA1	9.50	2940.0	2910.9	1.01
AA2	11.12	3780.0	3150.0	1.20
G2		3150.0	2547.6	1.07

Mean ± Standard Deviation (Coefft. Variation%)

Series A

0.85 ± 0.24 (27.9%)

A11 Series

0.84 ± 0.20 (23.4%)

* In reference to table 4.2 : This value governs in the Rangan - Hall's theory for all modes

TABLE 4.6. ANALYSIS OF TEST RESULTS BY McGEE - ZIA'S METHOD

BEAM	N/mm^2	N/mm^2	THEORY KNmm	TEST/ THEORY
A1	1.79	1.55	1638.8	0.69
A2	1.91	1.74	1730.8	0.74
A3	1.83	1.80	1746.7	0.80
A4	2.41	2.33	1949.4	0.53
A5	2.65	2.58	2088.9	0.60
A6	2.87	2.81	2202.6	0.95
A7	3.31	3.20	2387.1	0.96
A8	3.43	3.36	2476.9	0.96
A9	3.94	3.73	2608.1	0.97
A10	4.08	3.87	2697.2	1.26
A11	4.34	4.01	2763.6	1.28
B1	3.88	3.69	2621.3	0.54
B2	4.09	3.86	2698.3	0.96
B3	4.14	3.81	2678.4	0.86
B4	4.06	3.82	2676.2	0.71
B5	4.10	3.86	2702.4	1.07
B6	3.81	3.62	2579.1	0.87
C1	3.89	3.91	8721.5	0.71
C2	4.39	4.10	2813.7	0.83
C3	4.16	3.86	2702.3	1.01
C4	4.35	3.85	2700.1	0.93
D1	-	-	1866.7	0.69
D2	-	-	3628.9	0.76
D3	-	-	5212.3	0.65
E1	4.53	4.10	2839.7	1.23
E2	4.51	4.06	2811.0	1.13
E3	4.34	4.01	2738.5	1.00
E4	4.29	3.95	2320.4	0.48
F0	3.74	3.63	3990.1	0.53
F1	4.01	3.76	4083.7	0.98
F2	4.43	4.01	4140.4	0.59

continued

BEAMS	1	2	3	4
G1	4.17	3.85	2950.2	1.20
G2	4.04	3.85	2921.8	1.08
G3	4.48	4.11	2990.9	0.71
AA1	4.36	4.05	2752.9	1.07
AA2	4.29	4.03	2775.7	1.36

MEAN ± STANDARD DEVIATION (Coefft. VARIATION %)

SERIES A

0.89 ± 0.23)26%)

ALL SERIES

0.88 ± 0.23 (26%)

V_c = permissible flexural shear stress with torsion as defined by ACI Eq.(11-11) or (11-12)

c^* = permissible shear stress for torsion without flexural shear.

4.9. CONCLUSION

As a result of the analysis of the test beams by applying "all steel" and "stirrups only" at yield methods which are currently in use, it became evident that the experimental strengths were predicted neither accurately nor in a consistent manner. Serious discrepancies were noticeable when theoretical values and modes of failure were compared with the laboratorial observations. Consequently, generally poor coefficients of variation were obtained from those methods, in particular, the "all steel at yield" theories. Whilst the application of the partial steel yield methods improved the situation, the prestressing force in particular was not included satisfactorily. This is shown by the high coefficients of variation resulting from the comparison with the test beams of series I where the prestressing force was the main variable.

The difficulty, after predicting from an all yield method that the beams did not yield, is to determine the nature of their failure. Unfortunately none of these methods, except McMullen-Woodhead's iterative method, gives comparative relative values for alternative types of failure within the same mode e.g. by fully steel yield, longitudinal steel or stirrups only yield etc. This is crucial to determine the critical value of strength with which the member is more likely to fail depending not only on the applied loads but also on the materials strength. It was noticed from the foregoing sections of this chapter that the numerical predictions were not comparable between the theories, because such values were produced by equations derived from different assumptions and which contained different constants.

In an attempt to achieve a better and more realistic correlation with the experimental results of the test beams, it is proposed to extend the analysis by producing new theoretical expressions for the ultimate strength. This includes the ultimate strengths in the main modes of failure and the possible types of materials failure within the loading range of each mode, as controlled by the prestress, steel or concrete. Relevant interaction surfaces are also developed theoretically, with the prestressing force included explicitly, and applied to the test beams.

4.10 THEORETICAL SOLUTIONS FOR THE ULTIMATE STRENGTH OF PRESTRESSED CONCRETE BEAMS SUBJECTED TO TORSION, BENDING AND SHEAR WITH STIRRUPS (and/or longitudinal steel only - at yield)

In this section the following possible cases are considered for analysis:

- The all steel at yield case
- The case where only the stirrups yield
- The case where only the longitudinal steel yield.

In the first two cases the shear force is assumed to be taken entirely by the stirrups which yield. The longitudinal steel, however, is assumed to provide all of the vertical shear resistance in case three. The three cases for each of the three classical modes of failure are analysed and equations of general form for ultimate strength and interaction are presented.

4.10.1. An All-Steel at "Yield" Solution Mode 1 Form of Failure in Combined Torsion Bending and Shear :

1. For Mode One crack the section at the soffit by applying a moment Mo

2. Hence, taking moments about the transverse axis in the centroid of the concrete zone at top

$$M_1 + V_1 (d_1 - dn_1) \tan\beta = [A1\ fly - P\ell)\ \ell a_1 + Mo -$$

$$\frac{Asfsy}{S} (d_1 - dn_1)[\ (d_1 - dn)\ (\tan\alpha + \tan\beta)\ (\tan\alpha - \tan\beta) + b'\tan^2\alpha]$$

If $M_{1l} = A\ell\, f\ell y\ \ell a_1$ then after rearrangement :

$$\frac{M_1}{Mu_1} + \frac{P\ell a_1}{Mu_1} + \frac{V_1}{Mu_1} (d_1 - dn_1) \tan\beta = 1 + \frac{M_o}{Mu_1} -$$

$$r_1y \frac{(d_{11} - dn_1)}{\ell a_1} \left[\frac{d_1 - dn}{b'} + 1 \right) \tan^2\alpha$$

$$- \frac{(d_1 - dn)}{b} \tan^2\beta \Big] \qquad \text{----(1)}$$

3. Taking moments about the longitudinal axis, in the centroid of concrete zone at top

$$T_1 = \frac{Asfsy}{S}\ b'\tan\alpha\ \ell a_1 + \frac{Asfsy}{S} (d_1 - dn_1) \tan\alpha\ b'$$

$$\frac{T}{Mu_1} = r_1y \tan\alpha \left(1 + \frac{d_1 - dn_1}{\ell a_1}\right) \qquad \text{----(2)}$$

4. Resolving forces vertically,

$$V_1 = 2\ \frac{As\ fsy}{S} [d_1 - dn_1)\ \tan\beta$$

$$\frac{V_1}{Mu_1} = 2\ r_1y \frac{(d_1 - dn_1)}{b'\ \ell a_1} \tan\beta \qquad \text{----(3)}$$

5. Substituting equations 2 and 3 in equation 2,

$$\frac{M_1}{Mu_1} + \frac{P_1}{P_1y} + \left(\frac{V_1}{Mu_1}\right)^2 \frac{b\ \ell a_1}{2\ r_1y} = 1 + \frac{M_o}{Mu_1} - r_1y \frac{(d_1 - dn_1)}{\ell a_1} \Big[$$

$$\left[\left(\frac{d_1 - dn_1}{b'} + 1\right) \frac{T_1}{Mu_1} \frac{1}{r_1y\left(1 + \frac{d_1 - d_o}{\ell a1}\right)} - \left(\frac{d_1 - dn_1}{b'}\right) \left(\frac{V_1}{Mu_1} \frac{b'\ \ell a_1}{2\ r_1y}\right) (d_1 - dn_1)^2\right]$$

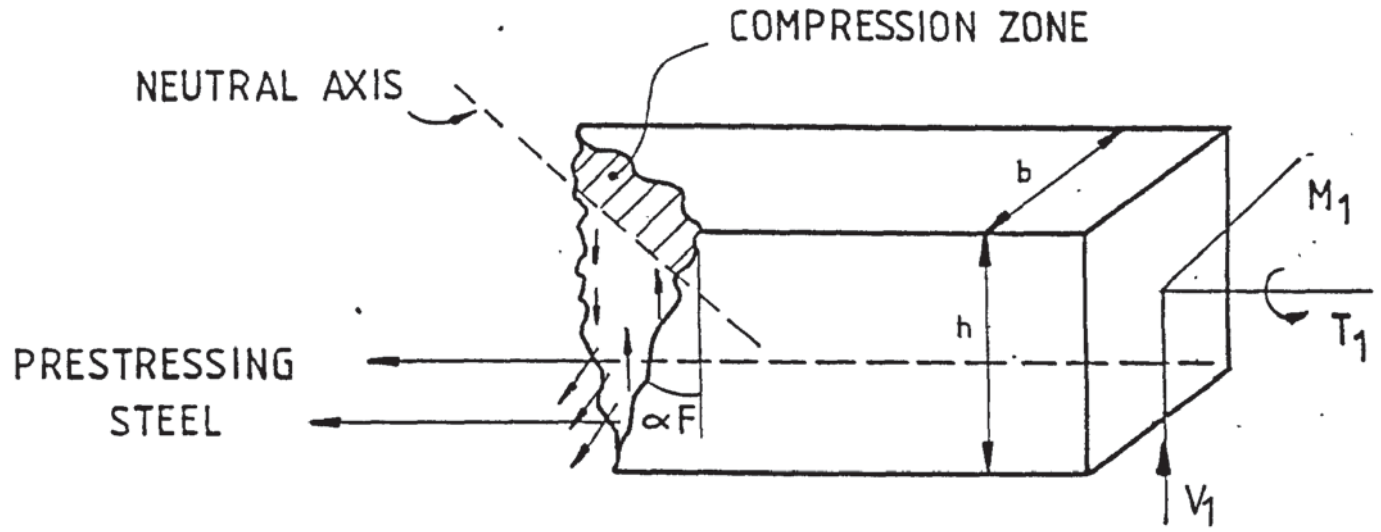

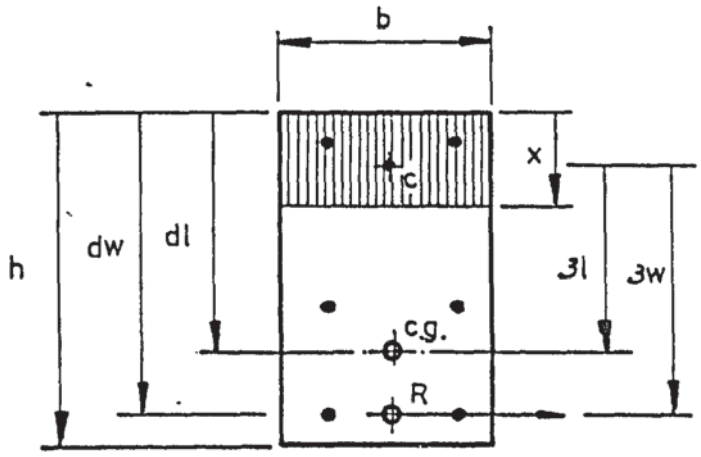

CROSS SECTION

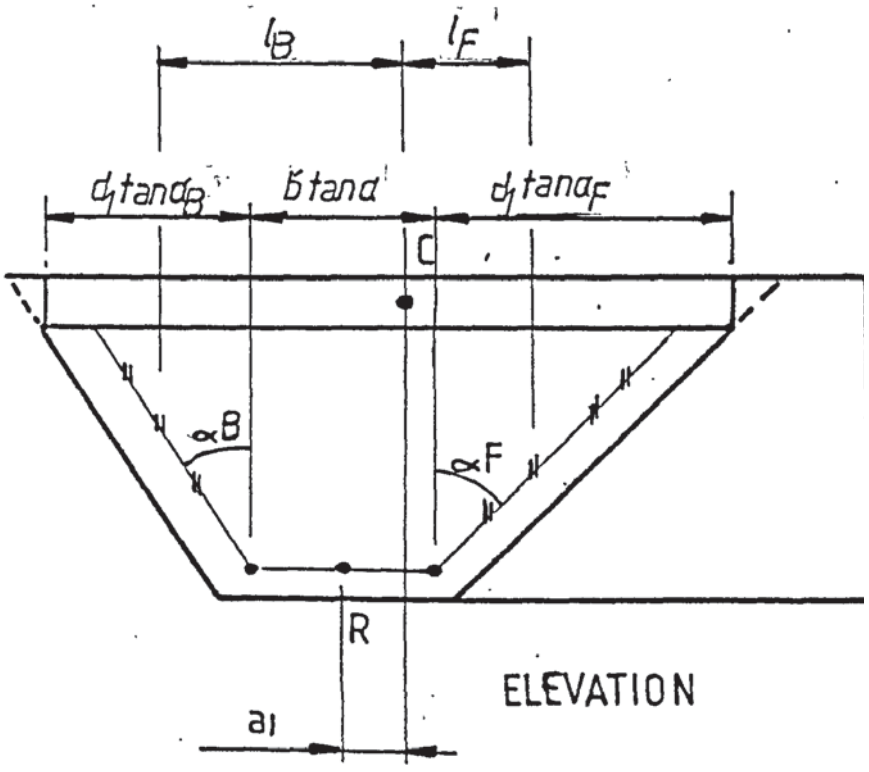

ELEVATION

$$2\,l_F = b\tan\alpha + (d_1 - d_{n1})\tan\alpha_F$$

$$2\,l_B = b\tan\alpha + (d_1 - d_{n1})\tan\alpha_B$$

$$\tan\alpha_F = \tan\alpha + \tan\beta$$

$$\tan\alpha_B = \tan\alpha - \tan\beta$$

FIGURE 4.10 MODE ONE OF FAILURE

$$\frac{M_1}{Mu_1} + \frac{P_1}{P_{1y}} + \left(\frac{V_1}{Mu_1}\right)^2 \frac{b' \ell a_1}{4\, r_{1y}} + \left(\frac{T_1}{Mu_1}\right)^2 \left[\frac{\left(\frac{d_1 - dn_1}{b'} + 1\right)(d_1 - dn_1)}{r_{1y}\left(1 + \frac{d_1 - dn_1}{\ell a_1}\right)^2 \ell a_1}\right] = 1 + \frac{M_o}{Mu_1}$$

$$\frac{M_1}{Mu_1} + \frac{P_1}{P_{1y}} + \left(\frac{V_1}{2Mu_1}\right)^2 \frac{b' \ell a_1}{r_{1y}} + \left(\frac{T_1}{2\, Mu_1}\right)^2 \frac{(1+ h/b)}{r_{1y}} = 1 + \frac{M_o}{Mu_1}$$

$$\frac{M_1}{Mu_1} + \frac{P_1}{P_{1y}} + \left[\frac{V_1}{Vu_1}\right]^2 + \left[\frac{T_1}{Tu_1}\right]^2 = 1 + \frac{M_o}{Mu_1} \qquad \text{---- (4)}$$

where :

$Mu_1 = A1\ fly\ \underline{\ell a_1}$

$$Tu_1 = 2\, Mu_1 \sqrt{\frac{r_{1y}}{1 + h/b}}$$

$$Vu_1 = 2\, Mu_1 \sqrt{\frac{r_y}{b' \ell a}} \qquad \text{and}$$

$$M_o = \frac{Ps}{bh}\ \frac{bh^3}{12y_d}\ \left[1 + \frac{12\, e\, y_d}{h^2}\right] + [0.36\ \ fc'/0.8]\ \frac{bh^3}{12y_d}$$

6. Rearranging equation (4) :

$$\left[\frac{T_1}{Tu_1}\right]^2 \left[1 + \left(\frac{Tu_1}{Vu_1}\right)^2 \left(\frac{V_1}{T_1}\right)^2 + \frac{P_1}{P_{1y}} \left(\frac{Tu_1}{T_1}\right)^2\right] + \left[\frac{T_1}{Tu_1}\right] \left[\frac{M_1}{T_1}\ \frac{Tu_1}{Mu_1}\right] = 1 + \frac{M_o}{Mu_1}$$

$$\frac{T_1}{Tu_1} = \frac{-\left[\frac{M_1}{T_1}\ \frac{Tu_1}{Mu_1}\right] + \sqrt{\left[\frac{M_1}{T_1}\ \frac{Tu_1}{Mu_1}\right]^2 + 4\Psi_1 \left[1 + \frac{M_o}{Mu_1}\right]}}{2\Psi_1}$$

$$\frac{T_1}{Tu_1} = \frac{-\left(\frac{1}{\alpha_1}\right) \frac{M_1}{T_1} + \sqrt{\left(\frac{1}{\alpha_1}\right)^2 \left[\frac{M_1}{T_1}\right]^2 + 4\Psi_1\, C_o}}{2\Psi_1} \qquad \text{---- (5)}$$

where :

$$\Psi_1 = 1 + \left(\frac{V_1}{T_1}\right)^2 \left(\frac{1}{\beta_1}\right)^2 + \frac{P_1}{P_{1y}} \left(\frac{Tu_1}{T_1}\right)^2$$

$$\alpha = \frac{Mu_1}{Tu_1}$$

$$\beta_1 = \frac{Vu_1}{Tu_1}$$

$$C_o = 1 + \frac{M_o}{Mu_1}$$

7. In equation 2 :

if $\ell a \cong d\ell - x$

$$\frac{T_1}{Mu_1} \cong 2\, r_{1y} \tan\alpha_1,$$

$$\frac{T_1}{Tu_1} \cong 2\,\alpha,\, r_{1y} \tan\alpha_1$$

Equating to equation 5:

$$\tan\alpha_1 = \frac{-\left(\frac{1}{\alpha}\right)\frac{M_1}{T_1} + \sqrt{\left(\frac{1}{\alpha_1}\right)^2\left[\frac{M_1}{T_1}\right]^2 + 4\,\Psi_1 Co}}{4\alpha_1\, r_{1y}\, \Psi_1}$$

$$= [1/(4\alpha_1^2\ r_{1y}\Psi_1)]\left\{\sqrt{\left(\frac{M_1}{T_1}\right)^2 + 4\alpha_1^2\Psi_1 Co} - \frac{M_1}{T_1}\right\}$$

$$\tan\alpha_1 = \frac{1}{(1 + h/b)\Psi_1}\left\{\sqrt{\left(\frac{M_1}{T_1}\right)^2 + \frac{(1 + h/b)\Psi_1\, Co}{r_{1y}}} - \frac{M_1}{T_1}\right\}$$

$$\tan\alpha_1(1 + h/b)\Psi_1 = \{\tan\theta_1\} \qquad \text{---- (6)}$$

Generally :

$$T_1 = 2\, Mu_1\, r_{1y} \tan\alpha_1 \qquad \text{---- (7)}$$

This can be further modified to form

$$T_1 = 2\,\frac{As\, fsy\, b'}{S}\, z_1 \tan\alpha_1 \qquad \text{----(7a)}$$

in which $z_1 = d_1 - k\ell\, dn_1$ is the lever arm ℓa_1 as based on the effective depth of the prestressing steel.

Also, equation 2 can be rewritten in terms of $d\omega$, the depth of the bottom legs of the stirrups, then :

$$T_1 = \frac{As\, fsy\, b'}{S}\,(d\tilde{\omega} - dn_1 + z_\omega)\ \tan\alpha_1 \qquad (2b)$$

Taking $z_\omega \cong d_\omega - dn_1$

$$T_1 = 2\,\frac{As\, fsy\, b'}{S}\, z_\omega \tan\alpha_1 \qquad (7b)$$

in which $z_\omega = d\omega - k\omega\, dn$ is the torsional lever arm ℓa_1 as based on the depth of the bottom legs of stirrups. Equations 7a, b are comparable and may be related by a ratio $\lambda_1 = \frac{z\ell}{z\omega} \cong \frac{d\ell}{d\omega}$.

A further approximation may be considered by determining the average of equations 7a and b taking $(z_\ell + z_\omega)/2 \cong d'$ Substituting in either equation 7a or b, gives a soltuion of the form :

$$T_1 = 2 \frac{As\ fsy\ b'd'}{S} \tan\alpha_1 \times [\Gamma_1] \qquad (8)$$

in which $\Gamma_1 = [\frac{\Gamma_\ell + \Gamma_\omega}{2}]$

8. In equation (7a) :

$$z_\ell = d_1 \left(1 - k_1 \frac{dn_1}{d1} \right)$$

$$= \lambda_\ell\ d' \left(1 - k_1 \frac{dn_1}{d1}\right) \quad \text{where} \quad d_\ell = \lambda_\ell\ d'$$

$$T_1 = 2 \frac{As\ fsy\ b'd'}{S} \tan\alpha_1 \times \Gamma_\ell \qquad (8a)$$

in which Γ_ℓ is a reduction factor.

$$\Gamma_\ell = \lambda_1 \left(1 - k_\ell \frac{dn_1}{d\ell}\right)$$

Also equation (7b) can be put in the form :

$$T_1 = [2 \frac{As\ fsy\ b'd'}{S} \tan\alpha_1 \cdot] \times \Gamma_\omega \qquad (8b)$$

in which Γ_ω is a factor :-

$$\Gamma_\omega = \lambda_\omega \left(1 - k_\omega \frac{dn_1}{d\omega}\right) \quad \text{where } d_\omega \cong \lambda_\omega\ d'$$

9. Assuming $\frac{d'}{b'} \cong \frac{h}{b}$ and the stirrups are closed and evenly distributed, the expression for $\tan\alpha_1$, equation (6) may be used to evaluate the depth of the compression zone with the following form containing an approximate value for ℓa_1 in the shear-prestress parameter :

$$\Psi_1 = 1 + \left(\frac{V_1}{T_1}\right)^2 \left(\frac{Tu_1}{Vu_1}\right)^2 + \frac{P\ell}{p\ell y} \left(\frac{Tu_1}{T_1}\right)^2 \qquad (6a)$$

Numerically equation (6a) may therefore be reduced to : $1 + \phi_1 \frac{h}{b}$ where $\phi_1 \geq 1$.

As for the parameter Co in equation 6 the lever arm ℓa may be taken equal to d' for the purpose of calculating the value of Mu_1 involved in the parameter Co only.

A theory for the determination of the compressive concrete zone dn_1 is also presented. The compression zone is subjected to a direct stress fm due to bending moment and a shear stress fct due to torsion only since the shear force is assumed to be entirely resisted by the stirrups. These stresses can be related to the steel stresses and areas and the dimensions of the section as follows.

Resolving forces parallel to the longitudinal axis of the member and ignoring the compression reinforcement :

$$(A_\ell \, fly - P_\ell) = Kcm \; b \; dn_1 fm \qquad (9)$$

Resolving forces at right angles to the longitudinal axis of the member and ignoring any dowel action :

$$\frac{As \; fsy \; b'}{S} \tan\alpha = K_{ct} \; b \; dn_1 \; fct \qquad (10)$$

fm and fct can now be related using a failure criterion for concrete. Following Martin's work (8) on reinforced concrete members, Cowan's criterion is applied :

$$\frac{fct}{fc'} = \frac{0.20}{\sqrt{1 + \left(\frac{fm}{2fct}\right)^2} - 0.3 \; \frac{fm}{fct}} \qquad (11)$$

Substituting equations (9) and (10) in the criterion :

$$\frac{As \; fsy \; b' \tan\alpha}{S \; Kct \; b \; dn_1 \; fc'} = \frac{0.20}{\sqrt{1 + \left(\frac{Kct. \; Po}{2Kcm \; r_\ell y \; \tan\alpha_1}\right)^2} - 0.3 \; \frac{Kct \quad Po}{kcm \; r_\ell y \; \tan\alpha_1}}$$

Rearranging

$$\frac{A_\ell \, fly \; . \; Po}{2 \; Kcm \; b \; dn_1} \left\{\sqrt{1 + \left[\frac{2 \; Kcm \; r_\ell y \quad \tan\alpha_1}{Kct \cdot Po}\right]^2} - 0.6 \right\} = 0.20 \; fc' \qquad (11a)$$

$$\frac{dn_1}{d_\ell} = \frac{\rho_\ell \, fly \cdot Po}{0.4 \; Kcm \; fc} \left\{\sqrt{1 + \left[\frac{2 \; Kcm \; r_\ell y \; \tan\alpha_1}{Kct \cdot Po}\right]^2} - 0.60 \right\} \qquad (12)$$

in which $\rho_\ell = \frac{A_1}{bd_\ell}$

and $Po = \left(1 - \frac{P_\ell}{P_{\ell y}}\right)$

The lever arm z_ℓ can be obtained from :

$$\frac{z_\ell}{d_\ell} = 1.0 - K_\ell \frac{dn_1}{d_\ell} \qquad (12a)$$

10. Setting the prestress to zero, equation (12) restores the form of solution as was originally produced by Martin (8) for reinforced concrete sections subjected to bending and torsional moments only. This is also the case for initially UNCRACKED prestressed sections for which, more generally in all the construction of the equations included in this subsection, the (Mo) terms are to be replaced by (P_ℓ $_\ell a_1$) and all the (P_ℓ) terms cancel out.

11. Partial-"yield" Case : Stirrups Only at "Yield"

The basic equation of moments, equation (1), is modified as follows:

$$M_1 + V_1(d_1 - dn_1)\tan\beta = \frac{[A_\ell\, fsy]\quad {}_\ell a_1}{\frac{As\, fsy}{S}(d_\ell - dn_1)} + Mo - [(d_1 - dn)(\tan^2\alpha - \tan^2\beta) + \beta \tan^2\alpha] \qquad (1)\ A$$

In which $[A_\ell\, fsy]$ is the change in the prestressing steel stress due to loading assumed to be related to the yield value of the stirrups steel. This can be expressed more generally :

$$flult. = P_\ell / A_\ell + fsy \qquad (a)$$

where flult. is the total stress value in the prestress steel at ultimate strength. Hency by replacing fly by flult., as given by equation (a), more generally all the derivation and the resulting equations in subsection 4.10.1. are simply modified to the present case.

Alternatively if $Msu_1 = A_\ell fsy\ {}_\ell a_1$, after rearrangement the modified interaction equation can be given in the following form :

$$\frac{M_1}{Msu_1} + \left[\frac{V_1}{Vu_1}\right]^2 + \left[\frac{T_1}{Tu_1}\right]^2 = 1 + \frac{Mo}{Msu_1} \qquad (4)\ A$$

where Msu1 = A_{ℓ} fsy ℓa_1 has replaced Mu_1 in equation (4).

$$Tu_1 = 2\ Msu_1 \sqrt{\frac{r_{\ell y}}{1+h/b}}$$

$$Vu_1 = 2\ Msu_1 \sqrt{\frac{r_{\ell y}}{b\ \ell a_1}} \quad \text{and} \quad r_{\ell y} = \frac{As\ fsy\ b}{A_{\ell}\ fsy\ S}$$

$$\frac{T_1}{Tu_1} = \frac{-(Tu_1/Msu1)\frac{M_1}{T_1} + \sqrt{(Tu_1/Msu1)^2[\frac{M}{T}) + 4\ \Psi_1\ Co.}}{2\Psi_1} \qquad (5)\ A$$

in which $\Psi_1 = 1 + (\frac{V_{\ell}}{T_{\ell}})^2\ (\frac{Tu_1}{Vu_{\ell}})^2$

and $Co = 1 + \frac{Mo}{Msu1}$

Equation 6 for $\tan\alpha_1$ is valid with the terms re-defined as above. A solution is given for ℓa_1 in the next subsection.

For cases where M < Mo i.e. UNCRACKED sections:

$$Co = 1 + \frac{P_{\ell}\ \ell a_1}{Msu1}$$ as the major difference.

Combined Torsion in Mode 2:

1. Taking moments about the transverse axis, in the centroid of the compression zone located at the vertical side of the beam on which the shear stresses (due to torsion and shear force) are subtractive:

$$\frac{As\ fsy}{S}(b_1-bn)\ \tan\alpha_2\ d'(\tan\alpha_2 + \tan\beta_1) + (b_1-bn)\ \tan\alpha = (A_{\ell 2}\ fly_2 - P_{\ell 2}) + P_S)\ \ell a_2$$

$$= [A_{\ell 2}\ fly_2 + P_{\ell}/2]\ \ell a_2$$

$$= A_{\ell 2}\ fly2\ \ell a_2 [1 + \frac{P_{\ell}}{2A_{\ell 2}\ fly}]$$

since $2\ A_{\ell 2}\ fly2 = A_{\ell 1}\ fly_1$

$$\frac{As\ fsy}{S}(b_1-bn]\ \tan\alpha_2[d'(\tan\alpha_2 + \tan\beta) + (b_1-bn)\ \tan\alpha_2]MU2[1 + \frac{P}{P_{\ell y}}]$$

2. Taking moments about the longitudinal axis,

$$T_2 + V_2(\frac{b}{2} - \frac{bn}{2}) = \frac{As\ fsy}{S}[d'(\tan\alpha + \tan\beta)\ \ell a_2 + (b_1-bn)\ \tan\alpha_2 d'] \qquad (2)$$

3. Resolving forces vertically

$$V_2 = \frac{2\ As\ fsy}{S}\ d'\ \tan\beta \qquad (3)$$

4. Substituting equation (3) in equation (2)

$$\frac{T_2}{A_{\ell 2}\ fly_2\ \ell a_2} + \frac{V_2}{2(A_{\ell 2}\ fly_2\ \ell a_2)}[b-bn] = \frac{As\ fsy\ d'}{SA_{\ell 2} fly_2\ \ell a_2}[\tan\beta\ \ell a_2 + (b_1-bn+\ell a_2)\tan$$

$$\frac{T_2}{Mu_2} + \frac{V_2}{2Mu_2}(b_1-bn-\ell a_2) = \frac{r_2 y}{\ell a_2}[\ell a_2 + b_1 - bn]\ \tan\alpha_2$$

If the error involved in assuming b-bn≅ ℓa_2 is reasonably small, the V_2 term on the left hand side cancels. In the right hand side, also if $\ell a_2 \cong b_1$-bn

$$\frac{T_2}{Mu_2} = 2\, r_{2y} \tan\alpha_2 \qquad (4)$$

5. Substituting equation (3) in the equation (1) :

$$\frac{As\ fsy}{S}(b_1-bn)(1+b/h)\ d' \tan^2\alpha_2 + \frac{As\ fsy}{S}(b_1-bn)\frac{d'V_2S\tan\alpha_2}{2Asfsy\ d'} = Mu\ (1+\frac{P_1}{P_{1y}})$$

$$\frac{r_{2y}(b_1-bn)(1+b/h)}{\ell a_2}\left[\frac{T}{2\,r_{2y}}\right]^2 + \frac{(b_1-bn)}{\ell a_2}\left(\frac{V_2\ell a_2}{2\,Mu_2}\right)\frac{T_2/Mu_2}{2\,r_{2y}} = 1+\frac{P\ell}{P_{1y}}$$

$$\left[\frac{T_2}{2Mu_2}\right]^2 \frac{1+b/h}{r_{2y}} + \frac{T_2V_2\ell a_2}{(2M_2)^2 r_{2y}} = 1+\frac{P_1}{P_{1y}}$$

$$\left[\frac{T_2}{2Mu_2\sqrt{\frac{r_{2y}}{1+b/h}}}\right]^2 + \frac{T_2}{2Mu_2\sqrt{\frac{r_{2y}}{1+b/h}}}\cdot\frac{V_2}{2Mu_2\sqrt{\frac{r_{2y}(1+b/h)}{\ell a_2^2}}} = 1+\frac{P_1}{P_{1y}}$$

or :

$$\left[\frac{T_2}{Tu_2}\right]^2 + \frac{T_2}{Tu_2}\frac{V_2}{Vu_2} = 1+\frac{P\ell}{P\ell y} \qquad (5)$$

$$\left[\frac{T_2}{Tu_2}\right]^2 \left[1+\frac{V_2}{T_2}/\frac{Tu_2}{Vu_2}\right] = 1+\frac{P\ell}{P_{1y}}$$

or :

$$\frac{T_2}{Tu_2} = \sqrt{\frac{1+P1/P_{1y}}{1+\frac{V_2}{T_2}/\frac{Tu_2}{Vu_2}}} \qquad (5a)$$

Equation (5) can also be rearranged further :

$$\left[\frac{T_2}{Tu_2}\right]^2 + \frac{V_2\ell a_2}{C_2\ 2Mu_2\sqrt{\frac{r_{2y}}{1+b/h}}}\cdot\frac{V_2\ell a_2}{2\,Mu_2\sqrt{r_{2y}^2(1+b/h)}} = 1+\frac{P\ell}{P\ell y}$$

in which $C_2 = \frac{V_2 b''}{T_2}$, and if $\ell a^2 \cong b'$:

$$\left[\frac{T_2}{Tu_2}\right]^2 + \frac{(V_2)^2}{(2Mu_2)^2\frac{r_{2y}}{b'\ell a^2}} = 1+\frac{P\ell}{P\ell y}$$

$$As\ Vu_2 = 2\,Mu_2\sqrt{\frac{r_{2y}}{b'\ell a^2}}\cdot(1+b/h)$$

$$\left[\frac{T_2}{Tu_2}\right]^2 + \frac{1}{C_2}(1 + b/h)\left[\frac{V_2}{Vu_2}\right]^2 = 1 + \frac{P\ell}{P\ell y}$$

or :

$$\left[\frac{T_2}{Tu_2}\right]^2 + \frac{T^2(1 + b/h)}{V^2 b'}\left[\frac{V_2}{Vu_2}\right]^2 = 1 + \frac{P\ell}{P\ell y}$$

and :

$$\left[\frac{T_2}{Tu_2}\right]^2 + \frac{1}{\Psi_0}\left[\frac{V_2}{Vu_2}\right]^2 = 1 + \frac{P\ell}{P\ell y}$$

where $\Psi_0 = \dfrac{V_2\ b'}{T_2\ (1 + b/h)}$ (5) A

which is the alternative form of equation (5).

For either equation (5) or (5)A to be useful a value for the lever arm ℓa_2 is required.

6. Proceeding similarly to Mode One, an expression for the lever arm ℓa_2 is derived

$$(A\ell_2 f l y_2 - P\ell/2) = Kcm\ bn\ h\ fm \qquad (6)$$

and

$$\frac{2As\ fsy\ (b_1 - bn)}{S}\tan\alpha_2 = Kct\ bn\ h\ fct \qquad (7)$$

Substituting in Cowan's simplified criterion the following equation is obtained

$$\frac{bn}{b_1} = \frac{\int\ell_2\ fly_2}{0.4\ Kcm\ fc'}\left(1 - \frac{P\ell}{P\ell y}\right)\left\{\sqrt{1 + \left[\frac{2\ Kcm\ r_{2y}\ \tan\alpha_2}{Kct(1 - P\ell/P\ell y}\right]^2} - 0.60\right\} \qquad (8)$$

in which $\int\ell_2 = \dfrac{A\ell_2}{hb_\ell}$ and $r_{2y} = \dfrac{Asfsy\ d'}{S\ A\ell_2\ fly_2}$

The angle $\tan\alpha_2$ is evaluated by equating equation (4) to equation (5a) and thus obtaining

$$2\ r_{2y}\ Mu_2\ \tan\alpha_2 = Tu_2\sqrt{\frac{1 + P_1/P\ell y}{1 + \frac{V_2}{T_2}\ \frac{Tu_2}{Vu_2}}}$$

Hence

$$\tan\alpha_2 = \frac{1}{\sqrt{r_{2y}(1 + b/h)\ \Psi_2}}\sqrt{1 + P\ell/P\ell y} \qquad (9)$$

where

$$\Psi_2 = 1 + \frac{V_2}{T_2} \quad \frac{Tu_2}{Vu_2} \quad \text{which can be further simplified into}$$

$$= 1 + \frac{V_2}{T_2} \frac{\ell a_2}{(1+ b/h)} \qquad (9a)$$

$$\frac{\ell a_2}{b\ell} = 1 - K_{\ell 2} \frac{bn}{b\ell} \qquad (8a)$$

7. Now equation (4) is reshaped into the general form :

$$T_2 = 2 \frac{As\ fsy\ d'\ b'}{S} \quad \tan\alpha_2 \qquad (11)$$

in which ℓa_2 is taken approximately equal to b'.

Alternatively the solution for all the steel yield case as governed by the concrete strength is

$$T_2 = [2 \frac{As\ fsy\ d'\ b'}{S}] \tan\alpha_2 \times \sqrt{2} \qquad (12)$$

in which $\sqrt{2} = \lambda_2 \quad (1-K\ell_2 \frac{bn}{b\ell})$

and $\lambda_2 = b_\ell / b'$

8. Combined Torsion in Mode 3:

In this mode, the compression zone is formed at the bottom of the beam. On turning the beam upside down, the interaction curve is exactly the same as for Mode 1, except that the bending moment tends now to rotate the section in the opposite direction. Thus putting $M_1 = -M_3$ in the basic interaction equation 1.5.(4) :

$$-\frac{M_3}{Mu_3} + \frac{P_3}{P_3 y} + [\frac{V_3}{Vu_3}]^2 + [\frac{T_3}{Tu_3}]^2 = 1 - \frac{Mo_3}{Mu_3} \qquad (1)$$

By interchanging the sign of M_1 and its subscript: all the equations for Mode 1, including the expression for the depth of the compressive zone, are equally valid in Mode 3 of failure. The top steel is interchanged by the bottom steel including the prestress forces. Accordingly Mo_3 is the moment necessary to overcome the prestress and crack the section at the top. Hence the general forms for T_3 are $T_3 = 2 \frac{Asfsy\ b'\ d'}{S} \tan\alpha_3$ (2)

and $T_3 = [2 \frac{Asfsy\ b'\ d'}{S} \tan\alpha_3] \times \sqrt{3}$ (3)

4.10.2. Alternative Solutions for Types of failure in Mode One:

All Steel at "Yield"

1. Following the same procedure in the section 4.10.1 the basic equation for mode 1 is constructed. Furthermore the shear torsional angle tan , which is evaluated by equation 10.1.6, is valid. In the form of this angle is absorbed the effect of the vertical shear force on the final cracking angles of the front and back faces of the beam which are crossed by the vertical legs of the stirrups. Hence

$$M_1 + V_1 (d\omega - dn_1) \tan\beta + P_{\ell} \ell a_1 = A1 fly\, \ell a_1 + Mo - \frac{Asfsy}{S} (d\omega - dn_1) [(d\omega - dn_1) (\tan\alpha_1) \cdot (\tan\alpha_1) + b' \tan^2\alpha_1] \qquad 10.2.1$$

2. Equations 10.1.2b and 10.1.7b are valid. Therefore :

$$\tan\alpha_1 = \frac{T_1}{Mu_1\ 2\ r1y} = \frac{T_1}{\frac{2As\ fsy\ b' z\omega}{S}} \qquad 10.2.2$$

3. Substituting in the last negative term of equation 10.2.1. and rearranging :

$$\frac{Asfsy}{S} (d\omega - dn_1)\, b' \left(1 + \frac{d\omega - dn_1}{b'}\right) \left[\frac{T_1}{\frac{2\ Asfsy\ b' z\omega}{S}}\right]^2$$

If $z\omega \cong (dw - dn_1) \cong d'$ and $\frac{d'}{b'} \cong \frac{h}{b}$

$$\frac{Asfsy}{S} z_{\omega}\, b' \left(1 + \frac{h}{b}\right) \left[\frac{T_1}{\frac{2As\ fsy\ b'd'}{S}}\right]^2$$

4. Now substituting in equation 10.2.1.

$$\frac{M_1}{Mu_1} + \frac{V_1}{A1\ fly\ \ell a_1} z\omega \tan\beta + \frac{P\ell}{P\ell y} + \frac{Asfsy\ b'}{A1Sfly} \frac{z\omega}{\ell a_1} \left(1 + \frac{h}{b}\right) \left[\frac{T_1}{Tsy}\right]^2 = 1 + \frac{Mo}{Mu}$$

$\frac{z\omega}{\ell a_1} \cong 1$ if for Tsy an average lever arm is also used

From equation 10.1.8.

$Tsy = \left(2 \frac{Asfsy}{S} b'd'\right) X \lceil 1$ where $\lceil 1$ is a ratio relating the strength to the compression zone failure. 10.1.8

$$\frac{M_1}{M_{u1}} + \frac{V_1}{A1fly}\tan\beta + \frac{P\ell}{P\ell y} + r\ell y\,(1 + h/b)\left[\frac{T_1}{Tsy}\right]^2 = 1 + \frac{Mo}{Mu_1}$$

or

$$\frac{T_1}{Tsy}\left[\frac{M_1}{T_1}\cdot\frac{Tsy}{Mu_1} + \frac{V_1}{T_1}\cdot\frac{Tsy}{A1fly}\tan\beta + \frac{P\ell}{T_1}\cdot\frac{Tsy}{P\ell y} + r\ell y\,(1+h/b)\frac{T_1}{Tsy}\right] = Co1$$

$$(T_1)\ \text{Theory} = \frac{Tsy\ Co_1}{\frac{M_1}{T_1}\left(\frac{Tsy}{Mu_1\lceil 1}\right) + \frac{V_1}{T_1}\left(\frac{Tsy}{A1fly}\right)\tan\beta + \frac{P\ell}{T_1}\left(\frac{Tsy}{P\ell y}\right) + r1y\,(1+h/b)\frac{T_1}{Tsy(\lceil 1)^2}}$$

$$\tan\beta u_1 = \sqrt{\left[\frac{M_1 + P\ell\ell a_1}{V_1 h}\right]^2 + \frac{1 + Mo/Mu_1}{r1y(h/b)}} - \left[\frac{M_1 + P\ell\ell a_1}{V_1 h}\right]$$

The terms $\lceil 1$ and $\ell a_1 = d'\lceil\ell$ are obtained from the analysis presented in 4.10.1. This applies when the solution is required based on the failure of concrete. However if dn was considered very small then $\lceil\ell = 1.0$.

Stirrups Only at "Yield"

1. Taking moments about a transverse axis through the centroid of the compressive zone at the top :

$$M_1 + V_1 a_1 + \frac{As\ fsy}{S}\,[d_1 - dn_1][b + d_1 - dn_1]\left[\frac{T_1}{Tsy}\right]^2 = A\ell fsy\ Sin\alpha\ell a_1 + Mo$$

2. Divided by $Msy_1 = A\ell fsy\ \ell a_1 \cong A\ell fsy\ Sin\alpha_o d'$

$$\frac{M_1}{Msy_1 Sin\alpha o} + \frac{V_1}{A\ell fsy}\cdot\frac{\tan\beta\omega y}{Sin\alpha_0} + R\,\frac{1}{Sin\alpha\ o}\,(1 + d'/b')\left[\frac{T_1}{Tsy}\right]^2 = 1 + \frac{Mo}{Msy1\ Sin\alpha o}$$

or

$$\frac{T_1}{Tsy} = \frac{(Sin\alpha o + Mo/Msy)}{\left\{\frac{M_1}{Msy_1}\cdot\frac{Tsy_1}{T_1} + \frac{V_1}{A1fsy}\tan\beta\ wy\cdot\frac{Tsy_1}{T_1} + R\,(1+d'/b')\,\frac{T_1}{Tsy}\right\}} = \tan\alpha\ wy$$

in which $Msy_1 = \frac{A1fsy}{\text{note no } Sin\alpha o}\,\ell a_1 = (A1fsy\ d')\ X\lceil\ell$

Mo = ditto

$Tsy = \left(2\,\frac{Asfsy\ b'd'}{S}\right) X\ \lceil w$

3. Alternatively $\tan\beta$ wy is evaluated and its solution is as follows:

$$\tan\beta wy = \sqrt{\left[\frac{M_1}{V_1 h}\right]^2 + \frac{[(Sin\alpha o) + Mo/Msy_1]}{R(h/b)}} - \left[\frac{M_1}{V_1 h}\right]$$

and

$$\left(\frac{dn_1}{d_1}\right) wy = \frac{\int \ell \; fsy \; Sin\alpha o}{0.4 \; Kcm \; fc'} \left[\sqrt{1 + \left(\frac{2 \; KCM \; R \; tan\alpha}{Kct \; Sin\alpha}\right)^2} - 0.6\right]$$

Longitudinal Steel Only at "Yield"

1. Taking moments about the transverse axis through the centroid of the compression zone at the top :

$$M_1 + V_1(d_1 - dn_1) \tan \beta \ell y + P\ell \; \ell a_1 + \frac{Asf\,s}{S} (d_1 - dn_1)(b' + d_\ell - dn_1) \left[\frac{T_1}{Tsy}\right]^2 = A\ell fly \ell a_1 + Mo$$

2. Divided by $M\ell y_1 = A1fly\ell a_1$

$$\frac{M_1}{M\ell y1} + \frac{V_1}{A1fly} (\tan \beta \ell y) + \frac{P\ell}{P\ell y} + (r\ell y \; Sin\alpha^{o}) (1 + d'/b') \left[\frac{T_1}{Tsy}\right]^2 = 1 + \frac{Mo}{M\ell y1}$$

or

$$\frac{T_1}{Tsy_1} = \frac{(1 + Mo/M\ell y1)}{\left\{\frac{M_1}{M_1 y_1} \frac{Tsy_1}{T_1} + \frac{V_1}{A1fly} \tan\beta\ell y \frac{Tsy_1}{T_1} + \frac{P\ell}{P\ell y} \frac{Tsy_1}{T_1} + (r\ell y_1 \; Sin\alpha o)(1 + d'/b')\frac{T_1}{Tsy_1}\right\}}$$

in which $M\ell y_1 = A\ell fly \; \ell a_1 = (A1fly \; d') \times \sqrt{\ell}$

$$Tsy_1 = 2 \frac{As \; fs \; b'd'}{S} \frac{fsy}{fsy} = \left(2 \frac{Asfsy \; b'd'}{S}\right)\left(\frac{fs}{fsy}\right) = \left(2 \frac{Asfsy \; b'd'}{S} Sin\alpha o\right) \times \sqrt{w}$$

3. Also:

$$\tan\beta\ell y1 = \sqrt{\left[\frac{M_1 + P\ell\ell a_1}{V_1 h}\right]^2 + \frac{[1 + Mo/M\ell y1]}{(r\ell y1 \; Sin\alpha o)(h/b)}} - \left[\frac{M_1 + P\ell\ell a_1}{V_1 h}\right]$$

4.11 Comparison with Test Results

For eleven beams of Series I the variation of actual strength with prestressing tendon force is represented in Figure (4.11.1). The Test Line is the line of a linear regression analysis. On the figure is imposed the predicted theoretical lines of equations:

4.10.2 -	for all yield
4.10.2 -	For longitudinal steel steel only at yield
4.10.2 -	for stirrups only at yield

It can be deduced that the experimental trend does not follow the lines of "all" or "longitudinal" steel at yield theories. This is conclusively indicated by the different slopes of the yield theoretical lines and the test line. As the test line passes well below the yield lines, it may, therefore, be concluded that failure was not due to yield of all steel or the longitudinal only. This is confirmed by the strain gauges readings which showed that neither of these reinforcements did yield.

It is noted, however, that the only stirrups yield line is apparently in good agreement with the tests. The conclusion must therefore be that failure may be governed by the stirrups only yield. In many cases this however did not occur in the tests.

For further comparison, the uncracked forms of the expressions (4.10) if presented graphically and imposed on the Test Line in Figure (4.11.1), the all yield line leads to similar conclusion. But the only stirrups at yield line shows good agreement with the test line. Hence the beams strength may be considered due to yielding of stirrups only.

FIGURE 4.11.1. VARIATION OF ULTIMATE STRENGTH WITH PRESTRESS COMPARED TO STEEL YIELDING METHODS - CRACKED SECTIONS

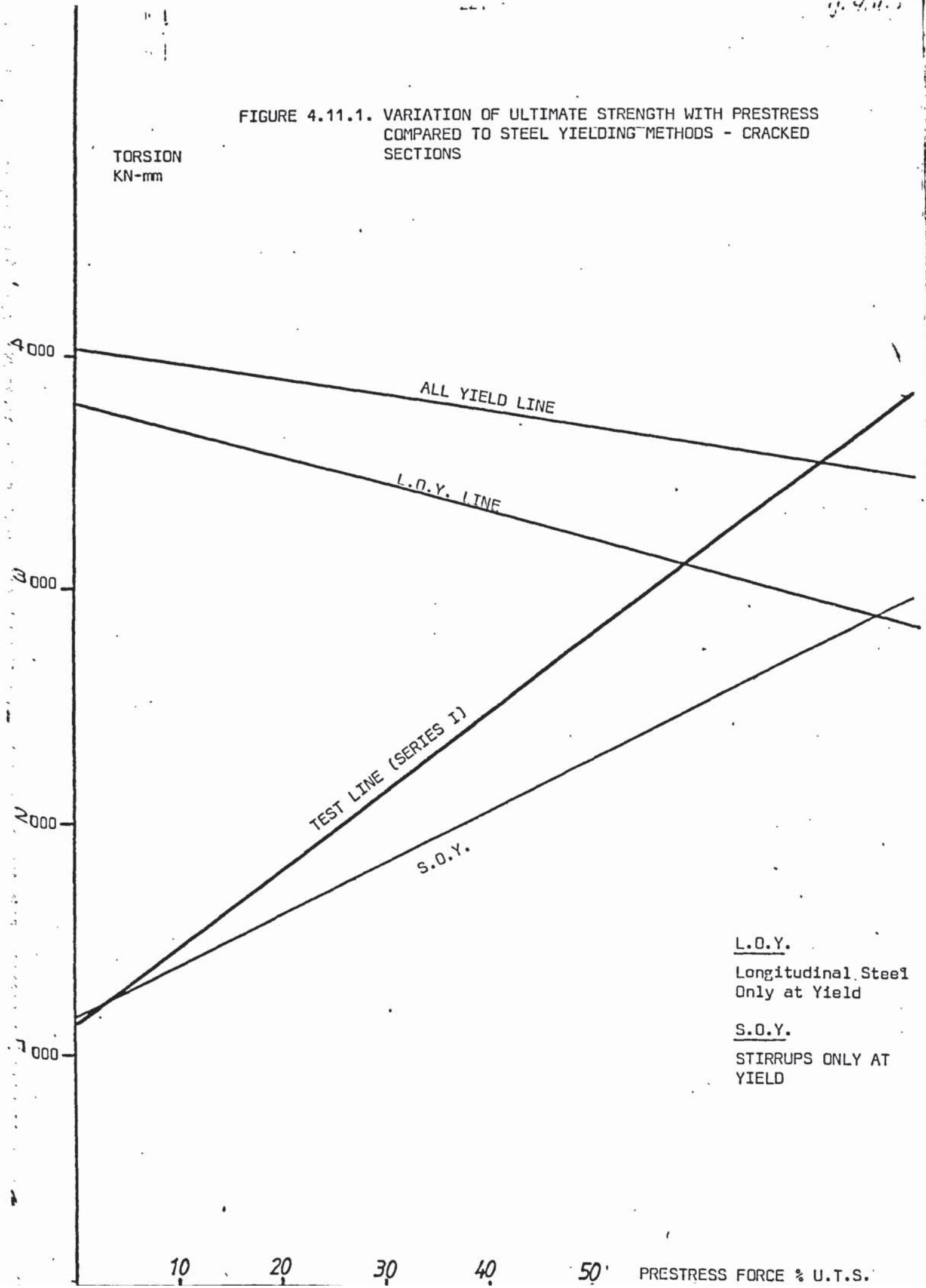

TABLE (4.11.1) DETAILED COMPARISON OF TEST BEAMS
WITH ALL-STEEL AT YIELD THEORY (uncracked).

BEAM	MODE 1	MODE 2	MODE 3	CR.MODE
A1	0.341	0.322	0.203	1
A2	0.325	0.355	0.318	2
A3	0.392	0.398	0.295	2
A4	0.341	0.306	0.169	1
A5	0.346	0.358	0.276	2
A6	0.550	0.595	0.508	2
A7	0.604	0.642	0.534	2
A8	0.574	0.656	0.664	3
A9	0.702	0.725	0.553	2
A10	0.878	0.953	0.838	2
A11	0.939	0.993	0.819	2
B1	0.443	0.453	0.353	2
B2	0.657	0.726	0.671	2
B3	0.448	0.534	0.606	3
B4	0.338	0.407	0.479	3
B5	0.471	0.580	0.747	3
B6	0.354	0.430	0.520	3
C1	0.481	0.534	0.499	3
C2	0.583	0.647	0.606	2
C3	0.675	0.760	0.736	2
C4	0.629	0.701	0.663	2
D1	0.368	0.481	0.488	3
D2	0.611	0.620	0.530	2
D3	0.668	0.646	0.505	1
E1	0.657	0.957	2.021	3
E2	0.722	0.876	1.048	3
E3	0.792	0.777	0.534	1
E4	0.690	0.432	0.104	1
F0	0.452	0.378	0.196	1
F1	0.605	0.691	0.711	3
F2	0.598	0.444	0.185	1
G1	0.720	0.866	1.016	3
G2	0.754	0.788	0.633	2
G3	0.641	0.551	0.288	1
AA1	0.802	0.83	0.647	2
BEAMS	number	mean	S.D.	C.V.
A	11	0.58	0.23	40%
B	6	0.58	0.12	20%
ALL-A	23	0.67	0.16	23%

TABLE (4.11.2) DETAILED COMPARISON OF TEST BEAMS WITH STIRRUPS ONLY AT YIELD THEORY (uncracked).

BEAM	MODE 1	MODE 2	MODE 3	CR.MODE
A1	1.29	0.58	0.22	1
A2	0.96	0.59	0.34	1
A3	1.09	0.63	0.31	1
A4	0.83	0.44	0.18	1
A5	0.72	0.48	0.29	1
A6	1.04	0.77	0.54	1
A7	1.01	0.77	0.57	1
A8	0.90	0.75	0.70	1
A9	0.97	0.76	0.59	1
A10	1.26	1.03	0.89	1
A11	1.25	1.02	0.87	1
C1	0.66	0.55	0.53	1
C2	0.76	0.65	0.65	1
C3	0.94	0.80	0.78	1
C4	0.89	0.75	0.70	1
E1	0.87	0.96	2.14	3 *
E2	0.96	0.89	1.11	3
E3	1.06	0.80	0.57	1
E4	0.93	0.42	0.11	1
BEAMS	number	mean	S.D.	C.V.
A	11	1.03	0.17	17%
C	4	0.81	0.11	14%
E	4	1.31	0.48	37%
Excldg.E1	3	1.03	0.08	7%

*pure torsion

In Table (4.11.1) the results of the predictions made on the basis of the all yielding theory are compared to the test strength. Test/Theory ratio is 0.58±0.23 (40%) for A beams and 0.67 (23%) for (23) beams from other series. This confirms the previous conclusions from the discussion.

For completeness the partial-yield theory of Section 10.11 is also used to analyse the test results. The results are tabulated in Table (4.11.2). The improved accuracy and coefficient of variation of 1.03±0.17 (17%) for Series A beams indicates that the strength may be governed by stirrups only at yield type of failure. Whilst that none of the prestressing steel yielded can be verified from the tests, it is difficult to substantiate that yield was always present in the stirrups.

CHAPTER 5:

ANALYSIS OF TEST BEAMS BY STEEL - NON-YIELDING METHODS AND CONCRETE FAILURE THEORIES

5.1. INTRODUCTION

In this Chapter the analysis of the test results is continued by considering the non-yielding conditions of failure and for this purpose an analytical method is presented. When necessary, suitable approximations are made. The average direct bending and shear stresses, are calculated from the experimental loads and depths of concrete compression zone whenever available. The test stresses are compared to the theoretical values which are determined from various failure criteria for concrete subjected to combined stresses. As a measure of accuracy the ratios of test/theory are determined for the criterion and further compared to the ratios which were calculated based on the steel yielding analysis in the previous chapter.

5.2. Non-Yielding Interaction Equations

In this section the basic interaction expressions are derived for three modes of failure. In mode one, two cases are considered when the stress at the bottom fibre due to the applied bending moment exceeds the prestress then a solution for a cracked section is applicable. The solution for the uncracked section, however, follows first.

5.2.1. Deduction of Non-yielding Interaction Equations:-

Mode One of failure (uncracked section in flexure)

1. Taking moments about a transverse axis through the centroid of the

compression zone which is located at the top of the failure sections :

$$M_1 + V_1(d_1 - x_1)\tan\beta_0 = [A1f\ell + P\ell]\,\ell_{01} - \frac{Asfs}{S}(d_1-x_1)(\tan\alpha_{01} + \tan\beta_0)$$
$$(\tan\alpha_{01} - \tan\beta_0) + b'\tan^2\alpha_{01}]$$

putting $M_{01} = (A1f\ell + P\ell)$
$= Kp\ A1f\ell\ \ell_{01}$ where $Kp = 1.0 + \frac{P\ell}{A1f\ell}$

Hence dividing both sides of the equation by M_{01}:

$$\frac{M_1}{M_{01}} + \frac{V_1}{M_{01}}(d_1-x_1)\tan\beta_0 = 1 - \frac{r\ell_0}{Kp}\frac{(d_1-x_1)}{\ell_{01}}\left[\left(\frac{d_1-x_1}{b'} + 1\right)\tan^2\alpha_{01} - \frac{(d_1-x_1)}{b}\tan^2\beta_0\right]$$

5.2.1.

in which $r\ell_0 = \frac{As\ fs\ b'}{S\ A1\ f\ell}$ thus if $fs/f\ell = Kr$ then $Kr\frac{As\ b'}{S\ A1} = Ro = Kr\ R$

2. Taking moments of forces about the longitudinal axis in the compression zone:

$$T_1 = \frac{As\ fs}{S}\,b'\tan\alpha_{01}\ell_{01} + \frac{As\ fs}{S}(d_1-x_1)\tan\alpha_{01}\,b'$$

$$\frac{T_1}{M_{01}} \quad (2\ Ro\ \tan\alpha_{01})\ \frac{1}{Kp} \qquad 5.2.2$$

3. Resolving forces vertically

$$V_1 = 2\frac{As\ fs}{S}(d_1-x_1)\tan\beta_0$$

(and hence all the shear force is taken by the stirrups)

$$\frac{V_1}{M_{01}} = 2\ Ro\ \frac{(d_1-x_1)}{b'\ell_{01}}\tan\beta_0\ \frac{1}{Kp} \qquad 5.2.3$$

4. Substitution of the last two equations in equation 5.2.1.:

$$\frac{M_1}{M_{01}} + \left(\frac{V_1}{M_{01}}\right)^2\frac{b'\ell_{01}}{2\ Ro} = 1 - \frac{Ro}{Kp}\frac{(d_1-x_1)}{\ell_{01}}\left[\left(\frac{d_1-x_1}{b'}+1\right)\left(\frac{KpTo_1}{M_{01}}\frac{1}{2Ro}\right)^2 - \frac{(d_1-x_1)}{b}\right.$$
$$\left.\left(\frac{Kp\ V_1}{M_{01}}\frac{b'\ell_{01}}{2Ro(d_1-x_1)}\right)^2\right]$$

On gathering terms and rearranging :

$$\frac{M_1}{M_{01}} + \left(\frac{V_1}{V_{01}}\right)^2 + \left(\frac{T_1}{T_{01}}\right)^2 = 1 \qquad 5.2.4.$$

in which $Kp = 1 + P\ell/P\ell o$ where $P\ell o = A\ell f\ell$ i.e.

$$Mo_1 = Kp\ A\ell f\ell \ell o_1$$

$$To_1 = 2Mo_1\sqrt{\frac{Ro}{1+h/b}}$$

$$Vo_1 = 2Mo_1\sqrt{\frac{Ro}{b'\ell o_1}}$$

This equation therefore defines the basic interaction surface for the four loading parameters involved. It can be further presented in the form :

$$Kp\frac{M_1}{(M\sigma_1')} + [\frac{V_1}{V\sigma_1'}]^2 + [\frac{T_1}{T\sigma_1'}]^2 = Kp^{-2} \quad \text{in which } M\sigma_1' = A\ell f\ell \ell o_1$$

or :

$$\frac{M_1}{M\sigma_1'} + \frac{1}{(1+F\ell/P\ell o)}\left\{[\frac{V_1}{V\sigma_1'}]^2 + [\frac{T_1}{T\sigma_1'}]^2\right\} = 1 + \frac{P\ell}{F\ell o} \qquad 5.2.4a$$

5. Rearranging terms of equation 5.2.4. and solving the resulting quadratic equation in $\frac{T_1}{To_1}$:

$$\frac{T_1}{To_1} = \frac{-[\frac{M_1}{T_1}\frac{To_1}{Mo_1}] + \sqrt{[\frac{M_1}{T_1}\frac{To}{Mo_1}]^2 + 4\ \Psi o_1}}{2\ \Psi o_1} \qquad 5.2.5$$

in which $\Psi o_1 = 1 + (\frac{V_1}{T_1})^2\ (\frac{To_1}{Vo_1})^2$ and

$$\frac{To}{Vo_1} = \sqrt{\frac{b'\ell o_1}{1+h/b}}$$

$$\frac{To}{Mo_1'} = 2\sqrt{\frac{Ro}{1+h/b}}$$

Mode One of failure (cracked section in flexure)

Similarly to the case of uncracked section moments are taken in the centroid of the compression zone about a transverse axis:

$$M_1 + V_1(d_1-x_1)\tan\beta o = A\ell\ f\ell\ \ell o_1 + Mo -$$

$$\frac{Asfs}{S}(d_1-x_1)\ [(d_1-x_1)(\tan\alpha_{oi} + \tan\beta o)(\tan\alpha oi - \tan\beta o) + b'\tan^2\alpha o_1]$$

putting $Mo_1 = A\ell f\ell\ \ell o_1$

$$Mo = \frac{bh^2}{12}\ \frac{h}{yd}\ [0.402\sqrt{f'c}] + Z\ \frac{h}{yd}\ [\frac{Ps}{bh}\ (1 + \frac{12eyd}{h^2})]$$

Henceforth the equations 5.2.1 through 5.2.3 retain the same format and are modified by interchanging the definition of Mo_1 term and setting Kp = 1. Equations 5.2.4, 5 become of the following forms:

$$\frac{M_1}{Mo_1} + \left(\frac{V_1}{Vo_1}\right)^2 + \left(\frac{T_1}{To_1}\right)^2 = 1 + \frac{Mo}{Mo_1} \qquad 5.2.4A$$

$$\frac{T_1}{To_1} = \frac{-\left[\frac{M_1}{T_1}\frac{To_1}{Mo_1}\right] + \sqrt{\left[\frac{M_1}{T_1}\frac{To_1}{Mo_1}\right]^2 + 4\,\Psi o_1 Co_1}}{2\,\Psi o_1} \qquad 5.2.5A$$

in which $\Psi o_1 = 1 + \left(\frac{V_1}{T_1}\right)^2 \left(\frac{To_1}{Vo_1}\right)^2$

$$Co_1 = 1 + \frac{Mo}{Mo_1}$$

6. To evaluate a value for the angle (αo_1) which is involved in the construction of equation 5.2.4A, equation 5.2.5A is equated to the value of $\frac{T_1}{To_1}$ from equation 5.2.2 :

$$\tan\alpha o_1 = \frac{1}{(1+h/b)\Psi o_1}\left\{\sqrt{\left(\frac{M_1}{T_1}\right)^2 + \frac{(1 + h/b)\,\Psi o_1 Co_1}{Ro}} - \frac{M_1}{T_1}\right\} \qquad 5.2.6$$

For the uncracked section $Co_1 = 1$

7. Now for either case of cracked or uncracked section equation 5.2.6 may be used with the appropriate angle (αo_1) and terms of Mo to express the T_1 in a general form, and the equation of the torsional moments in step 2 is :

$$T_1 = 2\,\frac{As\ fs\ b'}{S}\, z\ell o_1 \tan\alpha o_1 \text{ where } z\ell o = d_1 - K\ell o\, x_1 \qquad 5.5.2a$$

or :

$$T_1 + 2\,\frac{As\ fs\ b'}{S}\, k\ell o x_1 \tan\alpha_{o1} = 2\frac{As\ fsy\ b'd'}{S}\,\frac{fs}{fsy}\,\lambda_\ell \tan\alpha o_1$$

If $T_{x1} = 2\,\frac{As\ fs\ b'}{S}\, K_{\ell o} x_1 \tan\alpha o_1$

$$T_1\left[1 + \frac{Tx_1}{T_1}\right] = 2\,\frac{As\ fsy\ b'd'}{S}\left[\frac{fs}{fsy}\right]\lambda\ell \tan\alpha o_1 \text{ where } \lambda\ell = {}^{d1}/_{d'} \qquad 5.2.2b$$

Mode Two of failure

Similarly to Mode one, moments are taken about a transverse axis through the centroid of the compression zone which is located now at one of the wider sides of the beam and parallel to the line of action of the

vertical shear force which therefore does appear in this equation of moments:

$$M_2 = [A\ell_2 f\ell_2 + P\ell_2]\ \ell o_2 - \frac{As\ fs}{S}(b_\ell - x_2)[(b_1-x_2)(\tan\alpha_{02} + \tan\beta_0)(\tan\alpha_{02} - \tan\beta_0) + d'\tan^2\alpha_{02}]$$

putting $Mo_2 = (A\ell_2 f\ell_2 + P\ell_2)\ \ell o_2$

$= KpA\ell_2 f\ell_2 \ell o_2$ where $Kp = 1 + \frac{P\ell}{A1 f\ell}$ as in Mode 1

noting also that M_2 is very small.

$$Mo_2 \cong \frac{Asfs}{S}(b_1-x_2)[(b_1-x_2+d')\tan^2\alpha_{o2} - (b_1-x_2)\tan^2\beta_o]$$

$$1 \cong Kp\ \frac{Asfsd}{Al_2 S\ f\ell_2}(b_1-x_2)[(\frac{b_1-x_2}{d'}+1)\tan^2\alpha_{o2} - (\frac{b_1-x_2}{d'})\tan^2\beta_o]$$

Therefore interchanging b and h and their related dimensions in the equations constructed for Mode 1, the interaction equation for Mode 2 is :

$$[\frac{T_2}{To_2}]^2 + [\frac{V_2}{Vo_2}]^2 = 1 \qquad 5.2.7.$$

and $[\frac{T_2}{To_2}]^2 \left\{1 + [\frac{V_2}{Vo_2}]^2 [\frac{To_2}{T_2}]^2\right\} = 1$

$$\frac{T_2}{To_2} = \frac{1}{\sqrt{\Psi o_2}} \qquad 5.2.8.$$

where $\Psi o_2 = 1 + [\frac{V^2}{Vo_2}]^2 [\frac{To_2}{T_2}]^2$

Also

$$T_2 = 2\frac{As\ fs\ d'}{S} z\ell o_2 \tan\alpha o_2 \quad \text{in which } z\ell o_2 = b_1 - k\ell o_2 x_2 \qquad 5.2.9.$$

and

$$\tan\alpha o_2 = \frac{1}{\sqrt{(1 + b/h)\ \Psi o_2 Ro_2}} \quad \text{in which } Ro_2 = \frac{As\ d'}{A\ell_2\ S} \text{ and } A\ell_2 = \frac{A1_1 + A1_3}{2} \qquad 5.2.10.$$

5.2.2. Determination of average stresses acting on the compressive zone:

1. Average torsional shear stresses on the compression zone (ftv) is determined by taking moments of forces about a longitudinal axis in the tensile zone :

$$To_1 = K\Phi\ b x_1\ ftv\ ro_1 + \frac{As\ fs\ (d\omega - x_1)}{S} \tan\alpha o_1 b'$$

and

$$To_1 + \frac{As\ fs\ b'}{S} x_1 \tan\alpha o_1 = \frac{As\ fs\ b'\ d'}{S}\lambda\omega \tan\alpha o_1 + Kt\ bx_1 ftv\ ro_1$$

$$To_1\left[1 + \frac{Tx_1}{2To_1}\right] = Ktv\ bx_1 ftv\ (ro_1) + \frac{As\ fs\ b'\ d'}{S}\lambda\omega \tan\alpha o_1 \qquad 5.2.11.$$

in which $ro_1 \cong \ell o_1$, $\lambda\omega = \frac{d\omega}{d'}$

for $\frac{fs}{fsy} = \sin\alpha o_1$ equation 5.2.11 can readily be solved for ftv if xo_1 is known.

Note: Adding the equations 5.2.2b and 5.2.11 and dividing by 2 results in :

$$To_1\left[1 + 0.75\frac{Tx_1}{T_1}\right] = \tfrac{1}{2}kt\ b\ xo_1 ftv\ ro_1 + \frac{(2\lambda_1+\lambda\omega)}{2}\frac{As\ fsy\ b'\ d'}{S} X \left[\frac{fs}{fsy}\right] \tan\alpha o_1 \qquad 5.2.11b$$

in which $\left[\frac{fs}{fsy}\right] = \sin\alpha o_1$ by assumption.

2. Average vertical shear stress on the compression zone is determined by resolving forces vertically:

$$V_1 = kvbxo_1 fcv + 2\frac{As\ fs\ (d\omega - xo_1)}{S}\tan\beta o$$

and

$$V1 + \left[\frac{2\ As\ fsy\ xo_1}{S}\tan\beta o_1\right]\frac{fsv}{fsy} = kvbxo_1\ fcv + \left[2\frac{As\ fsy}{S}\ d\omega\tan\beta_{01}\right] X \frac{fsv}{fsy}$$

$$V_1\left[1 + \frac{Vx_1}{V_1}\right] = kvbxo_1 fcv + \left[2\frac{As}{S}\ fsy\ d\omega\ \tan\beta_{01}\right]\tan\beta_{01} \qquad 5.2.12.$$

in which $V_{x1} = \left[2\frac{As\ fsy\ xo_1}{S}\tan\beta o\right]\tan\beta o$ where $\frac{fsv}{fsy} = \tan\beta o$

The average vertical shear stress fcv is determined from Equation 5.2.12 on knowing xo_1.

3. Average direct bending stress on the compression zone is determined by taking moments about the centroid of the tensile steel about a transverse axis :

$$M_1 = Kcm\ b\ xo_1\ fcm\ \ell o_1 + 2\ \frac{As}{S}\ (fsy\ Sin\beta o)\left(\frac{d'\ tan\beta o}{2}\right)^2$$
$$- \frac{As}{S}\ (fsy\ Sin\alpha o)\ b'(1+ d'/b')\ tan\alpha o_1 d' \qquad 5.2.13.$$

The average direct stress fcm is determined from this equation when xo_1 is known.

4. Determination of xo_1 : elastic reduced by torsion.

5.3.1. Application to Test Beams - Ultimate Strength

To apply the general interaction equation 5.2.5. a value for the depth of the compression zone is needed. The stresses in the pre-stressing wires and stirrups, or their ratio, must also be known to achieve a solution. In this section these unknowns are obtained from the experimental measurements for the test beams.

Table (3.8.1) contains the experimental depths of the concrete zone in mode 1. In Table (3.7.1), the values of stresses in the stirrups legs and tendons have been presented. Thus the theory is applied by substituting these values. The outcome of the comparison with the test results is presented in Table (5.3.1.) in the form of ratios of test/theory.

For the eleven beams of Series I a mean of 1.68, a standard deviation of 0.22 and a coefficient of variable of 13.3% is obtained. Figure (5.3.1.) represents graphically the correlation between the non-yielding method and the test beams. The trend of the theoretical and experimental lines is similar but the theoretical line should be steeper. The coefficient of variation is good and suggests that the theoretical non-yielding analysis is correct and produces a safe lower limit for the test results. This line however, is too conservative.

In Figure (5.3.1.) also the theoretical line of the fully yielding method is reproduced for comparison with the non-yielding analysis. It is evident that the critical strength values are those predicted by the non-yield method. In reference to Figure (4.11.1.), it could be concluded that the non-yield line is also critical with respect to the partial yield method involving the yield of stirrups only.

TABLE 5.3.1 RATIOS OF TORQUE TEST/NON-YIELDING THEORY (CRACKED SECTION)

BEAM	TEST kNmm	THEORY CRACKED kNmm	RATIO	THEORY UNCRACKED kNmm	RATIO
A1	1120.0	790.16	1.42	N/A	-
A2	1274.0	773.36	1.65		
A3	1400.0	887.86	1.58	N/A	-
A4	1036.0	712.99	1.45	N/A	-
A5	1260.0	640.22	1.97	N/A	-
A6	2100.0	1160.01	1.81	N/A	-
A7	2282.0	1134.46	2.01	N/A	-
A8	2366.0	1684.90	1.40		
A9	2538.0	1769.80	1.43	N/A	-
A10	3402.0	1843.84	1.85	N/A	-
A11	3542.0	1884.30	1.88	N/A	-
MEAN ± S.D.		1.68 ± 0.22		-	
C.V. %		13.3%		-	

FIGURE 5.3.1. CORRELATION OF TEST BEAMS (ULTIMATE STRENGTH) AND NON-YIELDING METHOD FOR SERIES I

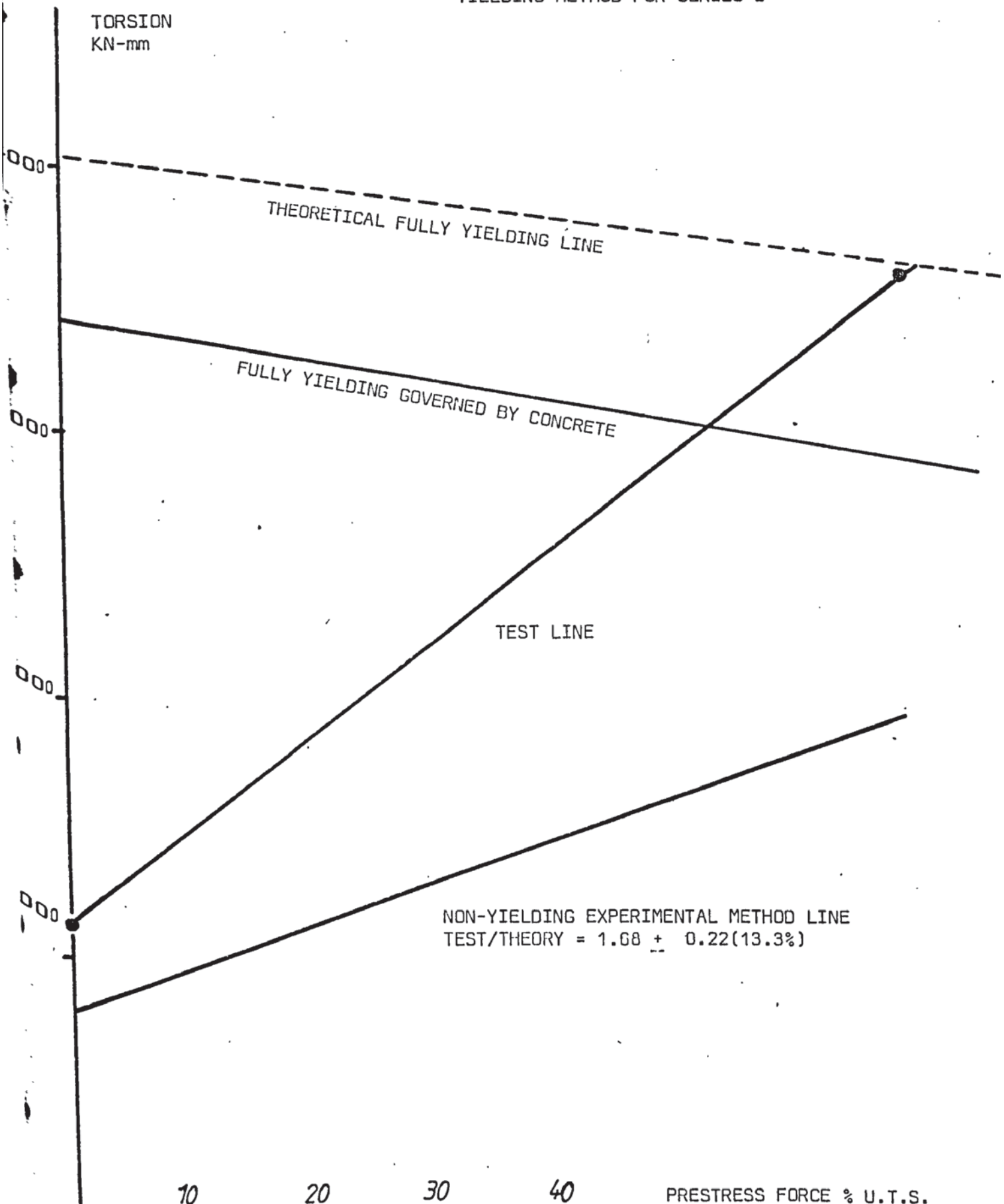

5.3.2. Application to Test Beams - Average stresses on the Compression Zone:

The average torsional and vertical shear stresses and direct bending stress are determined by using equation 5.2.11 and 13 with the experimental values of the depth of the compression zone. The experimental resultant shear stress frv is determined by vector addition:

$$frv = \sqrt{(fcv^2 + (fct)^2}$$

Hence the experimental ratio of the direct stress (fcm) to the resultant shear stress is obtained in terms of a ratio : $\frac{fm}{frv}$ experimental.

Now this ratio can be entered in various criteria of concrete failure subject to combined stresses. The outcome will be the theoretical stress according to the given criteria and therefore a ratio of frv Test/frv theory can be calculated and studied as a measure of correlation between the test results and the different concrete failure theories.

The following concrete failure criteria in rearranged forms, are applied in this subsection to analyse the test results:

Principal Tensile Stress Criterion:

$$(frv)\ \text{Theory} = fsp\sqrt{1 + \frac{fcm}{fsp}} \qquad \text{-------(5.3.2-a)}$$

Cowan Criterion:

$$(frv)\ \text{Theory} = \frac{0.2\ f\acute{c}}{\sqrt{1 + (\frac{fcm}{2\ frv})^2} - 0.3\ (\frac{fcm}{frv})} \qquad \text{------- (5.3.2-b)}$$

Seth Criterion:

$$(frv)\ \text{Theory} = \frac{fr}{\sqrt{1 + (\frac{fcm}{2frv})^2} - 0.78(\frac{fcm}{2frv})} \qquad \text{------- (5.3.2-c)}$$

Zia Criterion:

$$(frv)\ \text{Theory} = \frac{fr}{\sqrt{1 + (\frac{fcm}{2frv})^2} - (\frac{fcm}{2frv})\ S \text{ in } \lambda}$$

$$\text{in which } \tan^2\lambda = (\frac{0.25\ f\acute{c}}{fr_1})^2 - 1 \qquad \text{------- (5.3.2-d)}$$

These equations are presented in a graphical form in Figure (5.5.3.) in section (5.5) of this chapter where these criteria of failure are discussed.

In Table (5.3.2.) the computed values of the experimental average shear stress and direct stress (fcm) are presented. These values are based on the experimental measurements of the depth of the compression zone. The ratio of test average stress frv/theory using the criteria are presented in Table (5.3.3.). Seth criterion seems the critical one among the other theories, with an average of 0.71, a standard deviation of ±0.17 and c.v.= 23.5%. This result is good and suggests an agreement between Seth continuous criterion and the observed failures which were continuous from cleavage to crushing. In some cases, however, beams failed by crushing accompanied by extensive debris. Cowan criterion for concrete failure by crushing, produces a mean 0.57, a S.D. of 0.12 and 20.5% as coefficient of variation. It is noted that as the analysis is based on the experimental depths of the concrete which ranged between 0.29-0.63 of the effective depth of the steel, therefore the concrete accommodated a lower shear stress intensity to which Seth is apparently better related than Cowan's. Predictions made by Cowan criterion are represented graphically in Figure (5.3.1.).

It is concluded that Seth criterion is the more consistent when applied to the experimental results producing a mean value of 0.7 indicating that the test beams failed with combined stresses laying inside the range of the criterion. This should therefore be interpreted as an indication that the beams failed due to concrete failure.

To examine whether the steel reached yield before the concrete developed its useful strength, reference is made to Table (4.11.1) where the all steel yield theory was compared to the tests. Table (5.3.3)

TABLE 5.3.2 VALUES OF EXPERIMENTAL AVERAGE SHEAR (frv) STRESS AND DIRECT (fm) STRESS BASED ON THE MEASURED VALUES OF THE DEPTH OF COMPRESSIVE ZONE

BEAM	TEST VALUES dn/d	fm N/mm²	ft N/mm²	fv N/mm²	frv N/mm²	frv/fc	fm/fc	pc₂ /fc
A1	0.29	19.97	2.11	0.48	2.17	0.057	0.52	0.00
A2	0.35	13.86	1.76	-0.21	1.77	0.051	0.40	0.02
A3	0.38	16.58	2.15	-0.47	2.20	0.085	0.64	0.05
A4	0.45	13.91	1.40	-1.30	1.91	0.054	0.39	0.06
A5	0.45	12.05	1.56	-1.95	2.50	0.070	0.35	0.09
A6	0.54	14.65	2.63	-1.90	3.25	0.093	0.42	0.11
A7	0.54	16.17	2.93	-2.24	3.69	0.103	0.45	0.15
A8	0.51	14.07	3.06	-2.55	3.98	0.122	0.43	0.18
A9	0.71	15.71	2.82	-2.73	3.92	0.111	0.44	0.21
A10	0.62	19.66	4.27	-2.74	5.07	0.148	0.58	0.23
A11	0.63	21.89	4.49	-2.69	5.23	0.140	0.59	0.23

TABLE 5.3.3 RATIOS OF TEST AVERAGE STRESS (frv)/CRITERIA VALUES FOR TEST BEAMS USING EXPERIMENTAL (dni/dl)

BEAM	frv N/mm²	p.t.s. criterion	COWAN	ZIA	SETH	YIELD
A1	2.17	0.23	0.56	0.28	0.71	0.34
A2	1.77	0.23	0.43	0.22	0.51	0.36
A3	2.20	0.34	0.70	0.26	0.61	0.40
A4	1.91	0.25	0.43	0.23	0.52	0.34
A5	2.50	0.34	0.41	0.28	0.53	0.36
A6	3.25	0.48	0.52	0.36	0.67	0.60
A7	3.69	0.52	0.57	0.41	0.75	0.64
A8	3.98	0.55	0.59	0.45	0.75	0.66
A9	3.92	0.53	0.56	0.44	0.77	0.73
A10	5.07	0.60	0.75	0.57	0.98	0.95
A11	5.23	0.58	0.75	0.58	1.04	0.99
Mean ± S.D.		0.42±0.14	0.57±0.12	0.37± 0.12	0.71± 0.17	

includes the critical values of the two analyses and the higher ratio is indicated as that governs the strength and the type of failure.

In this comparison, as shown in Table (5.3.3), all the beams failed by concrete before that all of the steel could yield. This is confirmed by the readings from the strain gauges attached to the steel.

The analysis of the test beams is furthered by considering an elastic depth for compressive concrete zone.

The average shear and direct stresses calculated based on the elastic depth are presented in Table (5.3.4.). The results produced by the various criteria are tabulated in Table (5.3.5.). Seth seems to give the critical estimate when compared to Cowan and Zia. The trend of correlation is therefore basically identical to the one noticed when using the experimental depth of the concrete.

The ratios when compared to the steel yield results show decisively that the failure in all the beams was governed by concrete strength.

It is noted that to apply this method to a wider range of tests there is a need for a unified method to estimate the critical concrete stress. However the deployed criteria have a similar format as could be seen from equations (5.3.2. b,c and d). Nonetheless the basic assumptions and considerations involved in these criteria are different. As the tests seem to be more related to a concrete analysis than to a steel yield theory, the concrete criteria may therefore be considered further. In section (5.4.) existing concrete failure criteria are depicted and discussed. In section (5.5.), however, an attempt is made for a new formulation.

TABLE 5.3.4 VALUES OF EXPERIMENTAL AVERAGE SHEAR (frv) STRESS and DIRECT (fm) STRESS BASED ON ELASTIC VALUES OF THE DEPTH OF COMPRESSION ZONE

BEAM	Elastic value of dni/dl	fm N/mm²	ft N/mm²	fv N/mm²	frv N/mm²	frv/fc	fm/fc	pc_2 /fc
A1						0.067	0.163	0.00
A2						0.083	0.170	0.02
A3						0.118	0.210	0.05
A4						0.062	0.155	0.06
A5						0.076	0.150	0.09
A6						0.130	0.148	0.11
A7						0.134	0.138	0.15
A8						0.150	0.147	0.18
A9						0.158	0.142	0.21
A10						0.201	0.134	0.23
A11						0.192	0.123	0.23

TABLE 5.3.5 RATIOS OF TEST AVERAGE STRESS (frv)/CRITERIA VALUES FOR TEST BEAMS USING ELASTIC (dni/dl)

BEAM frv N/mm²	Principal t.Criterion	SETH	COWAN	ZIA
A1		0.481	0.283	0.335
A2		0.566	0.337	0.429
A3		0.858	0.473	0.673
A4		0.383	0.264	0.281
A5		0.550	0.308	0.415
A6		0.922	0.524	0.819
A7		0.911	0.545	0.829
A8		1.108	0.613	1.005
A9		1.086	0.650	1.006
A10		1.490	0.855	1.412
A11		1.623	0.822	1.528
MEAN ± S.D.				
C.V.%				

TABLE 5.3.6 RATIOS OF TEST AVERAGE STRESS (frv)/CRITERIA VALUES WITH 50° ANGLE

BEAM	COWAN
A1	0.57
A2	0.45
A3	0.74
A4	0.45
A5	0.47
A6	0.59
A7	0.64
A8	0.71
A9	0.67
A10	0.88
A11	0.86
MEAN	0.64
S.D.	±0.15
C.V.	22.6%

It is recalled that although Seth governed the strength of the test beams Cowan and Zia were shown to be closely related also, with the same S.D. ±0.12. This must be an indication that the failures may be linked to Cowan-Zia criterion by some mechanism which is not well established by Cowan or its modification by Zia.

The mean value of angle λ involved in Zia modified criterion for cleavage was 67.7° with a variation of 3.3% for the test beams. See equ.(5.3.2-d) for tan λ ; Cowan simplified criterion for crushing involves 37° angle. The average angle is therefore 52°. A value of 53° may thus be substituted in the two criteria.

A further modification of Cowan may be achieved by considering an average intercept of 0.1 fć. If this is taken as fr then equation (5.3.2.-d) for Zia is approximately identical to equation (5.3.2-c) for Seth and both may therefore be considered equal numerically.

5.4. FAILURE CRITERIA

The oldest classical theory for failure of materials is due to Coulomb (6). He also conducted an experimental study of the torsional phenomenon before Saint Venent. Coulomb experimented with metal wires of circular cross-section. Based on these experiments, the first solution of the torsional problem was proposed by Coulomb in 1784, in the form :

$$T = K\theta \qquad (a)$$

Although Coulomb never tested any concrete specimens in torsion, he contributed considerably to the theory of strength of materials, developing the idea of internal friction on which he based his failure criterion. As a value for the internal friction coefficient, $\mu = 0.75$ was used by Coulomb (19) to deal with problems in brickwork and soil mechanics.

Later Cowan (21) proposed his criterion of failure of concrete based on an angle of 37° from the internal friction theory of Coulomb, combined with Rankine's limiting tensile stress theory. The criterion was therefore a dual one although much use has been made of its compressive side for concrete failure in crushing. Zia (40), however, improved on the tensile branch of Cowan's criterion, modifying the slope of the line tangent to the tensile strength circle. This line was parallel to the shear axis according to Rankine-Cowan. Zia suggested an alternative inclined line joining the tangent to the pure shear circle with the intersection point of Cowan's envelope with the shear axis. See Figure (5.4.1). Better agreement was found between this modified Cowan criterion and failures in cleavage. The gain from the improved accuracy was not matched by simplicity provided by a continuous line of shear stress variation from tension to compression.

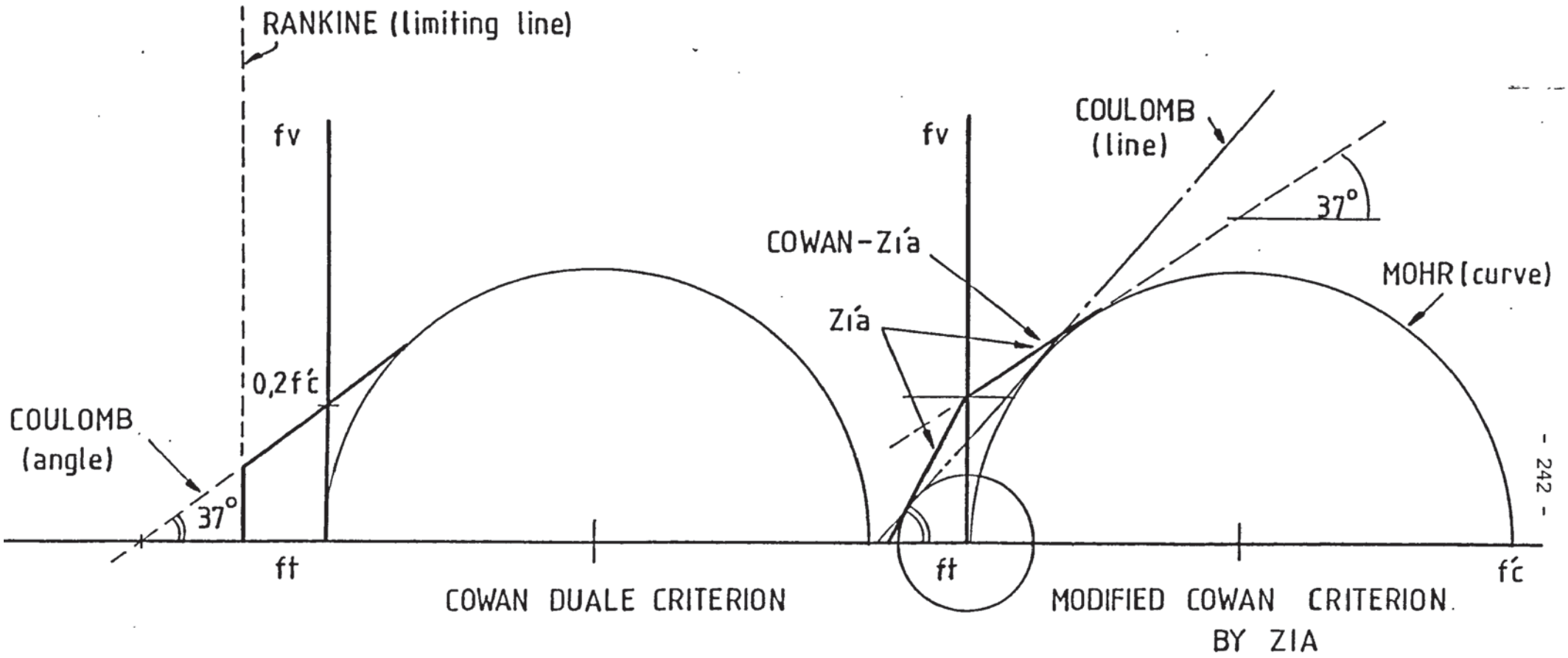
RANKINE (limiting line)
fv
0,2f'c
COULOMB
(angle)
37°
ft
COWAN DUALE CRITERION
fv
COULOMB
(line)
37°
COWAN-Zi'a
Zi'a
MOHR (curve)
ft
f'c
MODIFIED COWAN CRITERION
BY ZIA

DIAGRAM 5.4.1.

Zia's modification was however a notable contribution to bring the tensile stress criterion line closer to the Mohr envelope. Leon (19), however, was critical of Mohr's original generalization of Coulomb's theory because it could lead to inconsistency with tensile test results. In Zia's theory reference is made to an apparent "torsional stress" and the terms pure tensile and shear strength are interchangeable, although it is quite clear from the derivation that a shear stress circle is considered for equal tensile and compressive stresses. St.Venant, however, was the first to show that $\tau = 0.8ft$ (19) in an element under the action of equal tensile and compressive stresses. Zia's stress is therefore inaccurate and should be determined practically from directtensile concrete tests. Direct tensile tests introduce further difficulties because they may be measured and determined in various ways. Alternatively it is proposed in this thesis that a theoretical solution of the combined stress interaction can be obtained based on the shear-friction concept which can be related directly to laboratory tests.

Although Zia criterion was an improvement on Cowan, it was also discontinuous..

Practically failure is not a simple tensile/cleavage failure or a crushing failure but a transition failure in shear between these two extremes. This combined shear failure is common, because there is rarely a concrete structural member that fails exactly in pure crushing or cleavage. Nadai (19) came to a similar conclusion i.e. that the transition from rupture to crushing must be gradual. This conclusion is considered to be important, since it is more realistic to conceive the failure in different modes as curves which run smoothly into each other

rather than in abruptly sharp-intersection lines. Nadai (19) also preferred to refer to the "brittle" and "ductile" states of materials failure rather than to artificially classifying these materials into brittle and ductile.

By applying the skewed-bending axis theory, Martin and Cooper (38) derived the strength of a prestressed member in a mode 2 of failure subject to torsion, bending and shear which resulted in the stress equation : $f_{r2}\sqrt{1 + p_{c2}/f_{r2}}$. This equation will be developed further in this thesis. Martin and Wainwright (36) also produced the same solution, when shear force was absent and concluded that what was needed was to determine the precise nature of the failure criterion involved. In this chapter an attempt is made to synthesize such a general criterion which satisfies continuity from tension to compression.

In Figure (5.4.1) are depicted the criterion of Rankine, Coulomb, Mohr, Cowan and modified Cowan criterion. Another criterion, favoured by Indian researchers in combined torsion (53) and tensile diagonal cracking in pure shear (54) is named after its originator Seth (55). This criterion is basically different from the aforementioned criteria and thus it will be discussed later.

As a result of this survey, it is concluded that the basic failure criteria for concrete have been formulated as combinations, or modified versions, of older criteria which were formulated on the basis of semi-theoretical notions of materials failure. None were intended as a complete solution for concrete. These criteria were never confirmed experimentally in a systematic manner.

The notions of the slip-lines, plastic flow and the sand-heap

analogy as introduced by the plastic theory are unsound theoretically when applied to plain concrete which is not a "plastic" material in its mechanical properties. A plastic state cannot be assumed in concrete (reinforced or prestressed) because, as a general case, the steel does not yield. Nonetheless from lack of a better understanding, certain theoretical aspects of plasticity have been found by some research workers useful when applied to concrete problems involving uniform stress distribution and analogy solutions. Such attempts generally lack direct verification by concrete test specimens.

Experiments with Split-Cubes

Wainwright(36) simulated the state of combined normal and tangential stresses in the "compression zone" by loading 20 split-cubes to failure, as shown in Figure (6.2.1). The specimens were 150mm cubes which had been split in half by applying a knife-edge compressive force. The loading system was designed to apply a vertical compressive force to the horizontal unsplit face and a horizontal shear force. The predetermined force was applied first and then followed by the shear until failure was reached.

The test results are shown in a graphical form in Figure (6.2.1) and tabulated in Table (6) of Appendix III. The general trend of the shear resistance of the presplit cubes was to increase as the compressive direct force increased. The rate of shear increase, however, was reduced as the direct forces were reaching higher levels. Generally the failures occurred by a slip plane mechanism in which the two halves of a cube slid over the interface and shear resistance was provided by the friction induced between the two faces. Depending on the magnitude of the predetermined clamping force the modes of failure varied. With

increasing direct force the following failure problems can be distinguished:

1. Subject to a very low compressive stress, the failure was of a plane shear-friction type which involved basically a sliding push-off motion with very little evidence of aggregate cement paste bond breakdown. The failure surface was consequently debris free.
2. Aggregate-cement paste bond breakdown with little debris.
3. Shear failure of the weaker aggregate, with larger amount of debris present in addition to signs of the bond failure.
4. Aggregate failure predominant with the appearance of tensile diagonal cracking at the lower half of the cube which also spread to the upper half at higher direct forces.

As a consistent pattern the amount of the debris appearing on the failure surface increased with increasing the "prestress" direct force. The failure surface itself was clean and relatively smooth when subject to lower direct forces but with increasing compression the surface showed more distortion and the failures took place on a rough-textured surface.

Wainwright plotted the test results for a plane of shear stress versus direct stress, and showed that the actual split cube results did not follow the Cowan's failure envelope exactly. An attempt was made by him therefore, to fit the envelope to the measured results, by re-

rearranging and shifting the intercept on the shear stress - and the direct stress - axes. Although he found improved correlation with a shear stress intercept of approximately 2 N/mm² detecting what was described as an "apparent tensile strength of concrete", Wainwright recommended in view of these difficulties and the limited number of tests, that the problems should be investigated further and preferred for his thesis the use of Cowan's criterion until a more accurate formulation could emerge in future work.

5.5 A Continuous Criterion for Concrete Failure:

In Figure (5.5.1) is shown the Mohr stress circle of unconfined compression of cylinder strength test, $f\acute{c}$. With the axial stress axis, at an angle θ a tangent is drawn to Circle C_u. The shear axis is consequently intercepted at $(0, k_1 f\acute{c})$ point. Therefore it is possible to construct a circle C_i of $(1 - k_i) f\acute{c}$ diameter, which corresponds to the confined compression cylinder strength.

Also a circle C_2 is drawn representing the failure by diagonal crushing or cracking in pure torsion or shear which takes place at a skewed axis. Thus the C_2 circle has a radius of twice the modulus of rupture fr_1.

To complete the representation a circle C_3 is needed with a radius fr. representing shear failure subjected to two opposite and equal tensile stresses. It should also be noted that circle C_1 is for a shear failure subjected to compressive-compressive stresses, and circle C_2 is for a compression-tension shear failure.

The tangent is now drawn touching the three stress state circles of shear failure. This will intercept the axial axis with an angle θ.

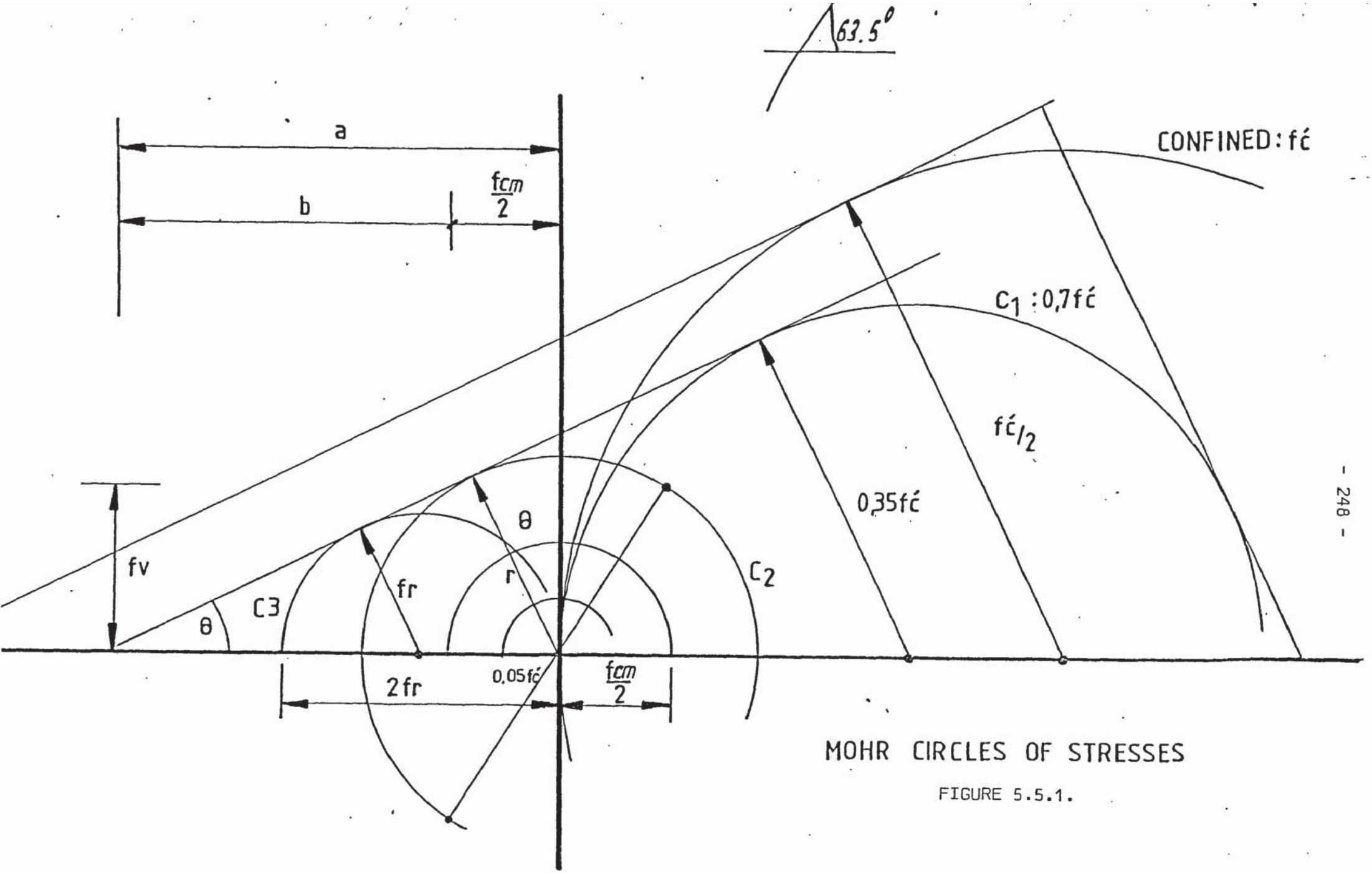

MOHR CIRCLES OF STRESSES

FIGURE 5.5.1.

From the geometry of the diagram :-

$$r = a \sin\theta \qquad (1)$$

$$\sqrt{(fvr)^2 + \left[\frac{fcm}{2}\right]^2} = r \qquad (2)$$

but :

$$a = \frac{fcm}{2} + b \qquad (3)$$

$$b = \frac{fr}{\sin\theta} \qquad (4)$$

$$a = \frac{fcm}{2} + \frac{fr}{\sin\theta} \qquad (5)$$

$$\sqrt{(fv)^2 + \left[\frac{fcm}{2}\right]^2} = a \sin\theta \qquad (6)$$

$$= fr + \left(\frac{fcm}{2}\right) \sin\theta \qquad (6a)$$

$$fv\sqrt{1 + \left(\frac{fcm}{2\ fv}\right)^2} = fr + \left(\frac{fcm}{2}\right) \sin\theta \qquad (7) \ *$$

Also from squaring both sides of equation (6a) :

$$(fv)^2 + \left(\frac{fcm}{2}\right)^2 = \left[fr + \left(\frac{fcm}{2}\right) \sin\theta\right]^2 \qquad (8)$$

or :

$$\left(\frac{fv}{fc}\right)^2 + \left(\frac{fcm}{2fc}\right)^2 = \left(\frac{fr_1}{fc}\right)^2 + 2\ \frac{fr_1}{fc}\ \frac{fcm}{2fc} \sin\theta + \left(\frac{fcm}{2fc}\right)^2 \sin^2\theta \qquad (9)$$

$$\left(\frac{fv}{fc}\right)^2 = \left(\frac{fr_1}{fc}\right)^2 + 2 \left(\frac{fr_1}{fc}\right) \frac{fcm}{2fc} \sin\theta - \left(\frac{fcm}{2fc}\right)^2 \cos^2\theta$$

if $C_o = \frac{fr}{fc}$

$$\left(\frac{fv}{C_o fc}\right)^2 = 1 + \frac{1}{C_o} \left(\frac{fcm}{fc}\right) \sin\theta - \left(\frac{fcm}{2\ C_o fc}\right)^2 \cos^2\theta \qquad (10) \ *$$

This is a general form of the criterion in terms of the interactive stresses and the failure plane angle of a skewed axis, θ.

Angle θ is evaluated as follows.

Evaluation of the angle θ :

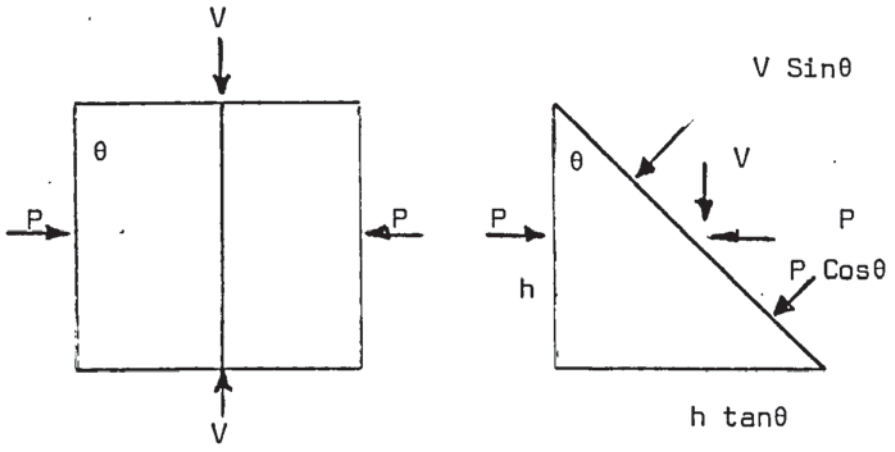

Making use of the shear-friction hypothesis - see verification later

$$\frac{\frac{V\ Sin\theta}{bh}}{Cos\theta} = C + \mu \frac{\frac{P\ Cos\theta}{bh}}{Cos\theta} \qquad (1)$$

or $\frac{V}{bh}\ Sin\theta\ Cos\theta = C + \mu \frac{P}{bh} \cdot Cos^2\theta$

V is upper bound in this equation with θ as a variable.

For min. V, $\frac{dv}{d\theta} = 0$

$$\frac{V}{bh} = \frac{C}{Sin\theta\ Cos\theta} + \mu \frac{P}{bh}\ Cot\theta \qquad \text{and} \qquad (2)$$

$$\left(\frac{dV}{d\theta}\right)\frac{1}{bh} = C\left\{\frac{1}{Cos\theta}\ (-Cosec\theta\ Cot\theta) + \frac{1}{Sin\theta}\ Sec\ \theta\ tan\ \theta\right\} - \mu \frac{P}{bh}\left(\frac{1}{Sin^2\theta}\right)$$

$$= C\left(-\frac{1}{Sin^2\theta} + \frac{1}{Cos^2\theta}\right) - \mu \frac{P}{bh}\left(\frac{1}{Sin^2\theta}\right) \qquad (3)$$

equating to zero, and after rearrangement :

$$tan^2\theta = 1 + \mu \frac{P}{bh} \qquad (4)$$

V is minimum when

$$\tan\theta = \pm\sqrt{1 + \mu \frac{pc_2}{C}} \qquad \text{where } pc_2 = P/bh \qquad (5)\ *$$

To take the positive value of (tanθ) critical for substitution in equation 1, the latter is rearranged :

$$\frac{V}{bhc} = \sqrt{1 + \tan^2\theta}\ \sqrt{1 + \frac{1}{\tan^2\theta}}\ \left[1 + \mu \frac{P}{bhC}\ \frac{1}{(1 + \tan^2\theta)}\right]$$

$$= [1 + \tan^2\theta\ ]\ \frac{1}{\tan\theta}\ \frac{(1 + \tan^2\theta) + \mu\ P/bhC}{(1 + \tan^2\theta)}$$

$$= \left[\frac{1}{\tan\theta} + \tan\theta\ \right] + \mu \frac{P}{bhC}\ \frac{1}{\tan\theta} \quad *$$

or

$$\frac{V}{bhC} = \tan\theta + \frac{1 + \mu\ p_{c_2}/C}{\tan\theta} \qquad (6)$$

$$(\tan\theta) \text{ critical} = \sqrt{1 + \mu \frac{p_{c_2}}{C}}$$

in equation (6) :

$$\frac{1 + \mu\, p_{c_2}/C}{\sqrt{1 + \mu\ p_{c_2}/C}} + \sqrt{1 + \mu\ p_{c_2}/C} = \frac{V}{bhC}$$

or :

$$\frac{\tau}{C} = 2\sqrt{1 + \mu \frac{p_{c_2}}{C}} \qquad \text{where } \tau = \frac{V}{bh} \qquad (7) \quad *$$

$$\tau = 2C\sqrt{1 + \mu \frac{p_{c_2}}{C}}$$

If $\mu = 0.75$ (See Chapter 6) and

max. $p_{c_2} = 0.20\ f'c$ } Note that only
min. $C = 0.05\ f'c$ } their ratio is involved

then in equation (5) :

$(\tan\theta)$ max. = 2.00 and thus $\theta = 63°.43$
$\cong 63.5$

also as $m_1 \times \frac{1}{m_2} = -1$

$(\tan\theta)$ min. = 0.50 $\quad \theta = 26°.5$

This latter value of $\theta = 26°.5$ is used in constructing the stress states circles.

Substituting the value $\theta = 63°.5$ in equation 10:

$$\left(\frac{f\nu}{C_o\ fc}\right)^2 = 1 + \left(\frac{fcm}{Co\ f\acute{c}}\right)(0.8949) - \left(\frac{fcm}{Co\ f\acute{c}}\right)^2 \frac{1}{4} \times 0.1991 \qquad (11a)$$

If $Co = 0.125$ and $K_i = 0.3$ i.e. $(1-k_1)fc = 0.7\ f\acute{c}$

$$f\nu = 0.125 \times 0.7\ f\acute{c}\sqrt{(1 + 10.2754\,x - 6.5012\ X^2)}$$

or

$$f\nu = 0.0878\ f\acute{c}\sqrt{(1 + 10.2754\ x - 6.5012\ X^2)} \qquad (11)$$

where $x = \frac{fcm}{f\acute{c}}$

The graphical form of this criterion equation is plotted in Figure (5.5.2.).

For a constant angle θ, $f\nu$ varies as a function of x. Differentiation of equation 11 w.r.t. x and equating to zero gives a maximum value of the shear stress:

$f\nu = 0.1975\ f\acute{c}$ at $\frac{fcm}{f\acute{c}} = 0.7903/1.6725 = 47.25\%$

Also $f\nu = 0.0132\ f\acute{c}$ when $\frac{fcm}{f\acute{c}} = 0.0900$ (tension)

and $= 0.0008\ f\acute{c}$ $= 1.6725$ (compression)

All these values can be seen on Figure (5.5.2.). It is noted in particular that a readjusted scale for the X - values directly related to $f\acute{c}$ as a unity may be desirable. Scale II on the diagram is therefore obtained by dividing $f\acute{c}$ by (1.6725). Using this figure the corrected value of the tensile intercept is $0.0554\ f\acute{c}$. This value is close to the value of $c = 0.05\ f\acute{c}$ used previously in the evaluation of angle θ.

A further adjustment of the axial axis values based on taking the full $f\acute{c}$ value as unity, is achieved by dividing by 1.7625. This figure is obtained by adding 0.09 to 1.6725 representing the total range between the tensile and compressive intercepts. The alternative of equation (11) is therefore :

$$f\nu = 0.087 f\acute{c}\sqrt{\left\{1 + 18.0265\ \frac{fm}{f\acute{c}} - 20.1954\ \left(\frac{fm}{f\acute{c}}\right)^2\right\}} \qquad (5.5.12)$$

This is plotted in Figure (5.5.3) which indicates the values of 0.05 f$\acute{c}$ and 0.94 for tensile and compressive intercepts. See Table (5.5.1) also. One interesting feature of the curve now is the approximately flat peak across the shear stress 0.1886 f$\acute{c}$ between 0.3f$\acute{c}$ to 0.6f$\acute{c}$ direct stresses. The maximum shear stress value is 0.1965f$\acute{c}$ occurring at 0.5f$\acute{c}$ direct stress and differs by only 4.2% from the average 0.1886f$\acute{c}$ shear stress value mentioned above.

TABLE 5.5.1 CRITERION VALUES OF DIRECT STRESS RATIOS X AND ASSOCIATED SHEAR STRESS fv

fv	x = fm/f$\acute{c}$	fv	x = fm/f$\acute{c}$
0.0184f$\acute{c}$	- 0.05	0.0852f$\acute{c}$	0.90
0.0878f$\acute{c}$	0.00	0.0372f$\acute{c}$	0.94
0.1196f$\acute{c}$	+ 0.05	0.00	0.95
0.1418f$\acute{c}$	0.10		
0.1714f$\acute{c}$	0.20		
0.1886f$\acute{c}$	0.30		
0.1965f$\acute{c}$	0.40		
0.1964f$\acute{c}$	0.50		
0.1882f$\acute{c}$	0.60		
0.1707f$\acute{c}$	0.70		
0.1405f$\acute{c}$	0.80		

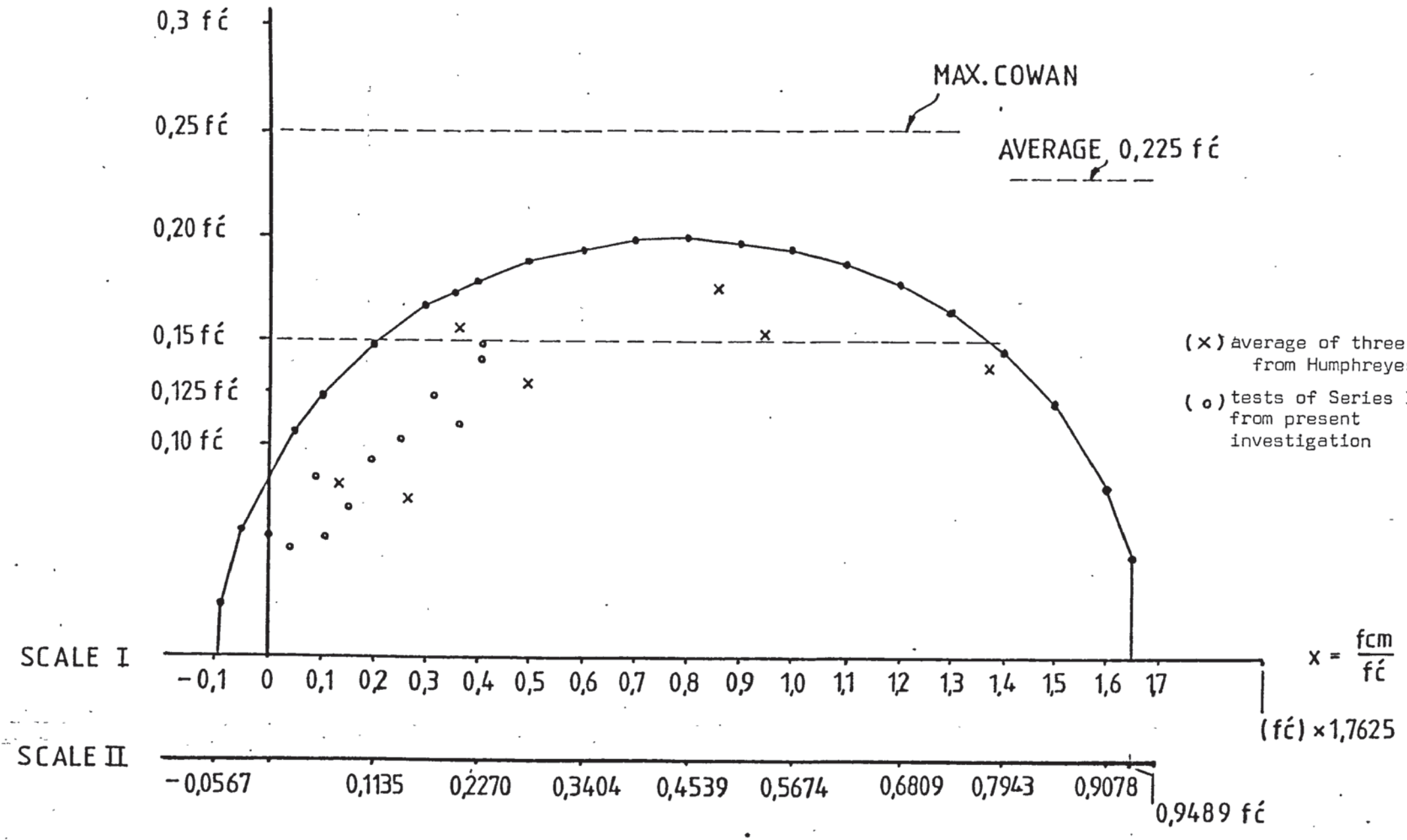

A CONTINOUS CRITION FOR CONCRETE FAILURE

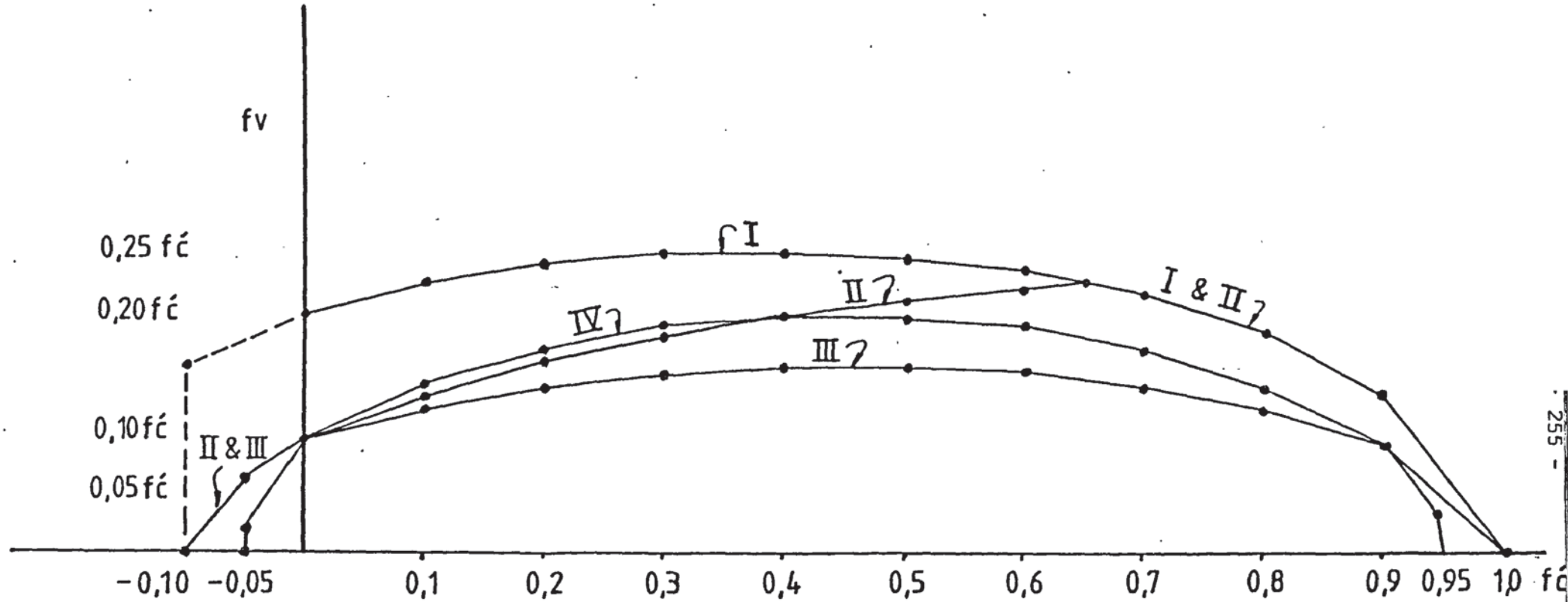

I COWAN
II ZIA
III SETH
IV EQN.5,5,12

CONCRETE CRITERIA

FIGURE 5.5.3.

A General Interaction Envelope:

In Figure (5.5.4) is presented an interaction envelope of shear stress - direct stress. It is a graphical representation of equation (12).

The procedure followed to construct this diagram is outlined as follows:

From Table 5.5.1 and Figure (5.5.3) is concluded that a parabola that fits the points on the ascending side is

$$f_v = 0.3444\, f_c' \sqrt{f_{cm}/f_c'} \qquad (a)$$

Also it is assumed that the area of the interaction diagram under the descending side is bounded by quarter of an ellipse. The total area consists therefore of a part of a parabola and a part of an ellipse. The problem is reduced to finding the maximum point of shear stress. This may be assumed to occur at a "neutral axis" of the area passing through the centroid. If the original area is that of a circular section, thus the required area is equivalent to the failure surface about a skewed axis of a distorted circle according to Martin (8) for plain concrete subjected to pure torsion.

Hence:

part of parabolaic area = 1/4 area of ellipse (b)

and for a D, diameter of a circle of f_c':

$$\tfrac{1}{2}\left[\tfrac{1}{2}\,\pi\, bc\right] \times \frac{4c}{3\pi} = \tfrac{1}{2}\left(\frac{4}{3}\, a\, b \times \frac{2}{5}\, a\right) \qquad (c)$$

$$c = 0.4721D$$

and the distance of the axis of maximum shear stress from the origin, taken at the vertical tangent point to the parabola Figure (5.5.4) is :

$$a = 0.5279D$$

or

$$a = 0.5279 f_c'$$

To complete the diagram the parabola of equation (a) above is intersected with the standard equation of an ellipse. The intersection point thus found is :

$(x, y) \equiv (0.5279, 0.2502)$

where $X = fm/f\acute{c}$ and $y = \frac{\nu c}{f\acute{c}}$

The equation of the ellipse is :

$$4.4863\, X^2 + 15.9744\, y^2 = 1 \qquad (d)$$

which added to the parabolaic part given by :

$$y = 0.3444\sqrt{X}$$

defines the boundary curve to the area of interaction of shear stresses - direct stresses.

The resulting diagram is a convenient graphical representation. The theory involved is important because it is included as the basis of the torsional theory presented in chapter 6.

The criterion of failure is also depicted on the diagram and the agreement is considered to be good. The criterion maximum shear stress level is also noticed to be lower by an $0.05\, f\acute{c}$ shear stress. The criterion equation (12) may therefore be modified simply by adding this amount of shear stress. Hence:

$$f_{r\nu} = f_t + f_\nu \qquad (a)$$

or

$$f_{r\nu} = 0.05\, f\acute{c} + 0.0878\, f\acute{c} \left\{ 1 + 18.0265 \frac{fm}{f\acute{c}} - 20.1954 \left(\frac{fm}{f\acute{c}}\right)^2 \right\}^{\frac{1}{2}} \qquad (13)$$

where $0.05 f\acute{c} = C$ the minimum stress in shear which has already been used when evaluating the angle . This term of 'C' can be regarded as a min.stress due to direct shear. According to the concept of shear-friction, which is expanded in the next chapter, it may be explained as a

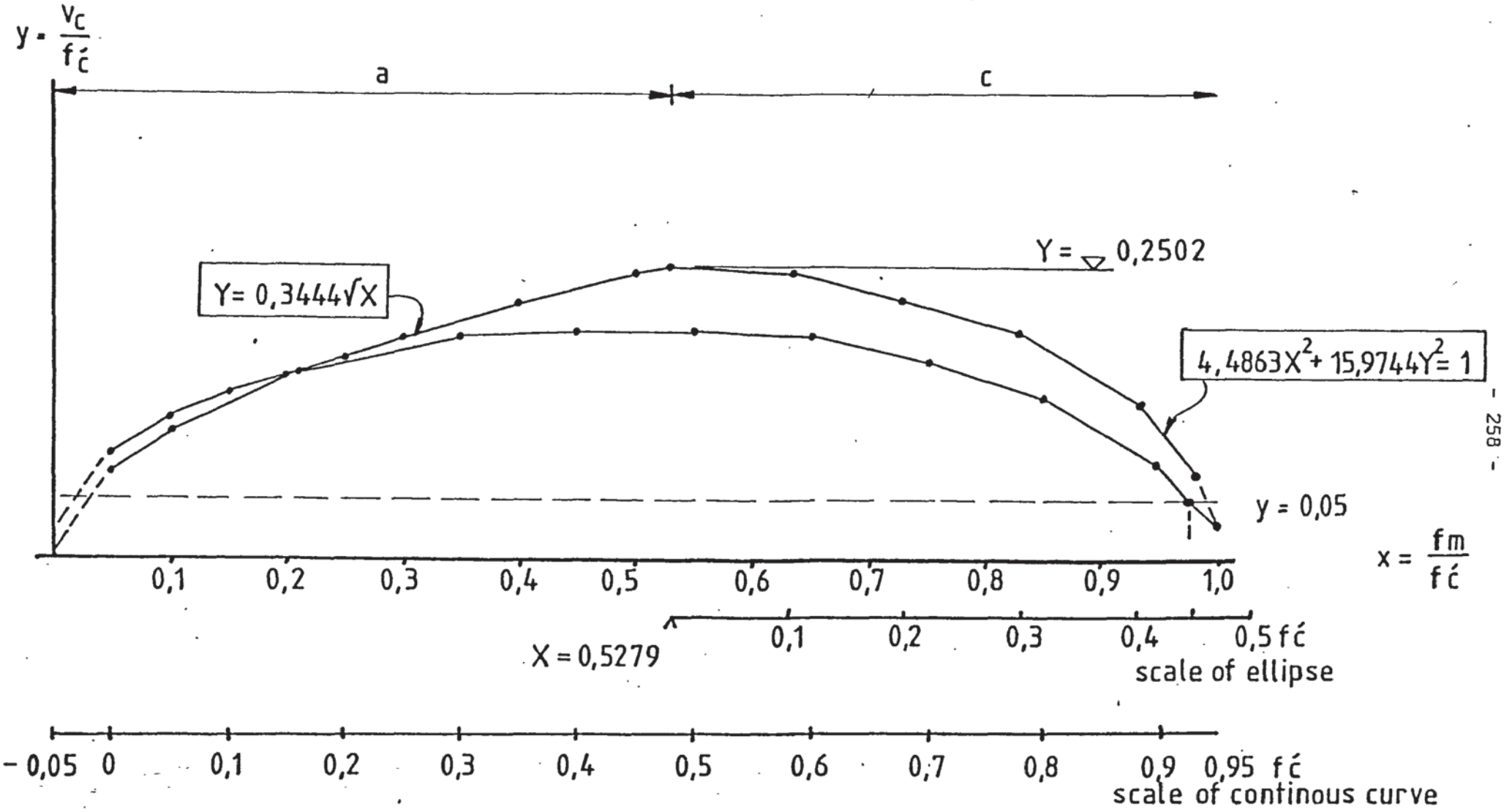

ENVELOPE FOR CONCRETE FAILURE

FIGURE 5.5.4.

min. confinement pressure necessary for concrete to mobilise its useful shear strength by friction when acted upon by external stresses.

TABLE 5.5.2 RATIOS OF TEST AVERAGE STRESS (frv)/CONTINUOUS CRITERION VALUES FOR TEST BEAMS USING EXPERIMENTAL (dn /dl)

BEAM	EQN. a f_m/f_c'	EQN. a p_{c2}/f_c'	EQN. b	EQN. c
A1	0.29	0.65	0.67	0.83
A2	0.26	0.50	0.55	0.74
A3	0.47	0.71	0.89	0.79
A4	0.28	0.43	0.56	0.75
A5	0.36	0.51	0.63	0.74
A6	0.47	0.64	0.83	0.80
A7	0.52	0.65	0.92	0.83
A8	0.62	0.73	1.09	0.83
A9	0.56	0.64	0.99	0.84
A10	0.78	0.83	1.29	0.90
A11	0.74	0.79	1.25	0.92
MEAN ± S.D. C.V.%	0.49 ± 0.17 35.0%	0.64 ± 0.12 18.0%	0.88 ± 0.25 29.0%	0.82 ± 0.06 7.0%

Eqn. a : Interactive Form,

$$frv = 0.0878 f_c' \sqrt{\left\{1 + 18.0265 \frac{fm}{f_c'} - 20.1854 \left(\frac{fm}{f_c'}\right)^2\right\}} \qquad (5.5.13)$$

Eqn. b : Non-interactive Form,

$$frv = \frac{0.05\ f_c'}{\sqrt{1 + \left(\frac{fm}{2frv}\right)^2} - \left(\frac{fm}{2frv}\right) \sin\theta} \qquad (5.5.14)$$

where $\sin\theta = \sin 63°.5 = 0.8949$

Eqn. c : Simplified Line,

$$frv = \frac{fr + (fm/2) \sin\theta}{\sqrt{1 + \left(\frac{fm}{2frv}\right)^2}} \qquad (5.5.15)$$

Equation (c) is in particular in good agreement with the test results. This equation may therefore be considered as a simplified line of criterion.

TABLE (5.6.4) DETAILED RESULTS OF COMPARISON OF TEST BEAMS WITH STEEL-YIELDING & CONCRETE CRITERIA

BEAM	CONCRETE	STEEL	CRITICAL
A1	0.45	0.34	C
A2	0.55	0.36	C
A3	0.76	0.40	C
A4	0.42	0.34	C
A5	0.52	0.36	C
A6	0.88	0.60	C
A7	0.93	0.64	C
A8	1.02	0.66	C
A9	1.08	0.73	C
A10	1.39	0.95	C
A11	1.36	0.99	C
B1	0.59	0.45	C
B2	1.03	0.73	C
B3	0.76	0.61	C
B4	0.66	0.48	C
B5	1.01	0.75	C
B6	0.76	0.52	C
C1	0.98	0.53	C
C2	0.92	0.65	C
C3	1.02	0.76	C
C4	0.77	0.70	C
D1	0.59	0.49	C
D2	0.59	0.62	S
D3	0.53	0.67	S
E1	1.23	2.02	S
E2	1.09	1.05	C
E3	1.03	0.79	C
E4	0.40	0.69	S
F0	0.86	0.45	C
F1	1.43	0.71	C
F2	0.80	0.59	C
G1	1.27	1.02	C
G2	1.27	0.79	C
G3	0.77	0.64	C
AA1	1.18	0.83	C
AA2	1.52		

TABLE (5.6.2.) DETAILED RESULTS OF COMPARISON OF TEST BEAMS WITH PROPOSED AND EXISTING CONCRETE CRITERIA

BEAM	RTC1	RTC2	RTC3	COWAN	ZIA	SETH	frv/fc'	fcm/fc'	pc2/fc
0	0.449	0.736	0.620	0.283	0.335	0.481	0.067	0.163	0.000
1	0.549	0.959	0.727	0.337	0.429	0.566	0.083	0.170	0.019
2	0.757	1.446	0.898	0.473	0.673	0.858	0.118	0.210	0.043
3	0.420	0.698	0.598	0.264	0.281	0.383	0.062	0.155	0.064
4	0.515	0.845	0.711	0.308	0.415	0.550	0.076	0.150	0.086
5	0.884	1.736	0.928	0.524	0.819	0.922	0.130	0.148	0.111
6	0.925	1.815	0.920	0.545	0.829	0.911	0.134	0.138	0.146
7	1.022	2.113	1.043	0.613	1.005	1.108	0.150	0.147	0.181
8	1.082	2.274	1.083	0.650	1.006	1.086	0.158	0.142	0.227
9	1.393	3.112	1.390	0.855	1.412	1.490	0.201	0.134	0.233
10	1.357	3.035	1.382	0.822	1.528	1.623	0.192	0.123	0.230
11	0.587	1.042	0.627	0.323	0.441	0.499	0.081	0.109	0.198
12	1.031	2.140	0.922	0.610	0.864	0.915	0.147	0.130	0.220
13	0.761	1.447	0.769	0.450	0.599	0.674	0.112	0.153	0.182
14	0.664	1.206	0.734	0.411	0.490	0.590	0.102	0.190	0.210
15	1.005	2.019	1.060	0.626	1.000	1.179	0.157	0.211	0.219
16	0.757	1.395	0.854	0.481	0.608	0.772	0.119	0.230	0.184
17	0.983	1.998	1.004	0.599	0.932	1.053	0.149	0.173	0.325
18	0.924	1.862	0.930	0.540	0.857	0.940	0.132	0.129	0.255
19	1.017	2.102	1.071	0.595	1.049	1.141	0.143	0.121	0.201
20	0.773	1.460	0.854	0.426	0.742	0.818	0.104	0.097	0.146
21	0.594	1.031	0.708	0.461	0.364	0.579	0.091	0.353	0.211
22	0.588	1.035	0.752	0.398	0.401	0.539	0.093	0.242	0.213
23	0.527	0.917	0.691	0.346	0.365	0.491	0.082	0.203	0.205
24	1.232	2.658	1.267	0.729	1.342	1.427	0.170	0.111	0.212
25	1.090	2.283	1.215	0.633	1.260	1.360	0.150	0.108	0.199
26	1.025	2.122	1.039	0.600	1.008	1.091	0.144	0.121	0.222
27	0.397	0.639	0.595	0.228	0.295	0.402	0.056	0.118	0.206
28	-0.014	-2.304	-0.397	-0.504	-1.127	-1.053	-0.002	0.126	0.213
29	0.857	1.639	0.831	0.507	0.703	0.773	0.126	0.147	0.213
30	1.426	3.195	1.391	0.872	1.545	1.633	0.203	0.128	0.193
31	0.798	1.545	0.927	0.452	0.818	0.921	0.111	0.115	0.197
32	1.266	2.767	1.269	0.768	1.393	1.495	0.182	0.133	0.194
33	1.270	2.761	1.274	0.783	1.383	1.498	0.188	0.153	0.231
34	0.774	1.485	0.833	0.449	0.683	0.775	0.112	0.135	0.234
35	1.175	2.518	1.256	0.701	1.334	1.441	0.166	0.125	0.237
36	1.534	3.467	1.655	0.942	1.997	2.125	0.218	0.131	0.249

RTC1 = frv test/Eqn. (5.5.13)
RTC2 = frv test/Eqn. (5.5.14)
RTC3 = frv test/Eqn. (5.5.15)

NOTE: Numbers 0 to 27 refer to beams A1 to E4 in the order shown in Table (5.6.1). Numbers 29 to 36 refer to beams FO to AA2 in the same order.

5.6. Analysis of Test Results and Comparison

The Continuous Failure Criterion is used to analyse the author's test beams using an elastic value for the depth of the compression zone and calculating the average stresses from the equations presented in section (5.2.2.).

For Series I beams the result of the analysis is presented in Table (5.6.2). Ratios of Test/Theory obtained from existing criteria are also included. The ratios produced by equation (5.5.12) seem to be critical in the majority of beams and close to the existing theories in the other cases.

For the tests in general, the concrete stress ratios are compared to the all steel yield ratios and presented in Table (5.6.1). It can be concluded that the values by the concrete method governs the members strength. This conclusion is substantiated by the experimental observations as reported in detail in Chapter 3. which did not indicate any case of all steel yield.

5.7. Conclusion

From the work in Chapter 5 it was confirmed, by comparing the yield steel analysis and concrete criterion, that failures of beams were governed by concrete failure. The concrete criterion, synthesised in section (5.5.) verifies this conclusion. Nonetheless the use of this new form of concrete criterion was limited, in section (5.6.), to provide a means for estimating the average shear stress. It is noted also that the straight line equation (5.5.19) shows an improvement on the predictions of equation (5.5.12). It may therefore be deduced that the test points lie higher than the straight line and generally

below the parabolic curve. From the better coefficient of variation obtained by the straight line equation, it can further be expected that the test average stress points followed a trend related to a straight line and not a parabolic variation.

Further analysis of the test results may therefore be based on a more general case where none of the steel yields and the member fails when concrete develops its useful strength.

CHAPTER 6

THEORETICAL ANALYSIS

6.1.1. INTRODUCTION

It is concluded from the previous theoretical work that the interaction equations between torsion, shear and/or bending can be expressed by one of the following methods : Skew-bending, truss analogy or the perpendicular axis approach.

The latter method is a general theoretical procedure which was used by Yudin, Evans et al and extended further by Martin and Elfgren et al. It is based on satisfying the equilibrium conditions along and about the flexural, torsional and shear transverse planes. The compatibility condition is not satisfied, but the other two methods share the difficulty of dealing with this aspect of the problem. This procedure has also been followed in Chapter 4 of this thesis. The skew bending and the truss analogy theories are based on two apparently different models. In an attempt to overcome some of the difficulties encountered by previous research workers, a mechanism of torsional shear-transfer by displacement-friction is proposed for the analysis of pure torsion and the interaction of torsion bending and shear.

This new approach is shown in this chapter to produce a form of the interaction equation which reduces to the simple cases of "pure" flexure, torsion and shear. The final result of using this approach agrees with current design methods.

In the following subsection the method is evaluated from experimental considerations. This is followed by a theoretical verification of the basis of the method and its format.

6.1.2. Hypothesis For the Evaluation of Torsional Strength

1. From the author's experiments reported and discussed in Chapter 3, it was concluded that no "all steel yield" case had occurred. Further examination of the strain gauge readings revealed that yield was never present in four legs of a gauged stirrup. Subsequently the analysis by the yield theory showed that the author's beams failed before their theoretical yield strength could be developed. Furthermore, this was confirmed by the concrete-based methods of Chapter 5, whose results when compared with the steel yield analysis were generally critical and indicated that the strength was governed by the concrete.

For the analysis of the test beams a further approach is, therefore, needed which is better related to the experimental observations particularly non-yield stress and concrete strength and cracking.

2. The experimental observation in this work showed that, in the majority of cases, visible cracks were present prior to failure. The cracks occurred initially in the soffit of the tested beams when the M/T ratio was relatively high. In all these test cases, the cracked concrete sections exhibited a sliding behaviour whereby the opposing two parts of the concrete apparently separated by the cracks slipped and/or rotated relative to each other. This slip in turn, caused the opposing parts of the concrete to separate further inducing a corresponding increase in the longitudinal steel, generally in tension. It is reasoned therefore, that as a reaction to these induced tensile stresses in the steel, equal compressive stresses, would be generated in the concrete across the crack. These compressive stresses, thus mobilised, will resist the slippage by friction along the interface of the rough, irregular and generally distorted crack surface. The

stirrups serve basically as a binder reinforcement holding the cracked concrete parts together and thus providing sufficient confinement for the concrete and the longitudinal steel to develop the shear-friction strength of the member.

3. The idea of perceiving the (shear) failure as a sliding motion is not new and the hypothesis of shear-friction has been in use since the late fifties to analyse problems of shear-transfer in reinforced concrete (Ref. Hofbeck et al 1969) and to design concrete corebels and concrete-steel connections (Ref. Mast 1968, Birkland and Birkland 1966, Witta and Basler 1966 etc.). The concept has not been explicitly used, however, to deal with the problem of torsion in plain, reinforced or prestressed concrete members.

In the present situation of prestressed concrete beams subject to combined torsion, bending and shear, the concrete cross section is subjected to direct stresses due to the prestressing force and the bending moments. It is also subjected to shear stresses due to the transverse shear force and the torsional moment. Previous investigators appreciated this complex state of stresses, and attempted, therefore, to relate the strength of the section to the concrete strength by means of a failure criterion. In an attempt to simulate the state of combined stresses in the "compression zone" of failure in mode 1, Wainwright (35) carried out (20) tests by loading split cubes as shown in Fig.(6.1.1.) These tests have been described in section (5.4.) of Chapter 5. His conclusion was that the failure did not follow Cowan's criterion exactly.

It is proposed that the specimens failed by shear-friction and

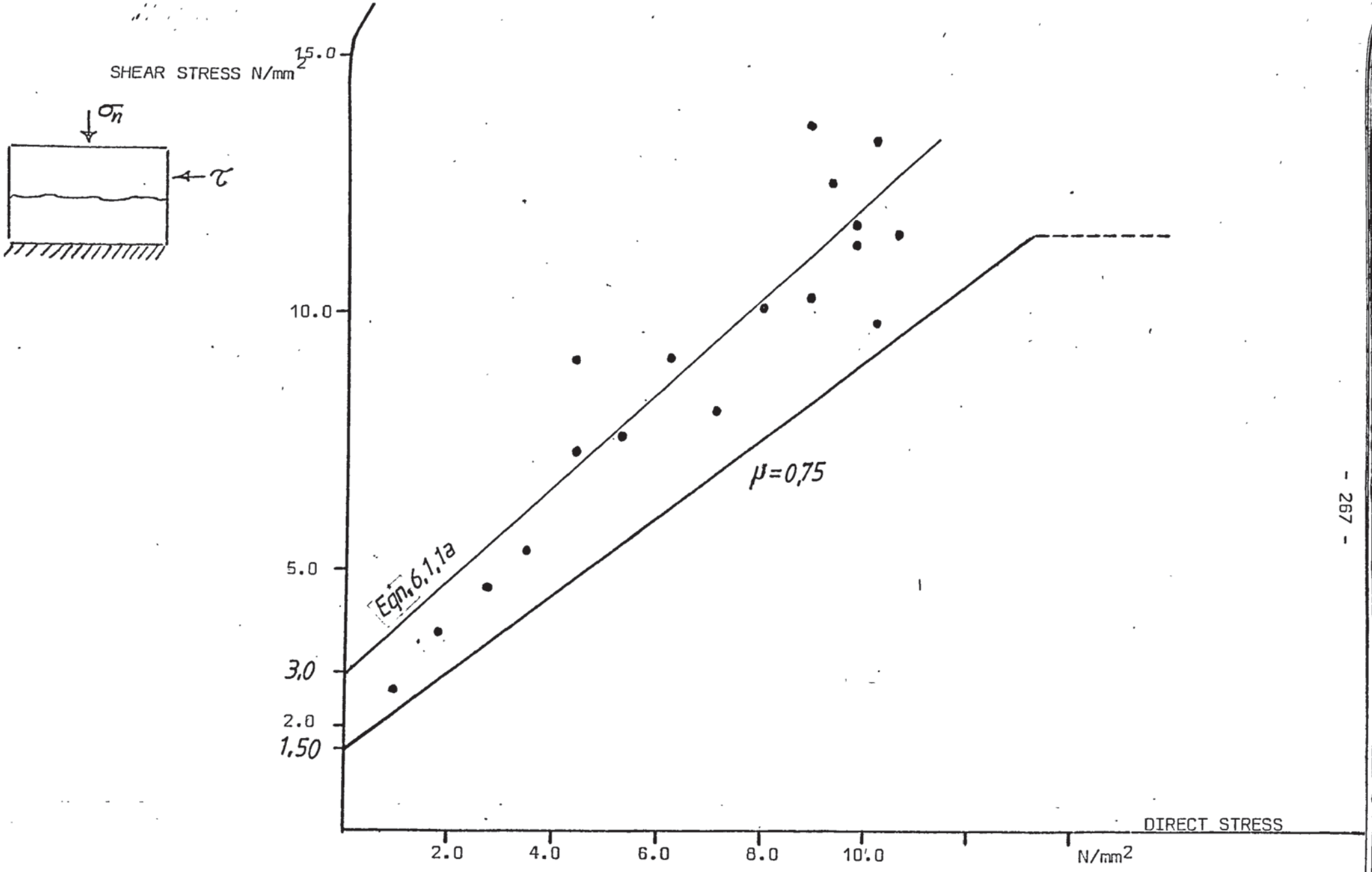

FIGURE 6.1.1. RESULTS OF SPLIT-CUBES PUSH-OFF TESTS BY WAINWRIGHT (35)

analysis may be based on this principle. This is supported by a detailed examination of the described patterns of failure of the cubes, Reference is made to section (5.4).

An alternative to Wainwright's approach, which attempted to fit the Cowan envelope to the test results, is to represent the variation of shear stress as a direct function of the normal (compressive) stress. The simplest function would be to assume a linear relationship between the direct stress and the shear stress.

A linear regression analysis of Waihwright's tests results in the straight line expressed by the following equation :

$$V = 2.99\ N/mm^2 + (0.9)\ (Ps/bh) \qquad (6.1\text{-}1)(a)$$

This line drawn on Fig.(6.1.1) gives a good correlation with the test results, with a correlation coefficient of 0.91. Wainwright's specimens did not include steel in the shear plane and the normal compressive stress is regarded as a prestress stress.

4. Other experimental results may be compared with those of Wainwright. Hofbeck et al (60) tested 49 uncracked and initially cracked push-off specimens including steel bars across the shear test plane, as shown in Fig.(6.2.1.). Mattock et al applied the shear-friction theory to these test results and proposed the following equation to estimate the strength of an initially cracked section :

$$V = 1.4\ \rho\ fy \qquad (b)$$

where $\rho = As/bd$

This assumes that the slip is sufficient to stress the steel to its yield point although no strain gauges appear to have been used

to substantiate this assumption. Mattock et al noticed from their test results that the shear resistance was a combination of cohesion and friction effects. Equation (b) is therefore based on ignoring the "cohesion effect" and consequently choosing larger value for the coefficient of friction. Mattock (64) however, suggested that :

$$v = 2.76 \text{ N/mm}^2 + 0.8 \text{ fy } (As/bd) \qquad (c)$$

was applicable within certain limits.

From the experimental work of Wainwright on plain concrete and Hofbeck et al on concrete sections including steel in the shear plane, a more general format of the shear-friction may be written as follows:

$$v = C + \mu (\rho fs + Ps/bh) \qquad (6.1\text{-}1)$$

Note: fs is not at yield.

where C and μ are determined from experiments.

For the value of (fs), the non-yield steel average stress, an empirical solution can be obtained from observed experimental behaviour and strain gauge readings.

5. Hsu (45) tested 53 beams with stirrups in pure torsion and reported details of the steel strain gauges readings. In many cases yield did not occur. From Hsu's beams results the following empirical solution for fs, the average steel stress, is proposed :

$$fs = 420 \ (1\text{-}0.4 \ b/h) \ (1\text{-}12 \ \frac{As}{bh}) \text{ N/mm}^2 \qquad (6.1.2.)$$

The line obtained by using this equation is shown in Fig.(6.1.2.) where Hsu's average experimental values for fs are plotted versus the b/h ratio.

In Fig.(6.1.3.) the experimental torsional shear stress values

are plotted versus the normal stresses for Hsu's beams of series B. The direct stress on the x-axis in the figure is experimental stress based on an average experimental stress of 238 N/mm^2 in the steel and stirrups as calculated from Hsu's strain gauge readings. A line with a slope of 0.75 and intercepting the shear axis at 1.50 N/mm^2 fits the test points. In comparison with equation (6.1-1) it can be deduced that the following numerical values for the shear intercept (c) and the coefficient of friction (μ) are :-

$$c = 1.5 \text{ N/mm}^2$$

$$\mu = 0.75$$

By examining Fig.(6.1.3), the agreement is good between the points based on fs, calculated from equation (6.1.2), and those based on the experimental reading. As for (c) and (μ) values, they are further justified by their apparent general agreement, for a lower limit, with Hofbeck et al and Wainwright's results as shown in Fig.(6.1.1)

6. The total shear resistance capacity of the section has therefore, been expressed in terms of average stresses. When the section is subjected to torsion, the external torsional shear moments are resisted by the internal shtresses in the cross section governed by an ultimate shear-friction criterion. Hence the torsional strength is expressed in the following form :

$$\boxed{\frac{ktT}{b^2h} = \bar{c} + \mu (\rho_\ell f_\ell)} \qquad (6.1-3)$$

in which

$$c = 1.5 \text{ N/mm}^2$$

$$\mu = 0.75$$

$$\rho_\ell = A_\ell / bh$$

and f_ℓ given by equation (6.1-2).

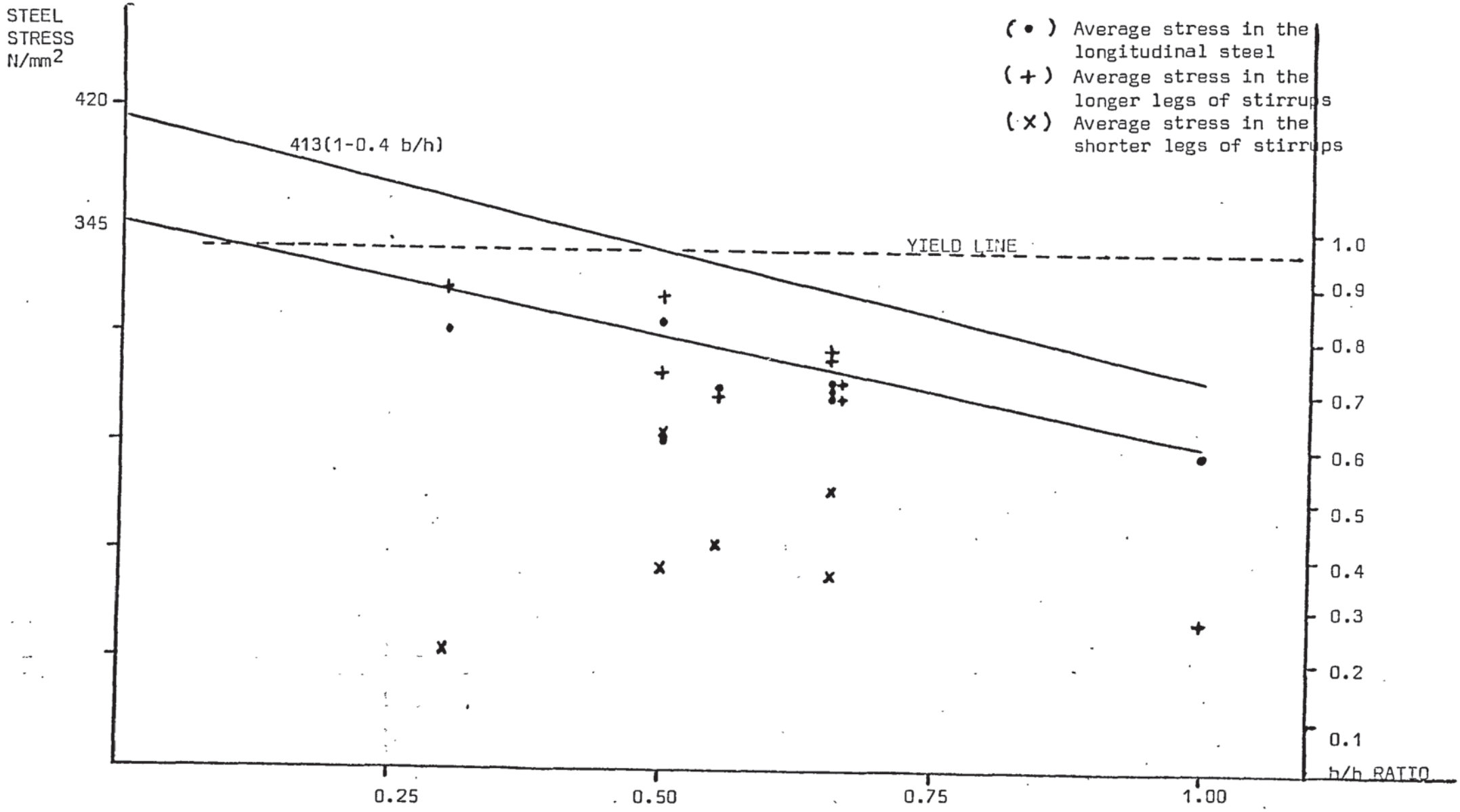

FIGURE 6.1.2. EXPERIMENTAL AVERAGE STEEL STRESS FROM HSU'S TEST BEAMS (45)

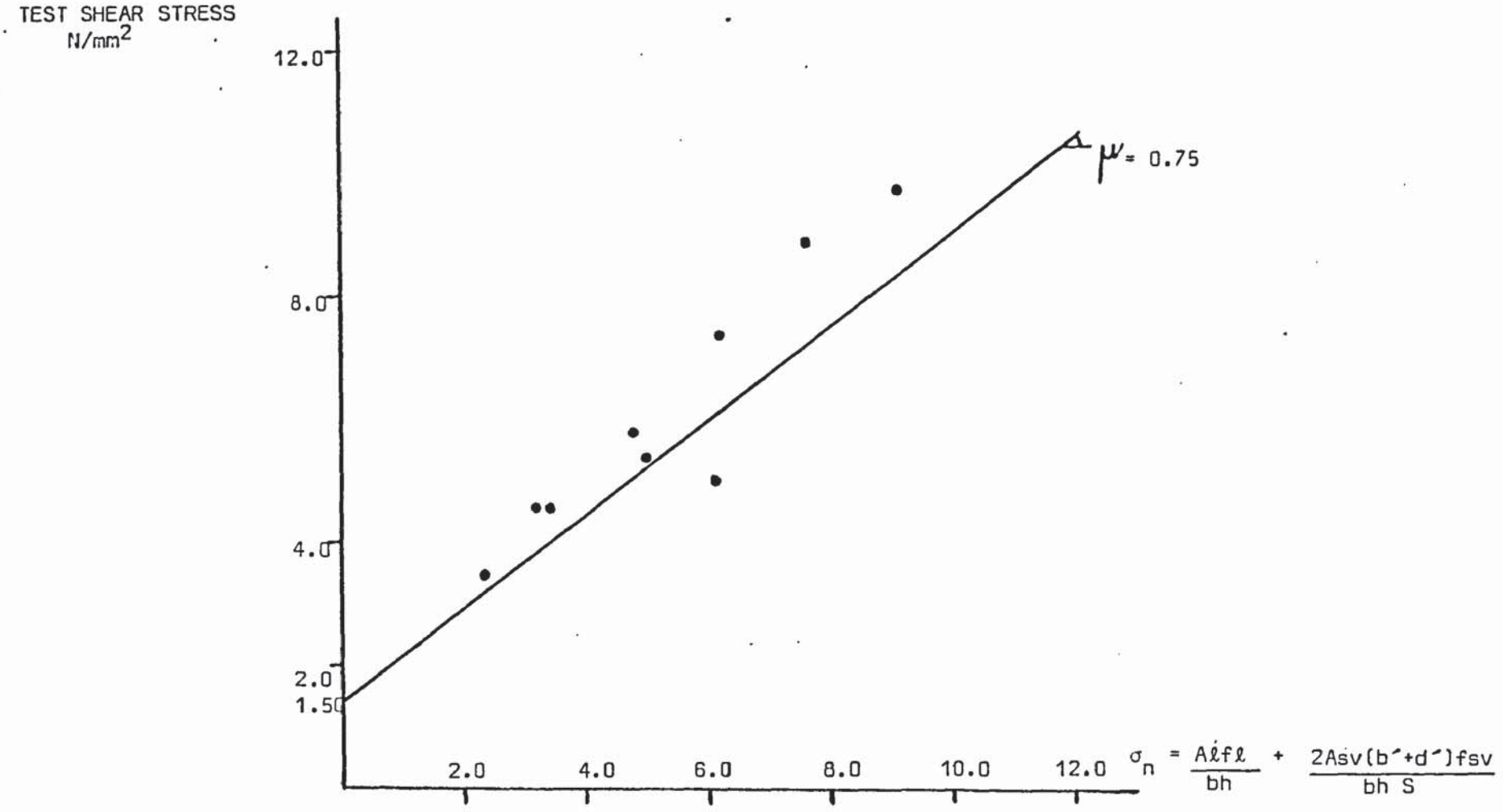

FIGURE 6.1.3. RESULTS OF TORSION TESTS BY HSU (45)

$$A\ell = \frac{A_1 + A_3}{2}$$

where A_1, A_3 longitudinal steel at bottom and top of the cross-sections.

In Fig.(6.23), taking moments about the transverse axis, in the centroid of the compression zone located at a vertical side of the beam:

$$\frac{As\ fsv}{S}(b_1-b_n)\tan\alpha\,[d'\tan\alpha + (b_1 - b_n)\tan\alpha]$$

$$= (A\ell\ f\ell\ la) \qquad (a)$$

If $b_\ell - b_n \cong b'$

$\ell a \cong b'$

$$\frac{Asfsv}{S} b'(d' + b')\tan^2\alpha = (A\ell f\ell b')$$

$$\frac{As\ fsv}{S}(d' + b')\tan^2\alpha = (A\ell\ f\ell) \qquad (b)$$

After dividing both sides by (bh), substituting of $(A\ell/bh)\ f\ell$ in equation 6.1-3 gives :

$$\frac{ktT}{b^2h} = c + \mu\frac{Asfsv\ (d' + b')}{S\ bh}\tan^2\alpha$$

$$= c + \mu\, \int wfsv\ \tan^2\alpha \qquad (6.1\text{-}4)$$

This is the equivalent strength equation governed by the stirrups. The lower torsional stress of the two given by equation (6.1-3) and (6.1-4) is to be considered critical and failure can thus be identified as due to longitudinal or stirrups strength accordingly.

A further useful form of the equation may be obtained by combining the longitudinal steel and the stirrups in a more general expression. In the presence of an external stress fle, equation (6.1-3) is modified to :

$$\frac{ktT}{b^2h} = c + \mu\,[\int\ell\ f\ell - \int\ell fle] \qquad (6.3\text{-}3a)$$

and taking moment about a transverse axis at the side of the beam:

$$M_2 = Al\ fle\ b' - \frac{Asfsvb'}{S}(d' + b')\tan^2\alpha$$

or

$$Al\ fle\ b' = M_2 - \frac{Asfsvb'}{S}(d' + b')\tan^2\alpha$$

By putting $M_2 \equiv 0$ and substituting of (Alfle b') in equation (6.1-3a). After rearrangement :

$$\frac{ktT}{b^2h} = c + \mu\int\ell f\ell + \mu\frac{Asfsv\ (d' + b')}{bhS}\tan^2\alpha$$

or

$$\frac{ktT}{b^2h} = c + \mu[\int\ell f\ell + \int w\ fsv] \qquad (6.1\text{-}5)$$

This simple format of the torsional expression reduces to the case of members with longitudinal steel only i.e. equation (6.1-3).

In the more practical case of beams containing stirrups equation (6.1-5) is substantiated by comparison with the test results and good agreement is found. From analysing Hsu's 49 beams (ref.45) a ratio of Test/Theory = 1.23 is obtained with a S.D. = $\pm$0.156 and 12.7% as a coefficient of variation. The detailed results are presented in Table (6.1.2). For further comparison the results using Hsu's equation (45) are also included. The latter produced an average of 1.018 $\pm$0.183 with a c.v. = 18%. It is important to emphasise the basic difference between the two theories because Hsu's, contrary to equation (6.1-5), is based on the asusmption that the stirrups yield. Only a few of his beams showed steel yielding, which indicates that the present method may be more realistic and close to the behaviour of the test beams.

In the following section the basic format of equation (6.1-5) is verified theoretically and is expanded to apply to problems of combined torsion, bending and shear.

TABLE (6.1.2)

Beam	Test/Theory	Hsu's Theory
B1	1.07	1.01
B2	1.12	1.05
B3	1.16	1.04
B4	1.21	1
B5	1.22	0.95
B6	1.19	0.87
B7	0.96	0.75
B8	0.83	0.46
B9	1.19	1.34
B10	1.03	1.57
M1	1.33	1.31
M2	1.45	1.36
M3	1.3	1.29
M4	1.23	1.16
M5	1.21	1.07
M6	1.18	0.98
I2	1.37	1.11
I3	1.42	1.16
I4	1.52	1.23
I5	1.54	1.14
I6	1.48	1.03
J1	1.03	1.07
J2	1.11	1.06
J3	1.09	0.98
J4	1.07	0.93
G1	1.03	0.92
G2	1.24	1.04
G3	1.26	1.04
G4	1.36	1.07
G5	1.27	0.92
G6	1.24	1.01
G7	1.29	1.04
G8	1.45	1.11
N1	1.31	1.00
N1A	1.29	0.99
N2	1.47	1.05
N2A	1.35	0.92
N3	1.41	1.03
N4	1.37	0.91
K1	1.29	0.82
K2	1.40	0.82
K3	1.28	0.73
K4	1.26	0.62

TABLE (6.1.2) Continued

Beam	Test/Theory	Hsu's Theory
C1	1.03	1.07
C2	1.05	1.02
C3	1.09	1.05
C4	1.12	1.02
C5	1.11	0.94
C6	1.11	0.84
No.of Beams	49	49
Mean	1.232	1.018
Standard deviation	$\pm$0.156	$\pm$0.183
Coeff. of variation	12.7%	17.96%

6.2.1. A Verification of the Format of Shear-Friction Hypothesis

In the loading system shown in Fig.(6.2.1i) a concrete specimen is presplit vertically by a knife-edge force, similar to Wainwright's presplit cubes descibred in Section 5.4. of Chapter 5. The specimen is subject to shear force V and a lateral compressive force P. It is asserted that provided the force P is not lower than a minimum and the force V does not exceed a maximum value then a linear relationship between V and P may be expressed by the shear-friction equation of the form :

$$\frac{V}{bh} = C + \mu \frac{P}{bh} \qquad (a)$$

In Fig.(6.2.1i) as the two faces of the confined concrete slide against one other along the preformed crack line, a-a, both faces will separate by a small horizontal displacement Δx corresponding to a vertical displacement Δy due to V. This separation creates tensile stresses which cause compressive stresses of equal amount across the crack.

Format of Equation (a) may now be verified by making use of the principle of virtual work. Taking downward movement as negative :

virtual work done by V :

$$= - V\Delta y$$

virtual work done against P :

$$= P\Delta x$$

virtual work of concrete along the action line of V :

$$= C'\Delta y$$

virtual work of conrete along the action line of P :

$$= C'\Delta x$$

where Δy, Δx are virtual displacements (not necessarily real) and C' is the force mobilized in the concrete across the cracks by the separation effecting displacements Δx and Δy.

But for equilibrium, Σ virtual work = 0

$$- V\Delta y + P\Delta x + C'\Delta y + C'\Delta x = 0 \qquad (1)$$

or

$$V\Delta y = C'\Delta y + C'\Delta x + P\Delta x \qquad (2)$$

Dividing by the area of the shear plane bh :

$$\frac{V}{bh}\ \Delta y = C_o\Delta y + C_o\Delta x + \frac{P}{bh}\Delta x \qquad (3)$$

Dividing throughout by Δy :

$$\frac{V}{bh} = C_o + \frac{\Delta x}{\Delta y}\left(C_o + \frac{P}{bh}\right) \qquad (4)$$

where :

$\frac{\Delta x}{\Delta y}$ is a factor depending on the shape of the relationship between shear force V versus force P. For a linear variation of V-P, the factor must be constant and independent of P and the shear plane area. Therefore we may put :

$$\mu = \frac{\Delta x}{\Delta y} = \text{coefficient of friction.}$$

and $$\frac{V}{bh} = C_o + \mu\left(C_o + \frac{P}{bh}\right) \qquad (5)$$

or if $C = C_o\ (1 + \mu)$:

$$\frac{V}{bh} = C + \mu\frac{P}{bh} \qquad (6)$$

as asserted in equation (a).

This has been verified experimentally as shown in Fig.(6.1.1).

It must be noted that P can be a longitudinal steel force : (As/bh) fℓ plus/or a prestress force. Therefore :

$$V = C + \mu(\rho_\ell f_\ell + Ps/bh) \qquad (7)$$

which is originally equation (6.1-1).

The specimen shown in Fig.(6.2.-1i) is basically a push-off test model which has been in use for shear tests.

In Fig.(6.2.-1ii), however, the push-off model is developed into a twist-off test model in order to verify the shear-friction format in case of pure torsion.

The format of the hypothesis of torsion-friction is verified as follows.

The specimens as similar to the one shown (6.2.-1i) but portion I is provided by a bracket near its centreline and linked to a lever arm as shown in Fig (6.2-1ii) to apply an accentrical load V_T which effects the torque T.

Provided that : $P_{min} < P < P_{max.}$ and $T > T_{max.}$, then as the two faces of the concrete in contact rotate against one other over the cracking surface, both portions I and II will separate by small horizontal displacement Δx corresponding to an angular rotation θ due to T. Consequently tensile stresses are created which are balanced by compressive stresses across the crack surface. Thus resistance is provided by friction over the crack interface.

Proceeding similarly and for equilibrium equating the sum of the virtual work to zero:

$$T.\theta = \acute{C}.\Delta x + \acute{C}.\Delta y + P.\Delta x \qquad (1)$$

where Δx is virtual displacement along the action line of P force whereas Δy is the virtual displacement along the preformed crack line.

From Fig.(6.2-2) it can be shown that $\theta = \frac{\Delta y}{(b/2)}$

$$\frac{T}{b} \times \Delta y = \Delta x \ \frac{\acute{C}}{2} + \Delta y \ \frac{\acute{C}}{2} + \frac{P}{2} \Delta x \qquad (2)$$

Divided by the twist plane area (bh) :

$$\alpha \times \frac{T}{b^2 h} \Delta y = C_o \Delta x + C_o \Delta y + \frac{P}{bh} \Delta x \qquad (3)$$

Divided by Δy and after rearrangement :

$$\alpha \frac{T}{b^2 h} = C_o + \frac{\Delta x}{\Delta y} (C_o + \frac{P}{bh}) \qquad (4)$$

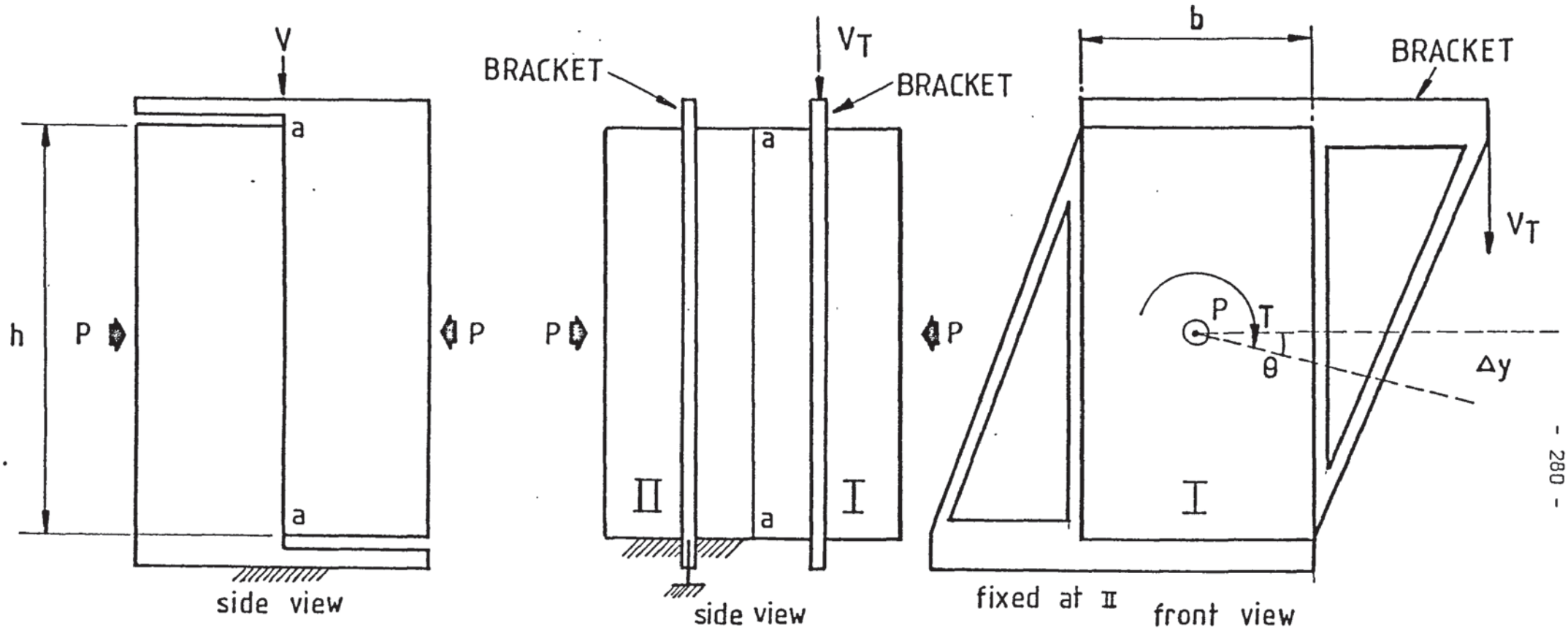

i PUSH-OFF MODEL

ii TWIST-OFF MODEL

MODELS FOR VERIFICATION OF SHEAR AND TORQUE-FRICTION HYPOTHESIS

FIGURE 6.2.1.

where :

$\frac{\Delta x}{\Delta y}$ is a factor that depends on the relationship connecting T and P For a linear relationship between T versus P this factor must be constant and independent of the twist plane area and the force P, which may be longitudinal steel force plus/or a prestress force.

Therefore if we put :

$$\mu = \frac{\Delta x}{\Delta y}$$

$$\alpha \frac{T}{b^2 h} = C + \mu \frac{P}{bh} \qquad (5)$$

where α is a nominal factor depending on the torsional stress distribution.

It must be noted that there are no available test data for the twist off model in Fig.(6.2.1ii) and therefore an experimental confirmation for the theoretical model is recommended for future research. However for the more complex problem of torsion combined with bending and shear, experimental evidence for format (5) has been produced in Series I of the author's beams which showed cracking prior to failure.

"Uncracked" Concrete Members

Since according to the virtual work method it is unnecessary that the displacements Δx, Δy take place in reality, therefore an identical procedure may be followed to verify the hypothesis in case of initially uncracked sections. The torque-friction concept can be applied by assuming that a crack surface exists which is "locked up" by the action of an "internal prestress" direct force sufficiently large to make the member behave as uncracked.

6.2.2. Basic Parameters of the Pure Torsional Equation

Torsion results from the action of an eccentrically applied load

acting normal to the longitudinal axis of a member. A concrete member resists torque by mobilising, at a given cross section, a shear flow. Subject to external torsion a twist-off action takes place and the two sides of a crack surface separate inducing direct tensile stresses.which are equalized by compressive stresses across the surface. Friction is generated as a result between the two faces of the crack and resistance to further torsion is provided by friction. With increasing torsion frictional resistance increases at a constant rate, i.e. coefficient of friction, and failure is reached when certain limits are exceeded.

An attempt is made in this subsection to consider some of the basic parameters involved and relevant values or expressions are proposed.

1. Considering a presplit concrete cylinder beam, an axially external force P is applied at the ends. It is assumed that the "prestressing" force P is large sufficiently for the cracking surface to be "locked up" and for the member to develop a strength equal to that of an uncracked member. The member can therefore be assumed to behave like uncracked member also. As the stress distribution is uncertain, uniform average stresses are assumed.

The cross section is uniformly loaded by force P which resists the applied torsional moment T. As resistance is due to a circulating shear flow arisen by friction, hence for an average shear stress τ_n tangential to the cross-sectional surface area :

$$\tau_n = \mu \frac{P}{\pi r^2} = \mu \sigma_n \qquad (a)$$

where : μ is the coefficient of friction. Taking an elemental area dA, at a varying distance r along the radius of the circular cross section, and a thickness dr

$$dA = r \cdot 2\pi . dr$$

by taking moment of dA about the central axis :

$$T = \int_0^{D/2} 2\Pi r.\ r.\ (\mu\sigma_n)\ dr \qquad (b)$$

or

$$T = \frac{1}{3} 2\Pi r^3 \mu\sigma_n + T_o \qquad (6.2.1)$$

in which T_o is a constant. Alternatively in a definite integrand form :

$$T = 2\Pi \left[\frac{r^3}{3} \right]_o^{D/2} \mu\sigma_n \qquad (c)$$

and $$T = \mu \left(\frac{\pi D^3}{12}\right) \sigma_n \qquad (6.2.2)$$

or

$$T = \left(\frac{\pi D^3}{12}\right) \text{(tangential shear stress)} \qquad (2a)$$

2. To achieve a solution from equation (6.2.2.) which contains the unknowns μ and σ_n, the deformation conditions of the failure surface must be considered. Visual evidence from experiments on circular <u>initially uncracked</u> sections reveals that the actual failure surface is complicated by the differing variation of the stresses along the axis of rotation. If such a distorted surface is considered for analysis a skew-bending approach may be used. A more complicated distorted surface, however, can be replaced by a projected surface area which is characterised by an elliptical-parabolic shape as shown in Fig.(6.2.2.). This theoretical equivalent shape was produced by Martin (8), who found the properties of the uncracked section :

the sectional modulus Z_2 (bottom) = (0.0813) $(D^3/\text{Cos}\ \theta'_2)$

by applying the skew-bending theory :

$$Tu'_2\ \text{Sin}\ \theta'_2 = Z_2\ fr_2$$

and

$$Tu'_2 = (0.0813)\ (D^3/\text{Sin}\ \theta'_2 \text{Cos}\ \theta'_2)\ fr_2$$

this is minimum when $\tan\theta'_2 = 1$

$$T = (0.83)\ \left(\frac{\pi D^3}{16}\right) fr_2 \qquad (6.2.3.)$$

3. Equating equations (6.2.2) and (6.2.3) assuming that the strength considered is due to friction resistance proportional to σ_n :

$$\mu \sigma_n \frac{1}{12} = (0.83)\, fr_2 \frac{1}{16} \qquad (a)$$

This states that the ultimate strength (or cracking strength) of plain concrete member is governed by the limiting average axial stress σ_n which is constant, and normal to the cross-section is of zero change. For this critical section, where both equations (6.2.2) and (6.2.3) are simultaneously satisfied, from (a) :

$$\mu = 0.75 \quad \text{if } \sigma_n = (0.83)\, fr_2$$
$$\mu = 0.623 \quad \text{if } \sigma_n = fr_2 \qquad (6.2.4)$$

4. Considering the shearing stress in the integral :

$$\int_A dV = \int (\mu \sigma_n)\, dA$$

is independent of the cross section shape, the solution for μ can be extended to rectangular sections. Therefore for a rectangular section of width (b) and overall depth (h) :

$$bh = (\pi D_o^2)/4 \qquad (6.2.5)$$

in which D_o is the theoretical equivalent diameter for the rectangle. In equation (6.2.1) :

$$T = \frac{1}{3} \mu \sigma_n (bh) \left(1.128 \sqrt{bh}\right) + T_o \qquad (6.2.6)$$

dividing both sides by $b^2 h$:

$$\frac{T}{b^2 h} = \frac{1}{3} \mu \sigma_n \left(1.128 \sqrt{\frac{h}{b}}\right) + \frac{T_o}{b^2 h}$$

if $3\sqrt{b/h} = \alpha$

$$\frac{\alpha T}{b^2 h} = \mu \sigma_n (1.128) + \tau_o \qquad (6.2.7)$$

In this equation if $\mu = 0.75$, $\tau_o = 0$ and $\alpha = 3$:

$$\frac{3T}{b^2 h} = (0.846)\, \sigma_n \qquad (6.2.8)$$

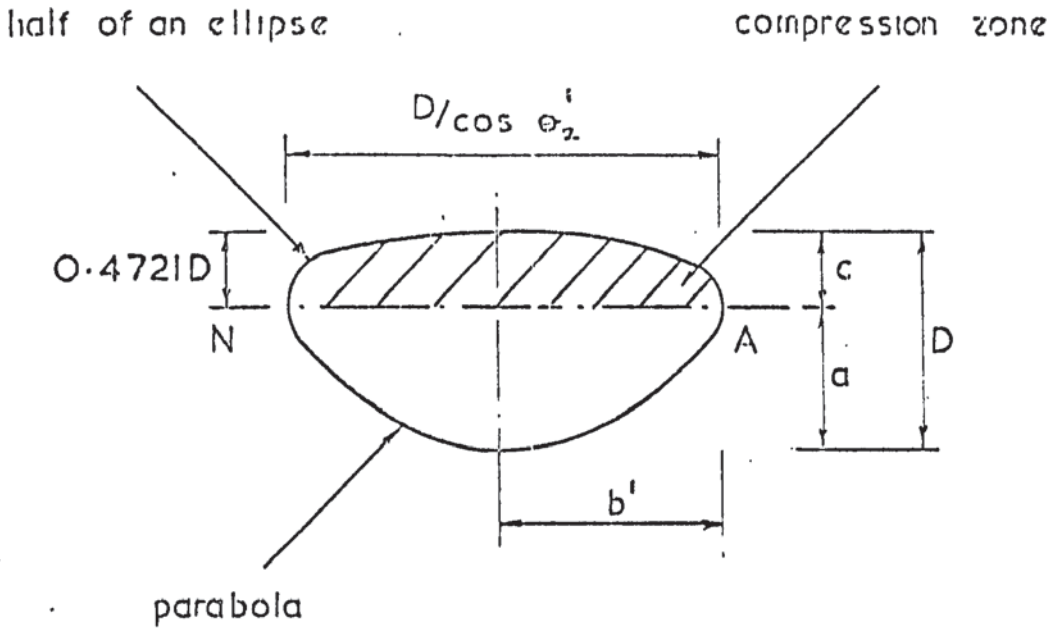

FIGURE 6.2.2. Theoretical Equivalent Shape of Distorted Failure Surface for Plain Concrete - Circular sections (Ref.8)

in which the numerical coefficient is approximately 0.85 introduced by Hsu (45) to account for the reduced strength of concrete in torsion. It should be noted, however, that in this equation : σ_n is related to fr_2, the modulus of rupture, by a factor of 0.83. The torsion-friction equation is apparently more conservative than Hsu's because τ_o is assumed to be zero.

From an analysis of a rectangular beam, using an idealized failure surface of a rectangular plane at a skewed axis of an angle θ with the vertical, it can be shown (8) that the capacity of the section is :

$$\frac{kt\,T}{b^2 h} = fr_2 \quad \text{for } \theta = 45^\circ \text{ and } kt = 3 \qquad (6.2.9)(a)$$

analysing a more realistic distorted failure surface, however, produced (8) :

$$\frac{kt\,T}{b^2 h} = fr_2 \quad \text{for } \theta' \quad \text{and } kt = 3 + \sqrt{\frac{b}{h}} \qquad (b)$$

where angle θ' was evaluated numerically for a minimum T on a distorted failure surface. The format : $3 + \sqrt{\frac{b}{h}}$ was intended as a theoretical basis for Hsu's reduction factor 0.85 by attributing the reduction to distortion.

Therefore for the same strength T, by equating the effects of distortion and twist-friction, equations (7) and (9) must be equivalent:-

$$\frac{3}{\mu}\sqrt{\frac{b}{h}} = 3 + \sqrt{\frac{b}{h}} \qquad (6.2.10)$$

simultaneously from equation (6.2.9)(a) :

$$fr_2 = 0.75 \times 0.83\, fr_2 \times 1.128 + \tau_o \qquad (a)$$

$$\tau_o = fr_2\,[1-0.702]$$

$$= 0.298\, fr_2 \qquad \text{for } \mu = 0.75 \qquad (6.2.11)(a)$$

More generally :

$$\tau_o = fr_2\,[1-0.936\mu] \qquad (6.2.11)$$

provided that $\mu = \mu_o$ and

$$\frac{1}{\mu_o} = \sqrt{\frac{h}{b}} + \frac{1}{3} \qquad (6.2.12)$$

This follows directly from the equality of geometrical distortion and friction effect as has been put forward in equation (6.2.10) and is the basis of equation (6.2.11)a.

Equation (6.2.12) substituted in equation (6.2.11) :

$$\tau_o = f r_2 \left[1 - \frac{0.936}{\sqrt{\frac{h}{b}} + \frac{1}{3}}\right] \qquad (6.2.13)$$

$$\mu = 0.75$$

$$kt = \frac{3}{\mu_o}\sqrt{\frac{b}{h}} = 3 + \sqrt{\frac{b}{h}}$$

Alternatively if it is preferred to hold μ_o constant for a given aspect ratio h/b, this may be discussed further where various forms of the torsional coefficient k_t are considered.

The theory may now be presented in the following form :

$$T = \frac{1}{kt}\,\mu\,[1.128\,\sigma_n]\,(b^2 h) + T_o \qquad (6.2.14)$$

or

$$\tau = \mu[1.128\,\sigma_n] + \tau_o$$

and

$$T = \frac{1}{kt}\,b^2 h\,(\tau) \qquad (6.2.15)$$

where all the parameters are as defined above.

5. The Torsion-Friction Equation may be derived for a concrete member subject to pure torsion with two forms of steel content : longitudinal bars and stirrups.

First, equation (6.2.14) is considered to be developed further to include the longitudinal steel. Taking a plane perpendicular to the axis of the beam and summing forces axially :

$$A1\,f\ell + bh\,\sigma_n = 0 \qquad (6.2.16)$$

this satisfies the condition that the sum of the normal stresses perpendicular to the plane of twist must be zero.

$$bh\ \sigma_n = A1\ f\ell$$

as σ_n is assumed compressive then $f\ell$ is tensile (stresses induced by separation due to twist-off effect) and :

$$\sigma_n = \frac{A1\ f\ell}{bh}$$

but from equation (6.2.4)

$$\sigma_n = 0.83\ fr_1$$

$$\overline{f\ell} = \frac{0.83\ fr_1}{\rho\ell} \qquad \text{where } \rho\ell = A1/bh \qquad (6.2.17)$$

note: all (A1) must be used in this equation for the average steel stress.

Hence equation (6.2.14) is rewritten as follows:

$$\tau = \tau_o + \mu\rho\ell \cdot f\ell \qquad (6.2.18)$$

The stirrup steel does not appear in this equation, but its action is regarded as transverse binder steel. The stirrups legs, however, can be treated as normal shear-friction steel, and will then contribute in this way to the ultimate torsional resistance. The member is cut by a horizontal plane section perpendicular to the previous plane used to expose the longitudinal steel stresses, and parallel to the plane containing the longitudinal steel. A unit length is taken along the beam axis :

$$\tau_H = C_H\ N/mm^2 + \mu\ \sigma_H \qquad (a)$$

and

$$bXSX\ \sigma_H = As\ fsv \qquad ; \quad As = \text{two legs}$$

$$\sigma H = \frac{As\ fsv}{bS}$$

into equation (a) :

$$\tau_H = C_H + \mu\ \frac{As\ fsv}{bS} \qquad (A)$$

for vertical legs of stirrups.

Similarly a third, vertical plan section is taken passing parallel to the plane of bending and normal to the plane of torsion. This will intercept the horizontal legs of a closed stirrup and be normal to them.

From this shear-friction plane the following two equations follow :

$$\tau_v = C_v \text{ N/mm}^2 + \mu\sigma_v \qquad (b)$$

and

$$bXSX\sigma_v = As\ fsh$$

$$\sigma_v = \frac{As\ fsh}{hS}$$

into equation (b):

$$\tau_v = C_v + \mu \frac{As\ fsh}{hS} \qquad (B)$$

for horizontal legs of stirrups.

In Fig.(6.2-) adding the shear flow stresses due to stirrups friction from equations (A,B) :

$$\tau_s = C_s \text{ n/mm}^2 + \mu \frac{As\ fsh}{hS} + \mu \frac{As\ fsv}{bS}$$

or

$$\frac{Kt\ Ts}{b^2 h} = C + \mu\left(\frac{As\ fsh\ b + As\ fsv\ h}{bhS} \right) \qquad (c)$$

Noting that torsional resistance, according to the basic concept underlying the present analysis, is composed of a tangential shear component in the plane of twist and a component of direct shear stress due to longitudinal displacement normal to the cross-section. Hence, for the plane of twist normal to the longitudinal steel, by summing the shear flow due to stirrups friction and longitudinal steel as shown in Fig.(6.2.), equation (6.2.18) is expanded into the form :

$$\tau = \tau_o \text{ N/mm}^2 + \mu \frac{A1 f\ell}{bh} + \mu \frac{As\ fsh}{hS} + \mu \frac{As\ fsv}{bS} \qquad (C)$$

By gathering terms :

$$\frac{KtT}{b^2 h} = C + \mu \Sigma \rho\ell f\ell + \mu \frac{As}{bhS} (fshb + fsvh) \qquad (6.2.19)$$

Also by taking : $\frac{d'}{h} = \frac{b'}{b} = 0.8$

hence (1/0.8) (fsv + fsh)/2 = fsv as an average stress in the horizontal and vertical legs, equation (19) may be simplified to give :

$$\tau = C + \mu(\rho\ell f\ell + \rho w\ fsv) \qquad (6.2.20)$$

note: ρw contains two legs of a closed stirrup.

This is the equation previously constructed from experimental consideration. They only differ in that $\tan^2\alpha$, from equation (6.1-5) is replaced now by a numerical value =2. Nonetheless, the basic difference is that equation (6.1-5) contained steel stresses determined by the empirical equation (6.1-2) whilst equation (6.2.20) is based on theoretical average stresses in the steel which are varying and their evaluation will be considered next.

Further Considerations

In the format of equation (6.2.20) the average stresses f_ℓ, fsh and fsv, in the longitudinal, horizontal and vertical legs of the stirrups respectively are involved. A method to determine these stresses follows.

1. Contribution of the Horizontal Legs of Stirrups

For the determination of the average stress in the horizontal legs of stirrups, fsh, the deformation conditions of failure on a distorted surface are considered. The distorted failure surface can be projected in one skewed rectangular plane with an axis inclined by an angle θ to the transverse axis of the beam. Only a summary of the method of solution is given here whilst a full derivation is included in an appendix to this Chapter.

By resolving torque and steel forces on the idealized failure surface the following equation is obtained :

$$\frac{ktT}{h^2 b} = \frac{C}{\sin\theta \cos\theta} + \mu(\rho_\ell f_\ell) \cot\theta + \mu(\rho_{sh} f_{sh}) \tan\theta \qquad (6.2.21)$$

where $\rho_{sh} = \frac{A_{sv} b'}{bhS}$

By differentiating equation (6.2.21) w.r.t.θ and setting $dT/d\theta = 0$, the failure surface can be defined in terms of $\tan\theta$:

$$\tan\theta = \sqrt{\frac{C + \mu\alpha}{C + \mu\beta_H}} \qquad (6.2.22)$$

in which $\alpha = \rho_\ell f_\ell$

$\beta_H = \rho_{sh} f_{sh}$

From equation (6.2.17) a value for f_1 may be obtained. This equation is re-presented as follows:

$$f_\ell = \left(\frac{1}{\rho_\ell}\right)(0.72)\left(1 + \frac{6\ 450}{b^2}\right)(f_c')^{1/3} \quad \text{for } b > 100\text{mm}$$

by applying Hsu's empirical formula for fr_2. (6.2.17) A

When neither category of steel yields and stress redistribution occurs the critical angle of failure θ is controlled by the cracking angle of concrete. The stresses in the steel are induced by the separation of the two faces of the cracking surface generating interface friction over this surface which, for a minimum torque capacity, is the failure surface. Therefore the critical angle of failure θ, from equation 6.2.22, may be controlled by the concrete failure angle of the shear-friction, equation 5.4.7 :

$$\tan\theta = \sqrt{1 + \mu\frac{\sigma_n}{C_o}} \qquad (6.2.23)$$

this, for consistent values of variables, gives

$$\tan\theta = 1.5$$

Into equation (6.2.22) and after rearrangement :

$$f_{sh} = (0.444\ f_\ell)(\rho_\ell/\rho_{sh}) - (0.555C)(1/\rho_{sh})(1/\mu) \qquad (6.2.24)$$

which is the average stress in the stirrups horizontal legs. For very low longitudinal steel content the horizontal legs may be compressive. Also as can be deduced from this equation, a similar effect may be expected in very deep cross sections where higher values for (C) is predicted as will be seen later.

2. Contribution of Vertical Legs of Stirrups

Proceeding similarly, in this case the distorted surface of failure is projected in one rectangular plane skewed with an angle θ to the

vertical. The following equations are produced :

$$\frac{ktT}{h^2 b} = \frac{C}{Sin\theta Cos\theta} + \mu(\int \ell f\ell)\ Cot\theta + \mu(\int sv\ fsv)\ \tan\theta \qquad (6.2.25)$$

$$\tan\theta = \sqrt{\frac{C + \mu\alpha}{C + \mu\beta v}} \qquad (6.2.26)$$

where $\beta_v = \int sv fsv$ and $\int sv = \frac{Asv d'}{bhS}$

Substituting $\tan\theta = 1.5$ from equation (6.2.23)

$$fsv = (0.444\ f\ell)(\int \ell / \int sv) - (0.555C)(1/\int sv)(1/\mu) \qquad (6.2.27)$$

In case of pure torsion, therefore, equations (27) and (24) are analogous with (d') replacing (b') respectively.

A Value for Term : C

If C is known in the above equations then equation (6.2.20) will contain no unknown and can be readily solved.

By inspecting equations (6.2.24,27) and recalling the shear-flow rule used in evaluating equation (20), it is possible to conclude that in the twist plane :

$$\tau_o = \frac{C}{Sin\theta Cos\theta} \qquad (a)$$

putting $\theta = 56.3°$ and

τ_o from equation (6.2.13) :

$$C = \frac{fr}{2.166}\left[1 - \frac{0.936}{\sqrt{\frac{h}{b} + \frac{1}{3}}}\right] \qquad (6.2.28)$$

for a square section : C = 0.138 fr.

3. Critical Steel Content

The critical total steel percentage is defined by the total steel present when failure occurs as simulatneously the concrete attains its shear strength and the steel reaches its average friction stresses. (These

stresses are expressed in equations 6.2.17A, 24 and 27).

- Critical concrete shear strength is given by :

$$V = 2\, C_o \tan\theta$$

$$C_o = 0.05\, fc' \qquad \text{Equation(5.4.7)}$$

$$\theta = 56^{o}.3$$

- Ultimat torsional load is given by :

$$\frac{ktT}{b^2h} = \tau_o + \mu(\rho_\ell f_\ell + \rho_w f_{sv}) \qquad \text{Equation(6.2.20)}$$

- Therefore for (T) governed by shear failure :

$$\frac{ktT}{b^2h} = 0.15\, fc'$$

- Hence :

$$\tau_o + \mu\frac{A_l}{bh} \cdot f_\ell + \mu\frac{A_{sv}\,(b' + d')}{bhS}\, f_{sv}\,(2) = 0.15\, fc' \qquad (a)$$

- Now to obtain an approximate expression a unified average stress is assumed in all the steel vzt, (fs) :

$$f_\ell = f_{sv} = f_s$$

furthermore fs may be determined from the empirical Formula (6.2.2).

After rearrangement and dividing by μf_s :

$$\frac{A_l}{bh} + \frac{A_{sv}(b' + d')}{bhS}\,(2) = \frac{0.15\, fc' - \tau_o}{\mu f_s}$$

where τ_o from equation (6.2.13) (6.2.29)

Also :

$$\rho_w\,(m + 2) = \frac{0.15\, fc' - \tau_o}{\mu f_s}$$

$$\text{critical } \rho_w = \frac{0.15\, fc' - \tau_o}{\mu(m + 2)\, f_s} \qquad (6.2.30)$$

one leg of stirrups

$$\text{critical } \rho_\ell = \frac{0.15\, fc' - \tau_o}{\mu(1 + 2/m) f_s} \qquad (6.2.31)$$

half longitudinal bars

if $\rho_t = (\rho_\ell + \rho_w)2$

$$\text{critical } \rho_t = \frac{2(1 + m)(0.15 fc' - \tau_o)}{\mu(2 + m)\, f_s} \qquad (6.2.32)$$

or may be approximated to :

$$\int t \cong \frac{2\,(1 + m)}{\mu\,(2 + m)}\,\frac{fr}{fs} \qquad \text{(b)}$$

where $fr \cong 0.1fc'$; $\tau_o \cong 0.05fc'$

6.2.3. Interaction of Torsion and Shear

The total torsion resistance capacity of the section has, therefore, been expressed in terms of average stresses. In the case when the section is subjected to an independent shear force also, the external shear forces and moments must be resisted by the internal stresses in the cross section governed by an ultimate torsional shear-friction criterion.

A concrete member which is initially cracked on the front face where the shear stresses due to flexural shear and torsion are additive fails by skew-bending (ref.39) on a failure surface as shown in Fig. (6.2.3). It is assumed that the critical torsional-friction shear stress τ_u occurs at a rectangular plane inclined with an angle θ_2 to the vertical.

Taking moments about the centroid of the section :

$$T_2 \operatorname{Sin}\theta_2 = \frac{hb^2}{6\operatorname{Cos}\theta_2}\left[\tau_u - \frac{V_2 \operatorname{Sin}\theta_2 \operatorname{Cos}\theta_2}{bh}\right] \qquad \text{(a)}$$

$$T_2 + \frac{V_2 b}{6} = \frac{hb^2}{6}\left[\frac{\tau_u}{\operatorname{Sin}\theta_2 \operatorname{Cos}\theta_2}\right] \qquad \text{(b)}$$

For a constant force V_2, differentiating T_2 w.r.t. θ_2 :

$$\frac{6}{bh^2}\,\frac{dT_2}{d\theta_2} = \tau_u\,(\operatorname{Sec}\theta_2(-\operatorname{Cosec}\theta_2 \operatorname{Cot}\theta_2) + \operatorname{Cosec}\theta_2 \operatorname{Sec}\theta_2 \tan\theta_2)$$

T_2 minimum when $dT_2/d\theta_2 = 0$:

after rearrangement

$$\tan^2\theta_2 = 1$$

or $$\tan\theta_2 = \pm 1 \quad \text{and} \quad \theta_2 = 45^o$$

Into the equation (b) :

$$T_2 + \frac{V_2 b}{6} = \frac{hb^2}{3} (\tau_u) \qquad (c)$$

and

$$\frac{3T_2}{hb^2} + \frac{V_2}{2bh} = \tau_u$$

if $V_2 = 0$ $\quad Tu_2 = \frac{hb^2}{3} (\tau_u)$

$T_2 = 0$ $\quad Vu_2 = 2bh (\tau_u)$

Following Cooper and Martin (38) the constant 3 in equation (c) may be modified to incorporate the effect of distortion on the idealized rectangular skew plane. Equation (c) becomes after rearrangement:

$$\frac{T_2}{b^2 h} + \frac{V_2}{6bh} = \frac{1}{3 + \sqrt{\frac{b}{h}} + 0.35 \sqrt{\frac{b}{h}} \sqrt{\frac{Pc_2}{fr_2}}} (\tau_u) \qquad (d)$$

this may be simplified by taking $kt = 3 + \sqrt{\frac{b}{h}}$:

$$\frac{ktT_2}{b^2 h} + \frac{V_2}{bh} \frac{Kt}{6} = \tau_u \qquad (e)$$

However if we consider the sum of the shear flow due to resist the shear force and the torsional moment and substituting for τ_u from equation (6.2.20) the following form is obtained :

$$\frac{ktT}{b^2 h} + \frac{V}{bh} = \tau_o + \mu (\int \ell f \ell + \int w \, fsv) \qquad (6.2.33)$$

in which $\int w = 0$ for members reinforced with longitudinal steel only.

In this equation $\tau_v = (V/bh)$ is an average shear stress with the (torsion/flexure shear) constant in equation (e) is taken as unity.

Modification for Prestressed Concrete

Simply the effect of prestress may be incorporated in the internal stress criterion of torsion-friction τ_u: By resolving the component of τ_u on an axis inclined at an angle θ_2 to the vertical :

$$\tau_u = \tau_o + \mu (2 \int \ell \, f \ell \cos^2 \theta_2 + pc_2 \cos^2 \theta)$$

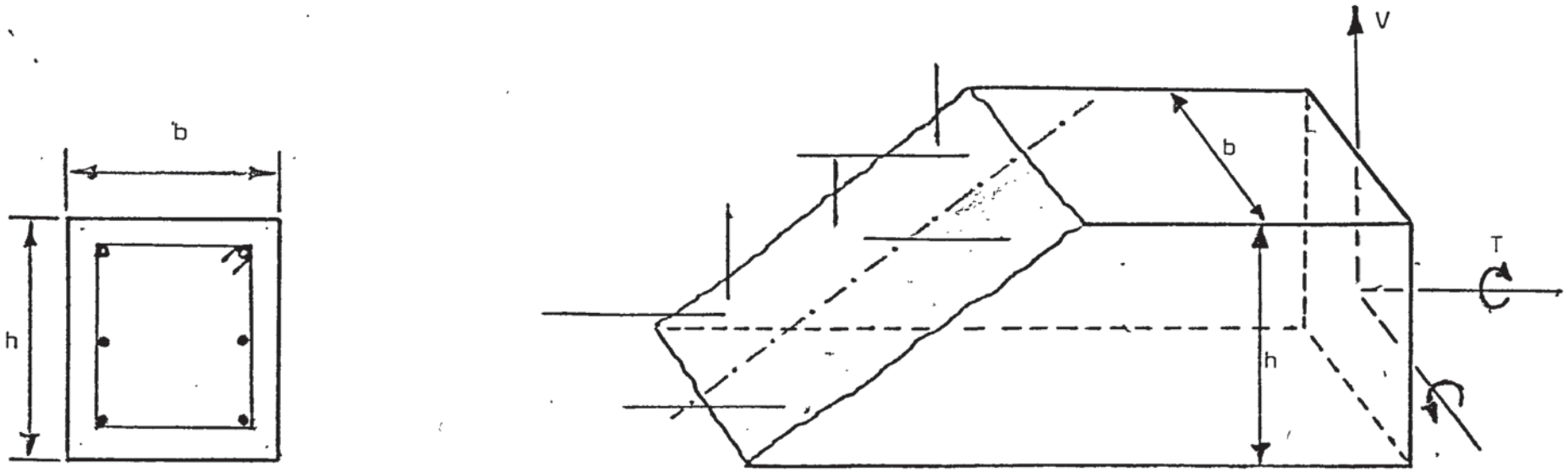

FIGURE (6.2.3.) FAILURE SURFACE IN TORSION & SHEAR.

It is important to note that the prestress $pc_2 = Ps/bh$ is assumed to be transmitted by the longitudinal steel Al(total) therefore ρ_l in this equation is multiplied by 2.

Substituting for a critical $\theta_2 = 45^o$

$$\therefore \quad \tau_u = \tau_o + \mu \rho_l f_l + \mu\left(\frac{pc_2}{2}\right)$$

Expanding the term $\rho_l f_l$ in equation (6.2.33):

$$\frac{ktT}{b^2h} + \frac{V}{bh} = \tau_o + \mu(\rho_l f_l + pc_2/2 + \rho_w f_{sv}) \qquad (6.2.34)$$

for prestressed members with stirrups.

Also :

$$\frac{ktT}{b^2h} + \frac{V}{bh} = \tau_u$$

or

$$T + \frac{Vb}{kt} = \frac{b^2h}{kt}\tau_u$$

if $V = 0 \qquad Tu = \frac{b^2h}{kt}\tau_u$

$$T = 0 \qquad Vu = bh\,\tau_u$$

Now dividing by Tu

$$\frac{T}{Tu} + \frac{Vb}{kt} \times \frac{kt}{b^2h\tau_u} = 1$$

or

$$\frac{T}{Tu} + \frac{V}{Vu} = 1 \qquad (6.2.35)$$

is the general interaction form in non-dimensional format.

6.3 Prestressed Concrete Beams with Stirrups Subject to Bending Combined with Torsion and Shear

Prestressed concrete members may be analysed depending on the ratio of the stress due to flexural moment to the prestress at the soffit of the beam. If

$$\frac{6M}{bh^2} > \frac{Ps}{bh}\left(1 + \frac{6e}{h}\right)$$

then the member is considered for a cracked section analysis. The method of analysis for such members is presented in Subsection (6.3.3) However, if the flexural stress does not exceed the prestress at the soffit then a theory for uncracked section is applicable. The analysis in this case depends on the level of the prestress at the soffit, mid-depth and the top of a beam eccentrically prestressed. The strength at these levels may be related to the longitudinal and/or stirrups steel. The analysis of uncracked sections is presented in Subsections (6.3.1 and 2).

In the analysis of cracked and uncracked sections, the torsion-friction method is applied and general non-dimensional interaction equations are presented in a linear format which reduces to the simple load cases.

6.3.1 Sections Uncracked in Flexure :

In the basic torsion-friction equation of the form :

$$\tau = \tau_o + \mu \sigma_n$$

since σ_n = constant normal to the cross section, thus in the presence of an external stress σ_e :

$$\sigma n = \sigma n - \sigma e$$

1. If this external stress is due to a bending moment M, then at the bottom fibres of a rectangular section, equation (6.2.34) assumes the following form :

$$\frac{ktT_1}{b^2h} + \frac{V_1}{bh} = \tau_o + \mu(\sigma_n - \sigma e)$$
$$= \tau_o + \mu\left[\sigma n + pc1/2 - \frac{6M_1}{bh^2}\right]$$

after rearrangement :

$$\frac{ktT_1}{b^2h} + \frac{V_1}{bh} + \frac{6M_1}{bh^2} = \tau_o + \mu[\sigma n + pc1/2] \qquad (6.2.36)$$

This equation can be further rearranged to give a more compact form :

$$\frac{ktT_1}{hb^2}\left[1 + \frac{V_1 b}{T_1 kt} + \mu\frac{6}{kt}\frac{M1}{T_1}\left(\frac{b}{h}\right)\right] = \tau_o + \mu(\sigma n + pc1/2)$$

and :

$$T_1 = \frac{1}{f1} Tu_1$$

or :

$$f1\,\frac{T_1}{Tu_1} = 1 \qquad (6.2.37)$$

in which :

$$f1 = 1 + \frac{V_1 b}{T_1 kt} + \frac{6}{Kt}\frac{M_1}{T_1}\left(\frac{b}{h}\right)$$

$$Tu_1 = (1/kt)\, b^2 h\, (\tau u_1)$$

$$\tau u_1 = \tau_o + \mu(\sigma n + pc1/2)$$

$$pc1 = (Ps/bh)\,(1 + 6e/h)$$

$$\sigma n = \rho_\ell f_\ell$$

subscript 1 is an index of the bottom level.

This is a form of the general interaction relationship including the loading factor f1.

For a non-dimensional form of interaction, equation (6.2.36) may be reduced to the simple loading cases :

if $V_1, M_1 = 0$ $\quad T_1 = Tu_1 = (1/kt)\, b^2 h\, (\tau u)$

if $M_1, T_1 = 0$ $\quad Vu_1 = bh\, (\tau u)$

and if $T_1, V_1 = 0$ $\quad Mu_1 = (1/6\mu)\, bh^2\, (\tau u)$

Multiplying equation (6.2.36) by (b^2h/kt) :

$$T_1 + \frac{V_1 b}{kt} + \frac{6\mu}{kt}\left(\frac{b}{h}\right) M_1 = Tu_1 \qquad \text{(a)}$$

dividing throughout by Tu_1

$$\frac{T_1}{Tu_1} + \frac{V_1}{Vu_1} + \frac{M_1}{Mu_1} = 1 \qquad (6.2.38)$$

2. At mid-depth, the bending moment effect is insignificant and therefore equation (6.2.34) applies as derived previously.

Also :

$$f_2 \frac{T_2}{Tu_2} = 1 \qquad (6.2.39)$$

in which $f_2 = 1 + \frac{V_2 b}{T_2 kt}$

$Tu_2 = (1/kt)\, b^2 h\, (Tu_2)$

$\tau u_2 = \tau_0 + \mu(\sigma n + pc2/2)$

$pc_2 = Ps/bh$

For the non-dimensional interaction format equation (6.2.35) is valid.

3. At the top face of uncracked beam and/or when M = 0 at the support interface :

$$\frac{ktT_3}{hb^2} + \frac{V_3}{bh} = \tau_0 + \mu[\sigma n + pc_3/2] \qquad (6.2.40)$$

Similarly :

$$f_3 \frac{T_3}{Tu_3} = 1 \qquad (6.2.41)$$

in which $f_3 = f_2$

$\tau u_3 = \tau_0 + \mu(\sigma n + pc3/2)$

$pc_3 = (Ps/bh)\,(1 - 6e/h)$

Also :

$$\frac{T_3}{Tu_3} + \frac{V_3}{Vu_3} = 1 \qquad (6.2.42)$$

as a non-dimensional form of interaction with :

$Tu_3 = (1/kt)\ b^2 h\ (\tau u_3)$

$Vu_3 = bh\ (\tau u_3)$

Equations (6.2.38 , 35 and 42) may be written in a more general form :

$$\frac{T_{1,2,3}}{Tu_{1,2,3}} + \frac{V_{1,2,3}}{Vu_{1,2,3}} + \frac{M_1}{Mu_1} = 1 \qquad (6.2.43)$$

in which the subscripts indicate the level for investigation. It is also noted that only the prestress in the equation for the pure shear-friction stress τu needs adjustment at different levels to calculate Tu , Vu, and Mu .

Modification for Longitudinal and Stirrups Steel

The effect of the stirrups is incorporated by expanding $\sigma n = \rho \ell f \ell$ in equations (6.2.36 through 43) to form :

$$\sigma n = \rho \ell f \ell + \underline{\rho w f s v} \qquad (a)$$

which restores the general form of Tu as expressed in equation (6.2.34) from which the derivations of the equations in this subsection were developed. Therefore :

$$\tau u = \tau_o + \mu(\rho \ell f \ell + \underline{\rho w f s v} + pci/2) \qquad (6.2.44)$$

for members containing longitudinal and stirrups and all the equations may therefore be modified by using this form for τu.

6.3.2 Sections Uncracked in Flexure : Stirrups Form

A further form of the torsion-friction equation may be desirable to check the stirrups strength. This is obtained by modifying equation (6.2.36) as follows:

1. At the bottom of the section :

$$\frac{ktT}{b^2 h} + \frac{V}{bh} = \tau_o + \mu(\rho \ell f \ell + pc1/2) - \mu \frac{6M}{bh^2} \qquad (a)$$

This equation contains only the longitudinal steel explicitly whilst the stirrups are assumed to act as confinement reinforcement provided that a minimum amount is present. The equation is based on a vertical plane perpendicular to the longitudinal axis of the beam. However by considering that the crack surface may initiate at angle α with the transverse at the bottom and continue approximately at the same angle at the front and back faces of the member, then the stirrups will contribute to the strength by providing an additional moment. Taking moment at level of the top steel :

$$\text{moment} = A\ell f\ell\ell a - \frac{As\ fsv\ d'}{S}(b' + d')\ \tan^2\alpha$$

Note: As is one leg area. (b)

In terms of stresses, by dividing by bh :

$$\frac{6M}{bh^2} \cong f\ell f\ell - \frac{As\ fsv\ b'}{bhS}\ (1 + d'/b')\ \tan^2\alpha \qquad (c)$$

by rearranging :

$$\frac{As\ fs\ b'}{bhS}\ (1 + d'/b')\ \tan^2\alpha = f\ell f\ell - \frac{6M}{bh^2} \qquad (d)$$

this means that the stirrups can act as normal shear-torsion friction steel and that their stress is induced by the separation action of twisting.

Now substituting of the R.H.S. in equation (a)

$$\frac{ktT_1}{b^2h} + \frac{V_1}{bh} = \tau_o + \mu\frac{As\ fsv\ b'}{bhS}\ (1 + d'/b')\ \tan^2\alpha + \mu\ (pc1/2) \qquad (6.2.45)$$

This equation is theoretically equivalent to equation (6.2.36) with M = 0 as the major difference. This indicates that a stirrups strength equation is independent of the interaction bending moment.

2. At mid-depth.

Equation (6.2.45) is modified by replacing pc1 with pc2.

3. At the top of the section :

The only difference is that pc1 to be replaced by pc3. This is also the case at the support interface where M = 0.

6.3.3 Sections Cracked in Flexure at Bottom:

In conditions where the M/T ratios are high, the member may crack in flexure at the soffit. After that the section has cracked torsion-friction will provide the resistance to the external loading. This case is governed by the equation :

$$\frac{6M}{bh^2} > \frac{Ps}{bh} \left(1 + \frac{6e}{h}\right)$$

1. Longitudinal Steel Form

Since $\sigma n = (A\ell/bh)f\ell$ is constant perpendicular to the plane in the presence of an external stress due to a bending moment M, σn is modified :

$$\sigma n = \frac{A}{bh}\left(f\ell - \frac{M}{A\ell\ell a}\right)$$

If M_o is the moment to cause zero stress at the section, σn is further modified :

$$\sigma n = \frac{A}{bh}\left(f\ell - \frac{M - M_o}{A\ell\ell a}\right)$$

Substituting into equation (6.2.35) :

$$\frac{ktT}{b^2 h} + \frac{V}{bh} = \tau_o + \mu_s \ell f\ell - \mu \frac{M}{bh\ell a} + \frac{M_o}{bh\ell a} (\mu)$$

lever arm: ℓa may be related to h by a factor k_1, also to avoid unduly complicated expression the ratio :

$$(\mu/\ell a) \cong (1/h)$$

in the M_o term.

After rearrangement :

$$\frac{ktT}{b^2h} + \frac{V}{bh} + \mu\frac{M}{k_1bh^2} = \tau_o + \mu\rho_{\ell}f_{\ell} + \frac{M_o}{bh^2} \qquad (6.2.46)$$

in which $M_o = \frac{Ps}{bh}\left(1 + \frac{12eyd}{h^2}\right)\frac{bh^3}{12yd} + 0.40\sqrt{f_c'}\,\frac{bh^3}{12yd}$.

$yd = d_{\ell} - h/2$, d_{ℓ} = effective depth of bottom steel A_{ℓ}.

Equation (6.2.46) is therefore the required strength expression in which the longitudinal steel only appears.

2. Stirrups Form

The crack surface is considered inclined to the transverse by angle α at the bottom and for sake of simplicity assumed to propogate with the same angle at the front and back faces. Taking moments about a transverse axis at a "compressive zone" at top of the section :

$$M = A_1f_{\ell}\ell_a - \frac{As\ fsv}{S}(d_1 - x)(b' + d_{\ell} - x)\tan^2\alpha$$

if x is taken conveniently small :

$$M = A_{\ell}f_{\ell}\ell_a - \frac{As\ fsv}{S}\,d'(b' + d')\tan^2\alpha$$

where $d_{\ell} - x \cong d'$

After rearrangement and dividing by bh:

$$\rho_{\ell}f_{\ell} - \frac{M}{bh\ell_a} = \frac{As\ fsv}{bhS}\,(1 + d'/b')\tan^2\alpha$$

where $\ell_a \cong d'$

Substituting in equation (6.2.46) :

$$\frac{ktT}{hb^2} + \frac{V}{bh} = \tau_o + \mu\frac{As\ fsv}{bhS}\,b(1 + d'/b')\tan^2\alpha + \frac{M_o}{bh^2} \qquad (6.2.47)$$

This is the stirrups strength equivalent of equation (46). It is noted that M does not appear in this form.

3. All Steel Form

A further more general expression may be obtained by combining the

longitudinal and stirrups steel. Similarly, moments are taken about a transverse axis and :

$$A\ell f\ell a = M - \frac{As\ fsv}{S}\ d'(b' + d')\ \tan^2\alpha$$

Divided by $(bh\ell a)$:

$$\int\ell f\ell e = \frac{M}{bh\ell a_1} - \frac{As\ fsv\ b'(1 + d'/b')}{Sbh}\ \tan^2\alpha$$

where $\ell a \cong d'$

Substituting into equation (6.2.46) :

$$\frac{ktT}{b^2h} + \frac{V}{bh} = \tau_o + \mu \int\ell f\ell - \mu\frac{M}{bh\ell a} + \mu\frac{As\ fsv\ (1 + d'/b')}{bhS}\ \tan^2\alpha$$

and if $\ell a_1 \cong 0.85h$:

$$\frac{ktT}{b^2h} + \frac{V}{bh} + \mu\ \frac{M}{0.85bh^2} = \tau_o + \mu\ [\int\ell f\ell + \int wfsv] + \frac{Mo}{bh^2} \qquad (6.2.48)$$

This is the required form of the strength equation including the total steel content.

This equation can be further rearranged to obtain a more versatile form :

$$\frac{ktT}{b^2h}\ \left[1 + \frac{Vb}{Tkt} + \mu\frac{1}{0.85kt}\ \frac{M}{T}\ \left(\frac{b}{h}\right)\right] = \tau_o + \mu\sigma n + pco \qquad (6.2.49)$$

and

$$T = \frac{1}{f}\ Tu$$

or

$$f\ \frac{T}{Tu} = 1 \qquad (6.2.50)$$

in which :

$$f = 1 + \frac{Vb}{Tkt} + \frac{1}{0.85kt}\ \frac{M - \acute{M}_o}{T}\ \left(\frac{b}{h}\right)$$

$$Tu = (1/kt)b^2h\ (\tau u)$$

$$\tau u = [\tau_o + \mu\sigma n]$$

$$pco = \frac{M_o}{bh^2} \qquad M_o = \text{ditto} \quad , \acute{M}_o = M_o\ (0.85/\mu)$$

$$\sigma n = \int\ell f\ell + \int wfsv$$

Equation (6.2.50) is a general interaction form characterized by linearity and including a combined loading factor f for combined torsion, bending and shear.

Similarly to the procedure followed in deriving Equation (6.2.38) for uncracked sections in flexure, the non-dimensional form of the interaction for cracked sections may be obtained, by manipulating Equation (6.2.48)

$$\frac{T}{Tu} + \frac{V}{Vu} + \frac{M - Mo'}{Mu} = 1 \qquad (6.2.51)$$

in which :

$$Tu = (1/kt)\, b^2 h\, (\tau u)$$

$$Vu = bh\, (\tau u)$$

$$Mu = (0.85/\mu)\, bh^2\, (\tau u)$$

and all other terms as defined in Equation (6.2.50).

6.4 Further Considerations

6.4.1 The Concrete Form of Torsional Strength:

The torsional strength has been presented in a form based on the strength of the steel and it has been assumed that the concrete is capable of providing the necessary friction for the steel stress to develop. From experiments, in many cases, the member failed at a lower strength due to the failure or disintegration of the concrete section. It is, therefore, important that an alternative concrete strength form of the torsional equation be considered.

This case is presented in this subsection for cracked and uncracked sections.

1. Cracked Sections

For an equivalent strength to Equation (6.2.48), governed by an average concrete stress (fcm):

$$b\, Cd\, (fcm) = \Sigma A\ell\, f\ell$$

where Cd = depth of compression zone to be determined from considering shear strain compatibility of steel and concrete, substituting

into Equation (6.2.48) :

$$\frac{ktT}{b^2h}(f) = \tau o + \mu\left(\frac{fcm}{2}\right)\left[\frac{Cd}{h}\right] + \frac{Mo}{bh^2} \qquad (6.2.52)$$

From the criterion Equation (5.5.12):

(fcm) max. = 0.60 fc′

$\therefore$ av. (fcm) = 0.30 fc′

Substituting into (6.2.52):

$$\frac{ktT}{b^2h}(f) = \tau_o + \mu(0.15\ fc')\left[\frac{Cd}{h}\right] + \frac{Mo}{bh^2} \qquad (6.2.53)$$

Equating shear stresses in concrete and steel:

$$\mu(0.15\ fc')\left[\frac{Cd}{h}\right] = \mu\left[\frac{A\ell f\ell}{bh} + \frac{Asf\ell(b'+d')}{bhS}\cdot 2\right] \qquad (1)$$

Noting that $\mu f\ell A\ell = \gamma_s G_s A\ell$:

$$\mu(0.15\ fc')\left[\frac{Cd}{h}\right] = \gamma_s G_s A\ell\,[1 + 1/m]\frac{1}{bh}$$

or $$\mu(0.15\ fc')\,Cdb = \gamma_s G_s A\ell\,[1 + 1/m] \qquad (2)$$

Considering that the concrete-steel shear strains are caused by torque-friction, the twist angle may be defined :

$$\theta = \frac{\gamma_c}{Cd} \qquad (3)$$

Assuming linear variation of shear strains for compatibility of shear strains in concrete and steel

$$\frac{\gamma_c}{Cd} = \frac{\gamma_s}{d\ell - Cd} \qquad (4)$$

where γ_c is the concrete shear strain

Substituting of γ_s from Equation (2) :

$$\mu(0.15fc')\,Cd\,b = \gamma_c\,\frac{(1-Cd/h)}{Cd/h}\,Gs\,A\ell[1 + 1/m]$$

after taking $\frac{Cd}{d\ell} \cong \frac{Cd}{h}$

Noting: $\gamma_c = \frac{\tau}{Gc}$ where $\tau = \mu\,0.15\ fc'$, after rearrangement and dividing both sides by (bh):

$$\frac{Cd}{h} = \frac{(1 - Cd/h)}{Cd/h}\,\frac{Gs}{Gc}\,[f\ell + fs] \qquad (5)$$

This is a quadratic in Cd, and

if $\frac{Gs}{Gc} = \alpha$, where Gc will be evaluated later, then

$$\frac{Cd}{h} = \sqrt{(\frac{1}{2}\alpha\,\rho t)^2 + 2\,(\frac{1}{2}\alpha\,\rho t)} - (\frac{1}{2}\alpha\,\rho t)$$

in which $\rho t = \rho\ell + \rho s$ is the steel content index. (6.2.54)

Therefore the deduced shear compression depth Cd depends on the relative modulus of rigidity of steel to concrete and the total steel content. The latter may be regarded as the main variable. To be strictly accurate this value for Cd must be interpreted as the depth produced by the steel reinforcement only since the prestress effect is not included. Cd can now be substituted in Equation (3) which may be solved for T which is the theoretical torque in the concrete form. The higher TEST/THEORY ratio obtained from Equations (a) and (3) is considered critical and the beam failure may be accordingly attributed to steel or concrete failure.

2. Uncracked Sections

By the same reasoning applied to cracked sections, replacing (b) by (h) in Equation (1) and considering a compressive zone located at the side on the beam, the original torque-friction equation for uncracked section can be written in the following form:

$$\frac{ktT}{b^2h} = \tau o + \mu(0.15\ fc') [\frac{Cd}{b}] + \mu (\frac{pc2}{2}) \qquad (6.2.55)$$

The derivation of $[\frac{Cd}{b}]$ value follows the same steps for cracked sections and it is found that :

$$[\frac{Cd}{b}] = [\frac{Cd}{h}] = \text{Constant}$$

obtainable from Equation (6.2.54).

Both of Equations (6.2.55) and (6.2.53) are expanded to the cases of combined loading by multiplying the theoretical torque T by (fi) the appropriate loading factor.

6.4.2 The Stiffness Form of The Torsional Equation

The concrete form equation has an advantage compared with the steel equation that the steel stress is not involved. Both equations, however, when applied give only an overall strength estimate of the member. In many cases, however, the ultimate strength may be determined by the angle of twist which may be reached before the torsional shear stress predicted by Equations (53) and (55) can develop. Since the failure load depends on the rotation-friction in the member, the steel and concrete contribute to the strength so long as the section is sufficiently rigid to resist the applied torque. Hence, the relative rigidity of the prestressed steel and concrete will be important.

It is proposed in this subsection to construct the stiffness relationship of the section using the torque-friction format.

$$\frac{KtT}{b^2h} = \tau o + \mu\left[\frac{Atf\ell}{bh}\right] + \mu\left[\frac{pc^2}{2}\right] \qquad (a)$$

where $At = A\ell + \frac{As(b' + d')\cdot 2}{S}$

Noting that: $\tau_s = \gamma_s G_s$ shear stress in steel

and assuming $\tau_s = \mu f\ell$

if $\tau_p = \mu\left(\frac{pc_2}{2}\right)$

$$T = \frac{1}{kt}\,\tau o\, b^2h + \frac{1}{kt}\,\gamma_s\, G_s\, Atb + \frac{1}{kt}\,\tau_p\, b^2h \qquad (1)$$

where $\tau o = G_c\,\gamma_c$ = constant.

Assuming equal modulus of elasticity in longitudinal and stirrups steel.

Defining the torsional rotation to cause failure by the angle of twist as :

$$\theta = \frac{\gamma_c}{b} \qquad (2)$$

Also assuming equal shear in concrete and steel

$$\gamma_c = \gamma_s$$

Equation (1) may now be written after substitution as :

$$T = \frac{1}{kt}\,\tau o\,[1 + \frac{\tau p}{\tau o}]\,b^2 h + \frac{1}{kt}\,\gamma_s\,G_s\,A\ell b$$

$$T = \frac{1}{kt} \cdot\theta\cdot Gc\,[1 + \frac{\tau p}{\tau o}]\,b^3 h + \frac{1}{kt} \cdot\theta\cdot Gs\,[\frac{At}{bh}]\,b^3 h$$

and

$$T = \frac{1}{kt}\,Gcb^3 h\,[1 + \frac{\tau p}{\tau o} + \frac{Gs}{Gc} \cdot\int t] \cdot\theta \qquad (6.2.56)$$

Defining the torsional stiffness (ref.45) as :

$$K = \frac{T}{\theta} \qquad (4)$$

$$\therefore \quad K = \frac{1}{kt}\,Gc\,b^3 h\,[\,1 + \frac{\tau p}{\tau o}\,]\,\{1 + \frac{Gs\int t}{Gc(1 + \frac{\tau p}{\tau o})}\}$$

or if $G\acute{c} = Gc\,[1 + \frac{\tau p}{\tau o}]$ which is visualized as increasing rigidity with increasing prestress,

$$K = \frac{1}{kt}\,G\acute{c}\;\; b^3 h\,\{1 + \int t\,\frac{Gs}{G\acute{c}}\} \qquad (6.2.57)$$

This is the stiffness of the section and can be considered as composed of a concrete stiffness component, which includes the prestress effect, and a steel stiffness component including the stirrups and the longitudinal steel rigidity. The torsional stiffness, K, may therefore be presented by rearranging Equation (6.2.56) :

$$K = \frac{1}{kt}\;\; G\acute{c}\;b^3 h + \frac{1}{kt}\,\int t\;Gs\;b^3 h \qquad (5)$$

or $$K = K\acute{c} + Ks \qquad (6.2.58)$$

where $$K\acute{c} = \frac{1}{kt}\,G\acute{c}\;b^3 h$$

$$Ks = \frac{1}{kt}\,\int t\;Gs\;b^3 h$$

It is noted that the steel stiffness Ks, can be expressed in terms of the longitudinal and stirrup contributions to the rigidity :

$$Ks = \frac{1}{kt}\,[\frac{A\ell}{bh} + \frac{Asv(b\acute{}+ d\acute{})}{bhS} \cdot 2]\;\; Gsb^3 h \qquad (6)$$

or $$Ks = K\ell + Ksv \qquad (6.2.58)A$$

where

$K\ell$ = stiffness due to longitudinal steel

Ksv= stiffness due to the stirrups steel

Using the torsional stiffness K and substituting for twist angle θ into Equation (4) :

$$T = K \left[\frac{\gamma_c}{b}\right] \qquad (6.2.59)$$

This is the relationship of the torque to the shear deformation.

For a fixed value of (τo) consistent values for γc and Gc must be used. It is suggested for instance that a value τo = 1.5 N/mm² may be related to the shear strain γc by a reduced value of Gc = 1000 N/mm² which may be taken as constant throughout. However, with (τo) obtained from Equation (6.2.13)

$$T = K \cdot \left[1 - \frac{0.936}{\sqrt{\frac{h}{b} + \frac{1}{3}}}\right] \frac{fr}{Gcb} \qquad (6.2.60)$$

This is the stiffness form of equation and has the advantage of containing neither the steel stress ($f\ell$) nor the average concrete stress ($0.15\ f\acute{c}$) involved in Equations (a) and (6.2.53).

For cracked sections in the derivations above $\mu(\frac{pc_2}{2})$ is replaced by $\frac{Mo}{bh^2}$

6.4.3 Critical Torsional Strength

For each type of section, cracked and uncracked, two main alternative forms of strength have been expressed with reference to steel or concrete. The critical strength of the member is governed by the lower strength the member can attain. However, for differing reinforced and prestressed beams the failure may occur at different stress levels in the concrete and, therefore, the direct stress is expected

to deviate considerably from the average stress used for the concrete in Equation (6.2.53). As a result the theoretical predictions will be affected.

Assuming several critical equilibrium conditions for ultimate shear strength established at various intervals of direct stress, the following critical shear stress levels are fixed by substituting the shear stresses from relationship (5.5.7) then

$$\begin{aligned} \tau u &= (0.30)\, f'c \qquad \frac{ktT}{b^2 h}(fi) \,/\, \tau u = C1 \\ &= (0.20)\, f'c \qquad\qquad = C2 \\ &= (0.15)\, f'c \qquad\qquad = C3 \\ &= (0.10)\, f'c \qquad\qquad = C4 \\ &= (0.05)\, f'c \qquad\qquad = C5 \end{aligned} \tag{a}$$

$(0.05)f'c$ is introduced as a lower limit and equal to the minimum shear stress τo.

From these ratios of (C1-5) the critical ratio can be deduced as:

$$Ci > 1$$

for which case the test beam exceeds the certain level of critical shear and failure will be imminent. However the critical shear level among several giving (C) ratios >1, is the shear stress producing :

$$C_{crt.} = \min.(Ci) \text{ where } Ci > 1$$

Therefore a concrete critical ratio of $\frac{\text{Test}}{\text{Theory}}$ has been obtained. This is controlled by concrete strength and may therefore be used to obtain a ratio of test to concrete strength as an alternative of using Equations (6.2.53, 55).

This has the advantage of identifying a critical shear zone within which the beam failure is expected to occur.

The critical concrete strength can be compared with the steel

strength to obtain the ultimate critical strength for the section.

6.5 Summary

In this chapter an attempt has been made to produce a simple and rational format for the torsional ultimate strength. A hypothesis of torque-friction is proposed for the analysis of pure torsion and interaction of torsion combined with bending and shear. The hypothesis is verified theoretically and by analysing experimental results from tests on reinforced concrete beams good agreement is found.

The basic parameters of the torsional equation have been considered and relevant expressions are produced when possible. However, for the expediency of the analysis it has been preferred to use an empirical formula for the average steel stress.

For members loaded in torsion and shear the approach produces a linear interaction equation which can also be derived using the existing skewed bending approach.

The analysis of members subject to bending moment, shear and torsion distinguishes two groups of members considering the crack state at the bottom due to flexure. Consequently the prestress is included directly in the uncracked sections whilst in the cracked group of section the prestress is considered to produce a moment stress to resist the external stress of applied bending moment. After cracking the reinforcement provides further resistance. This assumption is based on the experimental observations of the test beams which indicated that the ultimate strength was independent of the sequence of loading in torsion and bending. Nonetheless when M/T ratio was high then the crack started at the bottom in flexure.

For cracked and uncracked groups of sections, linear interaction relationships of general format are presented which extrapolate to simple loading cases by modifying a combined loading factor. Non-dimensional interaction equations are also presented in a linear form.

Furthermore, a torsional stiffness form of the torque-friction equation is derived relating the torsional rigidity of steel and concrete and prestress. This compact format may be pursued further to develop a rational method for predicting the stress level and the contribution of the longitudinal and stirrups steel in prestressed concrete beams.

APPENDIX TO CHAPTER 6

DERIVATION OF EQUATIONS (6.2.24, 27)

1. Determination of the average stress in the horizontal legs of stirrups; fsh:

The distorted failure surface is projected in one skewed plane with an axis inclined by an angle θ to the transverse axis of the beam.

Resolving moment and forces on this plane:

$$\frac{ktT}{h^2 b}\ \text{Cos}\ \theta\ \text{Sin}\ \theta = C + \mu\left(\frac{A\ell f\ell \text{Cos}\theta)}{bh}\right)\text{Cos}\ \theta + \mu\left(\frac{Asv\ \text{Sin}\theta\ \tan\theta\ b'\ fsh}{bhS}\right)\text{Cos}\theta$$

rearranging by gathering terms:

$$\frac{ktT}{h^2 b} = \frac{C}{\text{Sin}\theta\text{Cos}\theta} + \mu[\int\ell f\ell]\ \text{Cot}\theta + \mu[\int sh fsh]\ \tan\theta \qquad (6.2.21)$$

Note: in equation (20), $kt = 3\sqrt{\frac{b}{h}}$, thus

$$3\sqrt{\frac{h}{b}}\frac{T}{h^2 b} = 3\sqrt{\frac{b}{h}}\ \frac{T}{b^2 h} = 3\ \frac{T}{b^{1.5} h^{1.5}}$$

min. T is obtained from equation (21) by differentiation w.r.t.θ :

$$\frac{kt}{h^2 b}\ \frac{dT}{d\theta} = C\ \{\sec\theta\ (-\text{Cosec}\theta\text{Cot}\theta) + \text{Cosec}\theta\ \sec\theta\ \tan\theta\} + \mu[\int\ell f\ell]\ (-\text{Cosec}^2\theta) + \mu[\int sh fsh]\ \sec^2\theta$$

for $\frac{dT}{d\theta} = 0$:

$$0 = C\left\{-\frac{1}{\text{Sin}^2\theta} + \frac{1}{\text{Cos}^2\theta}\right\} + \mu[\int\ell f\ell]\ \left(-\frac{1}{\text{Sin}^2\theta}\right) + \mu[\int sh fsh]\ \left(\frac{1}{\text{Cos}^2\theta}\right)$$

and $C + \mu\alpha = C\tan^2\theta + \mu\beta\tan^2\theta$

or $\tan^2\theta\ [C + \mu\beta_H] = [C + \mu\alpha]$

$$\therefore\quad \tan\theta = \sqrt{\frac{C + \mu\alpha}{C + \mu\beta_H}} \qquad (6.2.22)$$

in which $\alpha = \int\ell f\ell$

$$\beta_H = \int sh\ fsh \quad ; \quad \int sh = \frac{Asv\ b'}{bhS} \cdot 2$$

fℓ is known from equation (6.2.17)

$$\tan\theta = \sqrt{1 + \frac{\sigma_n}{C_o}} \qquad (6.2.23)$$

as derived in Chapter 5

in which $\sigma_n = 0.83\, f_r$

$C_o = 0.05\, f_c'$, $\mu = 0.75$

$\tan\theta = 1.5$

and $\theta = 56°.3$

$$2.25C + 2.25\mu\beta_H = C + \mu\alpha$$

and $$\boxed{2.25\mu\beta_H = \mu\alpha - 1.25C} \qquad (6.2.24)$$

from which fsh can be determined.

2. <u>Determination of the average stress in the vertical legs of stirrups fsv</u> :

In this case the distorted failure surface is projected in one rectangular plane skewed with an angle θ to the vertical. Resolving moment and forces :

$$kt\,\frac{T}{hb^2} = \frac{C}{\sin\theta\cos\theta} + \mu\left\{\frac{A_{svd}' f_{sv}\sin\theta}{bhS\cos\theta} + \frac{(A_\ell f_\ell)\cos^2\theta}{bh\sin\theta\cos\theta}\right\} \qquad (6.2.25)$$

Minimising T w.r.t. θ gives after rearrangement :

$$C\tan^2\theta + \tan^2\theta\,\mu\beta_v = \mu\alpha + C$$

$$\text{or } \tan^2\theta\,(C + \mu\beta_v) = [C + \mu\alpha]$$

$$\tan\theta = \sqrt{\frac{C + \mu\alpha}{C + \mu\beta_v}} \qquad (6.2.26)$$

in which $\beta_v = \int_{sv} f_{sv}$; $\int_{sv} = \frac{A_{svd}'}{bhS}\cdot 2$

Substituting $\tan\theta = 1.5$ from equation (23) :

$$\boxed{2.25\mu\beta_v = \mu\alpha - 1.25C} \qquad (6.2.27)$$

from which (fsv) can be determined.

3. It is worth noting that Equations (6.2.24, 27) in their (α) terms are special cases because they will contain the bending moment and/or shear force when these combined loads are acting on the member. It is easier to consider that the stirrups contribute to the total resistance in proportional to their torsional rigidity. This is considered as follows:

Assuming that the applied torque is resisted by the concrete and the steel according to their rigidity :

$$\frac{(fi)T}{K} = \frac{T\acute{c}}{Kc'} = \frac{T\ell}{K\ell} = \frac{Tsv}{Ksv} = \bar{\theta} \qquad (1)$$

Stirrups contribution :

$$Tsv = \frac{Ksv}{K} \cdot T\,(fi) \qquad (2)$$

in which (fi) is the combined loading factor given in Equation (6.2.48) for cracked section or its modification for uncracked section.

Multiplying both sides of Equation (6.2.57) by $\bar{\theta}$, angle of twist, and expanding the stiffness Ks as in Equation (6.2.57A) :

$$\bar{\theta} \cdot K = \bar{\theta}\, Kc' + K\ell\bar{\theta} + Ksv\, \bar{\theta}$$

or

$$T = Tc' + T\ell + Tsv \qquad (3)$$

Noting that Equation (3) is developed from Equation (6.2.48) and by equating comparable terms :

$$Tsv = (\mu \int svfsv) \cdot \frac{1}{Kt}\, b^2 h \qquad (4)$$

or :

$$(fi)\, T = \frac{K}{Ksv} \cdot \frac{1}{Kt}\, b^2 h \cdot (\mu \int svfsv) \qquad (5)$$

from which a solution for (fsv) is possible.

However in the present case where a critical shear stress = 0.15 fc' is stated, then :

$$(fi)\, \frac{ktT}{b^2 h} = \frac{K}{Ksv} \cdot (\mu \int svfsv)$$

By simplifying the stiffness ratio :

$$fsv = \frac{(0.15fc')}{\mu \int sv} \cdot \frac{1}{[\frac{Gc'}{Gs} \cdot \frac{1}{\int sv} + 1]} \qquad (b)$$

is the required equation.

This solution can be extended to obtain an equation for the stress in the longitudinal steel, $f\ell$, for which the expression is written as follows:

$$f\ell = \frac{(0.15\ fc')}{\mu \int \ell} \cdot \frac{1}{[\frac{Gc'}{Gs} (\frac{1}{\int \ell}) + 1]} \qquad (7)$$

which is obtained by interchanging the stirrups and longitudinal steel contents, $\int sv$ and $\int \ell$ in Equation (6).

CHAPTER 7:

ANALYSIS OF TEST RESULTS.

7.1. INTRODUCTION

In this chapter the theoretical predictions by the methods of analysis presented in the foregoing chapters are compared to the experimental results.

The experimental results include the author's test beams and results by previous research workers. The test data of the specimens were compiled and prepared for use on ICL 1904S computer by which the analysis was carried out. The complete data file is listed in the Appendix, the main parameters involved in computation are also tabulated for each investigation and presented in Table (A.1.).

The results of the analysis of these tests are presented and discussed in the following sections.

7.2. The Empirical Formula of Chapter 3

This was derived originally to obtain a simplified method for comparison with the author's test results. The result of the comparison was presented in section (3.10) where the detailed predicted values and their ratio to the experimental torsional moments were included and discussed. The mean value of 1.02 ± 0.13 with a C.V.= 12% was produced for thirty-six beams tested by the author.

In this section the formula is compared with the test results available in the literature, which include beams subject to pure torsion and beams subjected to torsion, bending and shear.

Table (7.1.) summarises the comparison ratios between tests and formula. For a grand total of (207) beams, the formula produces a mean of Test/Theory = 1.19 and S.D. = ±0.27 with a C.V. = 22.5%. This result is good in view of the vast variation of the parameters involved in testing the beams and the simple format of the method.

The various forms of the formula presented in Equations (3.10.5 to 8) are presented in the following form by rearranging Equation (3.10.8):

$$(T/To)\ [1 + (V/T)\ (To/Vo) + (M/T)\ (To/Mo) + (Ps/T)\ (To/Po) + (Fs/T)\ (To/Fo)\ ] = 1 + pc^2/fsp$$

and if C.L., a factor of combined loading, is equal to the sum inside the large brackets :

$$T = (1/C.L.)\ (b^2 h/Kt)\ \sqrt{fc'}\ (1 + pc^2/fsp) \qquad 3.10.9.$$

where all the terms are defined in section (3.10).

For the computer program , when fsp fcu, fc' or fr were not all quoted in differing investigations, fsp was taken as the maximum of the following values:

$$\phi 1 = 0.05\ fcu + 0.7$$
$$\phi 2 = 0.07\ fc' + 0.7$$
$$\phi 3 = fsp$$
$$\phi 4 = 0.87\ fr \qquad 3.10.9a$$

Equation (3.10.9.) has the advantage of linearity and uses quoted values without the need to resort to more complicated empirical evaluations of fsp or fr.

The numerical coefficient C, see section (3.10), relating the axial stress to the tangential shear stress, was taken as the same used in Chapter 3 i.e.

$$C = 1.20$$

TABLE 7.1. CORRELATION OF EQUATION (3.10.9) WITH TEST RESULTS

INVESTIGATOR	NUMBER	MEAN	S.D.	C.V.%
ZIA (40)	6	0.802	0.01	1.0
MURASHKIN (43)	5	1.044	0.121	11.6
OKADA (44)	8	1.075	0.140	13.1
BISHARA (10)	8	1.169	0.223	19.1
GANGARAO (50)	13*	0.868	0.092	10.6
	27	1.169	0.175	15.0
EVANS et al (34)	14	1.143	0.150	13.1
MUKHERJEE (9)	44	1.238	0.243	19.6
McMULLEN (37)	17	1.376	0.253	18.4
	7+	1.386	0.227	16.0
HENRY (13)	32	1.418	0.226	15.9
McGEE (52)	6	1.417	0.075	5.3
	6*	1.022	0.106	10.4
BELOW (65)	14	0.896	0.137	15.2
Grand Total	207	1.191 1,145	0.26 mean	22.5 13.2

* uncracked

\+ no stirrups

The average longitudinal and web steel stress was taken equal to the value produced by the empirical (6.1-2) from Hsu's results.

The detailed results of the analysis for the different investigations are presented in tables from Table 7.4. Further remarks and discussions of the results are included in section (7.4.).

7.3. The Torsional Shear-friction Method of Chapter 6.

In this section the method is applied in simplified form using experimental constants. Therefore in the basic equations (6.2.17) and &6.2.24) the following values are assumed:

$$\theta = 45°$$
$$C = 1.5 \text{ N/mm}^2$$
$$\mu = 0.75$$

The average stress in a stirrup leg fsh is taken as equal to the average longitudinal steel stress $\bar{f}_\ell$, derived empirically from Hsu's strain gauge readings, multiplied by (1+d'/b1). The final form is therefore :

$$= 1.5 + \mu \rho_\ell \bar{f}_\ell + \mu^2 \frac{A_s' d'}{bh\ S} [1+b'/d'] \bar{f}_{sv}]$$

with the prestress effect duly included for the section when cracked or uncracked in flexure.

The comparison with the test results included (193) beams, seventy-three of which were found uncracked by flexure.

For the uncracked beams the coefficient of variation varied between 2-16.2% with a mean of 0.84 (min.) to 1.25 (max.) for (73) beams. The results of the comparison are presented in detail in Table (7.3.) for beams from nine investigations. It can be concluded that the correlation is generally good. The particularly good coefficient of

TABLE 7.2. CORRELATION OF EQUATION (6.2.24) WITH TEST RESULTS

INVESTIGATOR	NUMBER	MEAN	S.D.	C.V.%
ZIA (40)	6*	0.839	0.016	2.0
MURASHKIN (43)	5	0.845	0.100	11.9
OKADA (44)	6*	0.852	0.056	6.5
BISHARA (10)	6*	1.035	0.164	15.8
GANGARAO (50)	13*	1.064	0.172	16.2
	27	1.252	0.202	16.1
EVANS et al (34)	5*	1.077	0.047	4.4
	9	0.841	0.068	8.1
MUKHERJEE (9)	22*	1.169	0.162	13.9
	22	1.392	0.325	23.1
McMULLEN (37)	4*	1.034	0.088	8.5
	14	0.970	0.068	7.0
BELOW (65)	11	0.651	0.079	12.2
HENRY (13)	5*	1.162	0.057	4.9
	26	1.407	0.094	6.7
McGEE (52)	6*	1.253	0.092	7.3
	6	1.378	0.102	7.4
UNCRACKED	73	1,054	mean	8,8
CRACKED	120	1,092		11,6
	193	1,073		10,2

* uncracked

variation confirms the consistency of the method.

In Table (7.2.) also, the results of comparison with (120) beams, cracked in flexure, was presented. The agreement is very good taking into account the vast range of variation involved in the test data and the simplicity of the method. The coefficient of variation obtained varies between 23% as max., for (22) beams from Warwaruk's (9) and 6.7% as min., for twenty-six beams from Henry (13). Further discussions of the comparison is included in Section (7.4.).

The author's test beams are analysed and the results are presented in detail in Table (7.3). For a total of thirty-six beams the analysis produces a mean of 1.23 with a s.o. = ± 0.24 and a c.v. = 19.7%. However for the twenty seven sections cracked in flexure at bottom the mean is 1.176± 0.197 with a c.v. = 16.7%. The analysis for the uncracked nine beams is, however, more conservative and produces a mean of 1.397 ± 0.286 with c.v. = 20.5%.

7.4. Discussion

In Table (7.4) the results of the six rectangular beams tested by Zia (40) are presented. The mean is 0.802 with a S.D. = ±0.01 and c.v. = 1%. Equation (3.10.9) is therefore unconservative in predicting the strength of these beams. This may indicate that the actual stresses in the stirrups and tendons could be lower than the average stress values as calculated from the empirical Equation (6.1-2).

Table (7.5) contains results of five beams tested by Murashkin (43). The beams were tested in bending-torsion and all cracked in flexure. The mean is 1.04 with a c.v. = 11.6%.

In Table (7.6), Okada's (44) eight beams are compared. The beams were either cracked in flexure ur uncracked. Nevertheless a very good agreement with the equation is obtained with a mean = 1.08 and a c.v. = 13%. The results of eight beams tested in be nding-shear-torsion by Bishara (10) are presented in Table (7.7). Although the mean = 1.17 is apparently good, the c.v. = 19% is high. No concrete strength values of (fsp) or (ff) were quoted and the shear test span was much too short. This may affect the accuracy of the predictions.

Improved coefficient of variation is obtained from analysing thirteen beams, uncracked, tested by Gangarao(50). The equation produces c.v. = 10.6% with a mean = 0.87. However, for 27 beams, cracked, the formula produces a mean = 1.17(15%). For the total of forty beams the mean = 1.07 (19%) is obtained. The details are presented in Table (7.8).

The formula predicts the strength of 14 beams tested by Evans and Khalil(34) with an accuracy of 1.14 (13%) which is considered good. The detailed results are presented in Table (7.9).

In Table (7.10) is presented the results of comparison with McMullen and Woodhead's (37) beams. For a total of (14) beams, cracked, a mean = 1.47 (9.8%) is obtained. By including another three uncracked beams, however, the mean is lowered but the c.v. value is considerably affected giving a mean = 1.38 (18.4%) for 17 beams. It is noted that including a further seven beams with no stirrups will result in a mean = 1.36 (19.6%) for 24 beams. This may indicate that the formula may be extended for application to beams reinforced longitudinally only.

The result of the comparison for 32 beams tested by Henry (13)

is presented in Table (7.11). As is shown the prediction is on the conservative side with a mean = 1.42. Nonetheless the formula is reasonably consistent giving a c.v. = 15.9%. It is noted that all the beams were tested subject to combined torsion, bending and shear.

In Table (7.12) the test results reported by McGee (52) are compared. For 6 beams, cracked in flexure, the accuracy is 1.42 (5.3%) which is considerably good. The consistency is affected however, unfavourably when a further 6 beams, uncracked, are considered. For the total of 12 beams a mean = 1.22 (17.9%) is produced, which is acceptable for an approximate method.

Table (7.13) contains the result of comparison of 14 beams from Below (65). The formula produces a mean of 0.90, a S.D. = ±0.14 and a c.v. = 15%. This is considered good in view of the variable parameters involved in the design of the test beams.

It can be concluded, therefore, that the empirical format (3.10.9) is in a good agreement with the available test results. The replacement of the assumption of a yield stress in the steel by an average steel stress related to the cross-section and the steel content is considered justified. The strength of the member is governed by the concrete shear strength which is related to the split or rupture tensile strength, and the average prestress.

The general format of the method for the interaction of torsion, bending, shear and prestressing force is favourably supported by the comparison with the test results and may therefore be considered for use in analysis and practical purposes.

TABLE (7.3) DETAILED CORRELATION OF THE AUTHOR'S TEST RESULTS AND THEORY.

	1	2	3	4		5	6
	BEAM	TEST/ THEORY	CRITICAL CONCRETE	CRITICAL STRENGTH RATIO	TYPE	SHEAR FAILURE ZONE	BALANCED SECTIONS*
	A1	1.164	1.086	1.086	C	I	1.1
	A2	1.021	1.116	1.021	S	I	1.0
	A3	1.213	1.008	1.008	C	III	-
	A4	0.942	1.167	1.167	C	I	-
	A5	0.891	1.182	1.182	C	I	-
	A6	1.328	1.049	1.049	C	III	-
	A7	1.317	1.114	1.114	C	III	-
	A8	1.186	1.150	1.150	C	III	-
	A9	1.374	1.444	1.374	S	III	1.4
*	A10	1.028	1.028	1.038	C	IV	-
*	A11	1.012	1.012	1.012	C	IV	-
+	B1	1.205	0.83	0.83	C	I	-
	B2	1.230	1.205	1.205	C	III	1.2
	B3	1.030	1.126	1.030	S	II	1.0
+	B4	1.405	1.08	1.08	C	I	-
	B5	1.199	1.32	1.199	S	III	1.2
	B6	1.019	1.061	1.019	S	III	1.0
+	C2	1.427	1.08	1.08	C	II	-
+	C2	1.629	1.377	1.377	C	I	-
	C3	1.263	1.135	1.135	C	III	-
	C4	1.197	[0.99]	[0.99]	C	II	-
+	D1	1.023	1.092	1.023	S	I	1.0
	D2	0.843	1.147	1.147	C	II	-
	D3	0.884	1.071	1.071	C	II	-
+	E1	1.042	1.112	1.042	S	II	1.0
+	E2	1.736	1.008	1.008	C	II	-
	E3	1.455	1.383	1.383	C	III	1.4
	E4	1.206	1.086	1.086	C	III	1.1
	F0	0.991	1.193	[0.99]	S	III	-
	F1	1.400	1.445	1.400	S	III	1.4
	F2	1.192	1.163	1.163	C	III	1.2
+	G1	1.883	1.210	1.210	C	II	-
	G2	1.510	1.587	1.510	S	III	1.5
	G3	1.201	1.188	1.188	C	III	1.2
	AA1	1.650	1.485	1.485	C	III	-
+	AA2	1.224	1.264	1.224	S	III	1.2

* $\tau_u > 0.33\ f_c'$

\+ uncracked

THEORY	BEAMS	NO.	MEAN	S.D.	C.V.%
STEEL (Col.2)	SERIES I	11	1.13	±0.16	13.9
	UNCRACKED	9	1.10	±0.15	13.4
	CRACKED	27	1.18	±0.20	16.7
	TOTAL	36	1.23	±0.24	19.7
CRITI-CAL (Col.4)	SERIES I	11	1.11	±0.10	9.4
	TOTAL	36	1.14	±0.15	13.2
BALANCED (Col.6)	TOTAL	16	1.18	±0.16	13.8

SHEAR FAILURE ZONES **

ZONE	SHEAR	NO. BEAMS FAILURES
I	$0.10f'_c$	8
II	$0.15f'_c$	8
III	$0.20f'_c$	18
IV	$0.30f'_c$	2

* Balanced Strength (Col.6) is defined as the failure strength of a beam reached simultaneously by steel and concrete. For a balanced section failure (Col.6), steel strength (Col.2) should be equal to the concrete strength (Col.3).

** See Section 6.4.3.

TABLE (7.4) CORRELATION OF ZIA'S (40) TEST RESULTS WITH THEORY

SPECIMENS AND DATA FILE DESIGNATION	THEORETICAL	EMPIRICAL
C BEAM:0RW1	UNCRACKED	
BEAM NO.: 0	0.857	0.810
C BEAM:0RW2	UNCRACKED	
BEAM NO.: 1	0.857	0.810
C BEAM:2RW1	UNCRACKED	
BEAM NO.: 2	0.817	0.794
C BEAM:2RW2	UNCRACKED	
BEAM NO.: 3	0.817	0.794
C BEAM:2.5RW1	UNCRACKED	
BEAM NO.: 4	0.842	0.803
C BEAM:2.5RW2	UNCRACKED	
BEAM NO.: 5	0.842	0.803
C BEAM:0.25TW	UNCRACKED	
BEAM NO.: 6	1.136	0.983
C BEAM:0.25TW	UNCRACKED	
BEAM NO.: 7	1.136	0.983
C BEAM:2.25TW	UNCRACKED	
BEAM NO.: 8	0.967	0.902
C BEAM:2.25TW	UNCRACKED	
BEAM NO.: 9	0.967	0.902
C BEAM:2.75TW	UNCRACKED	
BEAM NO.: 10	1.080	0.958
C BEAM:2.75TW	UNCRACKED	
BEAM NO.: 11	1.080	0.958
C BEAM:0.75IW	UNCRACKED	
BEAM NO.: 12	1.054	0.925
C BEAM:0.75IW	UNCRACKED	
BEAM NO.: 13	1.054	0.925
C BEAM:3IW1,2	UNCRACKED	
BEAM NO.: 14	1.199	0.997
C BEAM:3IW2	UNCRACKED	
BEAM NO.: 15	1.199	0.997
C BEAM:3.5IW1	UNCRACKED	
BEAM NO.: 16	1.226	1.011
C BEAM:3.5IW2	UNCRACKED	
BEAM NO.: 17	1.226	1.011
C BEAM: 0R1	UNCRACKED	
BEAM NO.: 18	0.731	0.745
C BEAM: 0R2	UNCRACKED	
BEAM NO.: 19	0.769	0.761
C BEAM: 0R3	UNCRACKED	
BEAM NO.: 20	0.775	0.762
C BEAM: 2R1	UNCRACKED	
BEAM NO.: 21	0.736	0.770
C BEAM: 2R2	UNCRACKED	
BEAM NO.: 22	0.837	0.791
C BEAM: 2R3	UNCRACKED	
BEAM NO.: 23	0.808	0.779
C BEAM: 2.5R1	UNCRACKED	
BEAM NO.: 24	0.757	0.755
C BEAM: 2.5R2	UNCRACKED	
BEAM NO.: 25	0.784	0.766
C BEAM: 2.5R3	UNCRACKED	
BEAM NO.: 26	0.714	0.738
C BEAM: 0.25T	UNCRACKED	
BEAM NO.: 27	1.212	0.969
C BEAM: 0.25T	UNCRACKED	
BEAM NO.: 28	1.233	0.979
C BEAM: 2.25T	UNCRACKED	
BEAM NO.: 29	0.849	0.808

TABLE (7.5) CORRELATION OF MURASHKIN'S (43) TEST RESULTS WITH THEORY.

SPECIMENS AND DATA FILE DESIGNATION	THEORETICAL	EMPIRICAL
BEAM NO.: 143	0.000	
C BEAM: A1	CRACKED	
BEAM NO.: 149	0.803	0.934
C BEAM: A3	CRACKED	
BEAM NO.: 150	0.938	1.076
C BEAM: A5	CRACKED	
BEAM NO.: 151	0.729	0.968
C BEAM: A7	CRACKED	
BEAM NO.: 152	0.987	1.267
C BEAM: A9	CRACKED	
BEAM NO.: 153	0.766	0.977
C BEAM: A11	CRACKED	
BEAM NO.: 154	0.895	1.463
C BEAM: B-2	CRACKED	
BEAM NO.: 155	0.730	0.890
C BEAM: B-4	CRACKED	
BEAM NO.: 156	0.871	1.028
C BEAM: B6	CRACKED	
BEAM NO.: 157	0.624	0.883
C BEAM: B-8	CRACKED	
BEAM NO.: 158	0.906	1.185
C BEAM: B-10	CRACKED	
BEAM NO.: 159	0.647	0.883
C BEAM: B-12	CRACKED	
BEAM NO.: 160	0.533	0.871

TABLE (7.6.) CORRELATION OF OKADA'S (44) TEST RESULTS WITH THEORY.

SPECIMENS AND DATA FILE DESIGNATION	THEORETICAL	EMPIRICAL
C BEAM: 1 R5-	UNCRACKED	
BEAM NO.: 161	0.920	0.956
C BEAM: 2 R5-	UNCRACKED	
BEAM NO.: 162	0.932	0.963
C BEAM: 3 R5-	UNCRACKED	
BEAM NO.: 163	0.804	0.962
C BEAM: 4 R5-	UNCRACKED	
BEAM NO.: 164	0.847	0.989
C BEAM: 5 R5-	UNCRACKED	
BEAM NO.: 165	0.824	1.076
C BEAM:6 R5-I	UNCRACKED	
BEAM NO.: 166	0.785	1.046
C BEAM:7 R5-I	CRACKED	
BEAM NO.: 167	1.489	1.355
C BEAM:8 R5-I	CRACKED	
BEAM NO.: 168	1.320	1.252
C BEAM:9 R5-I	CRACKED	
BEAM NO.: 169	0.000	1.252
C BEAM:10 R5-	CRACKED	
BEAM NO.: 170	0.000	1.252

TABLE (7.7) CORRELATION OF BISHARA'S (10) TEST RESULTS WITH THEORY.

SPECIMENS AND DATA FILE DESIGNATION	THEORETICAL	EMPIRICAL
C BEAM:OR1	CRACKED	
BEAM NO.: 171	-0.005	1.520
C BEAM:OR2	CRACKED	
BEAM NO.: 172	-0.005	1.249
C BEAM:OR3	UNCRACKED	
BEAM NO.: 173	0.892	0.957
C BEAM:OR4	UNCRACKED	
BEAM NO.: 174	0.923	0.943
C BEAM:2.5R1	UNCRACKED	
BEAM NO.: 175	1.261	1.522
C BEAM:2.5R2	UNCRACKED	
BEAM NO.: 176	0.827	0.980
C BEAM:2.5R3	UNCRACKED	
BEAM NO.: 177	1.102	1.081
C BEAM:2.5R4	UNCRACKED	
BEAM NO.: 178	1.205	1.097
C BEAM:OI1	CRACKED	
BEAM NO.: 179	-0.009	2.210
C BEAM:OI2	CRACKED	
BEAM NO.: 180	-0.010	2.101
C BEAM:OI3	CRACKED	
BEAM NO.: 181	-0.010	2.013
C BEAM:OI4	CRACKED	
BEAM NO.: 182	-0.009	1.859
C BEAM:3.5I1	UNCRACKED	
BEAM NO.: 183	1.843	2.042
C BEAM:3.5I2	UNCRACKED	
BEAM NO.: 184	1.768	1.694
C BEAM:3.5I3	UNCRACKED	
BEAM NO.: 185	1.582	1.456
C BEAM:3.5I4	UNCRACKED	
BEAM NO.: 186	2.248	1.793
C BEAM:OT1	CRACKED	
BEAM NO.: 187	-20.493	2.399
C BEAM:OT2	CRACKED	
BEAM NO.: 188	-17.140	1.896
C BEAM:OT3	CRACKED	
BEAM NO.: 189	-36.057	1.709
C BEAM:OT4	UNCRACKED	
BEAM NO.: 190	1.900	1.586
C BEAM:2.75T1	CRACKED	
BEAM NO.: 191	1.794	2.305
C BEAM:2.75T2	UNCRACKED	
BEAM NO.: 192	1.706	1.629
C BEAM:2.75T3	UNCRACKED	
BEAM NO.: 193	1.598	1.455
C BEAM:2.75T4	UNCRACKED	
BEAM NO.: 194	1.581	1.391

TABLE (7.8) CORRELATION OF GANGARAO'S (50) TEST RESULTS WITH THEORY.

SPECIMENS AND DATA FILE DESIGNATION	THEORETICAL	EMPIRICAL
C BEAM:1/1	UNCRACKED	
BEAM NO.: 61	0.941	0.838
C BEAM:1/2	CRACKED	
BEAM NO.: 62	1.142	0.920
C BEAM:1/4	CRACKED	
BEAM NO.: 63	1.044	0.973
C BEAM:1/C	CRACKED	
BEAM NO.: 64	0.800	0.936
C BEAM:2/1	UNCRACKED	
BEAM NO.: 65	1.221	0.982
C BEAM:2/2	CRACKED	
BEAM NO.: 66	1.372	1.062
C BEAM:2/3	CRACKED	
BEAM NO.: 67	1.337	1.119
C BEAM:2/4	CRACKED	
BEAM NO.: 68	1.239	1.116
C BEAM:2/8	CRACKED	
BEAM NO.: 69	1.218	1.196
C BEAM:3/1	UNCRACKED	
BEAM NO.: 70	1.017	0.939
C BEAM:3/2	CRACKED	
BEAM NO.: 71	1.124	1.003
C BEAM:3/3	CRACKED	
BEAM NO.: 72	1.135	1.077
C BEAM:3/4	CRACKED	
BEAM NO.: 73	1.127	1.128
C BEAM:3/8	CRACKED	
BEAM NO.: 74	1.027	1.163
C BEAM:3/C	CRACKED	
BEAM NO.: 75	1.279	1.016
C BEAM:4/1	UNCRACKED	
BEAM NO.: 76	1.235	1.020
C BEAM:4/2	CRACKED	
BEAM NO.: 77	1.764	1.306
C BEAM:4/3	CRACKED	
BEAM NO.: 78	1.314	1.135
C BEAM:4/4	CRACKED	
BEAM NO.: 79	1.495	1.310
C BEAM:4/8	CRACKED	
BEAM NO.: 80	1.537	1.508
C BEAM:4/C	CRACKED	
BEAM NO.: 81	1.415	1.117
C BEAM:5/1	UNCRACKED	
BEAM NO.: 82	0.824	0.912
C BEAM:5/2	CRACKED	
BEAM NO.: 83	1.203	1.152
C BEAM:5/3	CRACKED	
BEAM NO.: 84	1.170	1.209
C BEAM:5/4	CRACKED	
BEAM NO.: 85	1.384	1.412
C BEAM:5/8	CRACKED	
BEAM NO.: 86	1.537	1.672
C BEAM:6/1	UNCRACKED	
BEAM NO.: 87	1.151	0.978
C BEAM:6/2	CRACKED	
BEAM NO.: 88	1.436	1.168
C BEAM:6/3	CRACKED	
BEAM NO.: 89	1.030	1.016
C BEAM:6/4	CRACKED	
BEAM NO.: 90	1.243	1.193

TABLE (7.8) - Continued

SPECIMENS AND DATA FILE DESIGNATION	THEORETICAL	EMPIRICAL
C BEAM:6/8	CRACKED	
BEAM NO.: 91	1.280	1.372
C BEAM:6/C	CRACKED	
BEAM NO.: 92	0.942	0.965
C BEAM:6/0	UNCRACKED	
BEAM NO.: 93	1.100	0.813
C BEAM:1/0	UNCRACKED	
BEAM NO.: 94	0.878	0.694
C BEAM:2/0	UNCRACKED	
BEAM NO.: 95	1.169	0.808
C BEAM:2/C	UNCRACKED	
BEAM NO.: 96	1.435	0.897
C BEAM:3/0	UNCRACKED	
BEAM NO.: 97	0.998	0.786
C BEAM:4/0	UNCRACKED	
BEAM NO.: 98	1.046	0.838
C BEAM:5/0	UNCRACKED	
BEAM NO.: 99	0.822	0.775
C BEAM:5/C	CRACKED	
BEAM NO.: 100	1.198	1.281

TABLE (7.9) CORRELATION OF EVANS ET AL (34) TEST RESULTS WITH THEORY.

SPECIMENS AND DATA FILE DESIGNATION	THEORETICAL	EMPIRICAL
C BEAM:EWT1	UNCRACKED	
BEAM NO.: 195	1.030	0.800
C BEAM:EW1	UNCRACKED	
BEAM NO.: 196	1.122	1.090
C BEAM:EW2	UNCRACKED	
BEAM NO.: 197	1.083	1.184
C BEAM:EW3	CRACKED	
BEAM NO.: 198	0.791	1.083
C BEAM:EW4	CRACKED	
BEAM NO.: 199	0.861	1.134
C BEAM:EW5	CRACKED	
BEAM NO.: 200	0.853	1.156
C BEAM:EW6	CRACKED	
BEAM NO.: 201	0.772	1.178
C BEAM:EW8	CRACKED	
BEAM NO.: 202	0.821	1.297
C BEAM:EWT2	UNCRACKED	
BEAM NO.: 203	1.015	0.831
C BEAM:EW11	UNCRACKED	
BEAM NO.: 204	1.133	1.199
C BEAM:EW12	CRACKED	
BEAM NO.: 205	0.961	1.195
C BEAM:EW13	CRACKED	
BEAM NO.: 206	0.928	1.286
C BEAM:EW15	CRACKED	
BEAM NO.: 207	0.845	1.265
C BEAM:EW18	CRACKED	
BEAM NO.: 208	0.734	1.305
C BEAM:EW8	CRACKED	
BEAM NO.: 209	0.000	

TABLE (7.10) CORRELATION OF McMULLEN AND WOODHEAD'S (37) TEST RESULTS WITH THEORY.

SPECIMENS AND DATA FILE DESIGNATION	THEORETICAL	EMPIRICAL
C BEAM I-1	CRACKED	
BEAM NO.: 262	0.000	1.287
C BEAM I-2	CRACKED	
BEAM NO.: 263	0.670	1.585
C BEAM I-3	CRACKED	
BEAM NO.: 264	0.751	1.623
C BEAM I-4	CRACKED	
BEAM NO.: 265	0.842	1.680
C BEAM: I-5	UNCRACKED	
BEAM NO.: 266	0.914	0.847
C BEAM: I-6	CRACKED	
BEAM NO.: 267	0.754	1.307
C BEAM: I-7	CRACKED	
BEAM NO.: 268	0.758	1.049
C BEAM: I-8	CRACKED	
BEAM NO.: 269	0.769	1.168
C BEAM: II-1	UNCRACKED	
BEAM NO.: 270	1.017	0.811
C BEAM: II-2	CRACKED	
BEAM NO.: 271	1.086	1.633
C BEAM: II-3	CRACKED	
BEAM NO.: 272	0.881	1.667
C BEAM: II-4	CRACKED	
BEAM NO.: 273	1.071	1.482
C BEAM: II-5	CRACKED	
BEAM NO.: 274	0.927	1.103
C BEAM: III-1	CRACKED	
BEAM NO.: 275	0.000	1.103
C BEAM: III-2	CRACKED	
BEAM NO.: 276	0.962	1.670
C BEAM: III-3	CRACKED	
BEAM NO.: 277	1.049	1.529
C BEAM: III-4	UNCRACKED	
BEAM NO.: 278	1.042	0.830
C BEAM: III-5	CRACKED	
BEAM NO.: 279	0.966	1.308
C BEAM: III-6	UNCRACKED	
BEAM NO.: 280	1.161	1.148
C BEAM: V-1	CRACKED	
BEAM NO.: 281	0.948	1.473
C BEAM: V-2	CRACKED	
BEAM NO.: 282	0.987	1.419
C BEAM: V-3	CRACKED	
BEAM NO.: 283	0.999	1.448
C BEAM: V-4	CRACKED	
BEAM NO.: 284	0.945	1.375
C BEAM: V-5	CRACKED	
BEAM NO.: 285	0.999	1.526
C BEAM: V-6	CRACKED	
BEAM NO.: 286	0.925	1.436
C BEAM: V-7	CRACKED	
BEAM NO.: 287	0.832	1.534

TABLE (7.11) CORRELATION OF HENRY'S (13) TEST RESULTS WITH THEORY.

SPECIMENS AND DATA FILE DESIGNATION	THEORETICAL	EMPIRICAL
C BEAM:IV/1/3	CRACKED	
BEAM NO.: 101	1.460	1.218
C BEAM:IV/2/3	CRACKED	
BEAM NO.: 102	1.345	1.196
C BEAM:IV/3/3	CRACKED	
BEAM NO.: 103	1.502	1.385
C BEAM:IV/4/3	CRACKED	
BEAM NO.: 104	1.562	1.630
C BEAM:IV/1/4	CRACKED	
BEAM NO.: 105	1.389	1.179
C BEAM:IV/2/4	CRACKED	
BEAM NO.: 106	1.425	1.368
C BEAM:IV/3/4	CRACKED	
BEAM NO.: 107	1.541	1.528
C BEAM:IV/4/4	CRACKED	
BEAM NO.: 108	1.590	1.655
C BEAM:IV/1/5	UNCRACKED	
BEAM NO.: 109	1.265	1.085
C BEAM:IV/2/5	CRACKED	
BEAM NO.: 110	1.330	1.128
C BEAM:IV/3/5	CRACKED	
BEAM NO.: 111	1.512	1.381
C BEAM:IV/4/5	CRACKED	
BEAM NO.: 112	1.400	1.322
C BEAM:IV/1/6	CRACKED	
BEAM NO.: 113	1.420	1.203
C BEAM:IV/2/6	CRACKED	
BEAM NO.: 114	1.384	1.249
C BEAM:IV/3/6	CRACKED	
BEAM NO.: 115	1.497	1.471
C BEAM:IV/4/6	CRACKED	
BEAM NO.: 116	-0.039	1.632
C BEAM: V/1/3	UNCRACKED	
BEAM NO.: 117	1.151	1.188
C BEAM: V/2/3	CRACKED	
BEAM NO.: 118	1.343	1.629
C BEAM: V/3/3	CRACKED	
BEAM NO.: 119	1.268	1.414
C BEAM: V/4/3	CRACKED	
BEAM NO.: 120	1.256	1.278
C BEAM: V/1/4	UNCRACKED	
BEAM NO.: 121	1.173	1.187
C BEAM: V/2/4	CRACKED	
BEAM NO.: 122	1.352	1.461
C BEAM: V/3/4	CRACKED	
BEAM NO.: 123	1.343	1.577

TABLE (7.11) - Continued

SPECIMENS AND DATA FILE DESIGNATION	THEORETICAL	EMPIRICAL
C BEAM: V/4/4	CRACKED	
BEAM NO.: 124	1.286	1.641
C BEAM: V/1/5	UNCRACKED	
BEAM NO.: 125	1.120	1.172
C BEAM: V/2/5	CRACKED	
BEAM NO.: 126	1.365	1.479
C BEAM: V/3/5	CRACKED	
BEAM NO.: 127	1.514	1.810
C BEAM: V/4/5	CRACKED	
BEAM NO.: 128	1.390	1.900
C BEAM: V/1/6	UNCRACKED	
BEAM NO.: 129	1.102	1.137
C BEAM: V/2/6	CRACKED	
BEAM NO.: 130	1.332	1.328
C BEAM: V/3/6	CRACKED	
BEAM NO.: 131	1.503	1.811
C BEAM: V/4/6	CRACKED	
BEAM NO.: 132	1.276	1.744

TABLE (7.12) CORRELATION OF McGEE'S (52) TEST RESULTS WITH THEORY.

SPECIMENS AND DATA FILE DESIGNATION	THEORETICAL	EMPIRICAL
C BEAM:W1E/3/	CRACKED	
BEAM NO.: 133	1.318	1.416
C BEAM:W1E/3/	UNCRACKED	
BEAM NO.: 134	1.263	1.132
BEAM:W1E/3/	UNCRACKED	
BEAM NO.: 135	1.285	1.059
C BEAM:W1E/0/	CRACKED	
BEAM NO.: 136	0.000	
C BEAM:W1E/4.	CRACKED	
BEAM NO.: 137	1.259	1.499
C BEAM:W1E/4.	CRACKED	
BEAM NO.: 138	1.287	1.330
C BEAM:W1E/4.	UNCRACKED	
BEAM NO.: 139	1.095	0.950
C BEAM:W1E/LC	CRACKED	
BEAM NO.: 140	0.000	0.950
C BEAM:W2E/3/	CRACKED	
BEAM NO.: 141	1.410	1.323
C BEAM:W2E/3/	UNCRACKED	
BEAM NO.: 142	1.267	1.124
C BEAM:W2E/3/	UNCRACKED	
BEAM NO.: 143	1.403	1.039
C BEAM:W2E/0/	CRACKED	
BEAM NO.: 144	0.000	1.039
C BEAM:W2E/4.	CRACKED	
BEAM NO.: 145	1.425	1.521
C BEAM:W2E/4.	CRACKED	
BEAM NO.: 146	1.560	1.412
C BEAM:W2E/4.	UNCRACKED	
BEAM NO.: 147	1.207	0.827
C BEAM:W2E/LC	CRACKED	

TABLE (7.13) CORRELATION OF BELOW'S (65) TEST RESULTS WITH THEORY.

SPECIMENS AND DATA FILE DESIGNATION	THEORETICAL	EMPIRICAL
C BEAM : P1	CRACKED	
BEAM NO.: 288	0.726	1.098
C BEAM : P2	CRACKED	
BEAM NO.: 289	0.758	1.058
C BEAM : P3	CRACKED	
BEAM NO.: 290	0.674	1.039
C BEAM : P4	CRACKED	
BEAM NO.: 291	0.710	1.074
C BEAM : P5	CRACKED	
BEAM NO.: 292	0.655	1.021
C BEAM : Q1	CRACKED	
BEAM NO.: 293	0.724	0.714
C BEAM : Q2	CRACKED	
BEAM NO.: 294	0.697	0.778
C BEAM : Q3	CRACKED	
BEAM NO.: 295	0.529	0.829
C BEAM : Q4	CRACKED	
BEAM NO.: 296	0.574	0.907
C BEAM : Q5	CRACKED	
BEAM NO.: 297	0.588	0.926
C BEAM : Q6	CRACKED	
BEAM NO.: 298	0.526	0.874
C BEAM : Q7	UNCRACKED	
BEAM NO.: 299	0.465	0.795
C BEAM : Q8	UNCRACKED	
BEAM NO.: 300	0.356	0.713
C BEAM : Q9	UNCRACKED	
BEAM NO.: 301	0.379	0.724

TABLE (7.14) CORRELATION OF MUKHERJEE'S (9) TEST RESULTS WITH THEORY.

SPECIMENS AND DATA FILE DESIGNATION	THEORETICAL	EMPIRICAL
C BEAM: A-101	CRACKED	
BEAM NO.: 210	0.000	
C BEAM: A-102	CRACKED	
BEAM NO.: 211	1.735	1.455
C BEAM: A-103	CRACKED	
BEAM NO.: 212	1.755	1.253
C BEAM: A-104	CRACKED	
BEAM NO.: 213	1.754	1.190
C BEAM: A-105	UNCRACKED	
BEAM NO.: 214	1.323	1.079
C BEAM: A-106	UNCRACKED	
BEAM NO.: 215	1.378	1.029
C BEAM: B-121	CRACKED	
BEAM NO.: 216	0.000	1.029
C BEAM: B-122	CRACKED	
BEAM NO.: 217	1.170	1.586
C BEAM: B-123	CRACKED	
BEAM NO.: 218	1.230	1.421
C BEAM: B-124	UNCRACKED	
BEAM NO.: 219	1.447	1.278
C BEAM: B-125	UNCRACKED	
BEAM NO.: 220	1.454	1.145
C BEAM: B-126	UNCRACKED	
BEAM NO.: 221	1.408	1.031
C BEAM: B-127	CRACKED	
BEAM NO.: 222	0.989	1.663
C BEAM: C-201	CRACKED	
BEAM NO.: 223	0.000	1.663
C BEAM: C-202	CRACKED	
BEAM NO.: 224	1.865	1.252
C BEAM: C-203	CRACKED	
BEAM NO.: 225	1.767	1.081
C BEAM: C-204	UNCRACKED	
BEAM NO.: 226	1.143	1.077
C BEAM: C-204	UNCRACKED	
BEAM NO.: 227	1.069	1.031
C BEAM: C-205	UNCRACKED	
BEAM NO.: 228	1.028	0.954
C BEAM: C-206	UNCRACKED	
BEAM NO.: 229	0.980	0.877
C BEAM: C-207	CRACKED	
BEAM NO.: 230	1.600	1.302
C BEAM: D-221	CRACKED	
BEAM NO.: 231	0.000	1.302
C BEAM: D-222	CRACKED	
BEAM NO.: 232	1.164	1.548
C BEAM: D-223	UNCRACKED	
BEAM NO.: 233	1.106	1.160
C BEAM: D-224	UNCRACKED	
BEAM NO.: 234	1.086	1.044
C BEAM: D-225	UNCRACKED	
BEAM NO.: 235	1.063	0.970

TABLE (7.14) - Continued

SPECIMENS AND DATA FILE DESIGNATION	THEORETICAL	EMPIRICAL
C BEAM: D-226	UNCRACKED	
BEAM NO.: 236	1.020	0.894
C BEAM: D-227	CRACKED	
BEAM NO.: 237	0.981	1.590
C BEAM: VA-10	CRACKED	
BEAM NO.: 238	0.000	1.590
C BEAM: VA-10	CRACKED	
BEAM NO.: 239	1.531	1.384
C BEAM: VA-10	CRACKED	
BEAM NO.: 240	1.770	1.207
C BEAM: VA-10	UNCRACKED	
BEAM NO.: 241	1.268	1.050
C BEAM: VA-10	CRACKED	
BEAM NO.: 242	1.096	1.280
C BEAM: VB-12	CRACKED	
BEAM NO.: 243	0.000	1.280
C BEAM: VB-12	CRACKED	
BEAM NO.: 244	1.174	1.739
C BEAM: VB-12	CRACKED	
BEAM NO.: 245	1.179	1.448
C BEAM: VB-12	UNCRACKED	
BEAM NO.: 246	1.358	1.275
C BEAM: VB-12	UNCRACKED	
BEAM NO.: 247	1.327	1.071
C BEAM: VB-12	CRACKED	
BEAM NO.: 248	0.925	1.688
C BEAM: VC-20	CRACKED	
BEAM NO.: 249	0.000	1.688
C BEAM: VC-20	CRACKED	
BEAM NO.: 250	1.913	1.420
C BEAM: VC-20	UNCRACKED	
BEAM NO.: 251	1.080	1.054
C BEAM: VC-20	UNCRACKED	
BEAM NO.: 252	1.061	0.991
C BEAM: VC-20	UNCRACKED	
BEAM NO.: 253	0.949	0.889
C BEAM: VC-20	CRACKED	
BEAM NO.: 254	1.450	1.315
C BEAM: VD-22	CRACKED	
BEAM NO.: 255	0.000	1.315
C BEAM: VD-22	UNCRACKED	
BEAM NO.: 256	1.066	1.165
C BEAM: VD-22	UNCRACKED	
BEAM NO.: 257	1.125	1.050
C BEAM: VD-22	UNCRACKED	
BEAM NO.: 258	0.982	0.919
C BEAM: VD-22	CRACKED	
BEAM NO.: 259	0.962	1.659
C BEAM: S1	CRACKED	
BEAM NO.: 260	1.158	1.646
C BEAM: S2	CRACKED	
BEAM NO.: 261	1.459	1.287

CHAPTER 8 CONCLUSIONS AND RECOMMENDATIONS FOR FUTURE WORK

CONCLUSIONS

8.1 Detailed conclusions from the experimental investigation are presented in Chapter 3, where it has been concluded that torsional strength varies directly proportional to the prestress, the concrete strength and the prestressing steel, and is inversely proportional to the aspect ratio. The variation of the torsional strength with the single variable parameters in this investigation is expressed empirically in a linear formula of the format :

$$\frac{kt}{b^2 h} T + \frac{V}{bh} + 1.20 \left\{ \frac{M}{0.85\ bh^2} + \frac{Ps}{bh} + \int tf\ell \right\} = 2\ fsp\ (1 + pc_2/fsp)$$

or in a non-dimensional interaction form :

$$\frac{T}{To} + \frac{V}{Vo} + \frac{M}{Mo} + \frac{Ps}{Po} + \frac{Fs}{Fo} = 1 + \frac{pc_2}{fsp}$$

This formula which is based on an average experimental steel stress lower than the yield point, produces a mean of 1.02 with a standard deviation of 0.13 and a coefficient of variation of 12% for 36 beams tested in this investigation.

In the analysis of a further 207 prestressed beams from previous investigations, the formula produces a mean = 1.19± 0.26 with a coefficient of variation of 22.5%.

8.2 Current approaches based on steel yielding asseumption are contradcited by the experimental evidence from the present investigation.

Analysis of the author's test beams by proposing an alternative partial stirrups yield theory in Section 4.10 with the assumption that

the ultimate steel stress = Ps/As + fsy produces a mean = 1.03± 0.17 with a coefficient of variation of 17% for eleven beams of Series I. This assumption is in better agreement with the experimental increases in the prestressing tendons which did not yield, but is contradicted by the experimental observation of non-yield in the stirrups legs.

8.3 A non-yielding analysis using average shear and direct stresses in the concrete is more consistent with the results of the test beams. The predictions of this method, making use of a continuous criterion for combining direct and shear stresses in the concrete at failure, confirm that member strength is governed by the concrete. This is shown from comparing the Test/Theory ratios obtained by the non-yield and yielding analyses. The conclusion is substantiated by the experimental observations which do not indicate cases of yield in all the steel.

It can further be concluded that the experimental ultimate stress points follow a straight line and not a parabolic variation as predicted by the concrete criterion. The results, however, lie higher than a straight line and below the parabolic curve.

8.4 For the analysis of the problem of torsion combined with bending and shear in concrete beams with stirrups, the method of torque-friction is proposed and developed using an average steel stress. The resulting ultimate torsional equation is of the general linear format :

$$(fi)\ \frac{ktT}{b^2 h} = to + \mu\sigma_n$$

where (fi) is a combined loading factor to modify the pure ultimate strength for differing cases of torsion combined with bending and/or shear.

A general linear interaction equation for combined torsion with bending and/or shear is proposed in the following format :

$$(fi)\ \frac{T}{Tu} = 1$$

It is concluded that the method predicts the strength of the author's beams reasonably well. For Series I beams, the method produces a mean = 1.13 ± 0.16 with a coefficient of variation of 13.9%. Whereas for 27 cracked beams the theory produces a mean of 1.18 ± 0.20 and a coefficient of variation of 16.7%. For the total of 36 beams, a mean = 1.23 ± 0.24 and coefficient of variation of 19.7% is obtained.

For 197 beams from eleven investigations available in the literature, the method produces a coefficient of variation ranging from 2.0 and 16.2%. However for 22 cracked beams from Mukherjee (9) a coefficient of 23.1% is obtained.

The basic method is also verified by comparison to Hsu's (45) 49 reinforced concrete beams for which a mean = 1.23 ± 0.16 with coefficient of variation = 12.7% is obtained.

8.5 The accuracy of the method may be improved by considering the critical strength based on the ultimate shear strength of concrete.

For the author's beams a mean = 1.11 ± 0.10 with a coefficient of variation of 9.4% is obtained for Series I beams. For 36 beams the mean is 1.14 ± 0.15 with a coefficient of variation of 13.2%.

Hsu's beams are predicted with a mean = 1.16 ± 0.13 and 10.8% as a coefficient of variation.

8.6 It is concluded that the torque-friction method provides a rational and simple basis for predicting the ultimate torsional strength. The method may also be developed into a design procedure.

However, for the further use of the method in analysis or design additional qualitative information concerning behaviour of concrete and concrete members subjected to torsion is needed.

Some recommendations for future research are made in the following sections.

RECOMMENDATIONS FOR FUTURE WORK

8.7 Experiments on the torque-friction model in plain, longitudinally reinforced concrete with and without stirrups and prestressed are needed.

Single parameters, similar to the experimental method followed in this thesis, should be investigated. In addition hollow specimens should also be tested.

Precracked and uncracked specimens should be used.

8.8 Experiments in pure torsion are needed on prestressed beams initially precracked. Confining reinforcement should be provided to cross the precrack surface to clarify the nature of the contribution of stirrups legs to strength and rigidity. In these experiments the prestress may be applied to the precracked member using post-tensioning or external prestressing.

Experiments should be extended to include torsion combined with bending and/or shear.

8.9 Tests are needed with single variable parameters on beams subjected to pure torsion to study their torsional stiffness. The expression given by Equation (6.2.60) should therefore be verified or developed further before applying to combined loading conditions.

As a result of these tests and the recommendation of Section 8.8, a theory for the assessment of steel stress in the stirrups legs and longitudinal steel may be accomplished.

8.10 Experiments of single variable parameters are needed on pre-tensioned and post-tensioned beams to assess the effect of bond on the steel stress. The tests should be carried out over a varying shear span.

8.11 Flanged and hollow sections should be tested to relate behaviour and strength to the torsional friction method.

8.12 Theoretical and experimental work is needed to clarify the exact nature of shear friction in concrete and reinforced concrete with particular reference to different bonding characteristics including anchorages and aggregate size.

8.13 Further research in the shear friction phenomenon should involve creep and impact tests.

8.14 Theoretical and experimental work is needed to clarify the exact mechanism of failure of beams in torsion and shear.

8.15 Experiments are needed on prestressed over-reinforced concrete beams to determine rational limits for over-reinforcements particularly in stirrups.

APPENDIX I CRACK PATTERNS AT FAILURE OF THE TEST BEAMS

Legend:

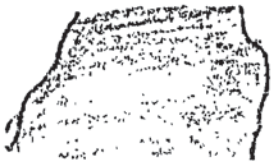

crushing of concrete

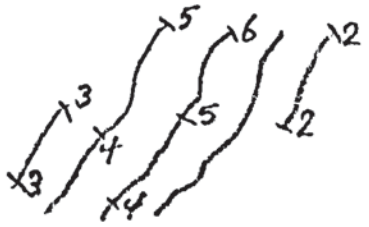

tensile cracks of concrete developed at different increments of applied load

C.L.	Centreline section of the test beam
G.L.	Concrete strain gauge-line
TOP	Top face of the beam
F.F.	Front face of the beam
BTM	Developed surface at the bottom of the beam
B.F.	Back face of the beam.

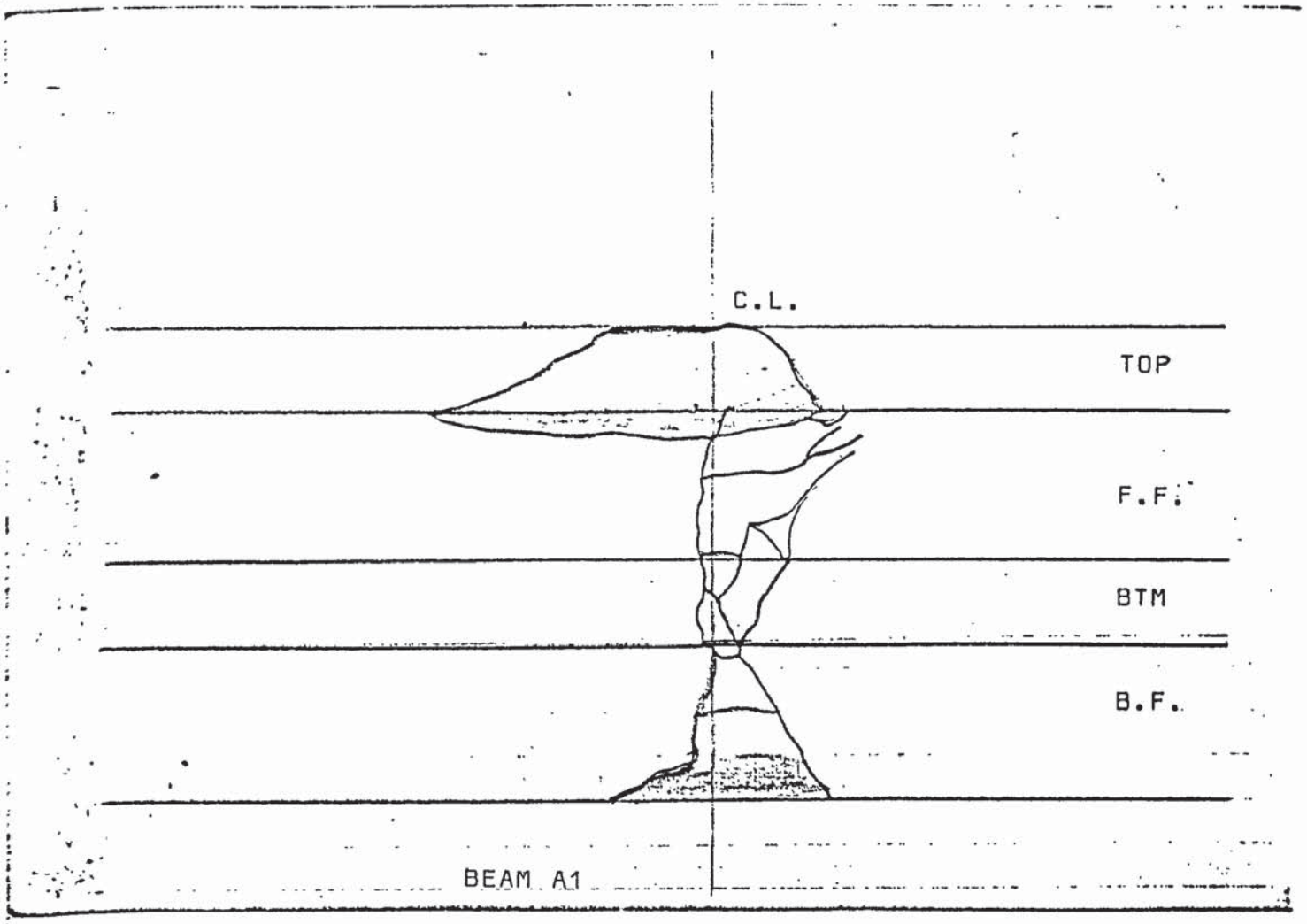

BEAM A1

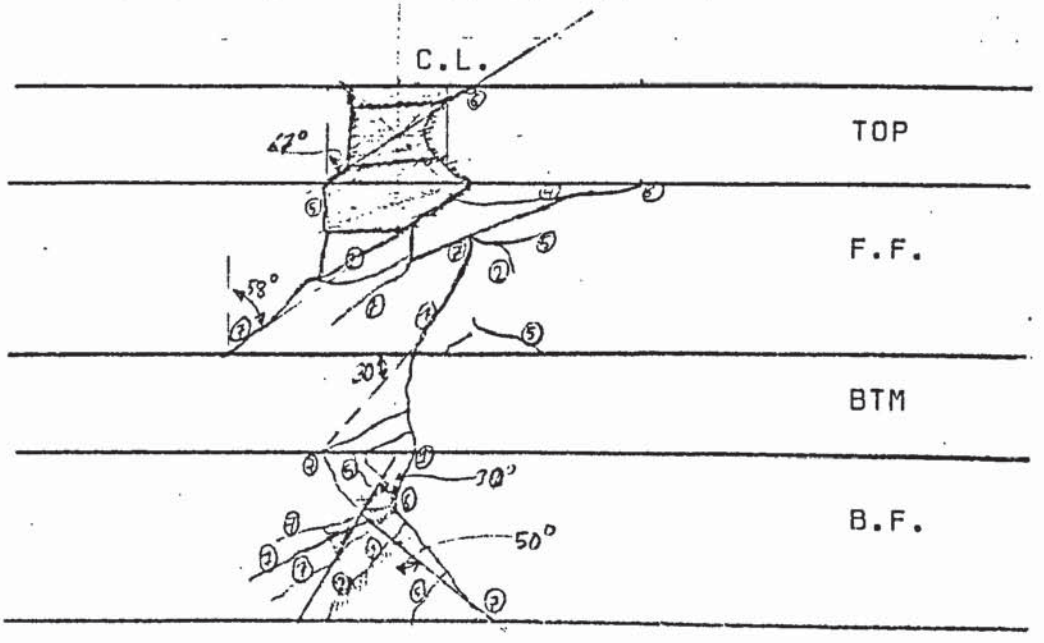

BEAM A3

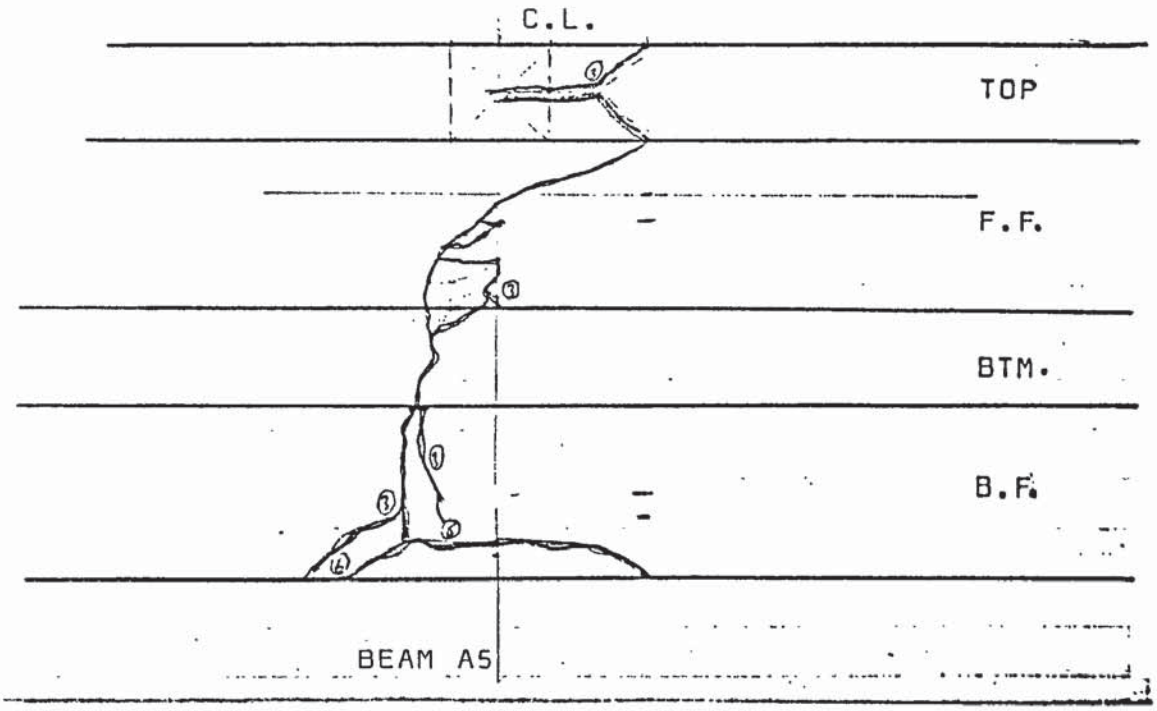
C.L.
TOP
F.F.
BTM.
B.F.
BEAM A5

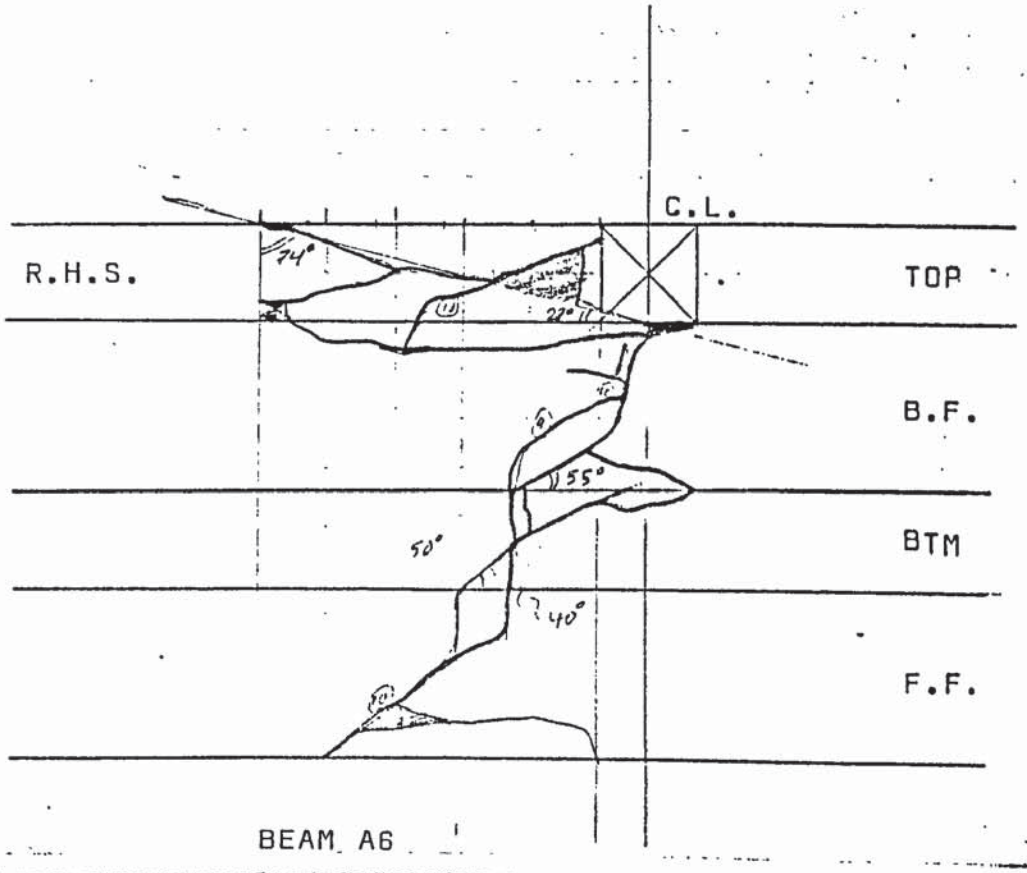
C.L.
R.H.S.
74°
22°
TOP
B.F.
55°
50°
BTM
40°
F.F.
BEAM A6

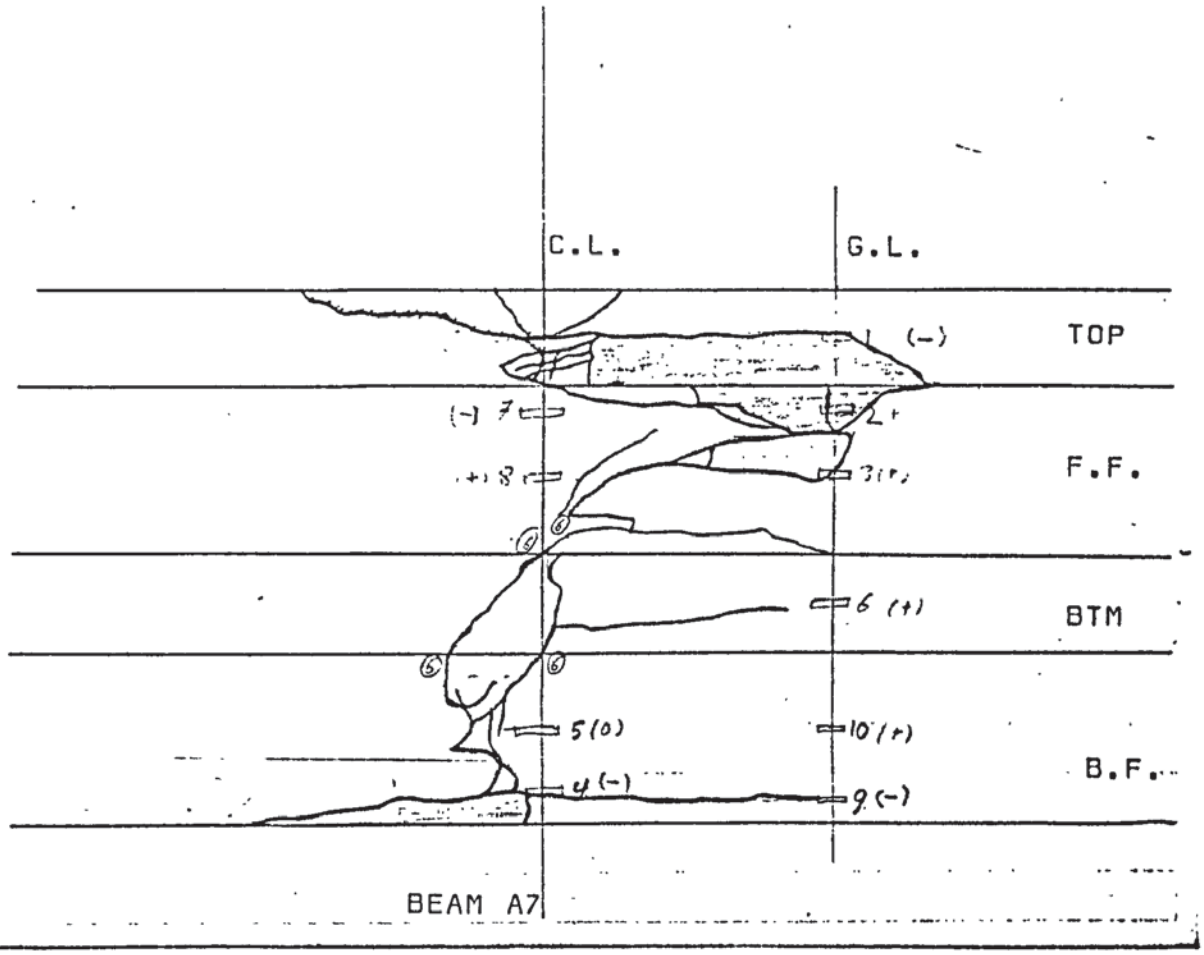

BEAM A7

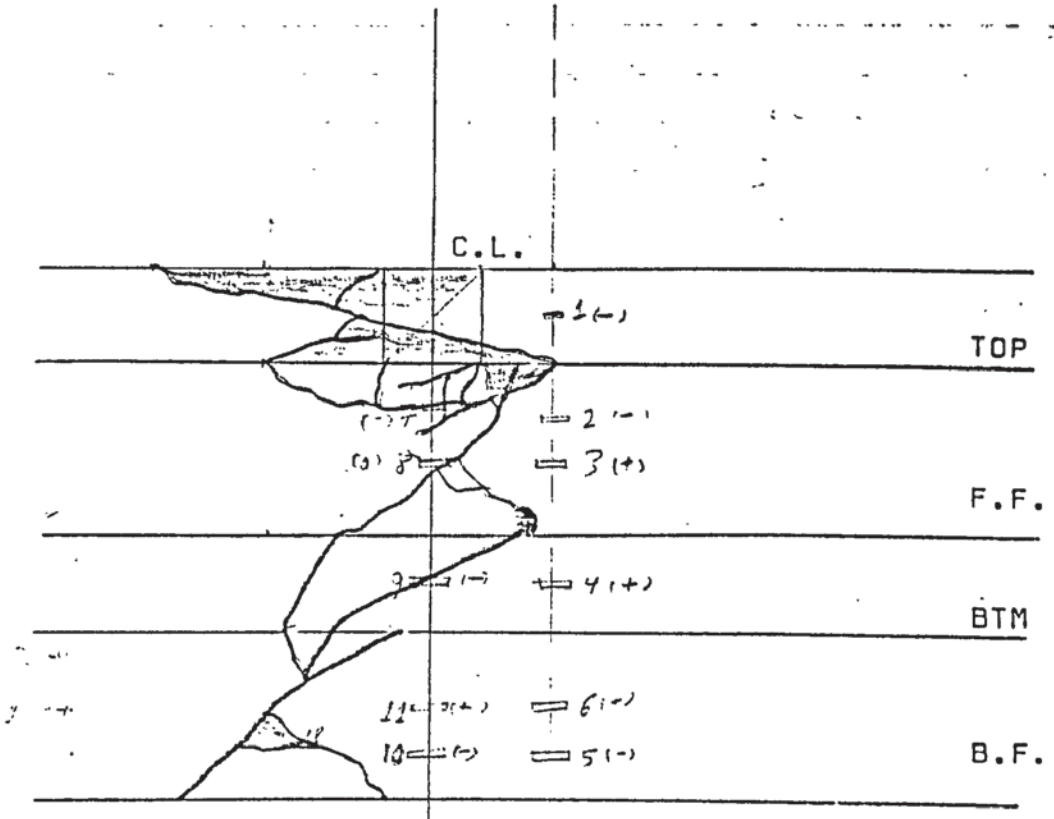

BEAM A8

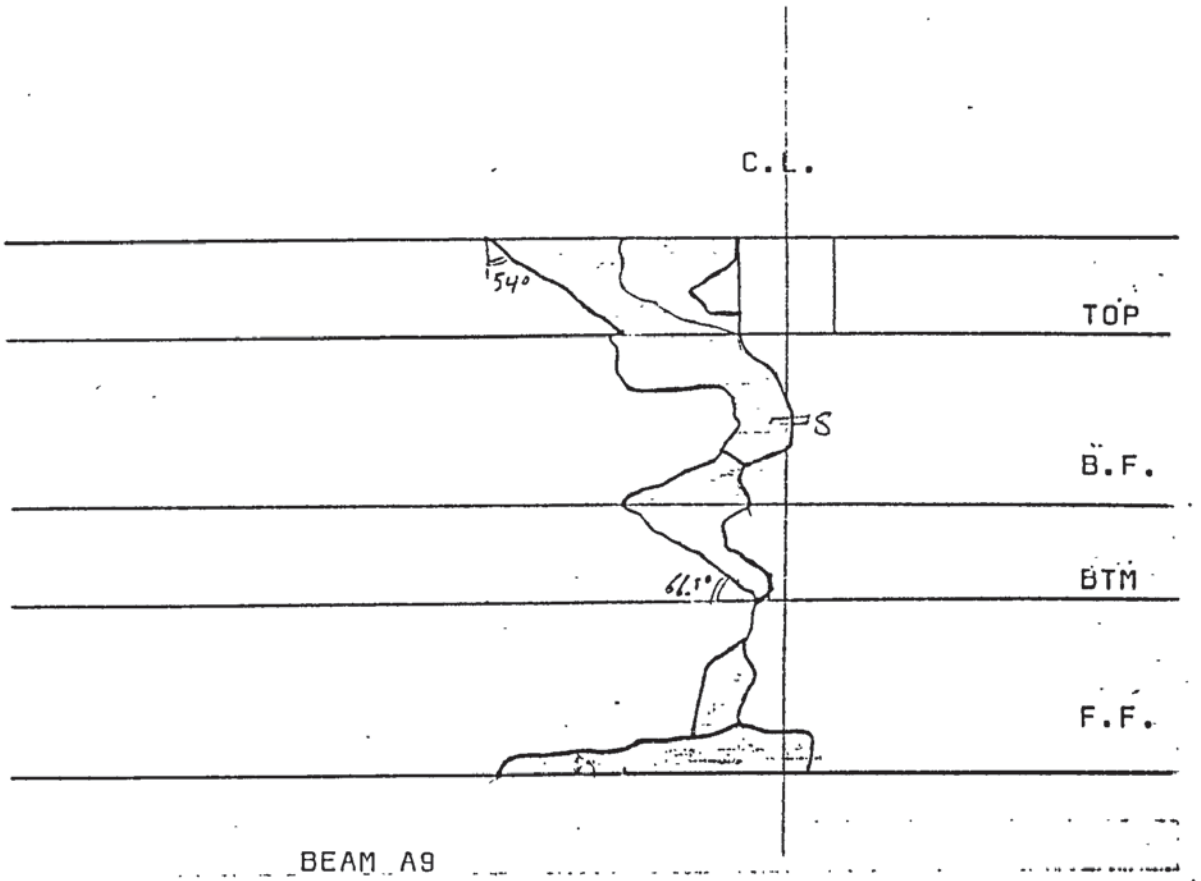

BEAM A9

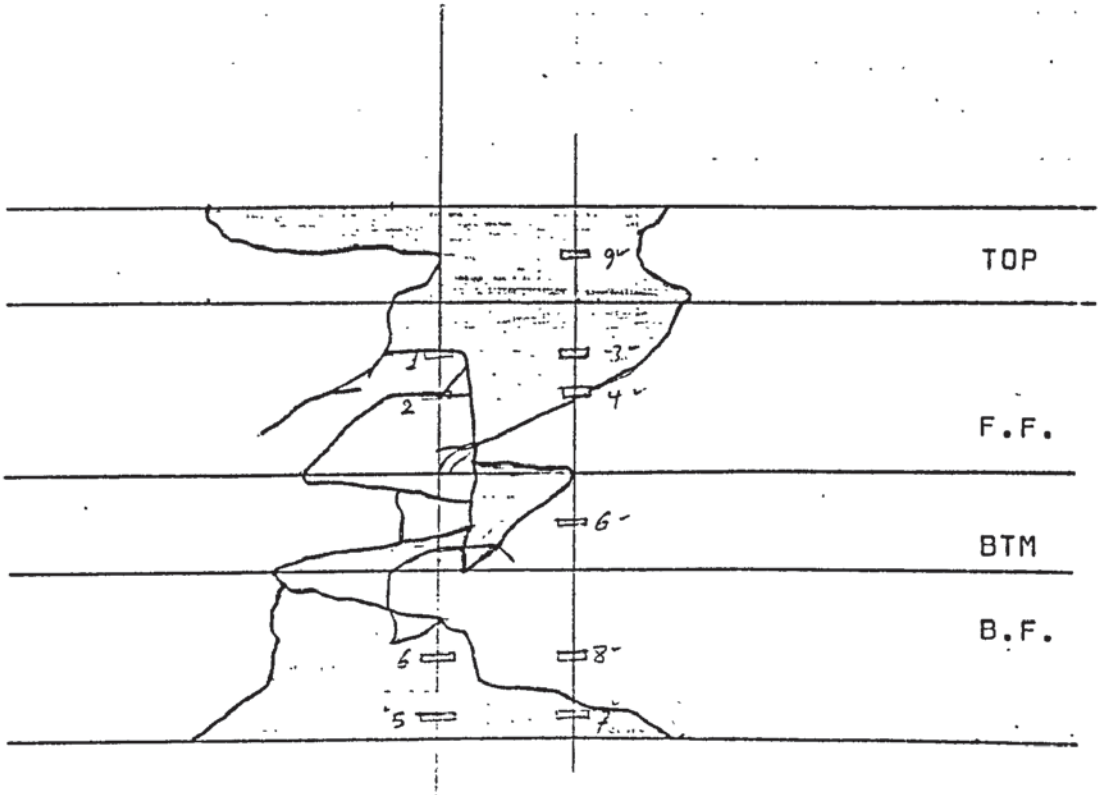

BEAM A10

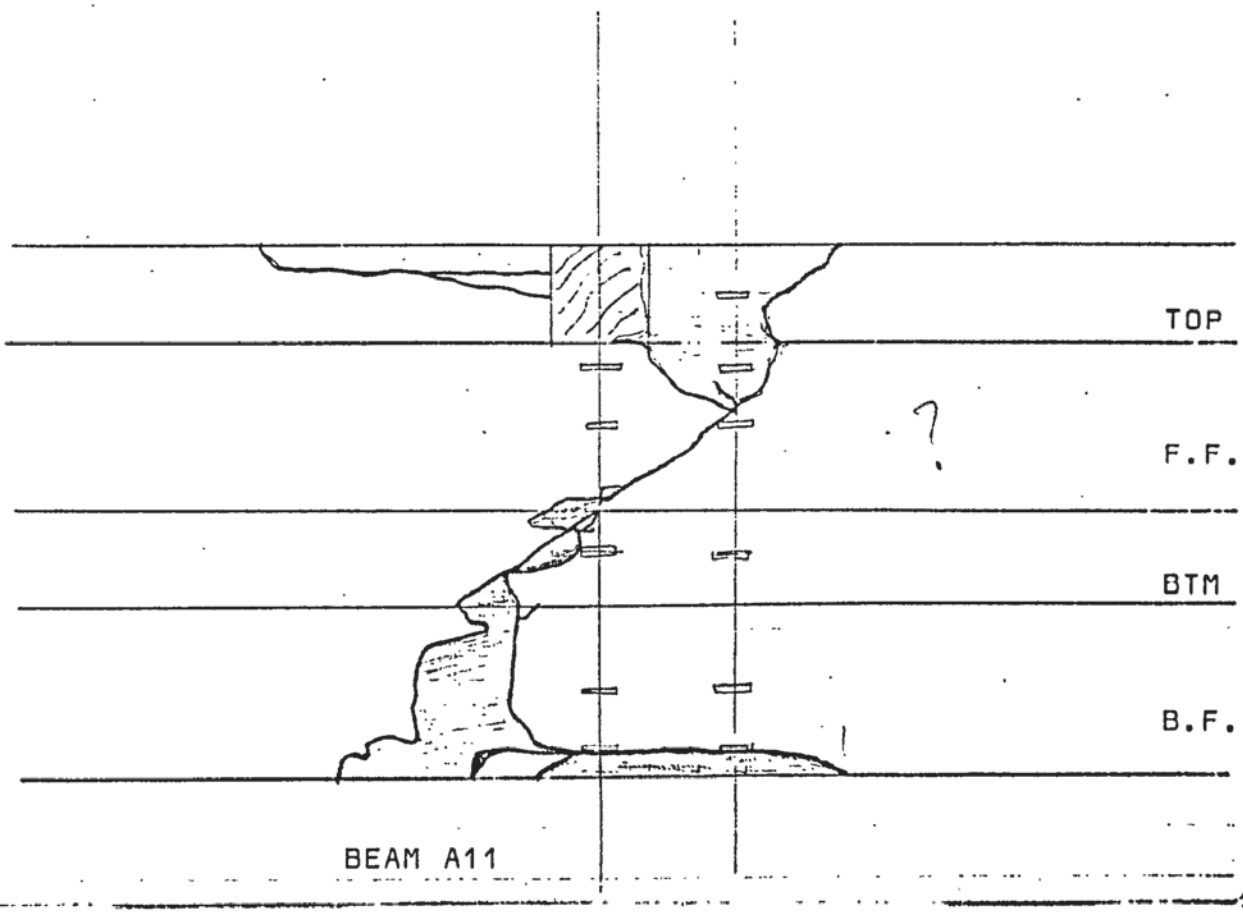

BEAM A11

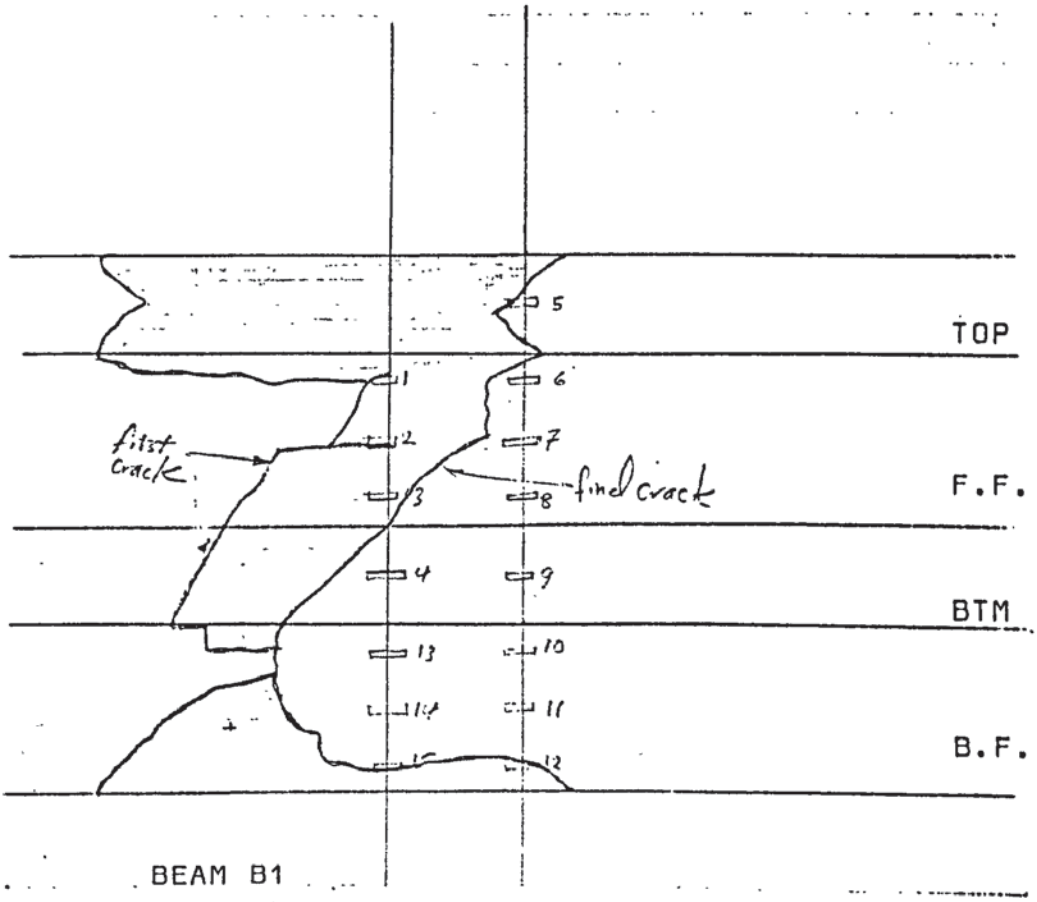

BEAM B1

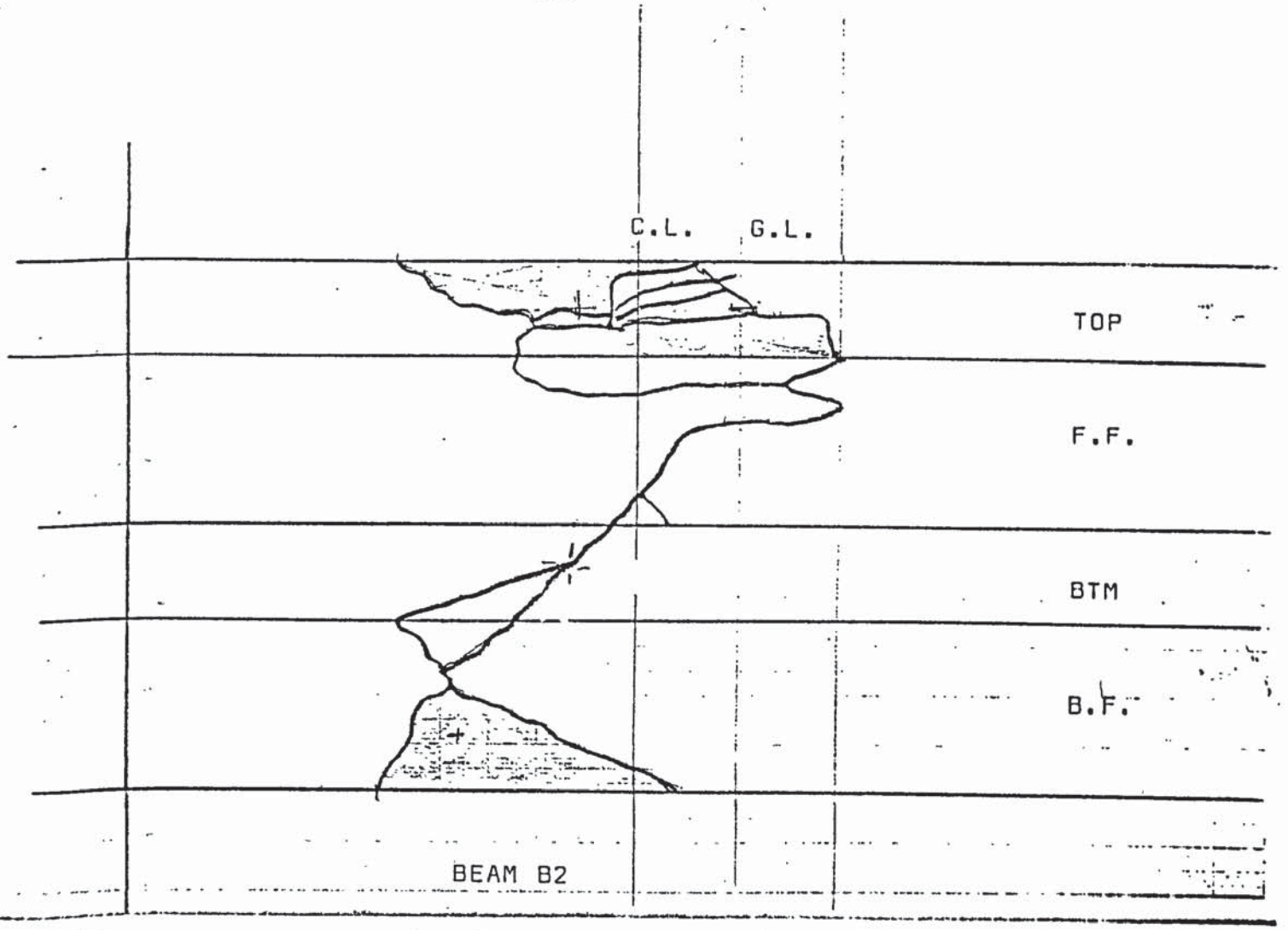
C.L.
G.L.
TOP
F.F.
BTM
B.F.
BEAM B2

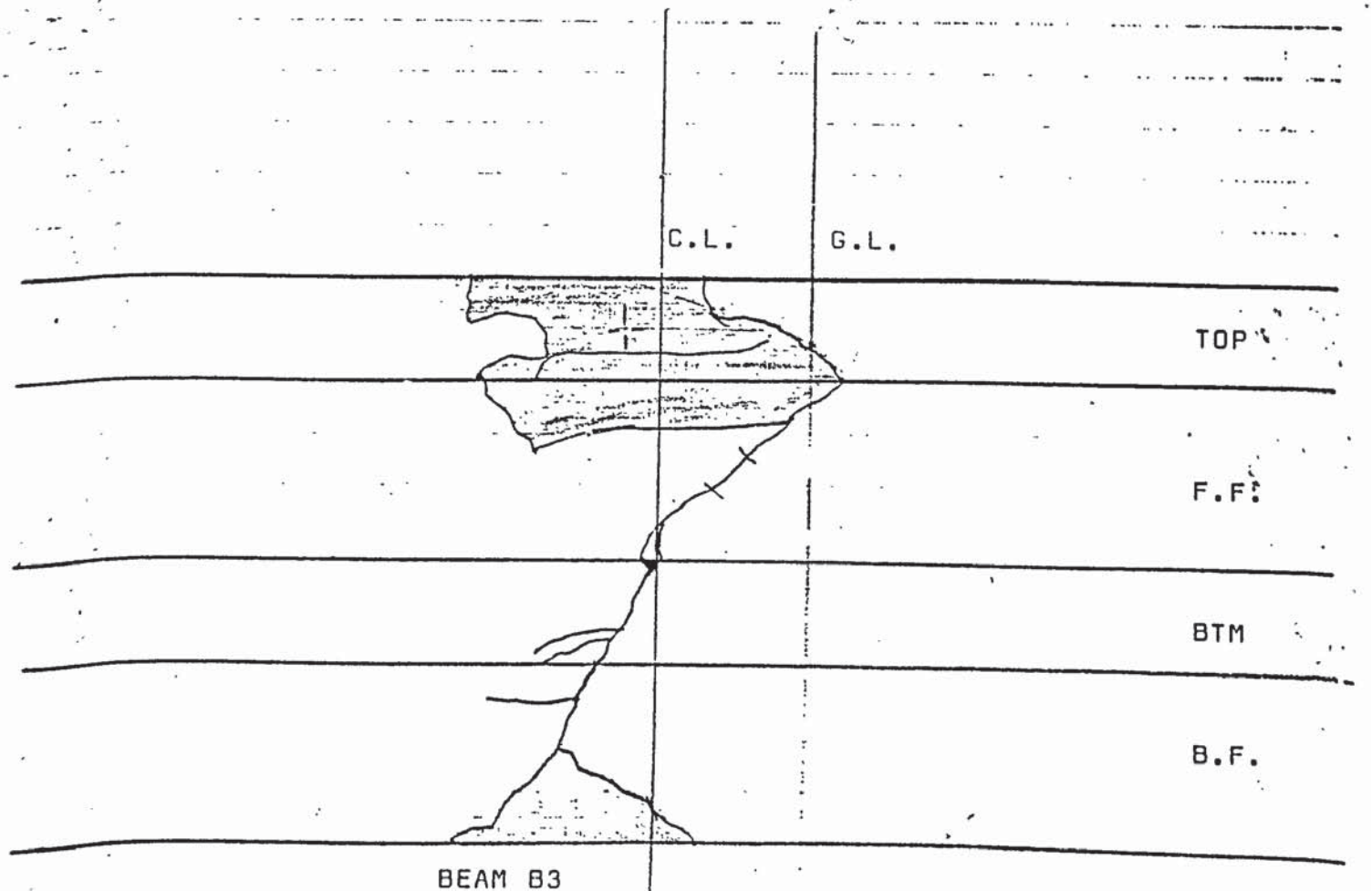
C.L.
G.L.
TOP
F.F.
BTM
B.F.
BEAM B3

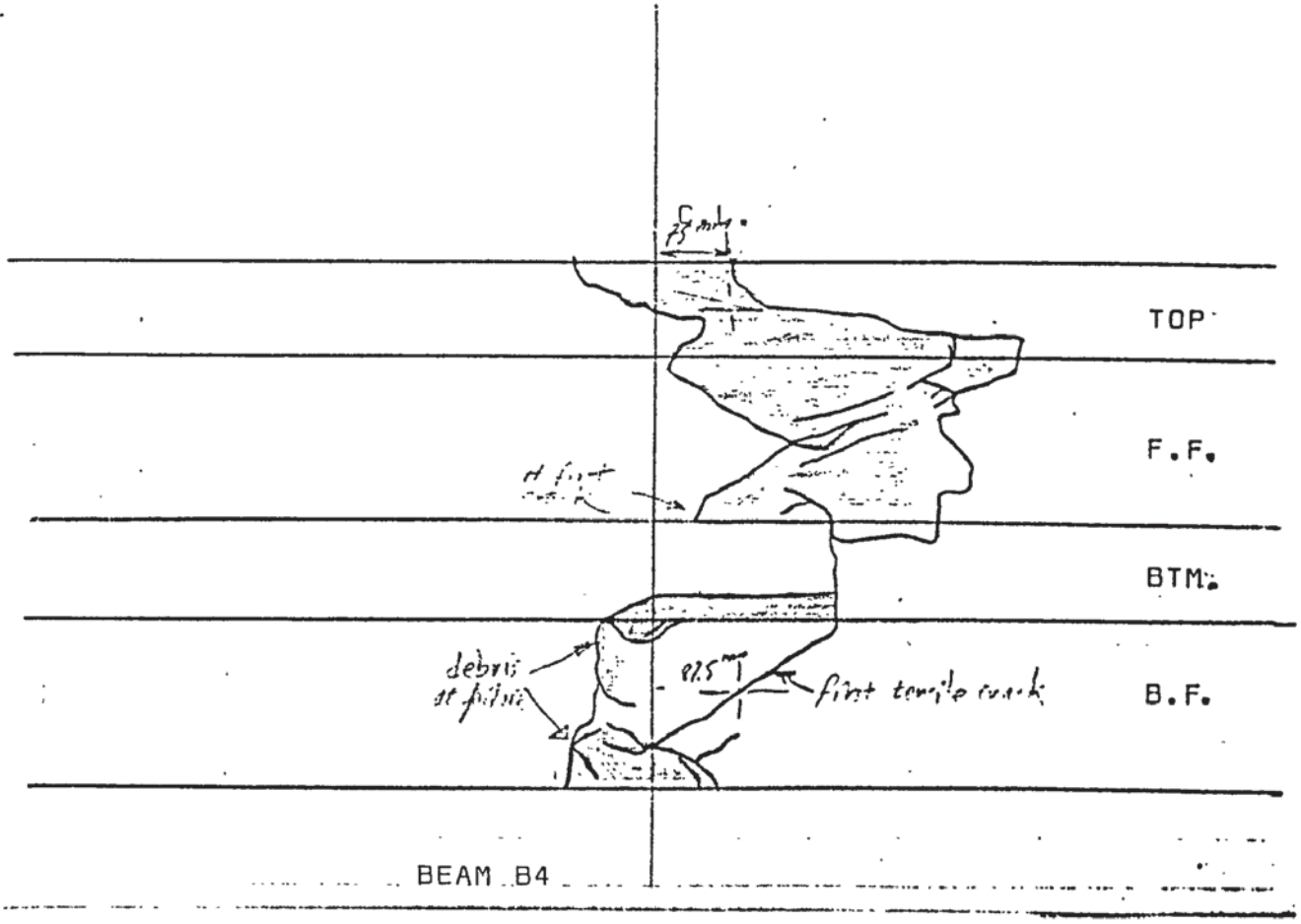

BEAM B4

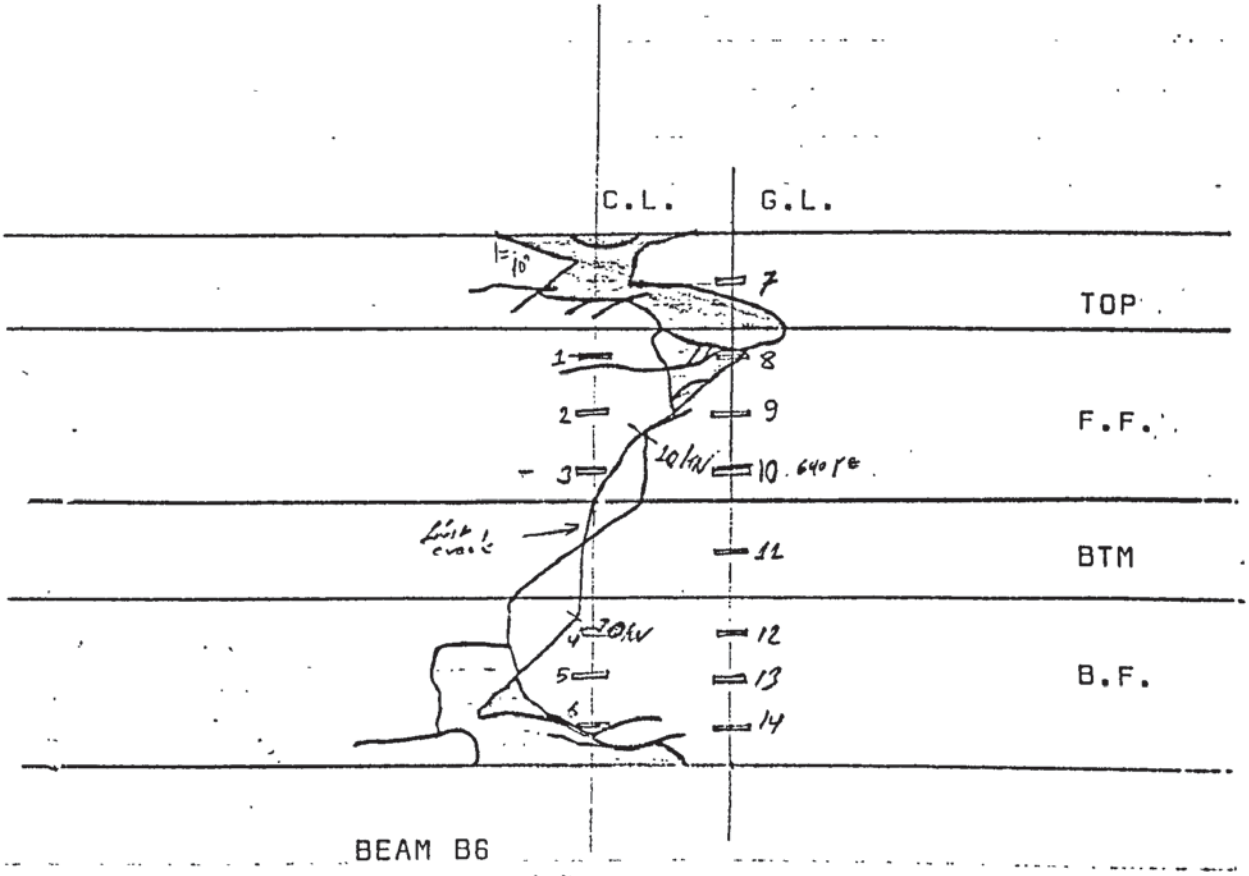

BEAM B6

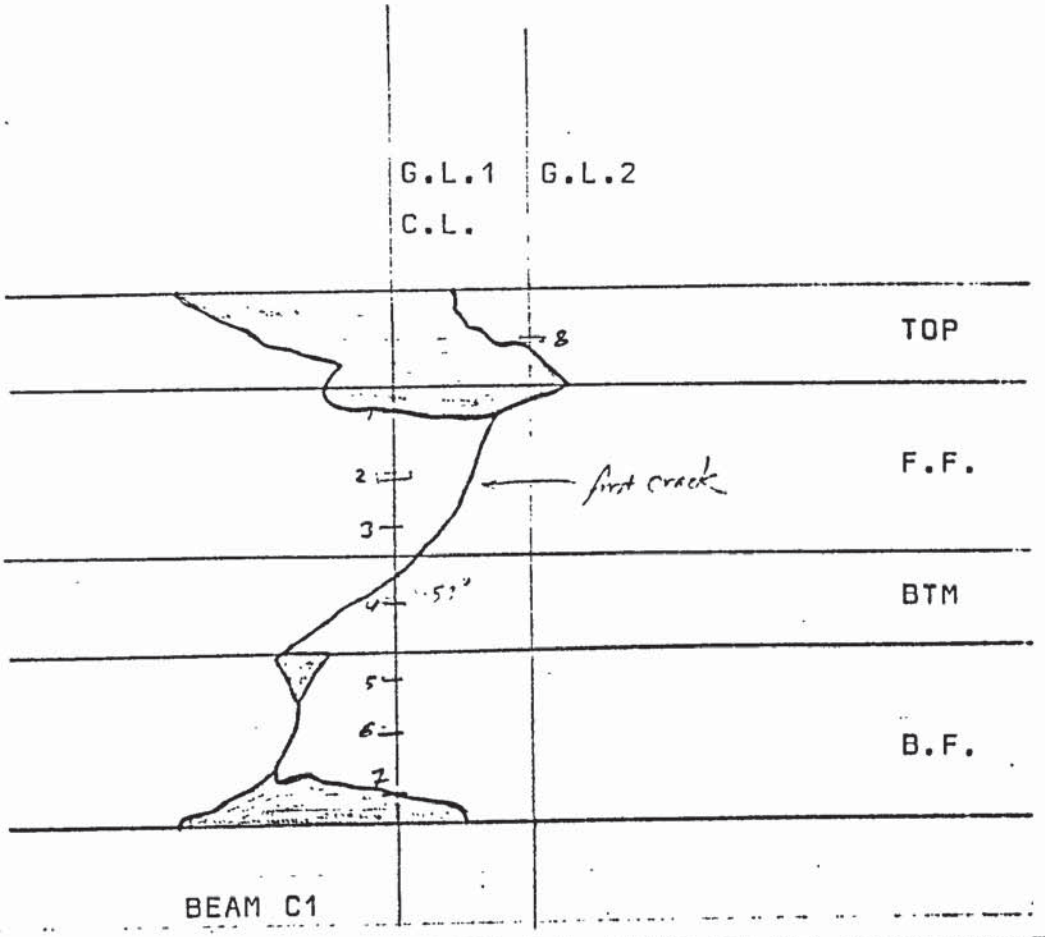

BEAM C1

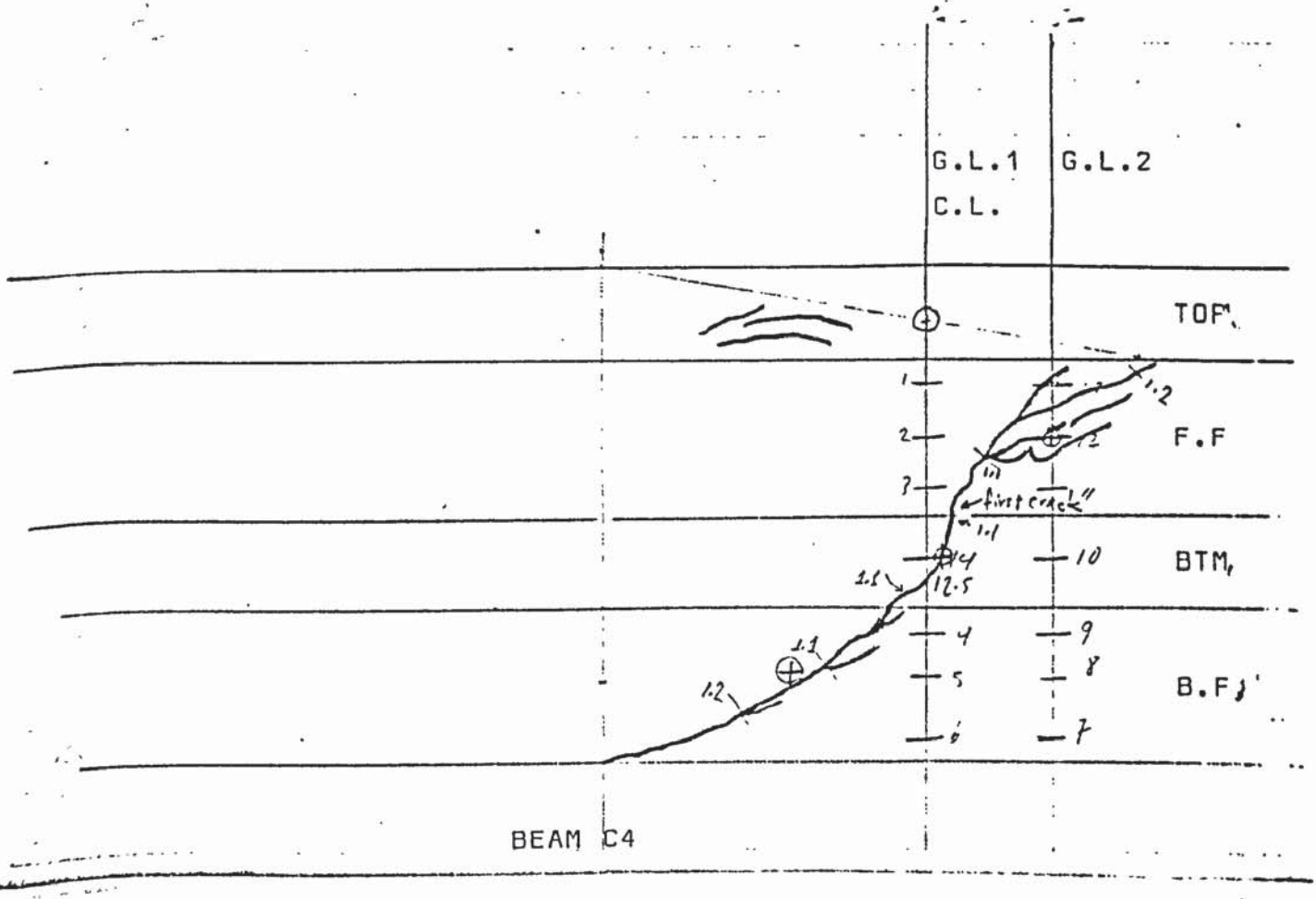

BEAM C4

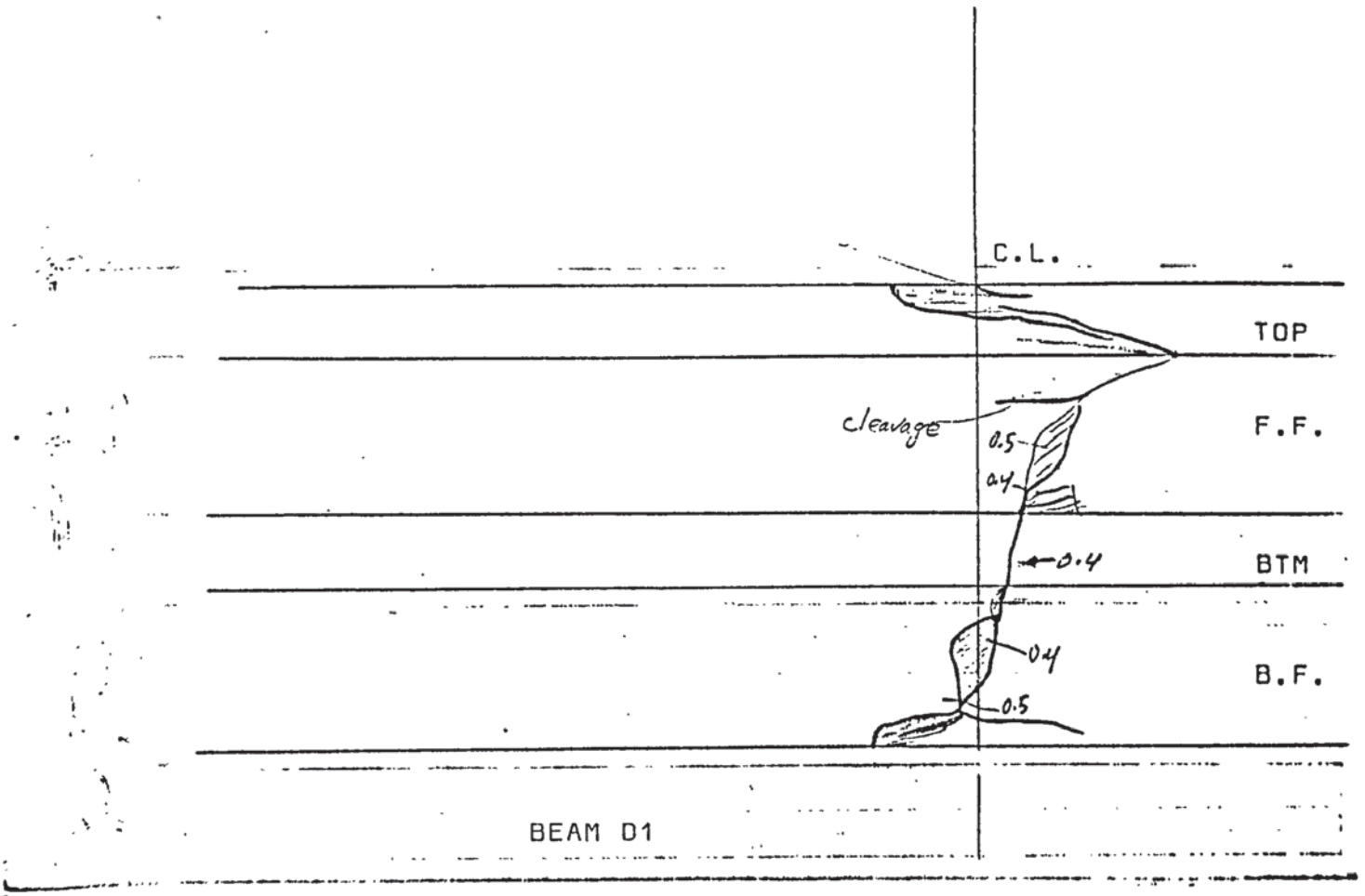

BEAM D1

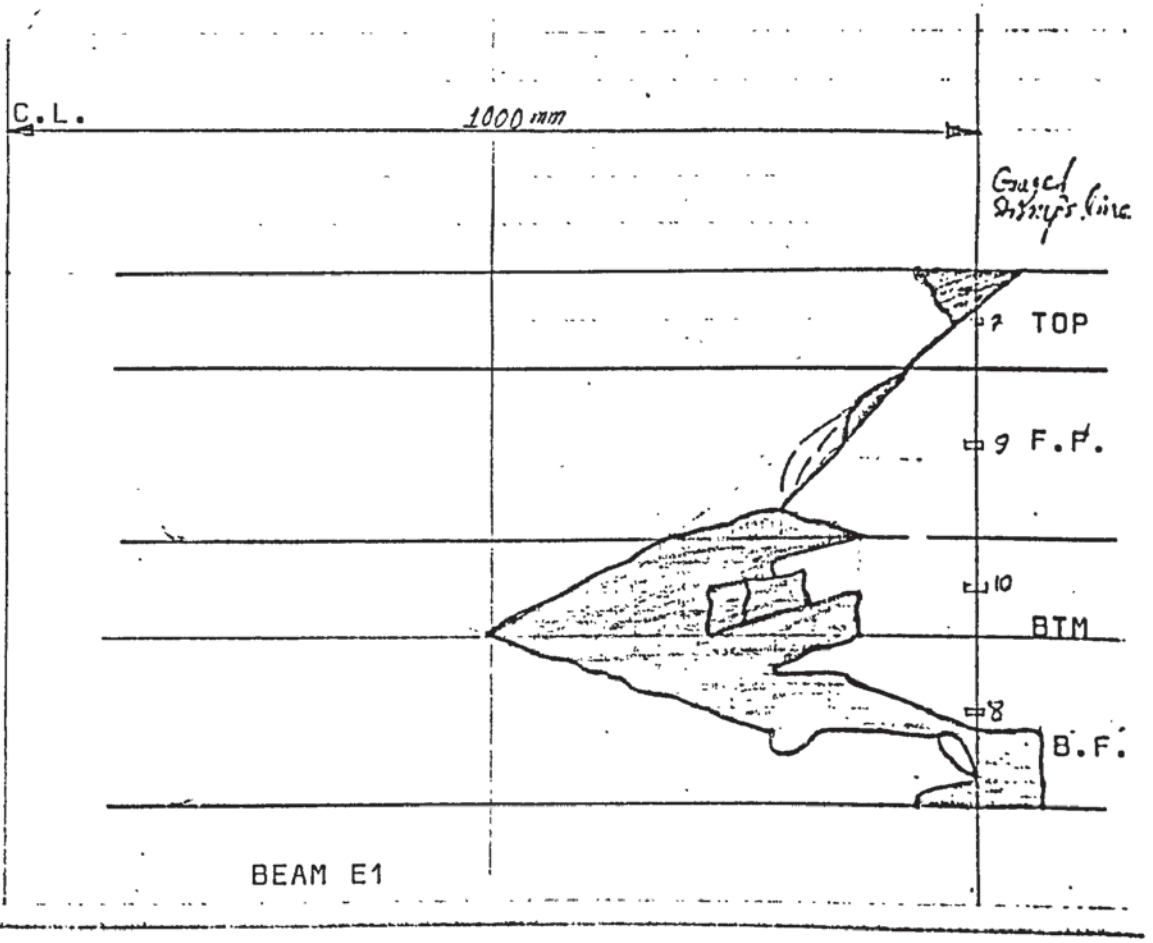

BEAM E1

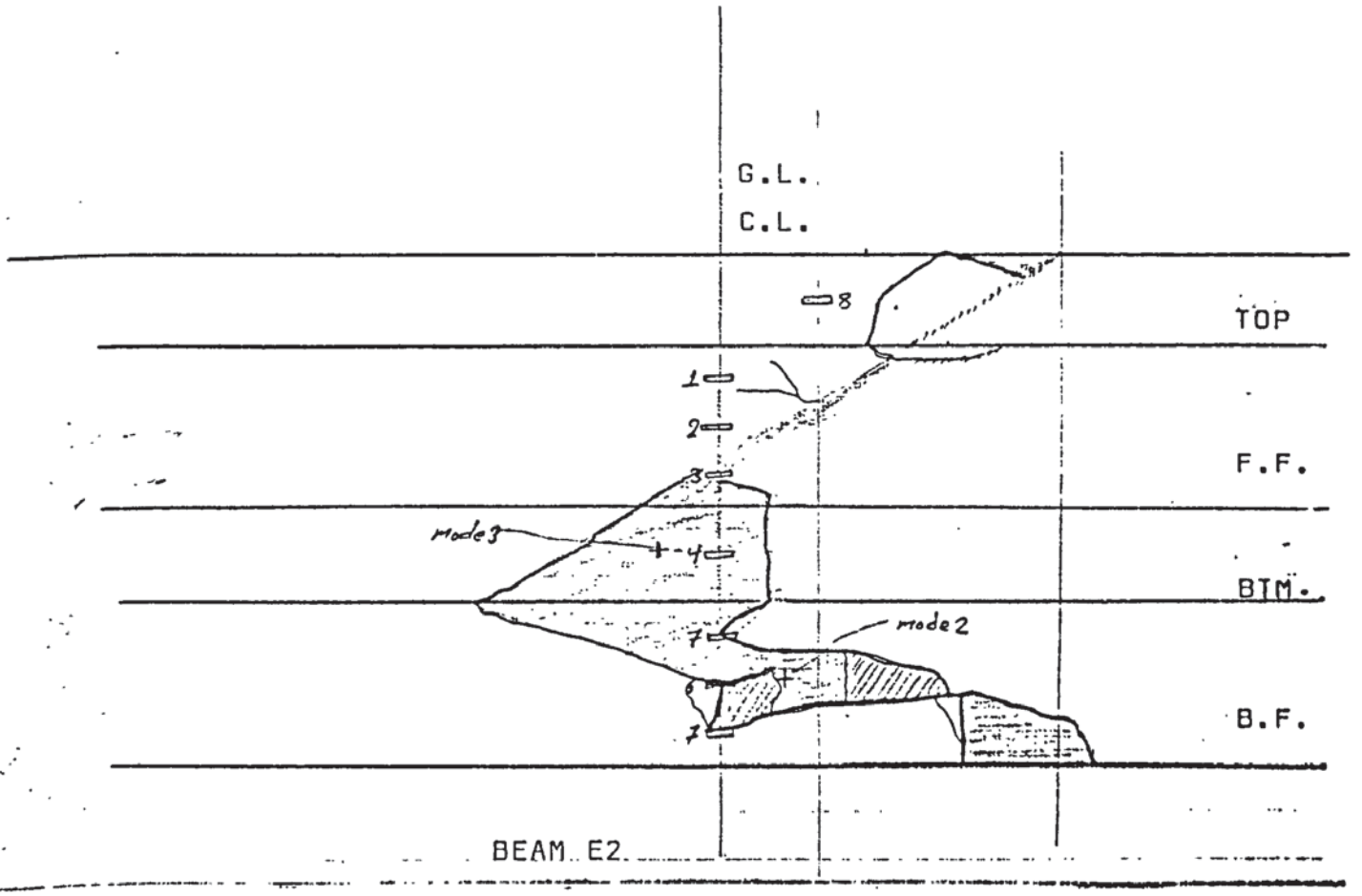

BEAM E2

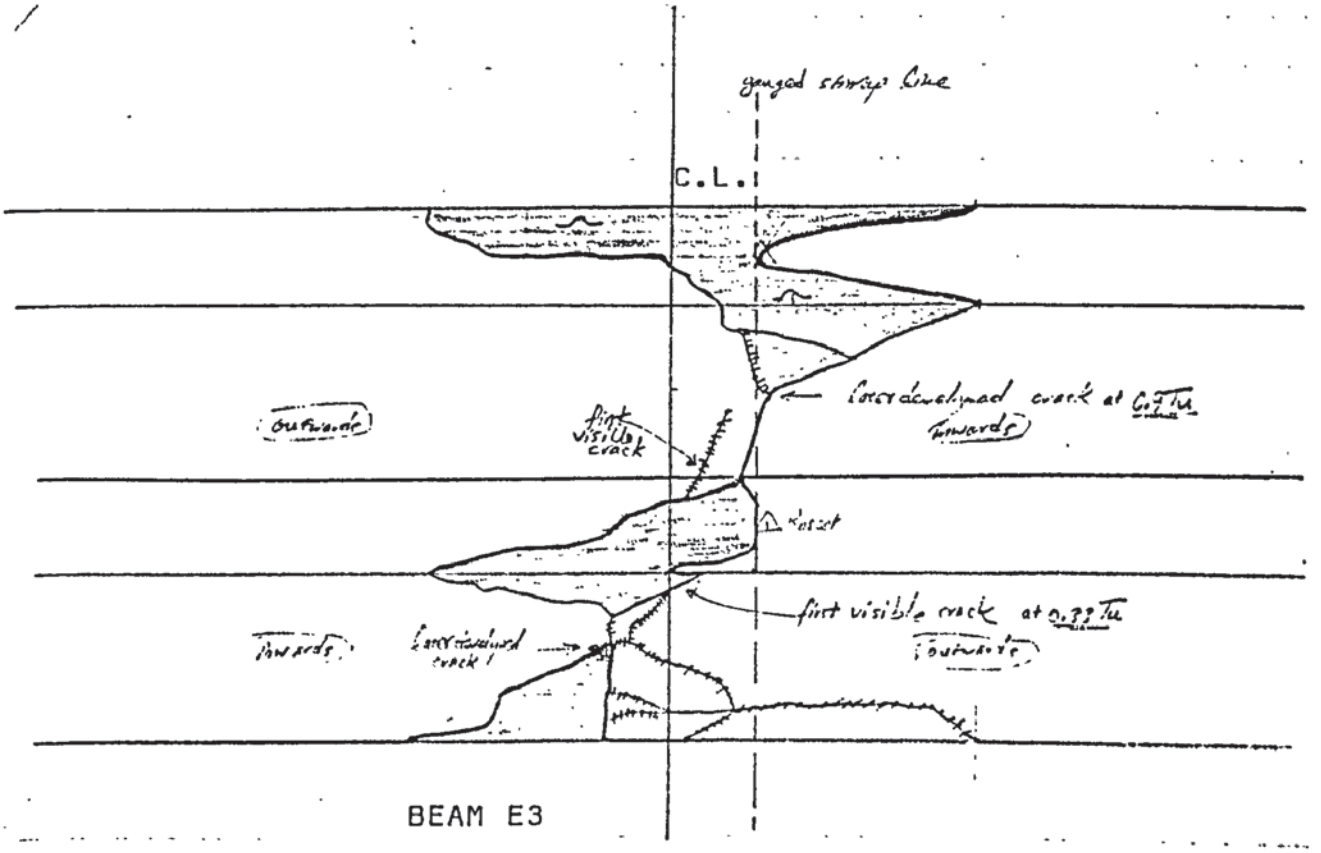

BEAM E3

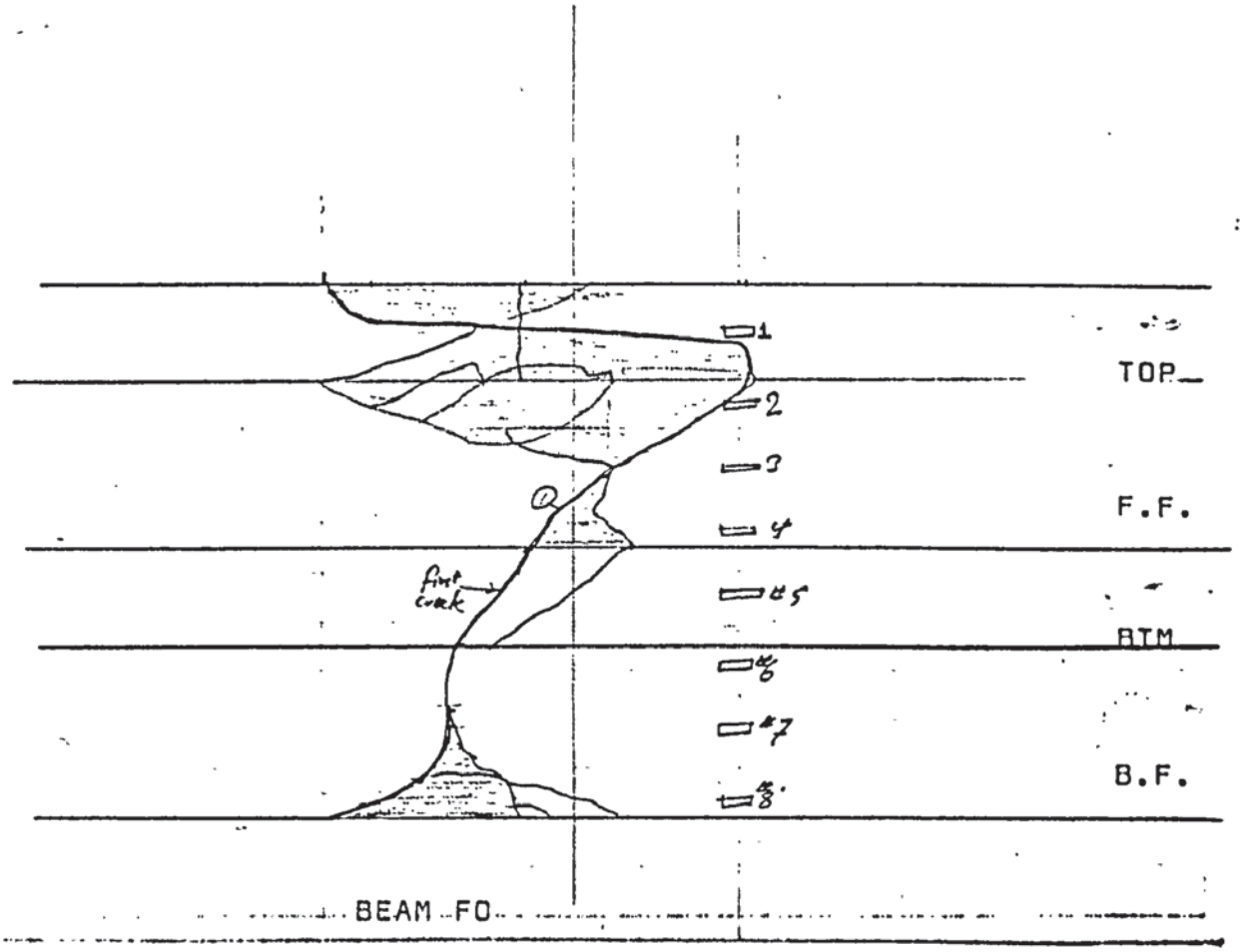

BEAM F0

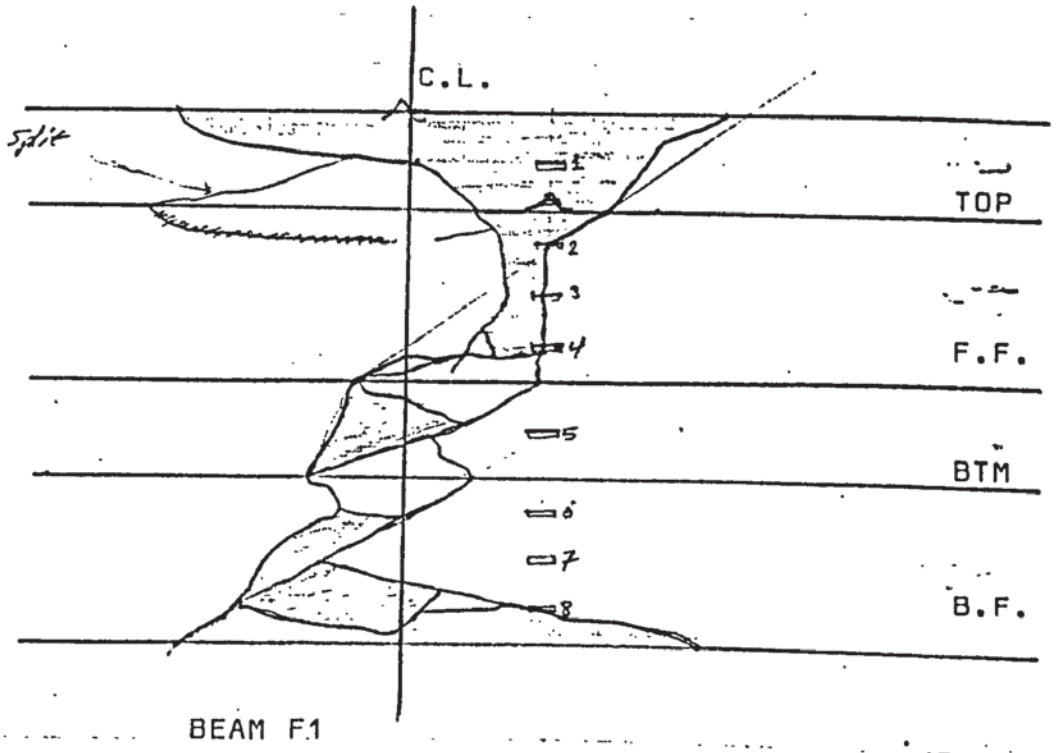

BEAM F1

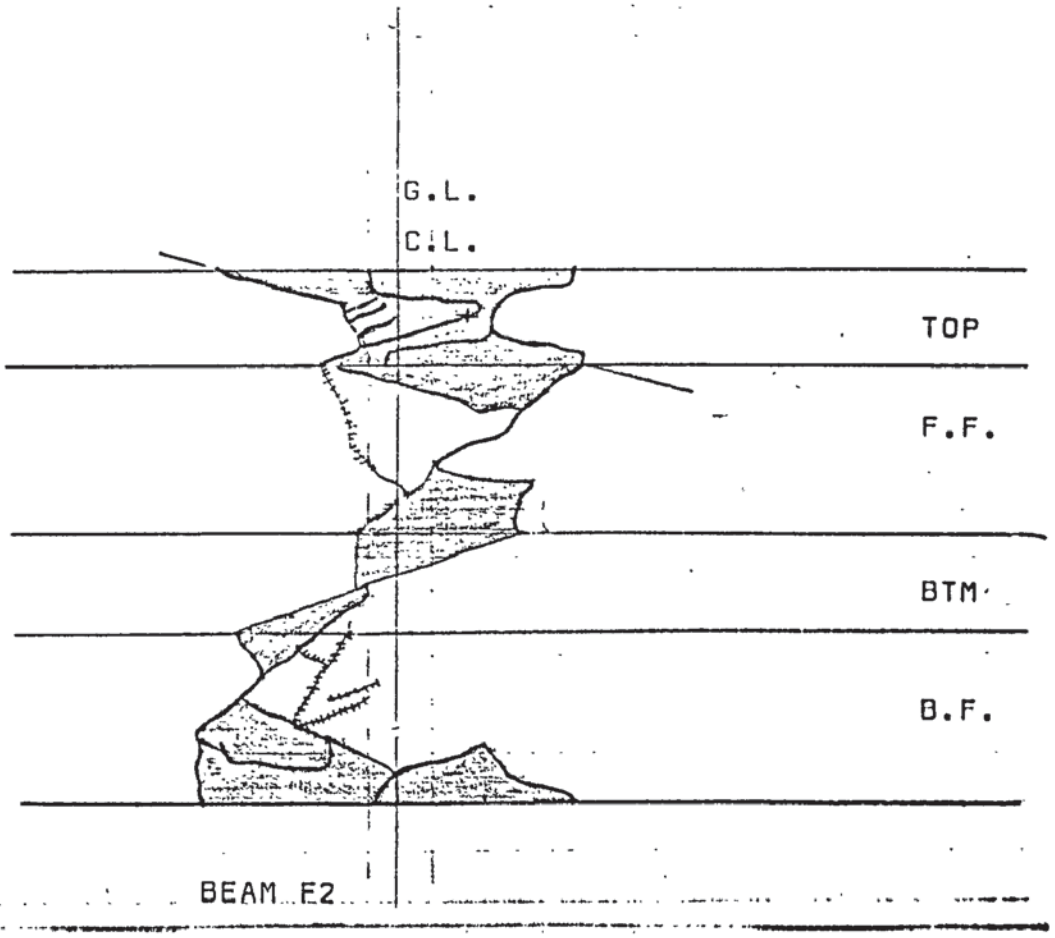

BEAM E2

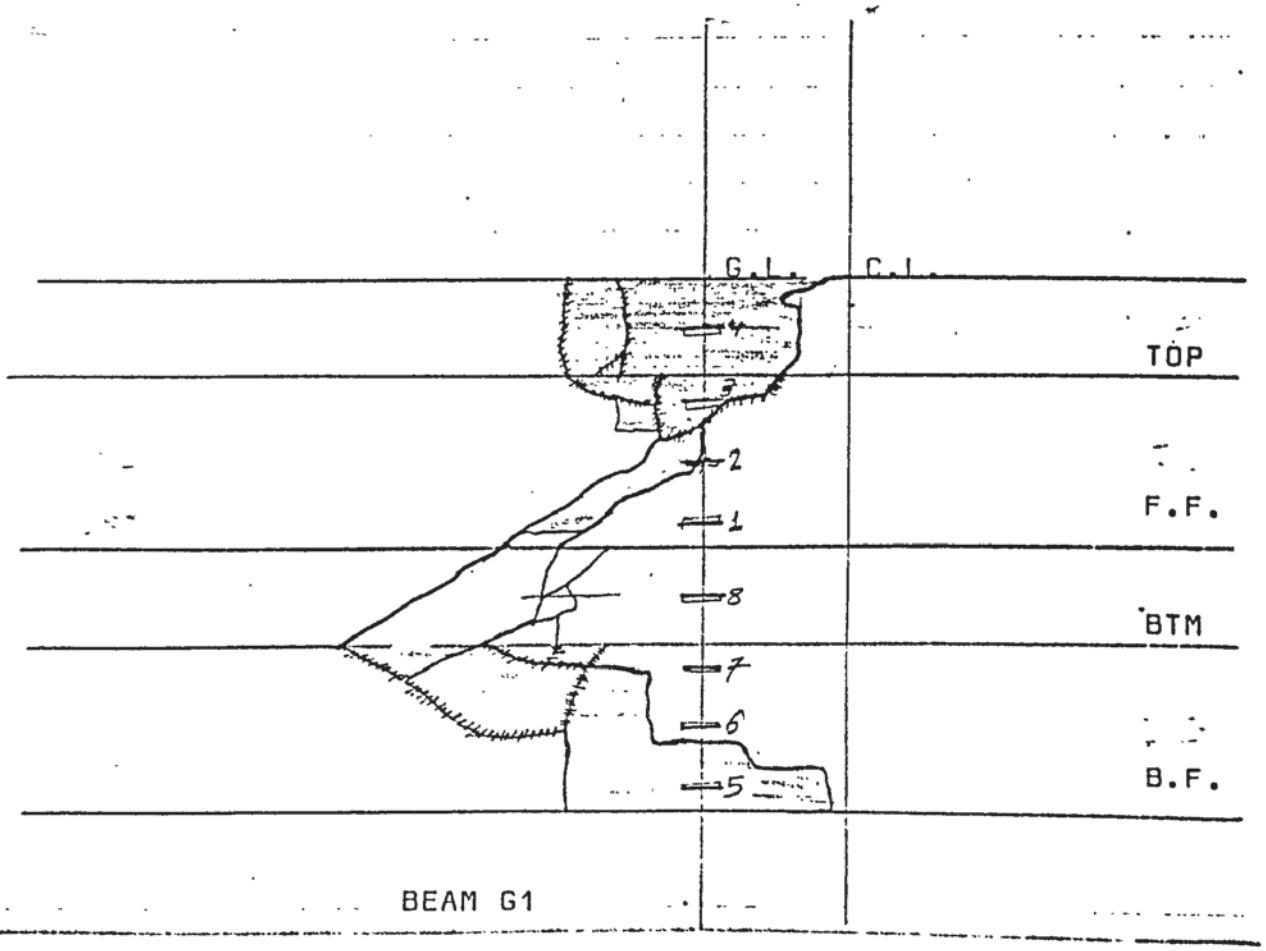

BEAM G1

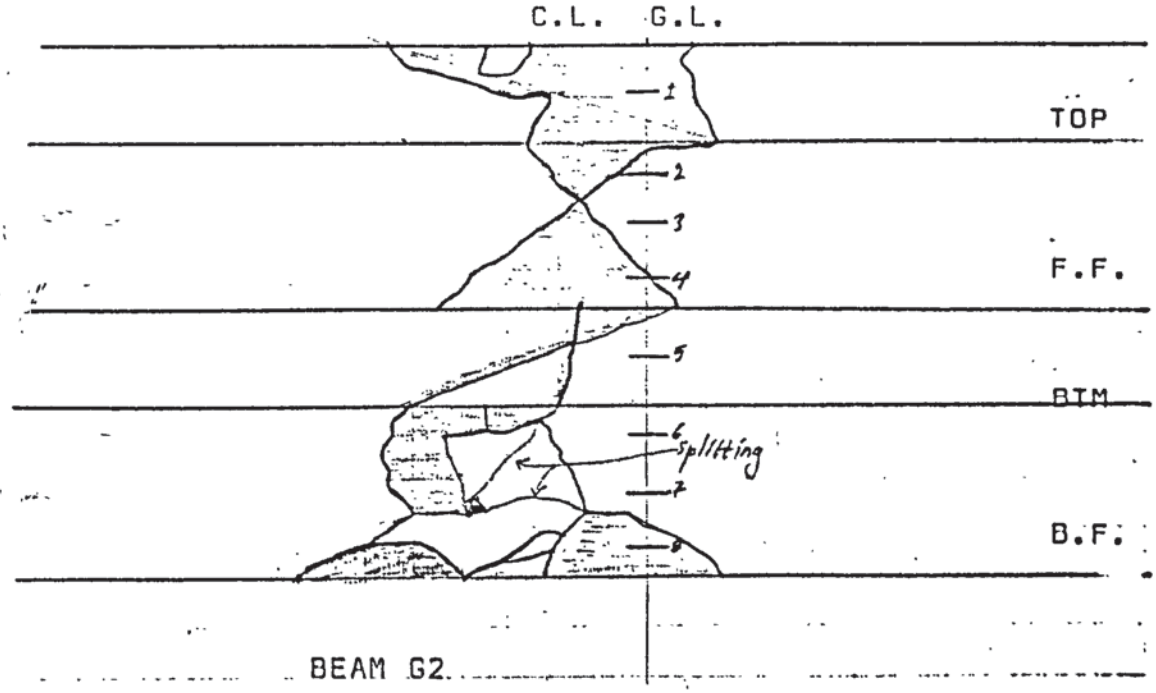

BEAM G2

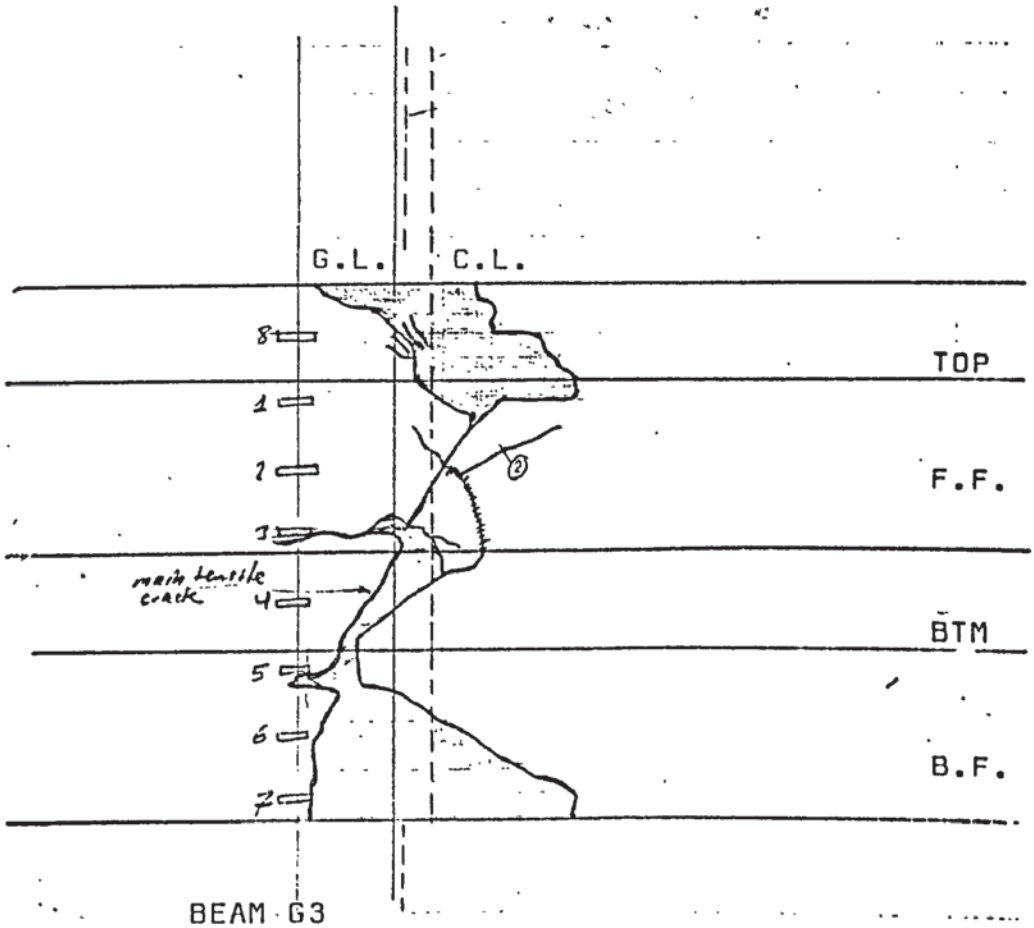

BEAM G3

APPENDIX I I

TABLE A.1. LISTING OF DATA FILE FOR TEST BEAMS USED IN THE COMPARISON OF TEST RESULTS WITH THEORY.

COLUMN

1	Beam Number in the data file
2	Torsion, KN-m
3	Bending Moment, KN-m
4	Shear Force, KN
5	Width, cm
6	Height, cm
7	Average Prestress, N/mm^2
8	Eccentricity, cm
9	Web Steel Ratio, $\rho_w = 2As\ (b' + d')/(bhS)$, (percentage)
10	Total Longitudinal Steel (prestressing and mild) Ratio, $\rho = (A_2 + A1)/(bh)$, (percentage)
11	Cylinder Compressive Strength of Concrete, N/mm^2
12	Modulus of Rupture of Concrete, N/mm^2
13	Yield - stress of Stirrups Steel, KN/mm^2
14	"Yield - stress" of Prestressing Steel, KN/mm^2

1	2	3	4	5	6	7	8	9	10	11	12	13	14
0	6.1	0.0	0.0	10.2	30.5	7.0	0.0	0.6	0.9	49.5	0.0	0.2	1.8
1	6.1	0.0	0.0	10.2	30.5	7.0	0.0	0.6	0.9	49.5	0.0	0.2	1.8
2	5.9	0.0	0.0	10.2	30.5	7.2	5.1	0.6	0.9	47.9	0.0	0.2	1.8
3	5.9	0.0	0.0	10.2	30.5	7.2	5.1	0.6	0.9	47.9	0.0	0.2	1.8
4	6.0	0.0	0.0	10.2	30.5	6.9	6.3	0.6	0.9	47.9	0.0	0.2	1.8
5	6.0	0.0	0.0	10.2	30.5	6.9	6.3	0.6	0.9	47.9	0.0	0.2	1.8
6	5.9	0.0	0.0	8.9	26.7	6.6	0.6	0.7	1.2	45.4	0.0	0.2	1.8
7	5.9	0.0	0.0	8.9	26.7	6.6	0.6	0.7	1.2	45.4	0.0	0.2	1.8
8	5.0	0.0	0.0	8.9	26.7	6.3	5.7	0.7	1.2	46.8	0.0	0.2	1.8
9	5.0	0.0	0.0	8.9	26.7	6.3	5.7	0.7	1.2	46.8	0.0	0.2	1.8
10	5.5	0.0	0.0	8.9	26.7	6.1	7.0	0.7	1.2	47.4	0.0	0.2	1.8
11	5.5	0.0	0.0	8.9	26.7	6.1	7.0	0.7	1.2	47.4	0.0	0.2	1.8
12	5.9	0.0	0.0	8.9	30.5	5.9	1.9	0.7	1.1	32.8	0.0	0.2	1.8
13	5.9	0.0	0.0	8.9	30.5	5.9	1.9	0.7	1.1	32.8	0.0	0.2	1.8
14	6.6	0.0	0.0	8.9	30.5	5.7	7.6	0.7	1.1	36.3	0.0	0.2	1.8
15	6.6	0.0	0.0	8.9	30.5	5.7	7.6	0.7	1.1	36.3	0.0	0.2	1.8
16	6.8	0.0	0.0	8.9	30.5	5.7	8.9	0.7	1.1	36.3	0.0	0.2	1.8
17	6.8	0.0	0.0	8.9	30.5	5.7	8.9	0.7	1.1	36.3	0.0	0.2	1.8
18	5.0	0.0	0.0	10.2	30.5	7.0	0.0	0.69	0.7	55.5	0.0	0.0	1.8
19	5.2	0.0	0.0	10.2	30.5	7.0	0.0	0.0	0.7	55.5	0.0	0.0	1.8
20	5.3	0.0	0.0	10.2	30.5	7.0	0.0	0.0	0.7	56.5	0.0	0.0	1.8
21	5.4	0.0	0.0	10.2	30.5	7.2	5.1	0.0	0.7	58.6	0.0	0.0	1.8
22	5.8	0.0	0.0	10.2	30.5	7.2	5.1	0.0	0.7	58.9	0.0	0.0	1.8
23	5.6	0.0	0.0	10.2	30.5	7.2	5.1	0.0	0.7	58.9	0.0	0.0	1.8
24	5.2	0.0	0.0	10.2	30.5	7.0	6.3	0.0	0.7	58.9	0.0	0.0	1.8
25	5.3	0.0	0.0	10.2	30.5	7.0	6.3	0.0	0.7	58.9	0.0	0.0	1.8
26	4.9	0.0	0.0	10.2	30.5	7.0	6.3	0.0	0.7	58.9	0.0	0.0	1.8
27	5.8	0.0	0.0	8.9	26.7	6.7	0.6	0.0	0.9	45.4	0.0	0.0	1.8
28	5.9	0.0	0.0	8.9	26.7	6.7	0.6	0.0	0.9	45.4	0.0	0.0	1.8
29	4.0	0.0	0.0	8.9	26.7	6.3	5.7	0.0	0.9	46.8	0.0	0.0	1.8
30	3.7	0.0	0.0	8.9	26.7	6.3	5.7	0.0	0.9	46.8	0.0	0.0	1.8
31	3.8	0.0	0.0	8.9	26.7	6.2	7.0	0.0	0.9	46.8	0.0	0.0	1.8
32	3.7	0.0	0.0	8.9	26.7	6.2	7.0	0.0	0.9	47.4	0.0	0.0	1.8
33	5.3	0.0	0.0	8.9	30.5	5.9	1.9	0.0	0.8	32.8	0.0	0.0	1.8
34	5.2	0.0	0.0	8.9	30.5	5.9	1.9	0.0	0.8	32.8	0.0	0.0	1.8
35	5.1	0.0	0.0	8.9	30.5	5.7	7.6	0.0	0.8	36.3	0.0	0.0	1.8

1	2	3	4	5	6	7	8	9	10	11	12	13	14
36	5.7	0.0	0.0	8.9	30.5	5.7	7.6	0.0	0.8	36.3	0.0	0.0	1.8
37	6.1	0.0	0.0	8.9	30.5	5.7	8.9	0.0	0.8	42.8	0.0	0.0	1.8
38	6.0	0.0	0.0	8.9	30.5	5.7	8.9	0.0	0.8	42.8	0.0	0.0	1.8
39	3.4	0.0	0.0	10.2	30.5	0.0	0.0	0.6	0.9	47.9	0.0	0.2	1.8
40	3.5	0.0	0.0	8.9	26.7	0.0	0.0	0.7	1.2	45.4	0.0	0.2	1.8
41	4.1	0.0	0.0	8.9	30.5	0.0	0.0	0.7	1.1	36.3	0.0	0.2	1.8
42	3.2	0.0	0.0	10.2	30.5	0.0	0.0	0.69	0.0	41.4	0.0	0.0	0.0
43	3.0	0.0	0.0	10.2	30.5	0.0	0.0	0.0	0.0	42.8	0.0	0.0	0.0
44	2.7	0.0	0.0	10.2	30.5	0.0	0.0	0.0	0.0	43.8	0.0	0.0	0.0
45	2.8	0.0	0.0	10.2	30.5	0.0	0.0	0.0	0.0	43.8	0.0	0.0	0.0
46	3.2	0.0	0.0	10.2	30.5	0.0	0.0	0.0	0.0	44.1	0.0	0.0	0.0
47	3.6	0.0	0.0	10.2	30.5	0.0	0.0	0.0	0.0	44.1	0.0	0.0	0.0
48	3.2	0.0	0.0	10.2	30.5	0.0	0.0	0.0	0.0	49.5	0.0	0.0	0.0
49	3.4	0.0	0.0	10.2	30.5	0.0	0.0	0.0	0.0	44.8	0.0	0.0	0.0
50	3.5	0.0	0.0	10.2	30.5	0.0	0.0	0.0	0.0	47.9	0.0	0.0	0.0
51	3.8	0.0	0.0	8.9	26.7	0.0	0.0	0.0	0.0	45.4	0.0	0.0	0.0
52	3.6	0.0	0.0	8.9	26.7	0.0	0.0	0.0	0.0	46.8	0.0	0.0	0.0
53	3.3	0.0	0.0	8.9	26.7	0.0	0.0	0.0	0.0	47.4	0.0	0.0	0.0
54	4.5	0.0	0.0	8.9	30.5	0.0	0.0	0.0	0.0	42.8	0.0	0.0	0.0
55	4.8	0.0	0.0	8.9	30.5	0.0	0.0	0.0	0.0	46.2	0.0	0.0	0.0
56	4.4	0.0	0.0	8.9	30.5	0.0	0.0	0.0	0.0	46.2	0.0	0.0	0.0
57	4.9	0.0	0.0	8.9	30.5	0.0	0.0	0.0	0.0	46.2	0.0	0.0	0.0
58	4.5	0.0	0.0	8.9	30.5	0.0	0.0	0.0	0.0	46.2	0.0	0.0	0.0
59	3.9	0.0	0.0	8.9	30.5	0.0	0.0	0.0	0.0	32.8	0.0	0.0	0.0
60	4.0	0.0	0.0	8.9	30.5	0.0	0.0	0.0	0.0	36.3	0.0	0.0	0.0
61	9.7	10.7	0.0	15.2	30.5	6.0	0.0	0.5	0.2	30.6	0.0	0.3	1.9
62	9.0	19.4	0.0	15.2	30.5	6.0	0.0	0.5	0.2	30.7	0.0	0.3	1.9
63	8.8	29.7	0.0	15.2	30.5	6.0	0.0	0.5	0.2	30.5	0.0	0.3	1.9
64	4.0	33.6	0.0	15.2	30.5	5.9	0.0	0.5	0.2	33.7	0.0	0.3	1.9
65	13.1	13.1	0.0	15.2	30.5	5.8	0.0	0.6	0.2	38.8	0.0	0.3	1.9
66	11.7	23.4	0.0	15.2	30.5	5.7	0.0	0.6	0.2	39.1	0.0	0.3	1.9
67	10.3	31.7	0.0	15.2	30.5	5.7	0.0	0.6	0.2	39.1	0.0	0.3	1.9
68	8.9	35.5	0.0	15.2	30.5	5.7	0.0	0.6	0.2	39.5	0.0	0.3	1.9
69	7.4	45.8	0.0	15.2	30.5	5.7	0.0	0.6	0.2	39.5	0.0	0.3	1.9
70	12.0	12.0	0.0	15.2	30.5	5.6	0.0	0.9	0.2	39.5	0.0	0.3	1.9
71	10.6	21.1	0.0	15.2	30.5	5.6	0.0	0.9	0.2	35.6	0.0	0.3	1.9

1	2	3	4	5	6	7	8	9	10	11	12	13	14
72	9.7	29.2	0.0	15.2	30.5	5.6	0.0	0.9	0.2	36.9	0.0	0.3	1.9
73	8.9	35.6	0.0	15.2	30.5	5.6	0.0	0.9	0.2	37.9	0.0	0.3	1.9
74	6.4	47.2	0.0	15.2	30.5	5.6	0.0	0.9	0.2	37.9	0.0	0.3	1.9
75	13.1	15.4	0.0	15.2	30.5	5.6	0.0	0.9	0.2	37.9	0.0	0.3	1.9
76	16.0	8.8	0.0	15.2	30.5	5.8	0.0	0.6	0.7	42.1	0.0	0.3	1.9
77	20.0	22.4	0.0	15.2	30.5	5.8	0.0	0.6	0.7	42.1	0.0	0.3	1.9
78	14.1	23.4	0.0	15.2	30.5	5.8	0.0	0.6	0.7	43.8	0.0	0.3	1.9
79	15.0	35.9	0.0	15.2	30.5	5.8	0.0	0.6	0.7	43.8	0.0	0.3	1.9
80	12.9	58.0	0.0	15.2	30.5	5.8	0.0	0.6	0.7	43.8	0.0	0.3	1.9
81	16.3	16.3	0.0	15.2	30.5	5.8	0.0	0.6	0.7	44.1	0.0	0.3	1.9
82	12.1	13.3	0.0	15.2	30.5	7.4	2.0	0.6	0.8	45.4	0.0	0.3	1.9
83	14.6	30.4	0.0	15.2	30.5	7.4	2.0	0.6	0.8	44.1	0.0	0.3	1.9
84	12.9	40.5	0.0	15.2	30.5	7.5	2.0	0.6	0.8	44.1	0.0	0.3	1.9
85	14.1	57.2	0.0	15.2	30.5	7.5	2.0	0.6	0.8	44.1	0.0	0.3	1.9
86	13.1	85.5	0.0	15.2	30.5	7.5	2.0	0.6	0.8	44.1	0.0	0.3	1.9
87	14.1	14.1	0.0	15.2	30.5	7.2	2.0	0.6	0.4	40.6	0.0	0.3	1.9
88	14.5	31.3	0.0	15.2	30.5	7.2	2.0	0.6	0.4	40.7	0.0	0.3	1.9
89	9.6	29.3	0.0	15.2	30.5	7.2	2.0	0.6	0.4	42.7	0.0	0.3	1.9
90	10.6	43.6	0.0	15.2	30.5	7.2	2.0	0.6	0.4	42.7	0.0	0.3	1.9
91	8.4	66.8	0.0	15.2	30.5	7.2	2.0	0.6	0.4	42.7	0.0	0.3	1.9
92	6.8	26.5	0.0	15.2	30.5	7.2	2.0	0.6	0.4	42.7	0.0	0.3	1.9
93	13.5	0.0	0.0	15.2	30.5	7.2	2.0	0.6	0.4	39.0	0.0	0.3	1.9
94	9.0	0.0	0.0	15.2	30.5	6.0	0.0	0.5	0.2	29.5	0.0	0.3	1.9
95	12.6	0.0	0.0	15.2	30.5	5.8	0.0	0.6	0.2	35.8	0.0	0.3	1.9
96	15.4	0.0	0.0	15.2	30.5	5.7	0.0	0.6	0.2	39.5	0.0	0.3	1.9
97	11.8	0.0	0.0	15.2	30.5	5.6	0.0	0.9	0.2	35.1	0.0	0.3	1.9
98	13.5	0.0	0.0	15.2	30.5	5.8	0.0	0.6	0.7	43.2	0.0	0.3	1.9
99	12.1	0.0	0.0	15.2	30.5	7.5	2.0	0.6	0.8	43.2	0.0	0.3	1.9
100	12.3	49.1	0.0	15.2	30.5	7.5	2.0	0.6	0.8	44.1	0.0	0.3	1.9
101	13.6	24.3	60.5	15.2	30.5	5.5	0.0	0.6	0.8	49.9	0.0	0.3	1.8
102	11.5	27.4	66.3	15.2	30.5	5.5	0.0	0.6	0.8	49.9	0.0	0.3	1.8
103	11.3	42.1	76.4	15.2	30.5	5.5	0.0	0.6	0.8	49.9	0.0	0.3	1.8
104	8.5	68.3	89.9	15.2	30.5	5.5	0.0	0.6	0.8	49.9	0.0	0.3	1.8
105	13.8	19.1	41.9	15.2	30.5	5.4	0.0	0.6	0.8	40.7	0.0	0.3	1.8
106	11.3	38.7	57.8	15.2	30.5	5.4	0.0	0.6	0.8	40.7	0.0	0.3	1.8
107	11.3	51.3	57.4	15.2	30.5	5.4	0.0	0.6	0.8	40.7	0.0	0.3	1.8

1	2	3	4	5	6	7	8	9	10	11	12	13	14
108	10.2	63.3	65.0	15.2	30.5	5.4	0.0	0.6	0.8	40.7	0.0	0.3	1.8
109	15.8	11.2	16.1	15.2	30.5	5.4	0.0	0.6	0.8	41.7	0.0	0.3	1.8
110	13.6	18.9	30.0	15.2	30.5	5.4	0.0	0.6	0.8	41.7	0.0	0.3	1.8
111	13.0	39.5	41.9	15.2	30.5	5.4	0.0	0.6	0.8	41.7	0.0	0.3	1.8
112	11.9	38.0	38.3	15.2	30.5	5.4	0.0	0.6	0.8	41.7	0.0	0.3	1.8
113	15.8	14.1	15.3	15.2	30.5	5.4	0.0	0.6	0.8	37.9	0.0	0.3	1.8
114	14.1	20.8	26.2	15.2	30.5	5.4	0.0	0.6	0.8	37.9	0.0	0.3	1.8
115	13.0	39.3	34.7	15.2	30.5	5.4	0.0	0.6	0.8	37.9	0.0	0.3	1.8
116	11.3	55.4	37.7	15.2	30.5	5.4	0.0	0.6	0.8	37.9	0.0	0.3	1.8
117	15.6	13.4	35.3	15.2	30.5	7.2	1.9	0.6	0.9	33.8	0.0	0.3	1.8
118	8.1	62.8	109.2	15.2	30.5	7.2	1.9	0.6	0.9	33.8	0.0	0.3	1.8
119	10.2	40.4	95.5	15.2	30.5	7.2	1.9	0.6	0.9	33.8	0.0	0.3	1.8
120	13.0	24.1	70.2	15.2	30.5	7.2	1.9	0.6	0.9	33.8	0.0	0.3	1.8
121	16.3	6.7	22.7	15.2	30.5	7.1	1.9	0.6	0.9	30.9	0.0	0.3	1.8
122	14.5	31.0	43.7	15.2	30.5	7.1	1.9	0.6	0.9	30.9	0.0	0.3	1.8
123	11.9	44.8	63.9	15.2	30.5	7.1	1.9	0.6	0.9	30.9	0.0	0.3	1.8
124	9.1	55.4	81.0	15.2	30.5	7.1	1.9	0.6	0.9	30.9	0.0	0.3	1.8
125	15.8	9.6	15.8	15.2	30.5	7.1	1.9	0.6	0.9	29.6	0.0	0.3	1.8
126	14.1	36.1	42.5	15.2	30.5	7.1	1.9	0.6	0.9	29.6	0.0	0.3	1.8
127	11.9	66.8	69.2	15.2	30.5	7.1	1.9	0.6	0.9	29.6	0.0	0.3	1.8
128	7.7	64.3	68.2	15.2	30.5	7.1	1.9	0.6	0.9	29.6	0.0	0.3	1.8
129	15.6	14.4	15.5	15.2	30.5	7.1	1.9	0.6	0.9	35.0	0.0	0.3	1.8
130	14.7	31.7	32.9	15.2	30.5	7.1	1.9	0.6	0.9	35.0	0.0	0.3	1.8
131	10.2	53.6	54.5	15.2	30.5	7.1	1.9	0.6	0.9	35.0	0.0	0.3	1.8
132	6.2	87.8	57.7	15.2	30.5	7.1	1.9	0.6	0.9	35.0	0.0	0.3	1.8
133	7.6	43.4	69.7	15.2	30.5	4.8	4.3	0.3	0.6	37.0	0.0	0.3	1.8
134	11.6	15.1	47.1	15.2	30.5	4.8	4.3	0.3	0.6	37.0	0.0	0.3	1.8
135	13.0	9.4	19.9	15.2	30.5	4.8	4.3	0.3	0.6	37.0	0.0	0.3	1.8
136	8.0	82.2	122.3	15.2	30.5	4.8	4.3	0.3	0.6	37.0	0.0	0.3	1.8
137	6.2	54.5	53.1	15.2	30.5	4.8	4.3	0.3	0.6	37.0	0.0	0.3	1.8
138	9.4	36.0	37.7	15.2	30.5	4.8	4.3	0.3	0.6	37.0	0.0	0.3	1.8
139	11.1	7.1	17.0	15.2	30.5	4.8	4.3	0.3	0.6	37.0	0.0	0.3	1.8
140	0.0	64.1	71.2	15.2	30.5	4.8	4.3	0.3	0.6	37.0	0.0	0.3	1.8
141	7.9	38.4	70.2	15.2	30.5	4.7	4.2	0.2	0.6	38.7	0.0	0.3	1.8
142	10.7	19.8	41.9	15.2	30.5	4.7	4.2	0.2	0.6	38.7	0.0	0.3	1.8
143	13.0	10.2	19.4	15.2	30.5	4.7	4.2	0.2	0.6	38.7	0.0	0.3	1.8

1	2	3	4	5	6	7	8	9	10	11	12	13	14
144	0.0	75.4	121.2	15.2	30.5	4.7	4.2	0.2	0.6	38.7	0.0	0.3	1.8
145	6.3	58.3	55.4	15.2	30.5	4.7	4.2	0.2	0.6	38.7	0.0	0.3	1.8
146	10.4	41.3	41.1	15.2	30.5	4.7	4.2	0.2	0.6	38.7	0.0	0.3	1.8
147	11.9	0.0	0.0	15.2	30.5	4.7	4.2	0.2	0.6	38.7	0.0	0.3	1.8
148	0.0	60.1	66.6	15.2	30.5	4.7	4.2	0.2	0.6	38.7	0.0	0.3	1.8
149	7.6	19.1	0.0	17.0	21.0	7.0	-0.0	0.4	2.5	38.0	0.0	0.2	0.6
150	8.9	22.3	0.0	17.0	21.0	5.5	1.6	0.4	2.5	38.0	0.0	0.2	0.6
151	6.7	16.8	0.0	17.0	21.0	4.2	3.1	0.4	2.5	29.4	0.0	0.2	0.6
152	7.6	19.1	0.0	17.0	21.0	1.9	-0.6	0.4	2.5	29.4	0.0	0.2	0.6
153	6.8	17.0	0.0	17.0	21.0	4.2	1.6	0.4	2.5	28.8	0.0	0.2	0.6
154	6.4	16.0	0.0	17.0	21.0	0.0	0.0	0.4	2.5	28.8	0.0	0.2	0.6
155	7.0	17.4	0.0	17.0	21.0	7.0	-0.0	0.39	2.5	38.0	0.0	0.0	0.6
156	8.3	20.7	0.0	17.0	21.0	5.5	1.6	0.0	2.5	38.0	0.0	0.0	0.6
157	5.7	14.3	0.0	17.0	21.0	4.2	3.2	0.0	2.5	29.4	0.0	0.0	0.6
158	7.0	17.5	0.0	17.0	21.0	1.9	-0.6	0.0	2.5	29.4	0.0	0.0	0.6
159	5.7	14.3	0.0	17.0	21.0	4.2	1.6	0.0	2.5	28.8	0.0	0.0	0.6
160	3.8	9.6	0.0	17.0	21.0	0.0	0.0	0.0	2.5	28.8	0.0	0.0	0.6
161	5.3	0.0	0.0	10.0	20.0	7.4	0.0	0.6	2.3	47.1	0.0	0.2	1.1
162	5.4	0.0	0.0	10.0	20.0	7.4	0.0	0.6	2.3	47.1	0.0	0.2	1.1
163	4.6	1.9	0.0	10.0	20.0	7.4	0.0	0.6	2.3	47.1	0.0	0.2	1.1
164	4.9	2.0	0.0	10.0	20.0	7.4	0.0	0.6	2.3	47.1	0.0	0.2	1.1
165	4.7	4.7	0.0	10.0	20.0	7.4	0.0	0.6	2.3	47.1	0.0	0.2	1.1
166	4.5	4.5	0.0	10.0	20.0	7.4	0.0	0.6	2.3	47.1	0.0	0.2	1.1
167	4.9	12.0	0.0	10.0	20.0	7.4	0.0	0.6	2.3	47.1	0.0	0.2	1.1
168	4.4	10.6	0.0	10.0	20.0	7.4	0.0	0.6	2.3	47.1	0.0	0.2	1.1
169	0.0	24.2	0.0	10.0	20.0	7.4	0.0	0.6	2.3	47.1	0.0	0.2	1.1
170	0.0	25.2	0.0	10.0	20.0	7.4	0.0	0.6	2.3	47.1	0.0	0.2	1.1
171	7.9	21.9	26.2	10.2	30.5	6.5	0.0	0.6	0.9	47.6	0.0	0.3	1.7
172	9.2	11.4	13.6	10.2	30.5	6.5	0.0	0.6	0.9	43.7	0.0	0.3	1.7
173	6.0	5.6	6.7	10.2	30.5	6.5	0.0	0.6	0.9	45.1	0.0	0.3	1.7
174	6.2	4.6	5.4	10.2	30.5	6.5	0.0	0.6	0.9	42.6	0.0	0.3	1.7
175	8.0	22.0	26.2	10.2	30.5	6.5	6.3	0.6	0.9	50.5	0.0	0.3	1.7
176	5.4	7.7	9.2	10.2	30.5	6.5	6.3	0.6	0.9	52.1	0.0	0.3	1.7
177	7.4	6.9	8.3	10.2	30.5	6.5	6.3	0.6	0.9	49.0	0.0	0.3	1.7
178	8.1	5.8	6.9	10.2	30.5	6.5	6.3	0.6	0.9	47.1	0.0	0.3	1.7
179	10.4	21.5	25.7	8.9	30.5	5.1	0.0	0.7	1.1	55.5	0.0	0.3	1.7

1	2	3	4	5	6	7	8	9	10	11	12	13	14
180	12.2	14.5	17.4	8.9	30.5	5.1	0.0	0.7	1.1	55.2	0.0	0.3	1.7
181	12.8	10.8	12.9	8.9	30.5	5.1	0.0	0.7	1.1	53.4	0.0	0.3	1.7
182	12.4	8.1	9.7	8.9	30.5	5.1	0.0	0.7	1.1	56.2	0.0	0.3	1.7
183	9.2	19.2	22.9	8.9	30.5	5.1	8.9	0.7	1.1	35.5	0.0	0.3	1.7
184	9.1	10.9	13.0	8.9	30.5	5.1	8.9	0.7	1.1	38.9	0.0	0.3	1.7
185	8.2	7.0	8.3	8.9	30.5	5.1	8.9	0.7	1.1	31.0	0.0	0.3	1.7
186	11.7	7.8	9.3	8.9	30.5	5.1	8.9	0.7	1.1	53.6	0.0	0.3	1.7
187	10.6	22.0	26.3	8.9	26.7	5.9	0.0	0.6	1.2	42.8	0.0	0.3	1.7
188	9.9	11.8	14.1	8.9	26.7	5.9	0.0	0.6	1.2	43.8	0.0	0.3	1.7
189	9.6	8.1	9.7	8.9	26.7	5.9	0.0	0.6	1.2	23.2	0.0	0.3	1.7
190	9.2	6.1	7.2	8.9	26.7	5.9	0.0	0.6	1.2	40.2	0.0	0.3	1.7
191	10.1	21.0	25.2	8.9	26.7	5.9	7.0	0.6	1.2	26.3	0.0	0.3	1.7
192	8.1	9.7	11.6	8.9	26.7	5.9	7.0	0.6	1.2	20.7	0.0	0.3	1.7
193	7.7	6.5	7.8	8.9	26.7	5.9	7.0	0.6	1.2	36.6	0.0	0.3	1.7
194	7.5	5.1	6.1	8.9	26.7	5.9	7.0	0.6	1.2	41.8	0.0	0.3	1.7
195	5.7	0.0	0.0	12.7	20.3	6.2	3.4	0.6	0.6	0.0	4.0	0.3	1.4
196	6.2	5.0	0.0	12.7	20.3	6.2	3.4	0.6	0.6	0.0	4.7	0.3	1.4
197	6.0	10.5	0.0	12.7	20.3	6.2	3.4	0.6	0.6	0.0	4.5	0.3	1.4
198	4.6	12.2	0.0	12.7	20.3	6.2	3.4	0.6	0.6	0.0	4.1	0.3	1.4
199	4.6	16.1	0.0	12.7	20.3	6.2	3.4	0.6	0.6	0.0	3.9	0.3	1.4
200	4.2	18.7	0.0	12.7	20.3	6.2	3.4	0.6	0.6	0.0	3.5	0.3	1.4
201	3.5	18.6	0.0	12.7	20.3	6.2	3.4	0.6	0.6	0.0	4.2	0.3	1.4
202	3.3	23.2	0.0	12.7	20.3	6.2	3.4	0.6	0.6	0.0	4.7	0.3	1.4
203	6.2	0.0	0.0	12.7	20.3	6.2	3.4	0.9	0.6	0.0	3.4	0.3	1.4
204	6.9	5.5	0.0	12.7	20.3	6.2	3.4	0.9	0.6	0.0	4.8	0.3	1.4
205	6.5	11.9	0.0	12.7	20.3	6.2	3.4	0.9	0.6	0.0	4.2	0.3	1.4
206	5.7	15.5	0.0	12.7	20.3	6.2	3.4	0.9	0.6	0.0	4.5	0.3	1.4
207	4.4	19.9	0.0	12.7	20.3	6.2	3.4	0.9	0.6	0.0	4.4	0.3	1.4
208	3.1	22.1	0.0	12.7	20.3	6.2	3.4	0.9	0.6	0.0	4.8	0.3	1.4
209	0.0	20.3	0.0	12.7	20.3	6.2	3.4	0.9	0.6	0.0	3.6	0.3	1.4
210	0.0	47.4	0.0	15.2	30.5	3.2	0.0	0.7	0.7	37.9	0.0	0.3	1.6
211	11.9	35.8	0.0	15.2	30.5	3.2	0.0	0.7	0.7	34.5	0.0	0.3	1.6
212	14.1	19.1	0.0	15.2	30.5	3.4	0.0	0.7	0.7	33.6	0.0	0.3	1.6
213	15.0	11.3	0.0	15.2	30.5	3.1	0.0	0.7	0.7	34.0	0.0	0.3	1.6
214	15.5	5.2	0.0	15.2	30.5	3.4	0.0	0.7	0.7	35.9	0.0	0.3	1.6
215	15.9	0.0	0.0	15.2	30.5	3.1	0.0	0.7	0.7	35.3	0.0	0.3	1.6

1	2	3	4	5	6	7	8	9	10	11	12	13	14
216	0.0	64.0	0.0	15.2	30.5	3.4	5.1	0.7	0.7	34.0	0.0	0.3	1.6
217	13.7	41.2	0.0	15.2	30.5	3.4	5.1	0.7	0.7	36.3	0.0	0.3	1.6
218	16.9	22.6	0.0	15.2	30.5	3.5	5.1	0.7	0.7	31.9	0.0	0.3	1.6
219	17.1	13.0	0.0	15.2	30.5	3.5	5.1	0.7	0.7	30.7	0.0	0.3	1.6
220	17.2	5.8	0.0	15.2	30.5	3.5	5.1	0.7	0.7	38.0	0.0	0.3	1.6
221	16.7	0.0	0.0	15.2	30.5	3.5	5.1	0.7	0.7	37.7	0.0	0.3	1.6
222	8.8	61.6	0.0	15.2	30.5	3.7	5.1	0.7	0.7	34.6	0.0	0.3	1.6
223	0.0	71.6	0.0	15.2	30.5	8.0	0.0	0.7	1.2	37.9	0.0	0.3	1.6
224	15.2	45.7	0.0	15.2	30.5	8.3	0.0	0.7	1.2	30.8	0.0	0.3	1.6
225	16.9	22.6	0.0	15.2	30.5	8.4	0.0	0.7	1.2	34.1	0.0	0.3	1.6
226	19.5	14.6	0.0	15.2	30.5	8.4	0.0	0.7	1.2	37.0	0.0	0.3	1.6
227	17.9	12.2	0.0	15.2	30.5	8.0	0.0	0.7	1.2	37.7	0.0	0.3	1.6
228	17.4	5.8	0.0	15.2	30.5	8.2	0.0	0.7	1.2	40.7	0.0	0.3	1.6
229	16.5	0.0	0.0	15.2	30.5	8.1	0.0	0.7	1.2	39.2	0.0	0.3	1.6
230	9.7	67.8	0.0	15.2	30.5	8.8	0.0	0.7	1.2	34.5	0.0	0.3	1.6
231	0.0	103.1	0.0	15.2	30.5	8.0	5.1	0.7	1.2	35.7	0.0	0.3	1.6
232	20.3	61.0	0.0	15.2	30.5	8.1	5.1	0.7	1.2	36.8	0.0	0.3	1.6
233	18.6	24.8	0.0	15.2	30.5	8.1	5.1	0.7	1.2	34.7	0.0	0.3	1.6
234	18.1	13.6	0.0	15.2	30.5	7.8	5.1	0.7	1.2	31.9	0.0	0.3	1.6
235	17.8	6.0	0.0	15.2	30.5	8.0	5.1	0.7	1.2	39.1	0.0	0.3	1.6
236	17.2	0.0	0.0	15.2	30.5	8.1	5.1	0.7	1.2	38.9	0.0	0.3	1.6
237	13.0	91.1	0.0	15.2	30.5	8.7	5.1	0.7	1.2	33.0	0.0	0.3	1.6
238	0.0	42.2	27.7	15.2	30.5	3.5	0.0	0.7	0.7	25.4	0.0	0.3	1.6
239	8.6	39.3	25.8	15.2	30.5	3.6	0.0	0.7	0.7	27.5	0.0	0.3	1.6
240	14.5	13.4	11.0	15.2	30.5	3.2	0.0	0.7	0.7	33.4	0.0	0.3	1.6
241	14.5	3.4	4.9	15.2	30.5	3.2	0.0	0.7	0.7	28.4	0.0	0.3	1.6
242	4.0	42.9	28.2	15.2	30.5	3.5	0.0	0.7	0.7	25.4	0.0	0.3	1.6
243	0.0	62.4	37.8	15.2	30.5	3.4	5.1	0.7	0.7	29.2	0.0	0.3	1.6
244	10.3	49.7	32.6	15.2	30.5	3.1	5.1	0.7	0.7	29.4	0.0	0.3	1.6
245	14.3	25.0	19.3	15.2	30.5	3.1	5.1	0.7	0.7	29.4	0.0	0.3	1.6
246	15.5	14.9	11.7	15.2	30.5	3.4	5.1	0.7	0.7	30.3	0.0	0.3	1.6
247	15.4	4.2	5.3	15.2	30.5	3.4	5.1	0.7	0.7	33.6	0.0	0.3	1.6
248	5.5	62.6	38.6	15.2	30.5	3.3	5.1	0.7	0.7	31.9	0.0	0.3	1.6
249	0.0	66.7	43.7	15.2	30.5	7.9	0.0	0.7	1.2	35.6	0.0	0.3	1.6
250	12.5	60.5	37.8	15.2	30.5	7.5	0.0	0.7	1.2	34.5	0.0	0.3	1.6
251	16.7	13.7	22.6	15.2	30.5	7.4	0.0	0.7	1.2	33.9	0.0	0.3	1.6

1	2	3	4	5	6	7	8	9	10	11	12	13	14
252	17.4	8.4	13.2	15.2	30.5	8.2	0.0	0.7	1.2	39.3	0.0	0.3	1.6
253	15.8	2.7	5.3	15.2	30.5	8.1	0.0	0.7	1.2	38.7	0.0	0.3	1.6
254	6.3	67.2	44.1	15.2	30.5	7.8	0.0	0.7	1.2	34.8	0.0	0.3	1.6
255	0.0	102.4	63.0	15.2	30.5	7.6	5.1	0.7	1.2	36.9	0.0	0.3	1.6
256	16.7	25.2	22.6	15.2	30.5	7.7	5.1	0.7	1.2	40.1	0.0	0.3	1.6
257	18.1	10.8	13.8	15.2	30.5	7.7	5.1	0.7	1.2	40.9	0.0	0.3	1.6
258	16.0	4.3	5.5	15.2	30.5	7.7	5.1	0.7	1.2	37.2	0.0	0.3	1.6
259	8.6	92.6	60.8	15.2	30.5	7.6	5.1	0.7	1.2	34.9	0.0	0.3	1.6
260	13.9	41.5	28.2	15.2	30.5	3.7	5.1	1.1	0.7	27.2	0.0	0.3	1.6
261	11.4	26.7	23.1	15.2	30.5	3.7	0.0	1.1	0.7	27.9	0.0	0.3	1.6
262	0.0	90.4	46.3	15.2	30.4	4.5	1.6	.1.06	0.9	47.2	3.4	0.0	1.7
263	1.0	81.5	41.6	15.2	30.4	4.5	3.8	0.0	0.9	47.2	3.4	0.0	1.7
264	2.5	87.7	44.8	15.2	30.4	5.5	3.8	0.0	0.9	49.5	3.7	0.0	1.7
265	4.4	82.1	41.9	15.2	30.4	4.8	3.7	0.0	0.9	49.5	3.7	0.0	1.7
266	13.5	0.0	0.0	15.2	30.4	5.3	3.1	0.0	0.9	39.7	3.8	0.0	1.7
267	7.3	48.4	31.7	15.2	30.4	5.2	3.9	0.0	0.9	39.7	3.8	0.0	1.7
268	11.3	19.2	12.9	15.2	30.4	4.7	3.2	0.0	0.9	51.1	3.9	0.0	1.7
269	9.6	31.6	21.4	15.2	30.4	4.7	2.9	0.0	0.9	51.1	3.9	0.0	1.7
270	11.9	0.0	0.0	15.2	30.4	4.8	4.5	0.4	0.9	36.8	3.8	0.2	1.7
271	7.9	67.6	34.5	15.2	30.4	4.8	4.3	0.4	0.9	36.8	3.8	0.2	1.7
272	3.2	82.0	41.9	15.2	30.4	5.5	3.9	0.4	0.9	39.9	4.4	0.2	1.7
273	10.2	46.2	26.7	15.2	30.4	4.7	3.6	0.4	0.9	39.9	4.4	0.2	1.7
274	11.9	21.6	13.0	15.2	30.4	5.0	4.1	0.4	0.9	38.1	3.8	0.2	1.7
275	0.0	103.0	52.4	15.2	30.4	8.4	3.9	0.4	0.9	45.0	3.9	0.2	1.7
276	4.0	103.0	52.4	15.2	30.4	7.5	4.0	0.4	0.9	45.0	3.9	0.2	1.7
277	9.3	78.0	40.4	15.2	30.4	7.6	4.2	0.4	0.9	41.8	3.5	0.2	1.7
278	14.1	0.0	0.0	15.2	30.4	7.4	4.3	0.4	0.9	41.8	3.5	0.2	1.7
279	11.9	52.5	31.1	15.2	30.4	8.1	4.4	0.4	0.9	45.4	3.7	0.2	1.8
280	15.3	27.1	16.7	15.2	30.4	7.7	4.7	0.4	0.9	45.4	3.7	0.2	1.7
281	10.1	83.0	44.1	15.2	30.4	9.3	4.6	0.7	0.9	39.5	3.8	0.2	1.7
282	8.9	73.3	38.9	15.2	30.4	8.3	4.2	0.3	0.9	39.5	3.8	0.2	1.7
283	9.3	76.0	40.4	15.2	30.4	8.6	4.7	0.2	0.9	46.3	3.9	0.2	1.7
284	8.9	70.2	38.9	15.2	30.4	8.8	4.5	0.2	0.9	46.3	3.9	0.2	1.7
285	10.1	84.1	44.1	15.2	30.4	8.6	4.2	0.7	0.9	38.1	3.8	0.4	1.7
286	8.6	71.5	37.5	15.2	30.4	8.1	4.0	0.5	0.9	38.9	4.1	0.4	1.7
287	9.9	81.5	43.4	15.2	30.4	8.7	4.2	1.9	0.9	38.9	4.1	0.4	1.7

1	2	3	4	5	6	7	8	9	10	11	12	13	14
288	14.9	31.0	0.0	20.3	20.3	6.8	2.5	3.8	1.1	36.0	0.0	0.3	1.6
289	13.9	29.0	0.0	20.3	20.3	6.8	2.5	1.5	1.1	40.0	0.0	0.3	1.6
290	10.6	22.5	0.0	20.3	20.3	3.2	2.5	3.8	0.7	43.0	0.0	0.3	1.6
291	11.2	23.6	0.0	20.3	20.3	3.2	2.5	4.6	0.7	44.0	0.0	0.3	1.6
292	11.8	24.2	0.0	20.3	20.3	5.4	2.5	4.7	1.0	22.0	0.0	0.3	1.6
293	5.4	6.4	0.0	20.3	20.3	0.8	2.5	0.4	0.2	23.0	0.0	0.3	1.4
294	6.6	7.9	0.0	20.3	20.3	1.7	2.5	0.6	0.3	24.0	0.0	0.3	1.5
295	7.0	8.3	0.0	20.3	20.3	2.1	2.5	1.7	0.6	17.0	0.0	0.3	1.6
296	8.4	9.7	0.0	20.3	20.3	2.6	2.5	2.1	0.7	16.0	0.0	0.3	1.5
297	9.8	11.2	0.0	20.3	20.3	3.2	2.5	2.6	0.8	19.0	0.0	0.3	1.5
298	9.2	10.5	0.0	20.3	20.3	3.6	2.5	2.8	0.8	17.0	0.0	0.3	1.4
299	8.4	9.7	0.0	20.3	20.3	4.4	2.5	3.6	0.9	18.0	0.0	0.3	1.5
300	6.7	8.1	0.0	20.3	20.3	4.9	2.5	3.9	1.0	14.0	0.0	0.3	1.6
301	7.5	8.8	0.0	20.3	20.3	5.6	2.5	4.2	1.1	15.0	0.0	0.3	1.4
302	7.5	0.0	0.0	8.0	30.0	3.7	3.4	2.9	1.1	43.0	0.0	0.3	1.4
303	7.7	15.4	0.0	8.0	30.0	3.7	3.4	2.9	1.1	43.4	0.0	0.3	1.4
304	8.2	16.4	0.0	8.0	30.0	3.7	3.4	2.9	1.1	41.9	0.0	0.3	1.4
305	7.7	23.2	0.0	8.0	30.0	3.7	3.4	2.9	1.1	35.5	0.0	0.3	1.4
306	8.2	32.7	0.0	8.0	30.0	3.7	3.4	2.9	1.1	43.4	0.0	0.3	1.4
307	7.1	35.5	0.0	8.0	30.0	3.7	3.4	2.9	1.1	35.5	0.0	0.3	1.4
308	6.8	41.0	0.0	8.0	30.0	3.7	3.4	2.9	1.1	43.0	0.0	0.3	1.4
309	7.4	8.2	12.3	8.0	30.0	3.7	3.4	2.9	1.1	38.6	0.0	0.3	1.4
310	7.7	6.2	31.0	8.0	30.0	3.7	3.4	2.9	1.1	35.2	0.0	0.3	1.4
311	6.8	41.0	34.2	8.0	30.0	3.7	3.4	2.9	1.1	38.6	0.0	0.3	1.4
312	5.9	35.6	71.2	8.0	30.0	3.7	3.4	2.9	1.1	35.2	0.0	0.3	1.4
313	11.5	0.0	0.0	8.0	30.0	3.7	3.4	3.3	1.3	44.1	0.0	0.4	1.4
314	12.2	24.4	0.0	8.0	30.0	3.7	3.4	3.3	1.3	44.1	0.0	0.4	1.4
315	9.9	39.5	0.0	8.0	30.0	3.7	3.4	3.3	1.3	44.1	0.0	0.4	1.4
316	7.5	0.0	0.0	8.0	30.0	2.6	1.2	2.9	0.9	44.0	0.0	0.3	1.4
317	7.8	15.7	0.0	8.0	30.0	2.6	1.2	2.9	0.9	44.5	0.0	0.3	1.4
318	6.8	27.3	0.0	8.0	30.0	2.6	1.2	2.9	0.9	44.2	0.0	0.3	1.4
319	5.7	34.3	0.0	8.0	30.0	2.6	1.2	2.9	0.9	44.2	0.0	0.3	1.4
320	12.2	0.0	0.0	8.0	30.0	2.1	0.0	4.6	0.9	36.5	0.0	0.4	1.4
321	11.6	23.1	0.0	8.0	30.0	1.6	11.2	4.6	1.0	36.5	0.0	0.4	1.4
322	9.5	38.1	0.0	8.0	30.0	2.1	9.9	4.6	1.1	37.3	0.0	0.4	1.4
323	9.1	54.5	0.0	8.0	30.0	2.6	8.7	4.6	1.2	37.3	0.0	0.4	1.4

1	2	3	4	5	6	7	8	9	10	11	12	13	14
324	7.6	15.3	0.0	8.0	30.0	3.7	1.2	2.9	0.9	40.5	0.0	0.3	1.4
325	6.5	26.0	0.0	8.0	30.0	3.7	1.2	2.9	0.9	40.5	0.0	0.3	1.4
326	5.5	32.9	0.0	8.0	30.0	3.7	1.2	2.9	0.9	46.0	0.0	0.3	1.4
327	2.9	0.0	0.0	12.7	12.7	8.7	0.0	2.85	0.0	0.0	3.8	0.0	0.0
328	3.3	0.0	0.0	12.7	12.7	12.3	0.0	0.0	0.0	0.0	3.8	0.0	0.0
329	4.7	0.0	0.0	12.7	12.7	19.2	0.0	0.0	0.0	0.0	3.8	0.0	0.0
330	5.4	0.0	0.0	12.7	12.7	24.9	0.0	0.0	0.0	0.0	3.8	0.0	0.0
331	6.0	0.0	0.0	12.7	12.7	30.5	0.0	0.0	0.0	0.0	3.8	0.0	0.0
332	5.1	0.0	0.0	12.7	12.7	42.1	0.0	0.0	0.0	0.0	3.8	0.0	0.0
333	6.0	0.0	0.0	12.7	25.4	6.0	0.0	0.0	0.0	0.0	3.8	0.0	0.0
334	8.2	0.0	0.0	12.7	25.4	14.1	0.0	0.0	0.0	0.0	3.8	0.0	0.0
335	9.2	0.0	0.0	12.7	25.4	18.1	0.0	0.0	0.0	0.0	3.8	0.0	0.0
336	11.2	0.0	0.0	12.7	25.4	29.2	0.0	0.0	0.0	0.0	3.8	0.0	0.0
337	9.0	0.0	0.0	12.7	38.1	4.2	0.0	0.0	0.0	0.0	3.8	0.0	0.0
338	14.2	0.0	0.0	12.7	38.1	15.3	0.0	0.0	0.0	0.0	3.8	0.0	0.0
339	19.1	0.0	0.0	12.7	38.1	26.4	0.0	0.0	0.0	0.0	3.8	0.0	0.0
340	2.1	0.0	0.0	7.6	22.9	4.3	0.0	0.0	0.0	0.0	4.5	0.0	0.0
341	3.3	0.0	0.0	7.6	22.9	11.8	0.0	0.0	0.0	0.0	4.5	0.0	0.0
342	4.2	0.0	0.0	7.6	22.9	18.4	0.0	0.0	0.0	0.0	4.5	0.0	0.0
343	3.5	0.0	0.0	7.6	30.5	4.4	0.0	0.0	0.0	0.0	4.5	0.0	0.0
344	4.9	0.0	0.0	7.6	30.5	11.4	0.0	0.0	0.0	0.0	4.5	0.0	0.0
345	5.8	0.0	0.0	7.6	30.5	23.2	0.0	0.0	0.0	0.0	4.5	0.0	0.0

APPENDIX III

TABLE 6. TEST RESULTS - SPLIT CUBES BY WAINWRIGHT

NO.	SHEAR STRESS N/mm²	DIRECT STRESS N/mm²	CUBE SPLITTING N/mm²
1	3.77	1.77	2.11
2	4.65	2.66	2.21
3	5.40	3.54	2.11
4	9.13	4.43	2.44
5	7.57	5.32	2.18
6	2.70	0.89	1.97
7	9.13	6.20	2.09
8	8.11	7.07	2.66
9	10.10	7.97	2.04
10	11.70	9.75	2.61
11	-	10.65	2.72
12	7.31	4.43	2.61
13	10.32	8.86	2.42
14	12.54	9.30	2.44
15	11.30	9.75	2.64
16	9.75	10.19	2.45
17	11.47	10.63	2.43
18	-	10.65	2.47
19	13.60	8.86	2.35
20	13.29	10.19	2.46

TABLE 6. TEST RESULTS - HOLLOW CYLINDERS BY WAINWRIGHT

NO.	SHEAR STRESS N/mm²	DIRECT STRESS N/mm²	fsp N/mm²	fc' N/mm²	fcn N/mm²
1	3.14	15.10	2.34	34.55	44.5
2	3.44	15.45	2.34	34.55	44.5
3	1.72	12.30	1.88	x20.79	35.4
5	1.89	17.03	2.25	30.43	44.94
15	3.07	x24.58	2.71	37.89	45.29
16	4.99	20.02	2.71	37.89	45.29
17	4.45	13.34	2.01	33.36	37.00
18	2.93	5.79	2.01	33.36	37.00
19	3.12	3.16	1.86	34.72	42.21
20	1.56	0.00	1.86	34.72	42.21
21	1.28	x21.95	2.28	31.37	40.80
22	3.97	10.19	2.28	31.37	40.80

LIST OF REFERENCES

1. Kollbrunner, C.F. and Basler, K. - "Torsion in Structures - An Engineering Approach", Springer-Verlag, New York 1969.

2. Kong, F.K. and Evans, R.H. - "Reinforced and Prestressed Concrete", Nelson, 2nd edition 1980.

3. Rowe, R.E. et al. Handbook on the Unified Code for Structural Concrete (CP110:1972), Cement and Concrete Association, 1972.

4. S.A.A. Code for Prestressed Concrete. Australian Standard No.CA35. Standards Association of Australia, Sydney, 1963.

5. Rangan, B.V. and Hall, A.S. - "Strength of Rectangular Prestressed Concrete Beams in Combined Torsion, Bending and Shear", Journal of the American Concrete Institute, Vol.70, April 1973,pp.270-278.

6. Cowan, H.J. and Lyalin, I.M. - "Reinforced and Prestressed Concrete in Torsion". Arnold 1965.

7. British Standard Institution. The Structural Use of Concrete, CP110:1972.

8. Martin, L.H. - "A Theoretical Investigation into the Ultimate Strength in Bending and Torsion of Plain and Reinforced Concrete Members", Ph.D. Thesis, 1973, The University of Aston in Birmingham.

9. Mukherjee, P.R. and Warwaruk, J. - "Torsion, Bending and Shear in Prestressed Concrete Beams", Journal of the Structural Division, Proceedings of the American Society of Civil Engineers, Vol.97, No.ST4, April 1971,pp.1063-1079.

10. Bishara, A. - "Prestressed Concrete Beams under Combined Torsion, Bending and Shear", Journal of the American Concrete Institute, Vol.66, No.7, July 1969,pp.525-538.

11. Lampert, P. - "Torsion and Bending in Reinforced and Prestressed Concrete Members", Proceedings of the Institution of Civil Engineers, Vol.50, Dec.1971,pp.487-505.

12. Lampert, P. and Collins, M.P. - "Torsion, bending and confusion - an attempt to establish the facts.", Proceedings of the American Concrete Institute, Vol.69, No.8, August 1972, pp.500-4.

13. Henry, R.L. and Zia, P. - "Prestressed Beams in Torsion, Bending and Shear", Journal of the Structural Division, Proceedings of the American Society of Civil Engineers, Vol.100, No.ST5, May 1974, pp.933-952.

14. St.Venant-Mem. sav etrangers, Vol.14, 1855 (Todhunter and Pearsons's History of the Theory of Elasticity, Cambridge, Vol.2, 1893, p.312).

15. Turner, L. and Davies, V.C. - "Plain and Reinforced Concrete in Torsion", Selected Engineering Paper, No.165, Institution of Civil Engineers, 1934.

16. Marshall, W.T. and Tembe, N.R. - "Experiments on Plain and Reinforced Concrete in Torsion", Structural Engineer, V.19, No.11, Nov.1941, pp.177-191.

17. Bach, C. - "Elastizität and Festigkeit", Verlag Julius Springer, Berlin, 1911.

18. Prandtl, L. - "Zur Torsion von prismatischen Stäben", Physikalische Zeitschrift, Leipzig, Vol.4, 1903, pp.758-9.

19. Nadai, A.- "Plasticity", McGraw-Hill, New York, 1931.
- "Theory of Flow and Fracture of Solids", McGraw-Hill, New York, 1950, pp.490-511.

20. Nylander, H. - "Vridning och Vridningsinspäning vid Betong Konstruktioner", (Torsion and Torsional Resistance by Concrete Structures), Statens Kommittee för Byggnadsforskning, Stockholm, Bulletin No.3, 1945.

21. Cowan, H.J. - "The Strength of Plain, Reinforced and Prestressed Concrete Under the Action of Combined Stresses with Particular Reference to the Combined Bending and Torsion of Rectangular Sections", Magazine of Concrete Research, V.5, No.14, Dec.1953, pp.75-86.

22. Hsu, Thomas T.C. - "Torsion of Structural Concrete - Plain Concrete Rectangular Sections.", Torsion of Structural Concrete, Special Publication No.18-8, American Concrete Institute, Detroit, 1966, pp.203-238.

23. Martin, L.H. - "Bending and Torsion of Plain Concrete Members", Building Science, Vol.6, No.4, Dec.1971, pp.253-265.

24. Hsu, Thomas T.C. - "Torsion of Structural Concrete - A Summary on Pure Torsion", Torsion of Structural Concrete, Special Publication No.18-6, American Concrete Institute, Detroit, 1966, pp.165-178.

25. Allos, A.E. and Martin, L.H. - "Plain Concrete Tee Beams Subject to Torsion, Bending and Shear.", Building and Environment, Vol.11.

26. Andersen, P. - "Experiments with Concrete in Torsion", Proceedings of the American Society of Civil Engineers, Vol.60, 1934, pp.641-652.
- "Design of Reinforced Concrete in Torsion", Vol.63, 1937, pp.1475-1483.
- "Rectangular Concrete Sections Under Torsion.", Journal of the American Concrete Institute, Vol.9, 1937, pp.1-11.

27. Hsu, Thomas T.C. - "Torsion of Structural Concrete - Interaction Surface for Combined Torsion, Shear and Bending in Beams without Stirrups.", Journal of the American Concrete Institute, Vol.65, No.1, Jan. 1968, pp.55-60.

28. Cowan, H.J. and Armstrong, S. - "Prestressed Concrete in Combined Bending and Torsion.", Final Report, Fourth Congress, International Association for Bridge and Structural Engineering (Zurich), Cambridge, 1953, pp.409-11.

29. Humphreys, R. - "Torsional Properties of Prestressed Concrete", Structural Engineer, Institution of Structural Engineers, London, Vol.35, 1957, pp.213-24.

30. Gardner, R.P.M. - "The Behaviour of Prestressed Concrete I - beams under Combined Bending and Torsion", Cement and Concrete Association, Technical Report TRA/329, 1960, p.66.

31. Swamy, N. - "The Behaviour and Ultimate Strength of Prestressed Concrete Hollow Beams under Combined Bending and Torsion.", Magazine of Concrete Research, Vol.14, 1962, pp.13-24.

32. Reeves, J.S. - "Prestressed Concrete Tee-Beams under Combined Bending and Torsion.", Cement and Concrete Association Technical Report TRA/364, 1962.

33. Hsu, Thomas T.C. - "Torsion of Structural Concrete - Uniformly Prestressed Rectangular Beams without Web Reinforcement.", Journal of Prestressed Concrete Institute, Vol.13, No.2, April 1968, pp.34-44.

34. Evans, R.H. and Khalil, M.G.A. - "The Behaviour and Strength of Prestressed Concrete Rectangular Beams subjected to Combined Bending and Torsion.", The Structural Engineer, Vol.48, No.2, Feb.1970, pp.59-73.

35. Wainwright, P.J. - "Ultimate Strength in Bending and Torsion of Prestressed Beams Reinforced with Longitudinal Steel Only.", Ph.D.Thesis, 1972, The University of Aston in Birmingham.

36. Martin, L.H. and Wainwright, P.J. - "Torsion and Bending of Prestressed Concrete Beams.", Journal of the Structural Division, Proceedings of the American Society of Civil Engineers, Vol.99, No.ST11, Nov.1973, pp.2229-2244.

37. McMullen, A.E. and Woodhead, H.R. - "Experimental Study of Prestressed Concrete under Combined Torsion, Bending and Shear.P, Journal of the Prestressed Concrete Institute, Oct.1973, pp.85-100.

38. Cooper, M.J. - "Prestressed Concrete Beams in Torsion, Bending and Shear", Ph.D.Thesis, 1976, The University of Aston in Birmingham.

39. Cooper, M.J. and Martin, L.H. - "Prestressed Concrete Beams with no Stirrups in Torsion, Bending and Shear.", Proceedings of the Institution of Civil Engineers, Part 2, 1977, Vol.63, June, pp.455-468.

40. Zia, P. - "Torsional Strength of Prestressed Concrete Members.", Journal of the American Concrete Institute, Vol.32, 1961, pp.1337-1359.

41. Cowan, H.J. - "Elastic Theory for Torsional Strength of Rectangular Reinforced Concrete Beams.", Magazine of Concrete Research, Vol.2, 1950, pp.3-8.

42. Lessig, N.N. - "Determination of the Load-carrying Capacity of Reinforced Concrete Elements with Rectangular Cross-section under Simultaneous Action of Flexure and Torsion.", Betoni Zhelezobeton, No.3, 1959, pp.109-113, Translated from Russian as Portland Cement Association, Chicago, Foreign Literature Study No.348.

43. Murashkin, G.V. - "Influence of Prestressing on the Carrying Capacity and Cracking loads of Reinforced Concrete Beams under Combined Bending and Torsion.", Betoni Zhelezabeton, 1965, Vol.10, pp.29-33.

44. Okada, K. et al. - "Experimental Studies on the Strength of Rectangular Reinforced and Prestressed Concrete Beams under Combined Flexure and Torsion.", Trans. of Japan Soc.Civ.Engineers, 1966, Vol.131, July, pp.39-51.

45. Hsu, Thomas T.C. - "Torsion of Structural Concrete - Behaviour of Reinforced Concrete Rectangular Members,", Torsion of Structural Concrete, American Concrete Institute, Special Publication SP-18, 1968, pp.261-306.

46. Lampert, P. and Thurliman, B. - "Torsionsversuche an Stahlbetonbalken,", Institut fur Baustatik, ETH, Zurich, June 1968, p.101.

47. Hsu, Thomas T.C. and Kemp, E.L. - "Background and Practical Application of Tentative Design Criteria for Torsion.", Journal of the American Concrete Institute, Vol.66, No.1, Jan.1969, pp.12-23.

48. Hsu, Thomas T.C. - "Ultimate Torque of Reinforced Rectangular Beams.", Journal of Structural Division, American Society of Civil Engineers, Vol.94, No.ST2, Proc.Paper 5814, Feb. 1968, pp.483-510.

49. GangaRao, H.V.S. - "Rectangular Prestressed Concrete Beams under Combined Bending and Torsion.", Ph.D.Thesis, 1970, Department of Civil Engineers, North Carolina State University, Raleigh, North Carolina.

50. GangaRao, H.V.S. and Zia, P. - "Rectangular Prestressed Beams in Torsion and Bending.", Journal of the Structural Division, Proceedings of the American Society of Civil Engineers, Vol.99, No.ST1, Jan.1973, pp.183-198.

51. Woodhead, H.R. and McMullen, A.E. - "Torsional Strength of Prestressed Concrete Beams.", Journal of the Structural Division of the American Society of Civil Engineers, 1974, Vol.100, May, pp.881-900.

52. McGee, D. and Zia, P. ; "Prestressed Concrete under Torsion, Shear and Bending.", Proceedings of the American Concrete Institute, Vol.73, Tital No.73-2, January 1976, pp.26-32.

53. Roy, S.K. and Mukhopadhyay, M. - "Prestressed Concrete T-beams under combined Bending, Torsion and Shear.", Proceedings of Institution of Civil Engineers, Part 2, 1978, 65, Sept. pp.623-643.

54. Kar, Jitendra N. - "Diagonal Cracking in Prestressed Concrete Beams.", Proceedings of the American Society of Civil Engineers, Journal of the Structural Division, Vol.94, No.ST1, January, 1968, pp.83-109.

55. Seth, B.R. - "Non-Homogeneous Yield Condition.", Symposium on non-homogeneity in elasticity and plasticity. International Union of Theoretical and Applied Mechanics, Warsaw, 1958.

56. Collins, M.P., Walsh, P.F., Archer, F.E. and Hall, A.S. - "Ultimate Strength of Reinforced Concrete Beams Subjected to Combined Torsion and Bending.", Torsion of Structural Concrete, American Concrete Institute, Special Publication SP-18, 1968, pp.379-402.

ɔs, A.G., "Prestressed Concrete T-Beams Subjected to Torsion, Bending and Shear", Ph.D. Thesis, 1977, The University of Aston in Birmingham.

la, O.A.A., "Concrete Beams with Stirrups Subject to Torsion, Shear and Bending", Ph.D. Thesis, 1980, The University of Aston in Birmingham.

ɜren, L., Karlsson, I., and Losberg, A., "Torsion-bending-shear interaction for concrete beams", American Society of Civil Engineers Journal, August 1974, Proceedings Vol. 100, No.ST8, pp.1657-1676.

ɔeck, J.A., Ibrahim, I.O., and Mattock, A.H., "Shear Transfer in Reinforced Concrete" ACI Journal, Vol.66, No.2., February 1969, pp.119-128.

t, R.F., "Auxiliary Reinforcement in Concrete Connections", Journal of the Structural Division, ASCE, Vol.94, ST6, June 1968, pp.1485-1504.

keland, P.W., and Nirkeland, H.W., "Connections in Precast Concrete Construction", ACI Journal, Proceedings Vol.63, No.3, March 1966, pp.345-368.

ler, E., and Witta, E., Discussion of Ref.62, September 1966, pp.1027.

tock, A.H., "Shear Transfer in Concrete Having Reinforcement at an angle to the Shear Plane" American Concrete Institute Publication SP-42, Shear in Reinforced Concrete, 1974, pp.17-42.

ɔw, K.D., "Concrete Beams in Torsion and Bending", Ph.D. Thesis, 1975, The University of New South Wales.